

**Membrane Effects
of
Antimicrobial Peptides**

Xiaoqi Wang

Membrane Effects of Antimicrobial Peptides

Xiaoqi Wang

ISBN: 978-94-6419-966-6

DOI: <https://doi.org/10.33540/2009>

Cover and layout design: Xiaoqi Wang

Printed by: Gildeprint

The research described in this thesis was performed in the Membrane Biochemistry & Biophysics group at the Institute of Biomembranes and Bijvoet Center at Utrecht University.

© Xiaoqi Wang, 2023

All rights reserved. No part of this book may be reproduced in any form by any means without permission of the author

Membrane Effects of Antimicrobial Peptides

Membraaneffecten van antimicrobiële peptiden

(met een samenvatting in het Nederlands)

Proefschrift

ter verkrijging van de graad van doctor aan de
Universiteit Utrecht
op gezag van de
rector magnificus, prof.dr. H.R.B.M. Kummeling,
ingevolge het besluit van het college voor promoties
in het openbaar te verdedigen op

woensdag 6 december 2023 des ochtends te 10.15 uur

door

Xiaoqi Wang

geboren op 24 november 1991
te Hangzhou, China

Promotoren:

Prof. dr. J.A. Killian
Prof. dr. E.J. Breukink

Beoordelingscommissie:

Prof. dr. H.P. Haagsman
Prof. dr. O.P. Kuipers
Prof. dr. K. Lohner
Prof. dr. R.J. Pieters
Dr. S.A.J. Zaat

This thesis was accomplished with financial support from China Scholarship Council (CSC).

Table of contents

List of abbreviations

- Chapter 1** Introduction: Lantibiotics and two types of novel AMPs
- Chapter 2** Bacterial pH homeostasis, ion homeostasis and ATP synthesis
- Chapter 3** Analyzing mechanisms of action of antimicrobial peptides on bacterial membranes requires multiple complimentary assays and different bacterial strains
- Chapter 4** Exploring potential targets of the lantibiotic epilancin 15X on bacterial membranes
- Chapter 5** The interactions of brevicacillin and brevicacillin 2V with Lipid II
- Chapter 6** Summary and discussion

Appendices

Nederlandse samenvatting en discussie

Acknowledgements

Curriculum vitae

List of publications

List of abbreviations

ABC	ATP-binding cassette
Abu	2-aminobutyric acid
AMP	Antimicrobial peptides
C55-P	undecaprenyl phosphate
C55-PP	undecaprenyl pyrophosphate
CCCP	Carbonyl cyanide m-chlorophenyl hydrazone
CD	Circular Dichroism
CF	Carboxyfluorescein
CFDA, SE	5 (and 6-)-carboxyfluorescein diacetate succinimidyl ester
CFU	Colony forming unit
CL	Cardiolipin
CDP-DAG	1,2-Dioleoyl-sn-glycero-3-(cytidine diphosphate)
DAP	Diaminopimelic acid
DAPI	4',6-Diamidino-2-phenylindole
Dha	2,3-Dehydroalanine
Dhb	(Z)-2,3-Dehydrobutyrine
DiSC ₂ (5)	3,3'-Diethylthiadicarbocyanine iodide
DOPC	1,2-Dioleoyl-sn-glycero-3-phosphocholine
DOPG	1,2-Dioleoyl-sn-glycero-3-phosphoglycerol
FAME	Fatty acid methyl ester
HPTS	8-Hydroxypyrene-1,3,6-trisulfonic acid trisodium salt
ITC	Isothermal titration calorimetry
LAB	Lactic acid bacteria
Lac	Lactate
Lal	Lysinoalanine
Lan	Lanthionine
LUV	Large unilamellar vesicle
ManNAc	N-acetylmannosamine
MeLan	β-methylanthionine
MIC	Minimum inhibitory concentration
MoA	Mode of action
MraY	Phospho-MurNAc-pentapeptide translocase
MRSA	Methicillin-resistant <i>Staphylococcus aureus</i>
MurNAc-GlcNAc	N-acetylmuramic acid-N-acetyl-D-glucosamine
NRP	Mon-ribosomally produced peptide
Obu	2-Oxo butyrate
PBP	Penicillin binding protein
PE	Phosphatidylethanolamine
PG	Peptidoglycan
Pi	Inorganic phosphate
PMF	Proton motive force

PNPT	Polyprenyl-phosphate N-acetyl hexosamine 1-phosphate transferase
RCK	Regulator of K ⁺ conductance
SKT	K ⁺ transporters
ssNMR	Solid-state NMR
SUV	Small unilamellar vesicle
TagO	Phospho-GlcNAc transferase
TCA	Tricarboxylic acid
TFA	Trifluoroacetic acid
TPP ⁺	Tetraphenylphosphonium
TSB	Tryptic soy broth
VRE	Vancomycin-resistant <i>enterococci</i>
VRSA	Vancomycin-resistant <i>Staphylococcus aureus</i>
wTA	Wall teichoic acid

Chapter 1

Introduction:

Lantibiotics and two types of novel AMPs

This chapter is partly based on:

Xiaoqi Wang, Qing Gu, and Eefjan Breukink. "Non-Lipid II Targeting Lantibiotics." *Biochimica et Biophysica Acta (BBA) - Biomembranes* 1862, no. 8 (2020/08/01/2020): 183244. <https://dx.doi.org/https://doi.org/10.1016/j.bbamem.2020.183244>.

1.1 Cell wall synthesis pathway

The cell wall of gram-positive bacteria maintains the structural strength and shape of the cell and protects the cell from osmotic lysis. It is the first barrier that gram-positive bacteria have put up to face outside threats. The enzymes and precursors in cell wall biosynthesis pathways are popular targets for many antibiotics. In general the gram-positive cell wall is composed of a peptidoglycan (PG) layer to which wall teichoic acids are attached, and the PG layer is tethered to the plasma membrane by lipoteichoic acids [1]. Peptidoglycan makes up for most of the weight of the cell wall and is composed of a polymer of N-acetylmuramic acid-N-acetyl-D-glucosamine (MurNAc-GlcNAc) units which are crosslinked by polysaccharides [2]. The wall teichoic acid (wTA) composition varies in different strains [3]. For instance, the wTA of *Bacillus subtilis* 168 contains a linkage unit of two sugars of GlcNAc and N-acetylmannosamine (ManNAc) on which glycerol-phosphate units are polymerized [4]. Additionally, the polymerized glycerol-phosphate units can be decorated with glucoses [4]. The wTA of *Staphylococcus aureus* contains a GlcNAc-ManNAc-glycerol-phosphate-glycerol-phosphate linkage unit to which a polymer of ribitol-phosphate units is attached [5]. These polymerized ribitol-phosphate units can be decorated with MurNAcs [5]. The wall teichoic acid biosynthesis cycle is tightly connected with peptidoglycan synthesis as both pathways have the same precursor undecaprenyl phosphate (C55-P) (Fig. 1A).

The membrane located steps of the peptidoglycan synthesis pathway start with the synthesis of Lipid I [6]. Here, the membrane embedded enzyme phospho-MurNAc-pentapeptide translocase (MraY) transfers a phospho-MurNAc-pentapeptide moiety from UDP-MurNAc-pentapeptide to C55-P forming Lipid I [6]. Then, another membrane enzyme MurG, a glycosyltransferase, couples a GlcNAc moiety from UDP-GlcNAc to Lipid I to produce Lipid II [7]. Lipid II is flipped to the outside of the membrane by a flippase. The Lipid II flippase identification is under dispute for now, with different researches claiming the flippase could be either MurJ or FtsW [8, 9]. Lipid II in the outside of membrane is incorporated into peptidoglycan network by penicillin binding proteins (PBPs) [10, 11]. The undecaprenyl pyrophosphate (C55-PP) remaining in the membrane after the polymerization step of PBPs is dephosphorylated to C55-P by BacA [12]. C55-P is recycled to the inside of the cell and is then available for another synthesis cycle.

As an example of a wTA pathway, we describe the biosynthesis of *Bacillus subtilis* 168 wTA (Fig. 1A) [4, 13], which starts with the synthesis of Lipid α [14]. This step is performed by the membrane embedded enzyme phospho-GlcNAc transferase (TagO) that transfers a phospho-GlcNAc moiety from UDP-GlcNAc to C55-P thus forming Lipid α [14]. TagO and MraY are both members of the polyprenyl-phosphate N-acetyl hexosamine 1-phosphate transferase (PNPT) superfamily that are responsible for the

synthesis of cell envelope polymers. The next step in the wTA synthesis is performed by another membrane enzyme TagA, which couples a ManNAc moiety from UDP-ManNAc to Lipid α to produce Lipid β [15]. The third membrane enzyme TagB catalyzes an sn-glycerol-3-phosphate unit from CDP-glycerol to Lipid β to form Lipid $\phi.1$ [16]. Then, a polymer of sn-glycerol-3-phosphate units is assembled on this lipid by the fourth enzyme TagF [17]. The polymerized Lipid $\phi.n$ is decorated with glucose units by TagE and then it is flipped to the external leaflet of the cell membrane by TagGH [18, 19]. At last, the wTA polymer is transferred to PG which is done by TagTUV [1, 20]. Like in the peptidoglycan synthesis pathway, C55-p will be recycled to become available for another cycle.

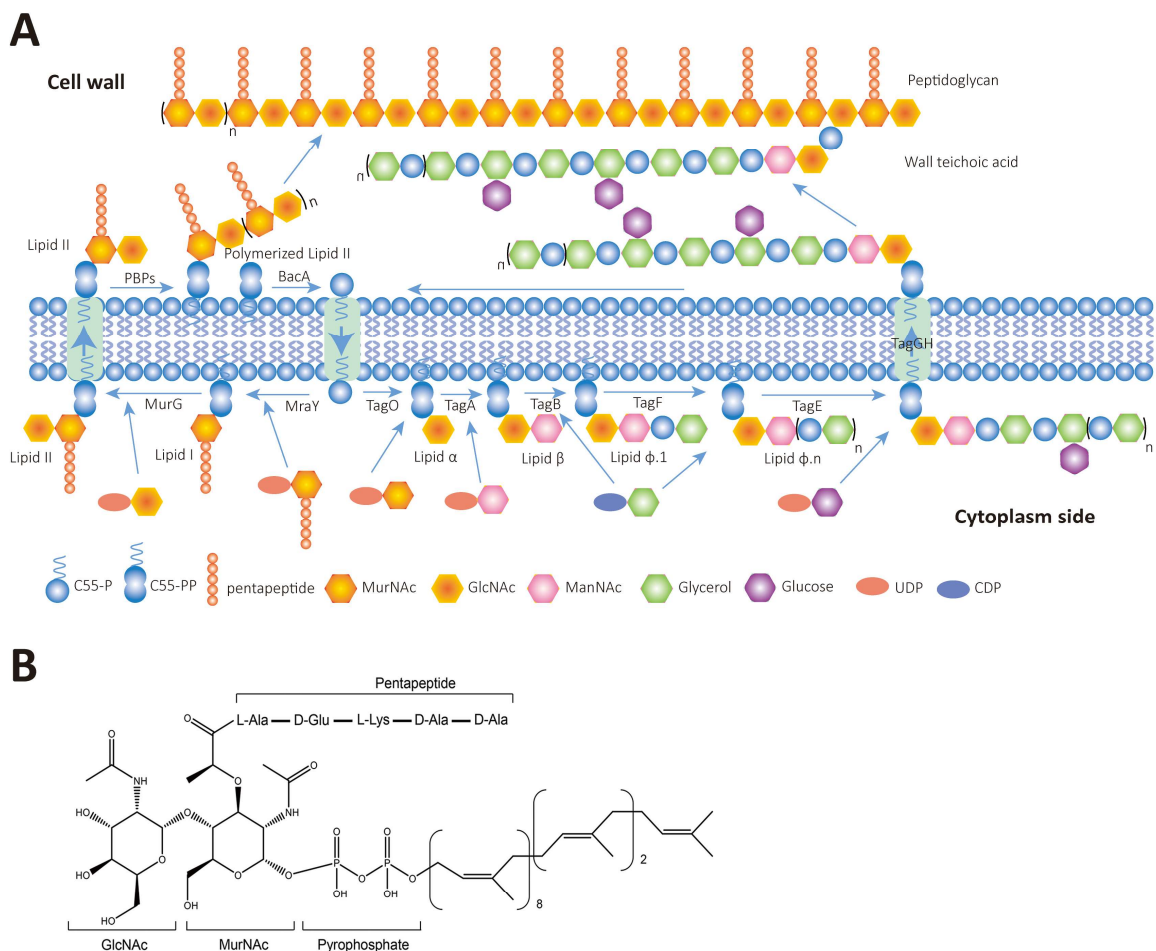


Figure 1. (A) Membrane steps of bacterial cell wall synthesis pathway. (B) Chemical structure of Lipid II. This figure is modified from [13, 21].

1.2 Lantibiotics

In the microbial world the continuous struggle for survival has led to the evolution of secreted peptides, proteins and other compounds that are able to inhibit the growth of

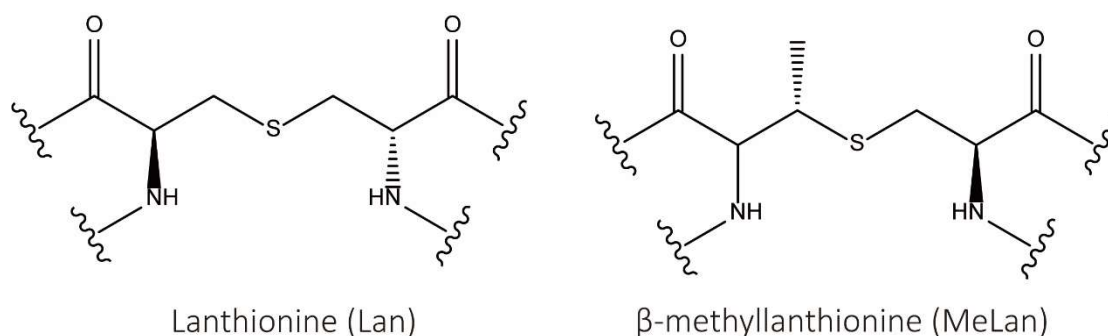


Figure 2. The chemical structure of lanthionine (Lan) and β -methylanthionine (MeLan).

or even kill competitors. These peptides and proteins are, by virtue of their activity, called bacteriocins. The first bacteriocin, Colicin V, was found in 1925 and ever since bacteriocins have been continuously discovered [22, 23]. The first lantibiotic, nisin, was discovered in 1928 [24] and much later, in 1971, its structure was determined [25]. Many more lantibiotics have been discovered since and they have their own class within the bacteriocins (Class I) [26]. The most distinguishing features of the lantibiotics are the thioether-linked rings and the dehydrated amino acids, which are introduced in the peptides post-translationally. The typical thioether linkages, provided by the lanthionine (Lan) or β -methylanthionine (MeLan) have first been found in wool, which is why this family of peptides has been called lantibiotics, derived from the Latin word *lana* (wool) [27] (Fig. 2). Lantibiotics are ribosomally synthesized and mostly produced by gram-positive bacteria [27, 28]. Their post-translational modifications are essential for antimicrobial activity. Lantibiotics are active against antibiotic-resistant bacteria such as methicillin-resistant *S. aureus* (MRSA) and vancomycin-resistant enterococci (VRE), thus they are considered promising candidates to deal with the antibiotic-resistance problem. Furthermore, lantibiotics have great potential for application as food additives and veterinary medicine as they are active against food borne pathogens such as *Listeria monocytogenes*, *Salmonella typhimurium* and *S. aureus*. Nisin, the most well studied lantibiotic, is the only one commercialized in pure form as food preservative and in animal care products to date [29]. The elucidation of the mode of action of nisin has taught us that the low, nanomolar range, minimum inhibitory concentration (MIC) of lantibiotics against pathogens often involves a specific target [30], to which the lantibiotics bind with high affinity. Studying the antimicrobial mechanisms of lantibiotics helps us to understand how they kill, and can possibly provide us with novel ways to tackle important pathogens.

Among the lantibiotics, compounds have been found that do not possess antimicrobial activity but serve other purposes [31-33]. Hence the term lanthipeptides was coined for these type of peptides [34]. Lantibiotics are sub-divided into a type-A and a type-B group. Type-A lantibiotics are positively charged peptides with an elongated shape whereas type-B lantibiotics are neutral or negatively charged peptides with a more globular shape [27]. Besides these differences in charge and shape, type-A and type-B lantibiotics are differently post-translationally modified. In principle, these modifications performed by a series of enzymes, are necessary to obtain full antibiotic activity. The lantibiotic biosynthetic genes are situated in a single gene cluster that is responsible for the lantibiotics' production, modification, export, regulation of expression and self-immunity. The precursor peptides of lantibiotics referred to as pre-peptides are encoded by the *lanA* genes [35]. These precursors contain a leader peptide at the N-terminus, rendering them biologically inactive [27]. The pre-peptides need to be modified by dehydration and cyclization to introduce the dehydrated amino acids and the Lan/MeLan rings. These modifications are performed by the dehydratase LanB and the cyclase Lan C for the type-A lantibiotics, and by the bi-functional enzyme LanM (for both activities) for the type B lantibiotics [36]. Proteases that remove the leader peptide of the lantibiotics and the proteins responsible for the secretion also differ between the type-A and type-B lantibiotics. For type-A lantibiotics, the ATP-binding cassette (ABC) transport protein LanT secretes leader peptide attached lantibiotics, which is followed by cleavage of the leader peptide extracellularly by the serine protease LanP [37, 38]. For type-B lantibiotics, proteolysis and secretion are mediated by the bifunctional enzyme LanP, which is a transport protein containing a proteolytic domain [36]. The gene encoding the protease is sometimes found outside the *lan*-gene cluster. For instance, there is no protease gene in the gene cluster of the strain producing subtilin, although its leader peptide is removed, suggesting that the leader peptide of this lantibiotic is cleaved by another protease [39]. Removal of the leader can also be done by a protease before the lantibiotics are secreted (e.g., cinnamycin) [37, 40]. In addition to the genes involved in processing, regulatory genes and self-immunity genes are important for the production of lantibiotics. The two-component regulation system LanKR is often found in both type-A and type-B producing strains [41]. The histidine kinase LanK functions as a receptor and the transcriptional regulator LanR works as a response regulator for the production of lantibiotics [42]. The products of the three genes *lanEFG* together form an ABC-like transporter that is responsible for active extrusion of the lantibiotics from the membrane, thus keeping the concentration at the membrane of the lantibiotic below a certain threshold [43]. Additionally, bacteria producing lantibiotics such as pep5, cytolysin and lactocin S require protection by LanI [27, 44-47]. The LanI protein is present mostly at the external leaflet of the plasma membrane where it is anchored to the membrane either by a lipid anchor (e.g. for Spal and Nisl) or via one or more transmembrane

segments (e.g. PepI and LtnI). There are several mechanisms postulated how the LanI proteins protect the producing cell from the action of the lantibiotic [48, 49]. For instance, NisI, the immunity lipoprotein of nisin, has been shown to bind to nisin thereby preventing nisin from killing the cell [48]. The immunity mechanism of PepI, the immunity protein of pep5, is still unknown. The potential target of pep5 is assumed to be on the membrane, and is likely an anionic compound considering the highly positively charged nature of pep5. PepI also contains 8 positive charged amino acids in a C-terminal domain of 20 amino acids, hence it was postulated that PepI protects the producing cell from pep5 by preventing the interaction with its target [49].

1.2.1 Two types of lantibiotic-Lipid II binding motifs

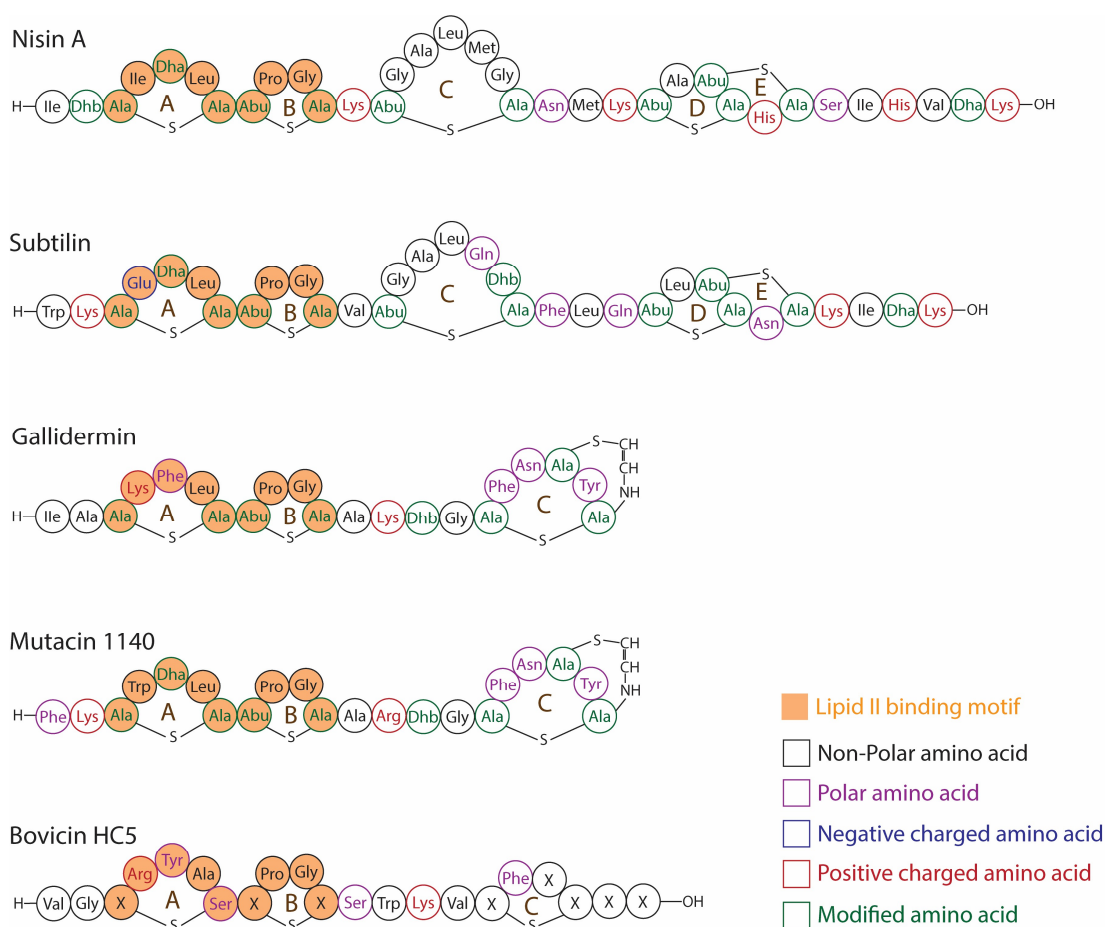


Figure 3. Lantibiotics of the nisin group that bind to Lipid II. Structures of the lantibiotics nisin A, subtilin, gallidermin, mutacin 1140, NAI-107 and bovicin HC5. NAI-107 has two congeners namely HO-Pro14 and di HO-Pro14. Some of the amino acids in bovicin HC5 are not identified yet, and are marked with an X. The lipid II binding motif is highlighted in orange.

The most common target for lantibiotics is the polyisoprenoid-linked cell wall precursor Lipid II [30] (Fig. 1B). Two different Lipid II-binding modes can be distinguished within the lantibiotics family, namely the pyrophosphate cage formed by the A/B-ring system of nisin and related lantibiotics (Fig. 3) and the mersacidin type of binding mode that is also present in the lactacin 481 group (Fig. 4) as well as in the two-component lantibiotics lactacin 3147 and haloduricin (Fig. 5). Nisin, the most well-known lantibiotic, uses Lipid II as an anchor molecule to form pores in the target cell's membrane [50-52]. The A and B rings of nisin form a pyrophosphate cage and bind to the pyrophosphate moiety of Lipid II, forming nisin-Lipid II complexes. The D and E rings of nisin are important for insertion and pore-formation in the membrane leading to cell death [50, 53, 54]. So far, all the lantibiotics that have similar A/B-ring systems, like mutacin 1140, gallidermin, epidermin, subtilin, NAI107 and bovicin HC5, have been shown to target Lipid II (Fig. 3) [55-59].

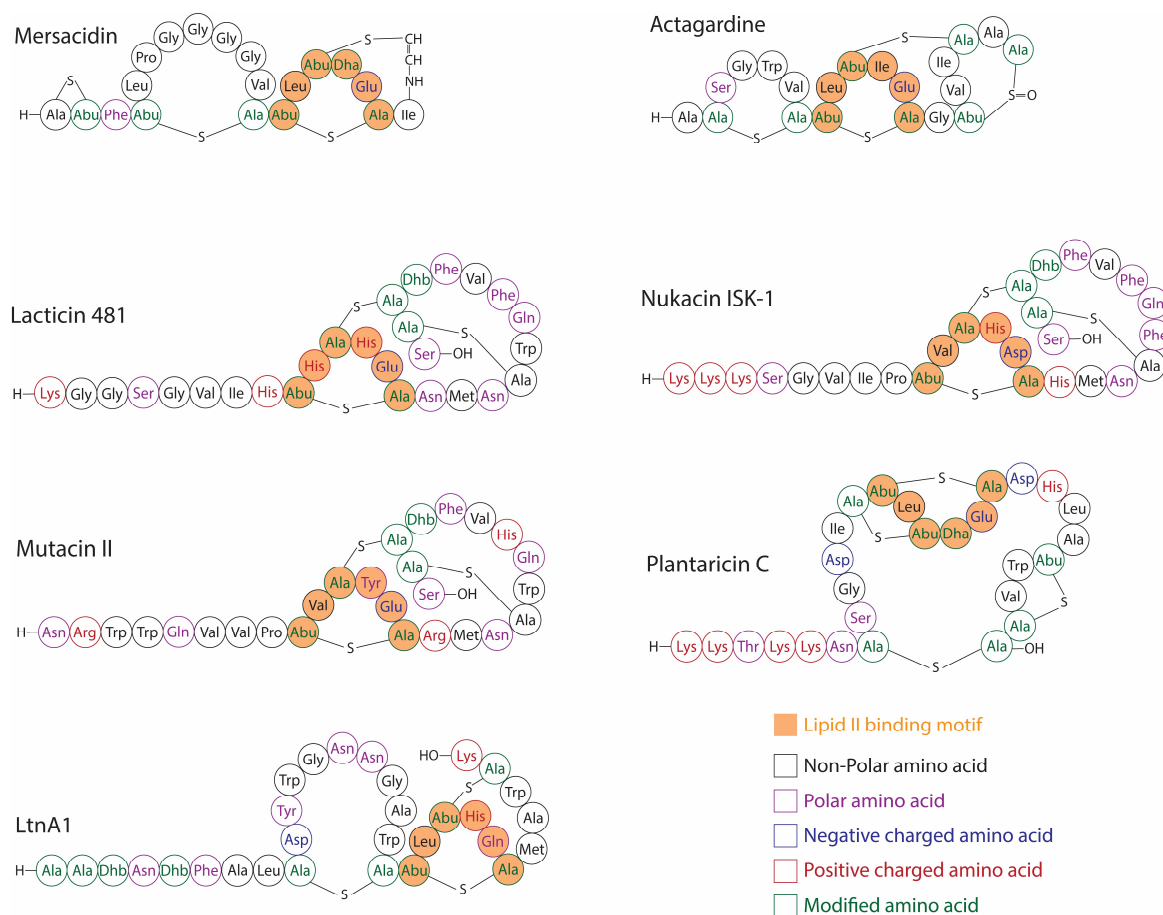


Figure 4. Lantibiotics that bind to Lipid II of the mersacidin group. Structures of the lantibiotics mersacidin group (mersacidin, actagardine), lactacin 481 group (lactacin 481, nukacin ISK-1, mutacin II), plantaricin C, LtnA1 of lactacin 3147, Hal α of haloduricin. The lipid II binding motif is highlighted in orange.

Lantibiotics from the mersacidin-group bind to Lipid II differently. Mersacidin was shown to also require the GlcNAc for binding and thus binds the complete headgroup of Lipid II [60], pp-MurNAc(pentapeptide)-GlcNAc, whereas for nisin Lipid I (lacking the GlcNAc sugar) is sufficient [61]. The lantibiotics from this group do not induce membrane leakage but rather inhibit cell wall synthesis by binding to Lipid II [62]. Notable is the presence of a negatively charged glutamate or aspartate in the conserved motif with which these lantibiotics bind to Lipid II (Fig. 4). The presence of this glutamate was shown to be essential as mersacidin was inactivated when Glu17 was replaced with Ala17 [63]. The essential role of this glutamate explains the requirement for Ca^{2+} for maximal activity, where a calcium ion is likely necessary for bridging the negatively charged pyrophosphate group of Lipid II to the negative charge of the glutamate side chain [60, 64].

An interesting combination of the two ways lantibiotics use Lipid II to kill bacteria is found in the two-peptide lantibiotics lactacin 3147 (LtnA1 and LtnA2) and haloduracin (Fig. 5) [65, 66]. The LtnA1 and Hal α peptides contain a mersacidin-like Lipid II binding motif and thus bind to Lipid II. However, this interaction does not lead to permeabilization of the target membrane. Only in the presence of the partner peptides (LtnA2 or Hal β) permeabilization of the membrane (presumably by pore-formation) is achieved [66].

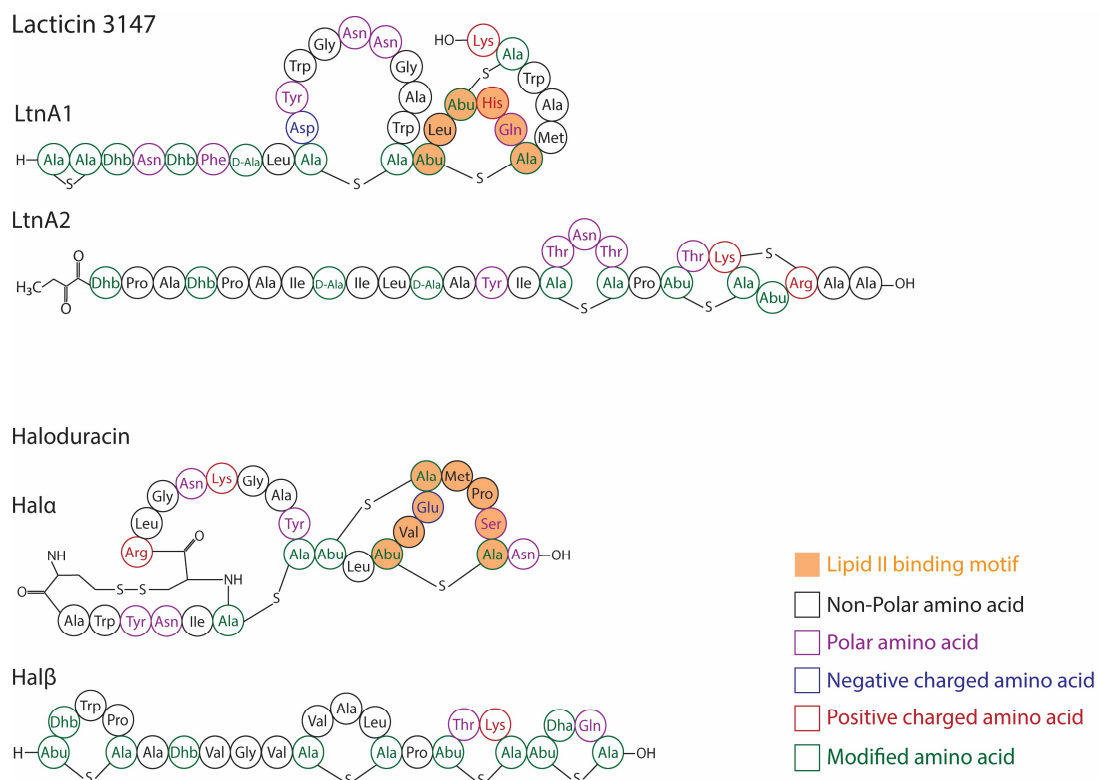


Figure 5. Two-peptide lantibiotics. Structures of the lactacin 3147 (LtnA1 and LtnA2), haloduracin (Hala and Hal β). The lipid II binding motif is highlighted in orange.

In addition to lantibiotics that bind to Lipid II, there are lantibiotics that have quite different modes of action. Some of these lantibiotics kill bacteria even more efficient than nisin and their antimicrobial mechanisms do not involve Lipid II, as will be discussed below.

1.2.2 Cinnamycin group lantibiotics (cinnamycin, duramycin, duramycin B, duramycin C and ancovenin)

Lantibiotics from the cinnamycin group are probably better known for their property of specifically binding to the phospholipid phosphatidylethanolamine (PE) than for their antimicrobial abilities. Cinnamycin, also named Ro 09-0198, was first isolated in 1952 and later others were found with a similar structure [67-70]. These lantibiotics are mainly produced by *Streptomyces* spp. and contain 19 amino acids, one Lan and two MeLan residues (Fig. 6) [69]. Cinnamycin, duramycin, duramycin B, and duramycin C have a special lysinoalanine (Lal) bridge between Ala6 and Lys19 and an erythro-3-hydroxy-L-aspartic acid at position 15 which is important for their antimicrobial activity [71]. This lysinoalanine bridge was not reported for ancovenin [72], but given the high structural resemblance of the peptides in this group it is likely that this bridge is present also in this peptide (Fig. 6).

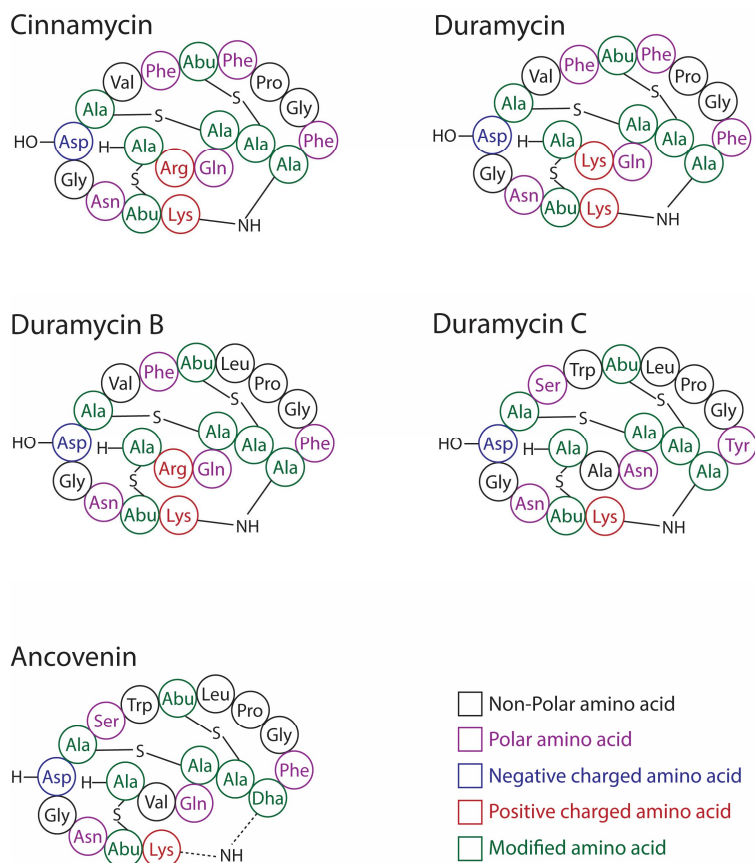


Figure 6. Cinnamycin group lantibiotics. Structures of the lantibiotics cinnamycin, duramycin, duramycin B, duramycin C and ancovenin.

Duramycin displays MICs in the range of 2–3.75 μM against *Bacillus* spp., 1.7 μM against *Paenibacillus* BC26, and it acts against *Herbospifillum* YR522, *Variovorax* CF313, *Chryseobacterium* CF314 G, *Sphingobium* AP49 with MICs of 17.5, 20, 21, 32.5 μM , respectively [73]. It also shows broad range activity against gram-negative bacteria, which may relate to its antimicrobial mechanism since PE is commonly present in relatively high amounts in both the outer and the plasma membrane of gram-negative bacteria.

The antimicrobial mechanism of the cinnamycin group lantibiotics is related to their ability to bind to PE at a 1:1 stoichiometry with high affinity [71, 74]. This property is also likely the cause of the interest for these peptides in fields unrelated to infectious diseases. Duramycin forms ion channels in both artificial and biological membranes and was reported to enhance chloride secretion in airway epithelium [75, 76]. Thanks to the latter property, it has entered clinical trials to relieve the burden of cystic fibrosis in patients [77].

Ancovenin was actually discovered in a screen that was set up to identify inhibitors of the angiotensin I converting enzyme which is a membrane-bound peptidyl dipeptidase [70, 78]. This may be related to the ancovenin-PE binding as well. Duramycins also show broad-spectrum inhibition of viral entry into mammalian cells [79]. Because of the PE-specific targeting of the peptides from the cinnamycin group, they have been labeled fluorescently or with other tracers and employed to study the localization of PE in eukaryotic membranes [80]. In view of their overall performance in the above-described areas it's likely that the application of this lantibiotic group will eventually be restricted to PE-localization studies.

1.2.3 Lactocin S

Lactocin S (3761.9 Da) produced by *Lactobacillus sakei* L45, was first isolated in 1989, and its amino acid sequence was determined in 1991 [81, 82]. It is encoded on the 50 kb plasmid pCIM1, which has been reported to be unstable and easily lost during bacterial reproduction [83, 84]. We had the same experience in our attempts to purify this lantibiotic (unpublished observations). Lactocin S is a lantibiotic of 36 amino acids with a relatively low amount of modifications with a lactate group blocking the N-terminus and containing the typical lantibiotic-related residues (Fig. 7). Notably, the peptide contains three D-Ala residues, which are post-translationally converted from L-serines of the pre-peptide [85]. Lactocin S contains 2 positively and 2 negatively charged amino acids. Additionally, it contains 2 histidine residues at ring B, which will render the peptide positively charged at pH conditions below the pKa of histidine (6.0) [86]. So far no homolog of lactocin S has been identified or characterized, making this a unique molecule within the lantibiotics family.

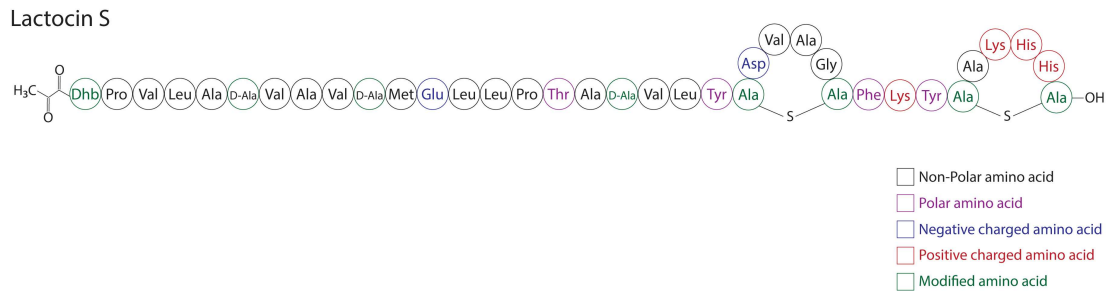


Figure 7. Structure of the lantibiotic lactocin S.

Lactocin S displays MICs in the range of 0.038–0.36 $\mu\text{g/ml}$ (10–96 nM) against lactic acid bacteria (LAB), 0.39–1.2 $\mu\text{g/ml}$ (103–319 nM) against *Staphylococcus* spp., 0.49–0.74 $\mu\text{g/ml}$ (130–197 nM) against *Listeria* spp., 0.43 $\mu\text{g/ml}$ (114 nM) against *E. faecalis* EF, and 2.0 $\mu\text{g/ml}$ (532 nM) against *B. cereus* [87]. Furthermore, lactocin S inhibits a broad range of food-borne pathogens. *Lactobacillus sakei* L45 is generally considered as safe for food products and is also used as a probiotic. Lantibiotic-producing lactic acid bacteria such as *L. sakei* L45 have probably their highest potential in food fermentation and preservation.

Likely due to the presence of the histidines, lactocin S only shows antimicrobial activity at pH values below 6.0, pointing to the importance of a positively charged C-terminal ring-system. Lactocin S and derived analogues have been fully synthesized chemically by the group of Vederas [82]. This allowed the first structure-activity study of this lantibiotic that showed that the antimicrobial activity of lactocin S was enhanced when the thioether bond of ring A was replaced by a methylene [88]. However, a similar replacement in ring B significantly reduced the activity [88]. These results together with the pH dependency of the activity point to an important role of ring B in the mode of action of this peptide. The low MIC towards LABs indicates that lactocin S uses a specific target, which remains to be identified. Considering the bactericidal activity of lactocin S below pH 6, it is likely that the peptide is membrane active.

1.2.4 Paenibacillin, subtilomycin, thuricin A4-4

The paenibacillin group is the lantibiotics group with the most posttranslational modifications per peptide (Fig. 8). Paenibacillin (m/z, 2984.6) is produced by *Paenibacillus polymyxa* OSY-DF and was structurally characterized in 2008 [89, 90]. Subtilomycin (m/z, 3235.6) and thuricin A4-4 (m/z, 2786.3), produced by *Bacillus* spp. were structurally characterized in 2013 and 2015, respectively [91, 92]. Paenibacillin has 30 amino acids and its first N-terminal amino acid is acetylated which is uncommon for lantibiotics [90]. Subtilomycin and thuricin A4-4 consist of 31 and 27 amino acids, respectively, and their N-terminal amino acids are modified with 2-oxo butyrate (Obu) [91, 92]. The structure of the B and C rings of the peptides in this group are similar to

the D and E rings of nisin.

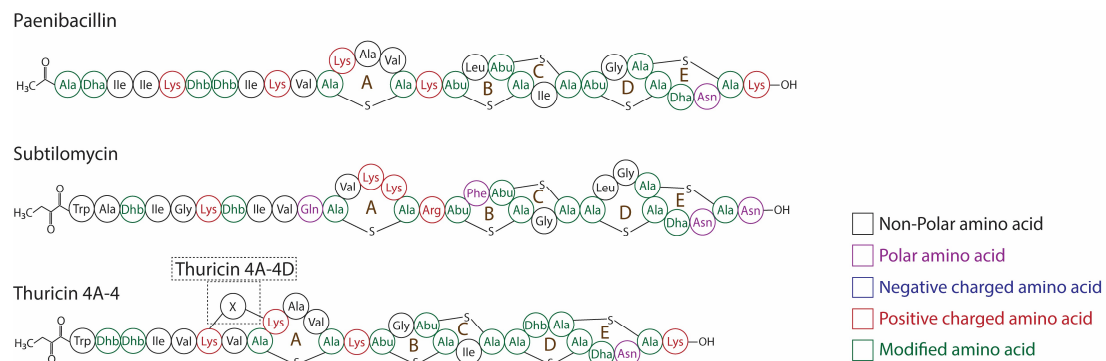


Figure 8. Paenibacillin group of lantibiotics. Structures of the lantibiotics paenibacillin, subtilomycin, thuricin 4A-4.

Paenibacillin displays MICs in the range of < 0.2 – $1.56 \mu\text{M}$ against MRSA, 0.1 – $0.78 \mu\text{M}$ against *E. faecalis* including VRE, and in the micromolar range against pathogenic gram-negative bacteria including those of the ESKAPE-group, i.e. six bacterial pathogens (*Enterococcus faecium*, *S. aureus*, *Klebsiella pneumoniae*, *Acinetobacter baumannii*, *Pseudomonas aeruginosa*, *Enterobacter* spp.) that are highly related to antimicrobial resistance [93]. Subtilomycin exhibits activity against a broad spectrum of gram-positive bacteria such as *B. cereus*, *L. monocytogenes* and *Clostridium sporogenes* [91]. It also inhibits a few gram-negative bacteria but these are less sensitive to subtilomycin compared to the gram-positive bacteria [91]. Thuricin 4A-4 display MICs in the range of 0.326 – $7.8 \mu\text{M}$ against *Bacillus* spp., 1.3 – $1.95 \mu\text{M}$ against *Staphylococcus* spp., but it is inactive against gram-negative bacteria [92].

Paenibacillin shows a higher ability to penetrate the outer membrane of bacteria as compared to nisin at concentrations up to $60 \mu\text{M}$, while it is not haemolytic nor cytotoxic to mammalian cells [93]. These properties led the authors to have high hopes for the paenibacillins “as a scaffold for further development as a next-generation antibacterial drug to fight difficult-to-treat pathogens”, however protease-sensitivity due to the presence of 5 lysines will likely prevent this. Very recently, subtilomycin was shown to act as a masking agent to reduce the defense of *Arabidopsis thaliana* and in effect promotes the (endophytic) colonization in the host plant for the producing strain [94]. Whether this is a general property of this lantibiotic group is unknown, but the producing bacteria (*P. polymyxa* and *B. subtilis*) are both endophytes that live inside plants. This raises a question about the main purpose of these peptides: antimicrobial activity or masking from host defense mechanisms.

1.2.5 Pep5 and epicidin 280

Pep5 (3487.8 ± 0.3 Da) and epicidin 280 (actually two compounds with MW 3133 ± 1.5 Da and 3136.0 ± 1.5 Da) produced by *S. epidermidis*, were discovered in 1989 and 1998, respectively [95-97]. Pep5 and epicidin 280 consist of 33 and 29 amino acids, respectively (Fig. 9). They carry three Lan/MeLan rings, and the spacer between ring A and the rings B and C of epicidin 280 is 3 amino acid residues shorter compared to that of pep5. The N-termini of both peptides are blocked, by an Obu moiety in pep5 and a lactate group in epicidin 280. The 8 positively charged amino acids of pep5 render it the most highly charged peptide of the lantibiotic family. Epicidin 280 exhibits 75% sequence similarity to pep5 and their biosynthetic genes share significant homology as well [98, 99]. This high similarity is probably the reason for the cross-immunity of their producing strains towards each other's peptide.

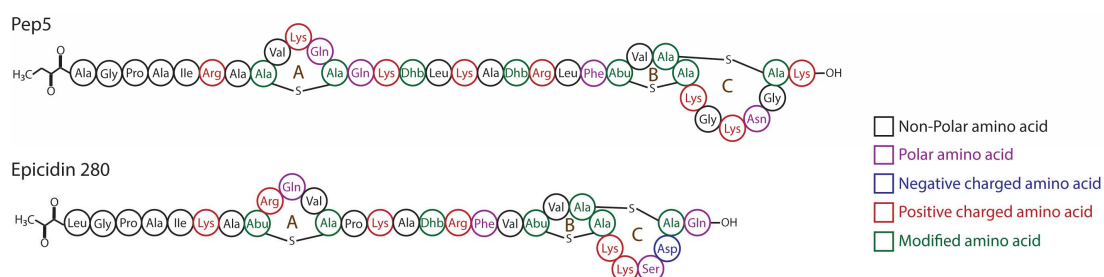


Figure 9. Pep5 group of lantibiotics. Structures of the lantibiotics pep5 and epicidin 280.

Pep5 has a highly selective antibacterial activity and displays MICs in the range of 0.001–19 $\mu\text{g/ml}$ (0.3-5448 nM) against *Staphylococcus spp.* and 1.2 $\mu\text{g/ml}$ (344 nM) against *Micrococcus luteus*. The most active epicidin 280 compound displays higher MICs in the range of 0.175–3.85 $\mu\text{g/ml}$ (55.8-1228 nM) against *Staphylococcus spp.* and 9.7 $\mu\text{g/ml}$ (3093 nM) against *M. luteus* [98]. Especially the low nanomolar MICs against staphylococci make pep5 a highly interesting lantibiotic, as apparently it uses a highly specific target.

Earlier research on the antimicrobial mechanism of pep5 showed that it causes membrane depolarization presumably via pore-formation [100, 101]. However, compared to the MIC values of pep5 against staphylococci and micrococci, the concentrations of pep5 causing membrane depolarization were magnitudes higher. This difference in concentrations suggests that pore-formation may not be the prime antimicrobial mechanism of pep5. High concentrations of cationic antimicrobial peptides tend to form pores in membrane as a barrel-stave, carpet or toroidal-pore, which depends more or less on their amphipathicity and hydrophobicity [102, 103]. In our hands, pep5 had no effect on the membrane potential at 50 \times the MIC and is bacteriostatic (unpublished). This is in line with previous research showing that trypsin

can rescue the growth of bacteria that were pre-treated with pep5, even after several hours [95]. The lack of signature Lipid II-binding domains in the sequence of pep5 argues against Lipid II as its target. Accordingly, pep5 did not cause leakage from Lipid II containing vesicles in vitro [51]. Moreover, pep5 does not interact with Lipid II in vitro (despite its high number of positive charges) as addition of Lipid II did not antagonize pep5 in an agar diffusion assay, whereas a clear inhibitory effect on nisin was observed (Fig. 10). Several pep5 structure-function studies have been performed, which showed that replacing the dehydrated amino acids at position 16 or 20 with an alanine already increased the MICs of very sensitive strains by a factor of 60–90. Incorporation of an extra lanthionine ring in the middle of the peptide abolished the activity of pep5 [104]. In our experience, pep5 is very sensitive to chemical modifications. Specific labeling of the N-terminus (via hydrazine-based coupling) or mild labeling using NHS-based probes destroyed all activity of pep5 (S.F. Oppedijk and E. Breukink, unpublished observations). These properties blocked our attempts to analyze the binding of the peptide to intact cells. There is no information on the antimicrobial mechanism of epicidin 280, thus we cannot compare the modes of action.

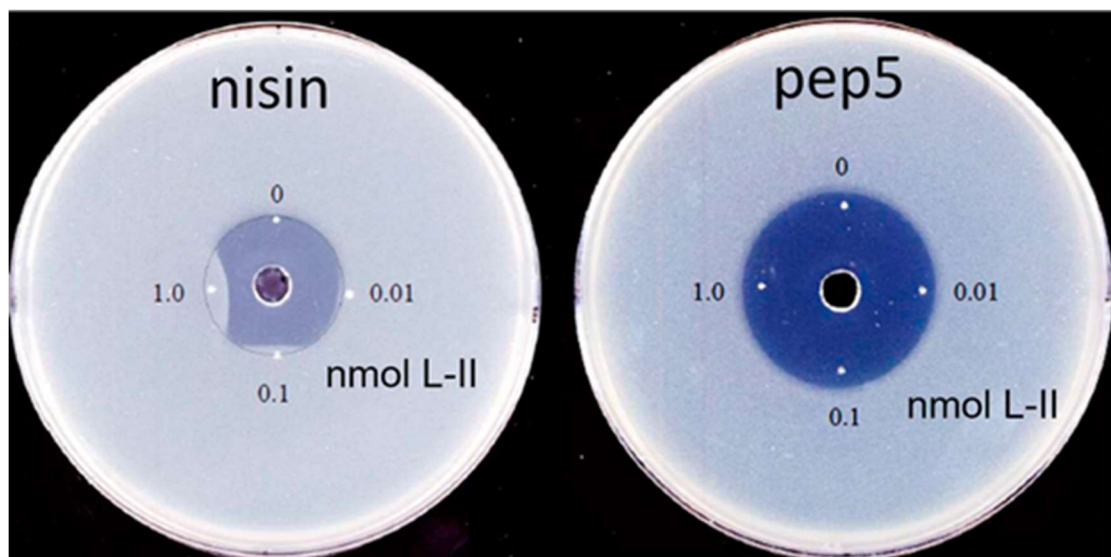


Figure 10. Test for antagonization of pep5 activity by Lipid II. Pep5 and nisin are placed on the agar which is pre-mixed with the indicator strain *Staphylococcus simulans*. Different amounts of Lipid II (0.01–1 nmol) dissolved in 10 mM Tris-HCl pH 7.5, 100 mM NaCl, 0.1% Triton X-100, are spotted on the edge of the (predicted) inhibition halo and incubated overnight at 30°C to allow growth of the indicator strain. The presence of Triton X-100 is to ensure that Lipid II is dissolved properly.

1.2.6 Epilancin group lantibiotics (epilancin 15X epilancin K7 and SWLP1)

Epilancin K7 (3032 ± 1.5 Da), epilancin 15X (3173 Da) and SWLP1 (2999 Da), the main members of this group, are produced by *Staphylococcus* spp. and were discovered in 1995, 2005 and 2009, respectively [105-108]. They share extremely high structural similarity (Fig. 11). Epilancins have a lactate group that blocks the N-terminus of which the specific function remains unknown. Replacement of the lactate with a pyruvate in epilancin 15X resulted in a very minor decrease in antimicrobial activity, which suggest that the nature of this group is not important for the activity. Its function is likely to protect the peptides from degradation by proteases [109, 110]. Besides a lanthionine (Ala12-S-Ala16) they contain a ring B and ring C system that is very similar to the D and E rings of nisin. The peptides have a high number of positively charge amino acids.

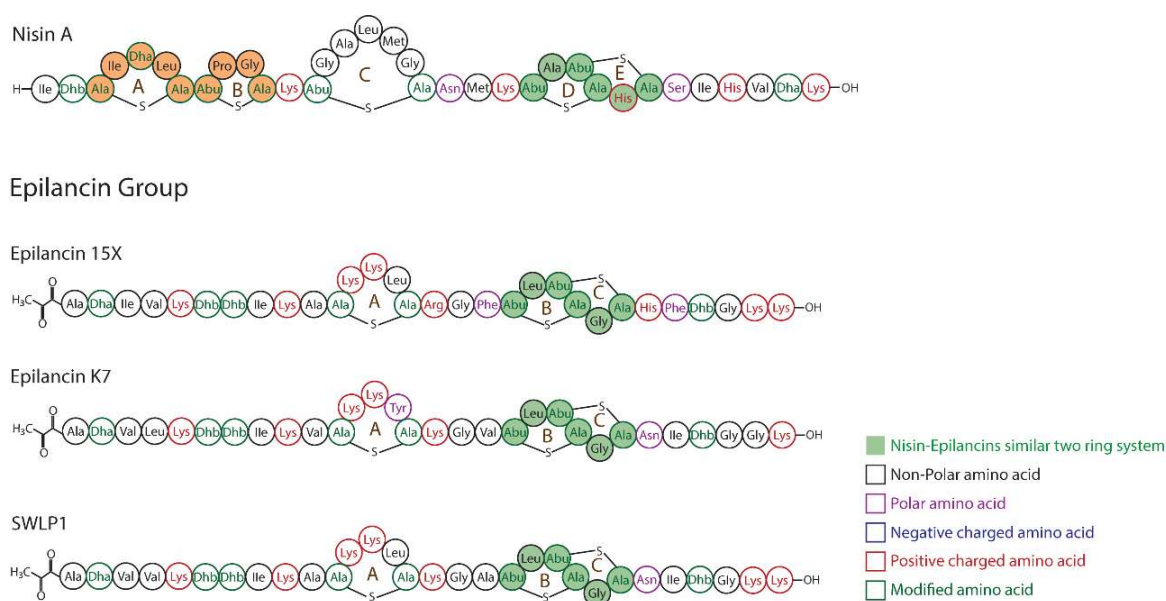


Figure 11. Nisin A and lantibiotics of the epilancin group. Structures of the lantibiotics nisin A, epilancin 15X, epilancin K7 and SWLP1. The lipid II binding motif is highlighted in orange The similar two C-terminal ring systems are highlighted in green.

Epilancin 15X displays MICs in the range of < 0.125–0.5 µg/ml (39-158 nM) against VRE and MRSA, 12.5–50 µg/ml (3.9-15.8 µM) against *Acinetobacter* spp., 0.25–100 µg/ml (0.08-31.5 µM) against *Escherichia. coli* spp., 0.25–1 µg/ml (79-315 nM) against *E. faecalis* spp., < 0.125–1 µg/ml (39-315 nM) against *S. epidermidis* spp. [111]. SWLP1 displays MICs in the range of 32–64 µg/ml (10.7-21.3 µM) against VRE spp., 1.5 µg/ml (0.5 µM) against vancomycin-resistant *S. aureus* spp.(VRSA), < 1–8 µg/ml

(0.3-2.7 μM) against *S. epidermidis* spp., 96 $\mu\text{g/ml}$ (32 μM) against *Klebsiella pneumoniae* [108]. In our hands it turned out that it was essential to remove residual trifluoroacetic acid (TFA) from the preparations after the final HPLC step in order to have maximal peptide activity (X. Wang and E. Breukink, unpublished observations). This may be required for all highly charged lantibiotics that are purified by HPLC using TFA-containing mobile phases.

The epilancins are active towards VRE implying that they target a different binding site than vancomycin. For nisin, the C-terminal part including the rings D and E has been suggested to be important for pore-formation [50]. Hence, the similar structure of the epilancins might be involved in pore-formation as well. This notion is in agreement with the disruption of the membrane potential of intact bacterial cells at relatively low peptide concentrations shown for an epilancin 15X variant [51, 109]. Notably, as is the case for pep5, the epilancins lack a signature Lipid II-binding element in their primary structure. Thus, it is reasonable to assume that the epilancin group lantibiotics do not target Lipid II. Indeed, it was shown for epilancin K7 that it could not induce leakage of contents from model membrane vesicles containing Lipid II [51, 109].

1.2.7 Outlook for lantibiotics

This chapter mainly focused on Lipid II & non-Lipid II targeted lantibiotics other two type of novel Lipid II targeting AMPs. The majority of the lantibiotics bind to Lipid II, which is not so surprising since it is a very good and accessible target that does not easily acquire resistance via mutations changing its structure because it is not gene-encoded. However, resistance that occurs by secreting an enzyme that specifically cleaves nisin has been described [28, 112-114]. We would not be surprised to see more strains obtaining a similar resistance mechanism against other Lipid II-binding lantibiotics, once they are used in the clinic.

Lantibiotics are easily degraded by proteases especially due to the abundant presence of positively charged amino acids, which make them non-ideal candidates for pharmaceutical applications. Yet, there are always exceptions to the rule, e.g. the Lipid II-targeting NAI-107 does not possess any lysine or arginine and was being developed for clinical use by Naicons (current status unknown) [115].

We noticed an interesting structural homology between the lantibiotics groups of which the targets have not been identified yet. Epilancin, pep5 and paenibacillin all have a ring composed of five amino acids (including the lanthionine residue) containing at least one positive charge. This ring is located approximately in the middle of the peptides. Two amino acids upstream of this ring a lysine is present in these peptides and in one case an arginine. At the C-terminal side of this ring there is another lysine or an arginine, but for the pep5 group this lysine is located one position further

downstream. We speculate that these groups may share the same or very similar targets, which would make them quite a substantial group next to the Lipid II-targeting lantibiotics. Whether or not this is true we can only learn by identifying the target of these lantibiotics.

1.3 Two types of other novel AMPs

Besides lantibiotics, many AMPs also have great potential to tackle the antimicrobial resistance problem. Here we introduce two other types of novel AMPs, teixobactins and brevicacillins, which are studied in this thesis.

1.3.1 Teixobactins

Teixobactin (1242.7 Da) is a non-ribosomal peptide antibiotic that was isolated from the gram-negative bacterium *Eleftheria terrae* in 2015 [116]. It is highly modified and contains 11 amino acids including four D-amino acids (D-N-Me-Phe1, D-Gln4, D-allo-Ile5, D-Thr8) and a rare amino acid L-allo-enduracididine at position 10 [116] (Fig. 12). Those D-amino acids and L-allo-enduracididine were shown to be important for antimicrobial activity [117, 118]. Teixobactin has been getting a lot of attention as it barely induces antibiotic resistance in *S. aureus* as well as *Mycobacterium tuberculosis* and shows efficacy towards resistant pathogens [116]. It displays MICs of 0.25 µg/mL (200 nM) against MRSA and MSSA, 0.5 µg/mL (400 nM) against VRE [116]. Structure-activity studies on teixobactin aimed at improving its activity and pharmacokinetic and dynamic properties haven't been focused on the L-allo-enduracididine. Although natural teixobactin is chemically accessible, removing the L-allo-enduracididine would significantly increase this accessibility as this residue is a major bottleneck for chemical synthesis. Replacing the L-allo-enduracididine with leucine or isoleucine did not change the activity of the peptide as identical MIC values against MRSA ATCC 33591 were obtained for these variants compared to the natural peptide [119]. The activity of teixobactin could even be significantly enhanced by replacing the glutamine at position 4 by an arginine (Fig. 12). This double mutant, [R4L10]-teixobactin, displayed lower MICs against MRSA (0.03-0.125 µg/mL, 24-100 nM) and VRE (0.06-0.5 µg/mL, 48-400 nM), and showed to have no cytotoxicity *in vitro* and *in vivo* [120].

Teixobactin inhibits the peptidoglycan and wall teichoic acid biosynthesis pathways by binding to the pyrophosphate part of the peptidoglycan precursor Lipid II and the wall teichoic acid precursor Lipid III in the bacterial membrane [116], which is the main reason why there is low resistance-development towards teixobactin. Solid state NMR results show that teixobactin and [R4L10]-teixobactin assemble into antiparallel β-sheets in the membrane [121, 122]. The antiparallel β-sheet structure is caused by

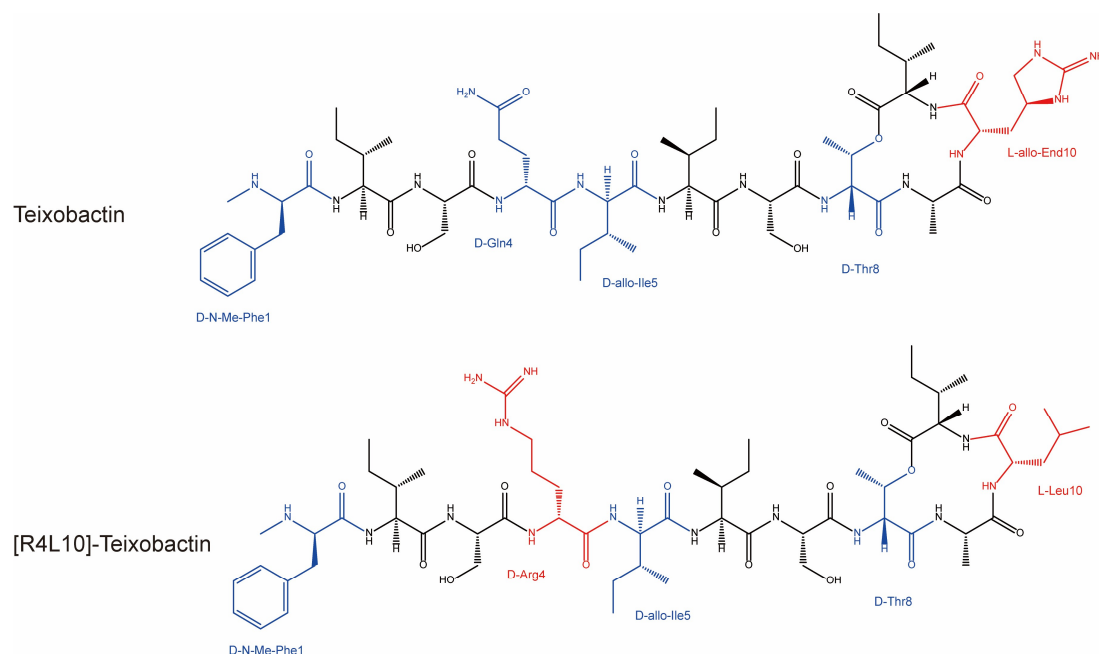


Figure 12. The chemical structure of teixobactin and its analogue [R4L10]-teixobactin. D-amino acids are labeled by blue (except D-Arg4 in [R4L10]-teixobactin) and the replaced amino acids are labeled by red.

teixobactin-Lipid II oligomerization in which the ring motif of teixobactin interacts with the pyrophosphate and MurNAc of Lipid II [121, 122]. The fast oligomerization step (time scale of seconds) follows with a slow cluster formation on a timescale of about 2 to 4 hours [121, 122]. This cluster contains a concentrated hydrophobic patch that results in local thinning of the membrane leading to membrane permeabilization [122]. Furthermore, polyprenyl tails of Lipid II are proposed to be involved in membrane perturbation as well [122].

1.3.2 Brevibacillins (Bogorol family)

Brevibacillin (1583.1 Da) produced by *Brevibacillus laterosporus*, was first isolated and identified in 2016 [123]. It is a non-ribosomal lipo-tridecapeptide antibiotic containing 13 amino acids and an N-terminal 6-Carbon fatty acid chain [123]. Structurally, brevibacillins share high similarity with bogorols and thus are considered as members of bogorol family [123-125]. The structure of bogorol A was elucidated in 2001 by MS and NMR [124]; bogorol A-E and brevibacillins have the following consensus sequence (identical amino acids in bold): fatty acid chain-**Dhb**-Leu/Val/Met- **Orn**-Ile/Val-Val/Ile-**Val-Lys**-Val/Ile-**Leu-Lys-Tyr-Leu-valinol**. In figure 13 the structures of brevibacillin, brevibacillin I, brevibacillin V and brevibacillin 2V are depicted. Their 4th, 5th, 8th amino acids are either Ile or Val, and their conserved cationic amino acids at positions 3(Orn), 7(Lys), and 10(Lys) provide them with an overall positive charge, which is proposed to

be important for their membrane permeabilizing activity [125, 126].

Brevibacillin displays MICs in the range of 1-4 $\mu\text{g}/\text{mL}$ (0.6-2.5 μM) against *B. cereus*, 1-2 $\mu\text{g}/\text{mL}$ (0.6-1.3 μM) against *Listeria spp.*, 1 $\mu\text{g}/\text{mL}$ (0.6 μM) against MRSA, and 4-8 $\mu\text{g}/\text{mL}$ (2.5-5 μM) against VRE [123]. Besides the ability against gram-positive pathogens including antibiotic-resistant bacteria, brevibacillins also have potential to be applied as antitumor drug [127]. Bogorol B-JX was found to inhibit the proliferation of ConA-activated spleen cells and human histiocytic lymphoma cell U-937 at concentration of 5 $\mu\text{g}/\text{mL}$ (3.2 μM) [127].

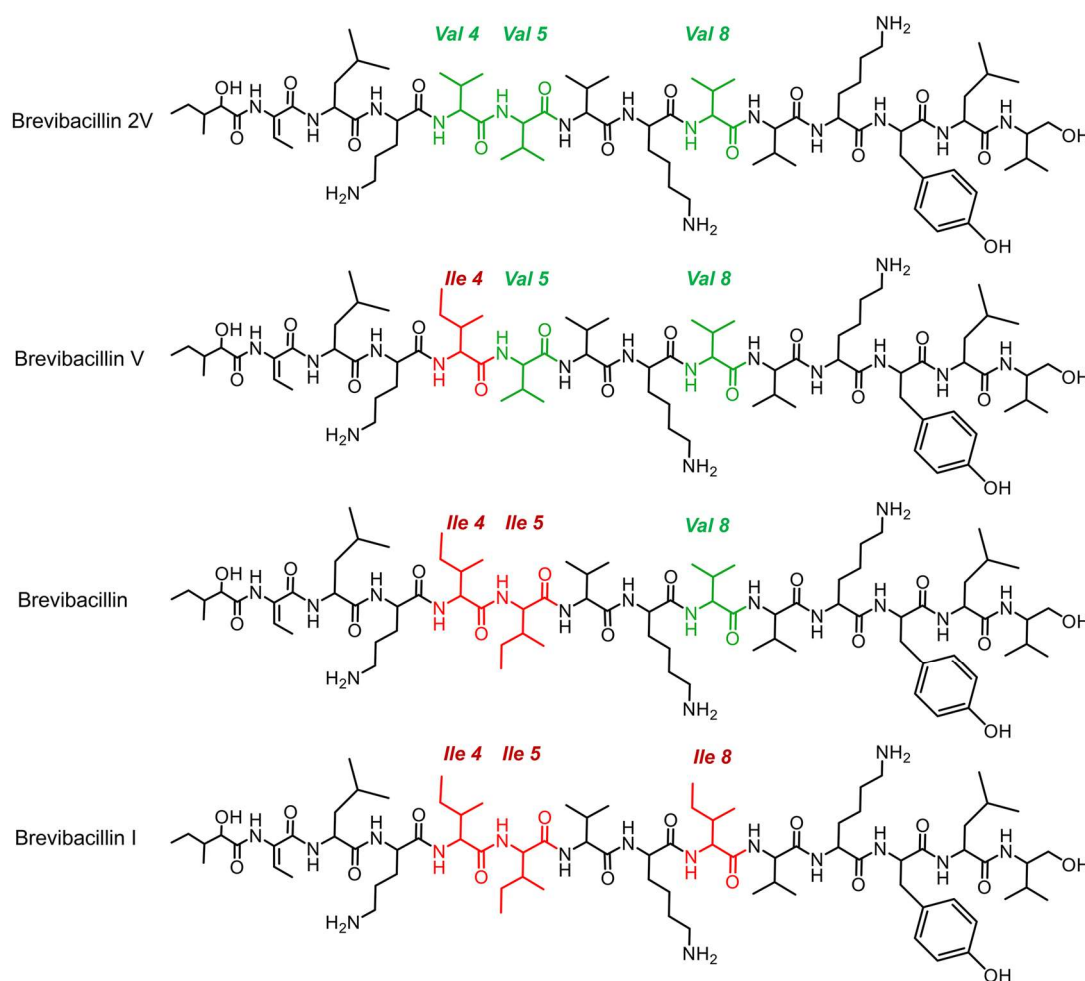


Figure 13. The chemical structure of Brevibacillins [128]. The differences between brevibacillins are labeled by red (Isoleucine, Ile) and green (Valine, Val).

Brevibacillin was found to bind to lipoteichoic acids that are present in the gram-positive cell wall while it didn't cause morphological changes in *S. aureus* [126]. Moreover, it was shown that brevibacillin caused membrane depolarization, K^+ leakage and permeabilizes cytoplasmic membrane of *S. aureus* by three fluoresce probe-based

assays respectively [126].

1.4 Scope of this thesis

The theme of this thesis is centered on studying the mode of action of antimicrobial peptides (AMPs) that have the potential to act against antibiotic-resistant bacteria. **Chapter 2** briefly explains the pH homeostasis, ion homeostasis and ATP synthesis of bacteria and how they affect each other. Protons are pumped out by the respiratory chain to generate a proton gradient (ΔpH) and in order to compensate for ΔpH , ions are taken up which establish a transmembrane electrical potential ($\Delta\psi$). The proton motive force (PMF) composed of ΔpH and $\Delta\psi$ is the driving force of ATP synthesis. Besides, a large number of pumps and channels are responsible for the regulation of protons, ions, and ATP level in bacteria. AMPs commonly target bacterial membranes and induce various membrane effects such as membrane depolarization and pore-formation. These effects inevitably interfere with the homeostasis of bacteria. Studying how antibiotics or AMPs influence bacterial pH homeostasis, ion homeostasis and ATP synthesis helps us understand how AMPs inhibit bacteria and may give novel insight in improving their efficacy. In **Chapter 3**, we used multiple assays and strains to draw an informative picture on the effects of AMPs on the bacterial membranes. Three AMPs (nisin, epilancin 15X, [R4L10]-teixobactin) are tested toward three strains (*S. simulans*, *Micrococcus flavus*, *Bacillus megaterium*), using different fluorescence or luminescence base approaches that measured the AMP's effect on the membrane potential, ATP level, intracellular pH and membrane permeability. This chapter generates a new picture on how AMPs, by targeting the bacterial membranes, interfere with pH and ion homeostasis of bacteria and the corresponding effects on ATP levels and synthesis. It illustrates the importance of always measuring changes in the three coupled phenomena when studying membrane effects of AMPs: pH homeostasis, ion homeostasis and ATP synthesis. In **Chapter 4** we study the mode of action of the lantibiotic epilancin 15X that has nano-molar range activity against *S. simulans*. An antagonism-based experiment pointed towards a possible interaction between epilancin 15X and Lipid II and this was confirmed by Circular Dichroism (CD) based experiments. However, this interaction did not lead to the formation of pores in model membranes. The membrane depolarization assay with intact bacteria showed that treatment of the bacteria by antibiotics known to affect the bacterial cell wall synthesis pathway decreased the effects of epilancin 15X. This suggested that epilancin 15X interferes with a pathway involving polyprenyl lipids. Then, we explored potential targets of epilancin 15X on bacterial membranes with specific focus on pathways involving polyprenyl lipids. The wall teichoic acid pathway is linked to the peptidoglycan biosynthesis pathway as they share undecaprenyl-phosphate as a common precursor. Antibiotics that specifically inhibit the wall teichoic acid synthesis did affect the activity

of epilancin 15X in the membrane depolarization assay. However, a *B. subtilis* TagO deletion mutant which lacks wall teichoic acid precursors was more sensitive to epilancin 15X than the wild type. Thus, wall teichoic acid precursors are not likely to be the target of epilancin 15X. The observed interaction between epilancin 15X with CDP-DAG points to the involvement of a lipid-linked pyrophosphate. Yet, unfortunately, the exact target remains obscure so far. **Chapter 5** studies the mode of action of brevibacillins, a novel class of non-ribosomally produced lipo-tridecapeptides which show potential against antimicrobial resistant bacteria. Brevibacillin and brevibacillin 2V displayed a clear interaction with Lipid II in the agar diffusion assay and the presence of Lipid II induced changes in the secondary structure of the brevibacillins. Moreover, using pyrene-labeled lipid II an interaction of the brevibacillins with Lipid II could also be observed. Brevibacillin and brevibacillin 2V both caused permeabilization of model membranes without the help of Lipid II. Additionally, binding to Lipid II even decreased the membrane permeabilization of brevibacillins in the CF leakage assay. We suggest that brevibacillin and brevibacillin 2V have two independent antimicrobial mechanisms: (1) binding to Lipid II to interfere with cell wall synthesis and (2) membrane permeabilization. Finally, **Chapter 6** summarizes the results and proposes (novel) modes of action of AMPs. New perspectives for further studying antibiotics' mechanism of action are also given.

1.5 References

1. Brown, S., J.P. Santa Maria, Jr., and S. Walker, *Wall teichoic acids of gram-positive bacteria*. Annual review of microbiology, 2013. **67**: p. 313-336.
2. Liu, Y. and E. Breukink, *The Membrane Steps of Bacterial Cell Wall Synthesis as Antibiotic Targets*. Antibiotics, 2016. **5**(3): p. 28.
3. Armstrong, J.J., et al., *882. Isolation and structure of ribitol phosphate derivatives (teichoic acids) from bacterial cell walls*. 1958: p. 4344-4354.
4. Formstone, A., et al., *Localization and interactions of teichoic acid synthetic enzymes in Bacillus subtilis*. J Bacteriol, 2008. **190**(5): p. 1812-21.
5. Brown, S., et al., *Staphylococcus aureus and Bacillus subtilis W23 make polyribitol wall teichoic acids using different enzymatic pathways*. Chem Biol, 2010. **17**(10): p. 1101-10.
6. Chung, B.C., et al., *Crystal structure of MraY, an essential membrane enzyme for bacterial cell wall synthesis*. Science, 2013. **341**(6149): p. 1012-1016.
7. de Kruijff, B., V. van Dam, and E. Breukink, *Lipid II: a central component in bacterial cell wall synthesis and a target for antibiotics*. Prostaglandins, leukotrienes and essential fatty acids, 2008. **79**(3): p. 117-121.
8. Sham, L.T., et al., *Bacterial cell wall. MurJ is the flippase of lipid-linked precursors for peptidoglycan biogenesis*. Science, 2014. **345**(6193): p. 220-2.
9. Mohammadi, T., et al., *Specificity of the transport of lipid II by FtsW in Escherichia coli*. J Biol Chem, 2014. **289**(21): p. 14707-18.
10. Jeong, J.H., et al., *Crystal structures of bifunctional penicillin-binding protein 4 from Listeria monocytogenes*. Antimicrob Agents Chemother, 2013. **57**(8): p. 3507-12.
11. Egan, A.J., et al., *Activities and regulation of peptidoglycan synthases*. Philos Trans R Soc Lond B Biol Sci, 2015. **370**(1679).
12. Manat, G., et al., *Membrane Topology and Biochemical Characterization of the Escherichia coli BacA Undecaprenyl-Pyrophosphate Phosphatase*. PLoS One, 2015. **10**(11): p. e0142870.
13. Sewell, E.W. and E.D. Brown, *Taking aim at wall teichoic acid synthesis: new biology and new leads for antibiotics*. J Antibiot (Tokyo), 2014. **67**(1): p. 43-51.
14. Soldo, B., V. Lazarevic, and D. Karamata, *tagO is involved in the synthesis of all anionic cell-wall polymers in Bacillus subtilis 168*. Microbiology (Reading), 2002. **148**(Pt 7): p. 2079-2087.
15. Zhang, Y.H., et al., *Acceptor substrate selectivity and kinetic mechanism of Bacillus subtilis TagA*. Biochemistry, 2006. **45**(36): p. 10895-904.

16. Bhavsar, A.P., R. Truant, and E.D. Brown, *The TagB protein in Bacillus subtilis 168 is an intracellular peripheral membrane protein that can incorporate glycerol phosphate onto a membrane-bound acceptor in vitro*. J Biol Chem, 2005. **280**(44): p. 36691-700.
17. Schertzer, J.W. and E.D. Brown, *Purified, recombinant TagF protein from Bacillus subtilis 168 catalyzes the polymerization of glycerol phosphate onto a membrane acceptor in vitro*. J Biol Chem, 2003. **278**(20): p. 18002-7.
18. Allison, S.E., et al., *Studies of the genetics, function, and kinetic mechanism of TagE, the wall teichoic acid glycosyltransferase in Bacillus subtilis 168*. J Biol Chem, 2011. **286**(27): p. 23708-16.
19. Lazarevic, V. and D. Karamata, *The tagGH operon of Bacillus subtilis 168 encodes a two-component ABC transporter involved in the metabolism of two wall teichoic acids*. Mol Microbiol, 1995. **16**(2): p. 345-55.
20. Kawai, Y., et al., *A widespread family of bacterial cell wall assembly proteins*. Embo j, 2011. **30**(24): p. 4931-41.
21. D'Elia, M.A., et al., *Probing teichoic acid genetics with bioactive molecules reveals new interactions among diverse processes in bacterial cell wall biogenesis*. Chem Biol, 2009. **16**(5): p. 548-56.
22. Gratia, A., *Sur un remarquable exemple d'antagonisme entre deux souches de coilbacille*. C. R. Seances Soc. Biol. Fil., 1925. **93**: p. 1040-1041.
23. Gratia, J.-P., *André Gratia: A Forerunner in Microbial and Viral Genetics*. Genetics, 2000. **156**(2): p. 471.
24. Rogers, L.A., *THE INHIBITING EFFECT OF STREPTOCOCCUS LACTIS ON LACTOBACILLUS BULGARICUS*. Journal of bacteriology, 1928. **16**(5): p. 321-325.
25. Gross, E. and J.L. Morell, *Structure of nisin*. Journal of the American Chemical Society, 1971. **93**(18): p. 4634-4635.
26. Yang, S.-C., et al., *Antibacterial activities of bacteriocins: application in foods and pharmaceuticals*. Frontiers in Microbiology, 2014. **5**: p. 241.
27. Bierbaum, G. and H.G. Sahl, *Lantibiotics: Mode of Action, Biosynthesis and Bioengineering*. Current pharmaceutical biotechnology, 2009. **10**(1): p. 2-18.
28. Chatterjee, C., et al., *Biosynthesis and Mode of Action of Lantibiotics*. Chemical Reviews, 2005. **105**(2): p. 633-684.
29. Dischinger, J., S. Basi Chipalu, and G. Bierbaum, *Lantibiotics: Promising candidates for future applications in health care*. International Journal of Medical Microbiology, 2014. **304**(1): p. 51-62.

30. Breukink, E. and B. de Kruijff, *Lipid II as a target for antibiotics*. Nature Reviews Drug Discovery, 2006. **5**: p. 321.
31. Kodani, S., et al., *The SapB morphogen is a lantibiotic-like peptide derived from the product of the developmental gene *ramS* in *Streptomyces coelicolor**. Proceedings of the National Academy of Sciences of the United States of America, 2004. **101**(31): p. 11448.
32. Kodani, S., et al., *SapT, a lanthionine-containing peptide involved in aerial hyphae formation in the streptomycetes*. Molecular Microbiology, 2005. **58**(5): p. 1368-1380.
33. Wang, H. and W.A. van der Donk, *Biosynthesis of the Class III Lantipeptide Catenulipeptin*. ACS Chemical Biology, 2012. **7**(9): p. 1529-1535.
34. Goto, Y., et al., *Discovery of unique lanthionine synthetases reveals new mechanistic and evolutionary insights*. PLoS biology, 2010. **8**(3): p. e1000339-e1000339.
35. Bierbaum, G., et al., *The biosynthesis of the lantibiotics epidermin, gallidermin, Pep5 and epilancin K7*. Antonie van Leeuwenhoek, 1996. **69**(2): p. 119-127.
36. Barbosa, J., T. Caetano, and S. Mendo, *Class I and Class II Lanthipeptides Produced by Bacillus spp*. Journal of Natural Products, 2015. **78**(11): p. 2850-2866.
37. Widdick, D., et al., *Cloning and engineering of the cinnamycin biosynthetic gene cluster from Streptomyces cinnamoneus cinnamoneus DSM 40005*. Proceedings of the National Academy of Sciences, 2003. **100**(7): p. 4316-4321.
38. Montalbán-López, M., et al., *Specificity and Application of the Lantibiotic Protease NisP*. Frontiers in microbiology, 2018. **9**: p. 160-160.
39. Schnell, N., et al., *Analysis of genes involved in the biosynthesis of lantibiotic epidermin*. European journal of biochemistry, 1992. **204**(1): p. 57-68.
40. Li, B., et al., *Structure and mechanism of the lantibiotic cyclase involved in nisin biosynthesis*. Science, 2006. **311**(5766): p. 1464-1467.
41. De Ruyter, P., et al., *Functional analysis of promoters in the nisin gene cluster of Lactococcus lactis*. Journal of bacteriology, 1996. **178**(12): p. 3434-3439.
42. Stock, A.M., V.L. Robinson, and P.N. Goudreau, *Two-Component Signal Transduction*. Annual Review of Biochemistry, 2000. **69**(1): p. 183-215.
43. Otto, M., A. Peschel, and F. Götz, *Producer self-protection against the lantibiotic epidermin by the ABC transporter EpiFEG of Staphylococcus epidermidis Tü3298*. FEMS Microbiology Letters, 1998. **166**(2): p. 203-211.
44. Reis, M., et al., *Producer immunity towards the lantibiotic Pep5: identification of the immunity gene *pepI* and localization and functional analysis of its gene product*. Appl. Environ. Microbiol.,

1994. **60**(8): p. 2876-2883.
45. Coburn, P.S., et al., *A Novel Means of Self-Protection, Unrelated to Toxin Activation, Confers Immunity to the Bactericidal Effects of the Enterococcus faecalis Cytolysin*. Infection and immunity, 1999. **67**(7): p. 3339-3347.
46. Skaugen, M., C. Abildgaard, and I. Nes, *Organization and expression of a gene cluster involved in the biosynthesis of the lantibiotic lactocin S*. Molecular and General Genetics MGG, 1997. **253**(6): p. 674-686.
47. Draper, L.A., et al., *Insights into Lantibiotic Immunity Provided by Bioengineering of LtnI*. Antimicrobial agents and chemotherapy, 2012. **56**(10): p. 5122-5133.
48. Khosa, S., M. Lagedroste, and S.H. Smits, *Protein defense systems against the lantibiotic nisin: function of the immunity protein NisI and the resistance protein NSR*. Frontiers in microbiology, 2016. **7**: p. 504.
49. Hoffmann, A., et al., *Localization and functional analysis of Pepl, the immunity peptide of Pep5-producing Staphylococcus epidermidis strain 5*. Applied and environmental microbiology, 2004. **70**(6): p. 3263-3271.
50. Wiedemann, I., et al., *Specific binding of nisin to the peptidoglycan precursor lipid II combines pore formation and inhibition of cell wall biosynthesis for potent antibiotic activity*. Journal of Biological Chemistry, 2001. **276**(3): p. 1772-1779.
51. Brötz, H., et al., *Role of lipid-bound peptidoglycan precursors in the formation of pores by nisin, epidermin and other lantibiotics*. Molecular Microbiology, 1998. **30**(2): p. 317-327.
52. Breukink, E., et al., *Use of the cell wall precursor lipid II by a pore-forming peptide antibiotic*. Science, 1999. **286**(5448): p. 2361-2364.
53. Hsu, S.-T.D., et al., *The nisin–lipid II complex reveals a pyrophosphate cage that provides a blueprint for novel antibiotics*. Nature Structural & Molecular Biology, 2004. **11**: p. 963.
54. Breukink, E. and B. de Kruijff, *The lantibiotic nisin, a special case or not?* Biochimica et Biophysica Acta (BBA) - Biomembranes, 1999. **1462**(1–2): p. 223-234.
55. Smith, L., et al., *Elucidation of the Antimicrobial Mechanism of Mutacin 1140*. Biochemistry, 2008. **47**(10): p. 3308-3314.
56. Bonelli, R.R., et al., *Insights into in vivo activities of lantibiotics from gallidermin and epidermin mode-of-action studies*. Antimicrob Agents Chemother, 2006. **50**(4): p. 1449-57.
57. Parisot, J., et al., *Molecular mechanism of target recognition by subtilin, a class I lanthionine antibiotic*. Antimicrob Agents Chemother, 2008. **52**(2): p. 612-8.
58. Donadio, S., et al., *Sources of novel antibiotics—aside the common roads*. Applied Microbiology and Biotechnology, 2010. **88**(6): p. 1261-1267.

59. Paiva, A.D., E. Breukink, and H.C. Mantovani, *Role of lipid II and membrane thickness in the mechanism of action of the lantibiotic bovicin HC5*. Antimicrobial agents and chemotherapy, 2011. **55**(11): p. 5284-5293.
60. Brötz, H., et al., *The lantibiotic mersacidin inhibits peptidoglycan synthesis by targeting lipid II*. Antimicrob Agents Chemother, 1998. **42**(1): p. 154-60.
61. 't Hart, P., et al., *New Insights into nisin's Antibacterial Mechanism Revealed by Binding Studies with Synthetic Lipid II Analogues*. Biochemistry, 2016. **55**(1): p. 232-237.
62. Brötz, H., et al., *Mode of action of the lantibiotic mersacidin: inhibition of peptidoglycan biosynthesis via a novel mechanism?* Antimicrobial agents and chemotherapy, 1995. **39**(3): p. 714-719.
63. Uguen, P., et al., *Maturation by LctT is required for biosynthesis of full-length lantibiotic lactacin 481*. Applied and environmental microbiology, 2005. **71**(1): p. 562-565.
64. Böttiger, T., et al., *Influence of Ca(2+) ions on the activity of lantibiotics containing a mersacidin-like lipid II binding motif*. Appl Environ Microbiol, 2009. **75**(13): p. 4427-34.
65. Wiedemann, I., et al., *The mode of action of the lantibiotic lactacin 3147 – a complex mechanism involving specific interaction of two peptides and the cell wall precursor lipid II*. Molecular Microbiology, 2006. **61**(2): p. 285-296.
66. Oman, T.J. and W.A. van der Donk, *Insights into the mode of action of the two-peptide lantibiotic haloduracin*. ACS chemical biology, 2009. **4**(10): p. 865-874.
67. Benedict, R.G., et al., *Cinnamycin, an antibiotic from Streptomyces cinnamoneus nov. sp.* Antibiotics & chemotherapy (Northfield, Ill.), 1952. **2**(11): p. 591-594.
68. Shotwell, O.L., et al., *Antibiotics against plant disease. III. Duramycin, a new antibiotic from Streptomyces cinnamomeus forma azacoluta2*. Journal of the American Chemical Society, 1958. **80**(15): p. 3912-3915.
69. ZIMMERMANN, N., et al., *Solution structures of the lantibiotics duramycin B and C*. European journal of biochemistry, 1993. **216**(2): p. 419-428.
70. Kido, Y., et al., *Isolation and characterization of ancovenin, a new inhibitor of angiotensin I converting enzyme, produced by actinomycetes*. The Journal of antibiotics, 1983. **36**(10): p. 1295-1299.
71. Märki, F., et al., *Mode of action of the lanthionine-containing peptide antibiotics duramycin, duramycin B and C, and cinnamycin as indirect inhibitors of phospholipase A2*. Biochemical pharmacology, 1991. **42**(10): p. 2027-2035.
72. Wakamiya, T., et al., *The structure of ancovenin, a new peptide inhibitor of angiotensin I converting enzyme*. Tetrahedron Letters, 1985. **26**(5): p. 665-668.

73. Hasim, S., et al., *Elucidating Duramycin's Bacterial Selectivity and Mode of Action on the Bacterial Cell Envelope*. *Frontiers in Microbiology*, 2018. **9**(219).
74. Zhao, M., Z. Li, and S. Bugenhagen, *99mTc-labeled duramycin as a novel phosphatidylethanolamine-binding molecular probe*. *Journal of Nuclear Medicine*, 2008. **49**(8): p. 1345-1352.
75. Cloutier, M.M., et al., *Duramycin enhances chloride secretion in airway epithelium*. *American Journal of Physiology-Cell Physiology*, 1990. **259**(3): p. C450-C454.
76. Sheth, T.R., et al., *Ion channel formation by duramycin*. *Biochimica et Biophysica Acta (BBA)-Biomembranes*, 1992. **1107**(1): p. 179-185.
77. Grasemann, H., et al., *Inhalation of Moli1901 in Patients With Cystic Fibrosis*. *Chest*, 2007. **131**(5): p. 1461-1466.
78. Riordan, J.F., *Angiotensin-I-converting enzyme and its relatives*. *Genome biology*, 2003. **4**(8): p. 225-225.
79. Huo, L., et al., *Insights into the Biosynthesis of Duramycin*. *Applied and environmental microbiology*, 2017. **83**(3): p. e02698-16.
80. Zhao, M., *Lantibiotics as probes for phosphatidylethanolamine*. *Amino acids*, 2011. **41**(5): p. 1071-1079.
81. Mørtvedt, C., et al., *Purification and amino acid sequence of lactocin S, a bacteriocin produced by Lactobacillus sake L45*. *Applied and Environmental Microbiology*, 1991. **57**(6): p. 1829-1834.
82. Ross, A.C., et al., *Synthesis of the Lantibiotic Lactocin S Using Peptide Cyclizations on Solid Phase*. *Journal of the American Chemical Society*, 2010. **132**(2): p. 462-463.
83. Ahn, C. and M.E. Stiles, *Plasmid-associated bacteriocin production by a strain of Carnobacterium piscicola from meat*. *Applied and environmental microbiology*, 1990. **56**(8): p. 2503-2510.
84. Mortvedt-Abildgaa, C., et al., *Production and pH-Dependent Bactericidal Activity of Lactocin S, a Lantibiotic from Lactobacillus sake L45*. *Applied and Environmental Microbiology*, 1995. **61**(1): p. 175-179.
85. Skaugen, M., et al., *In vivo conversion of L-serine to D-alanine in a ribosomally synthesized polypeptide*. *Journal of Biological Chemistry*, 1994. **269**(44): p. 27183-27185.
86. Nes, I.F., et al., *Lactocin S, a lanthionine-containing bacteriocin isolated from Lactobacillus sake L45*, in *Bacteriocins of lactic acid bacteria*. 1994, Springer. p. 435-449.
87. Cintas, L.M., et al., *Comparative antimicrobial activity of enterocin L50, pediocin PA-1, nisin A and lactocin S against spoilage and foodborne pathogenic bacteria*. *Food Microbiology*, 1998. **15**(3): p. 289-298.

88. Ross, A.C., S.M. McKinnie, and J.C. Vederas, *The synthesis of active and stable diaminopimelate analogues of the lantibiotic peptide lactocin S*. Journal of the American Chemical Society, 2012. **134**(4): p. 2008-2011.
89. He, Z., et al., *Isolation and Identification of a *Paenibacillus polymyxa* Strain That Coproduces a Novel Lantibiotic and Polymyxin*. Applied and Environmental Microbiology, 2007. **73**(1): p. 168.
90. Huang, E. and A.E. Yousef, *Biosynthesis of paenibacillin, a lantibiotic with N-terminal acetylation, by Paenibacillus polymyxa*. Microbiological Research, 2015. **181**: p. 15-21.
91. Phelan, W.R., et al., *Subtilomycin: A New Lantibiotic from Bacillus subtilis Strain MMA7 Isolated from the Marine Sponge Haliclona simulans*. Marine Drugs, 2013. **11**(6).
92. Xin, B., et al., *The Bacillus cereus group is an excellent reservoir of novel lanthipeptides*. Appl. Environ. Microbiol., 2015. **81**(5): p. 1765-1774.
93. Jangra, M., M. Kaur, and H. Nandanwar, *In-vitro studies on a natural lantibiotic, paenibacillin: A new-generation antibacterial drug candidate to overcome multi-drug resistance*. International Journal of Antimicrobial Agents, 2019. **53**(6): p. 838-843.
94. Deng, Y., et al., *Endophyte Bacillus subtilis evade plant defense by producing lantibiotic subtilomycin to mask self-produced flagellin*. Communications Biology, 2019. **2**(1): p. 368.
95. Sahl, H.-G. and H. Brandis, *Production, purification and chemical properties of an antistaphylococcal agent produced by Staphylococcus epidermidis*. Microbiology, 1981. **127**(2): p. 377-384.
96. Neis, S., et al., *Effect of leader peptide mutations on biosynthesis of the lantibiotic Pep5*. FEMS Microbiology Letters, 1997. **149**(2): p. 249-255.
97. Kellner, R., et al., *Pep5: Structure Elucidation of a Large Lantibiotic*. Angewandte Chemie International Edition in English, 1989. **28**(5): p. 616-619.
98. Heidrich, C., et al., *Isolation, characterization, and heterologous expression of the novel lantibiotic epicidin 280 and analysis of its biosynthetic gene cluster*. Applied and environmental microbiology, 1998. **64**(9): p. 3140-3146.
99. Schleifer, K. and U. Fischer, *Description of a new species of the genus Staphylococcus: Staphylococcus carnosus*. International Journal of Systematic and Evolutionary Microbiology, 1982. **32**(2): p. 153-156.
100. Kordel, M., R. Benz, and H.G. Sahl, *Mode of action of the staphylococcinlike peptide Pep 5: voltage-dependent depolarization of bacterial and artificial membranes*. Journal of bacteriology, 1988. **170**(1): p. 84-88.
101. Sahl, H.G., *Influence of the staphylococcinlike peptide Pep 5 on membrane potential of bacterial*

- cells and cytoplasmic membrane vesicles*. Journal of bacteriology, 1985. **162**(2): p. 833-836.
102. Brogden, K.A., *Antimicrobial peptides: pore formers or metabolic inhibitors in bacteria?* Nature Reviews Microbiology, 2005. **3**(3): p. 238-250.
103. Oren, Z. and Y. Shai, *Mode of action of linear amphipathic α -helical antimicrobial peptides*. Peptide Science, 1998. **47**(6): p. 451-463.
104. Bierbaum, G., et al., *Engineering of a novel thioether bridge and role of modified residues in the lantibiotic Pep5*. Applied and environmental microbiology, 1996. **62**(2): p. 385-392.
105. Van De Kamp, M., et al., *Sequence Analysis by NMR Spectroscopy of the Peptide Lantibiotic Epilancin K7 from Staphylococcus epidermidis K7*. European Journal of Biochemistry, 1995. **227**(3): p. 757-771.
106. Van De Kamp, M., et al., *Elucidation of the Primary Structure of the Lantibiotic Epilancin K7 from Staphylococcus epidermidis K7*. European Journal of Biochemistry, 1995. **230**(2): p. 587-600.
107. Ekkelenkamp, M.B., et al., *Isolation and structural characterization of epilancin 15X, a novel lantibiotic from a clinical strain of Staphylococcus epidermidis*. FEBS Letters, 2005. **579**(9): p. 1917-1922.
108. Petersen, J., et al., *Identification and characterization of a bioactive lantibiotic produced by Staphylococcus warneri*, in *Biological Chemistry*. 2009. p. 437.
109. Velásquez, J.E., X. Zhang, and W.A. Van Der Donk, *Biosynthesis of the antimicrobial peptide epilancin 15X and its N-terminal lactate*. Chemistry & biology, 2011. **18**(7): p. 857-867.
110. Knerr, P.J. and W.A. van der Donk, *Chemical Synthesis and Biological Activity of Analogues of the Lantibiotic Epilancin 15X*. Journal of the American Chemical Society, 2012. **134**(18): p. 7648-7651.
111. Verhoef, J., Milatovic, D., and Ekkelenkamp, M.B., *Antimicrobial compounds*. 2005.
112. Froseth, B.R. and L.L. McKay, *Molecular characterization of the nisin resistance region of Lactococcus lactis subsp. lactis biovar diacetylactis DRC3*. Applied and environmental microbiology, 1991. **57**(3): p. 804-811.
113. Draper, L.A., et al., *Lantibiotic resistance*. Microbiology and molecular biology reviews : MMBR, 2015. **79**(2): p. 171-191.
114. Jarvis, B., *Enzymic reduction of the C-terminal dehydroalanyl-lysine sequence in nisin*. The Biochemical journal, 1970. **119**(5): p. 56P-56P.
115. Brunati, C., et al., *Expanding the potential of NAI-107 for treating serious ESKAPE pathogens: synergistic combinations against gram-negatives and bactericidal activity against non-dividing cells*. Journal of Antimicrobial Chemotherapy, 2017. **73**(2): p. 414-424.

116. Ling, L.L., et al., *A new antibiotic kills pathogens without detectable resistance*. Nature, 2015. **517**(7535): p. 455-9.
117. Parmar, A., et al., *Efficient total syntheses and biological activities of two teixobactin analogues*. Chemical Communications, 2016. **52**(36): p. 6060-6063.
118. Yang, H., K.H. Chen, and J.S. Nowick, *Elucidation of the Teixobactin Pharmacophore*. ACS Chemical Biology, 2016. **11**(7): p. 1823-1826.
119. Parmar, A., et al., *Teixobactin analogues reveal enduracididine to be non-essential for highly potent antibacterial activity and lipid II binding*. Chem Sci, 2017. **8**(12): p. 8183-8192.
120. Parmar, A., et al., *Design and Syntheses of Highly Potent Teixobactin Analogues against Staphylococcus aureus, Methicillin-Resistant Staphylococcus aureus (MRSA), and Vancomycin-Resistant Enterococci (VRE) in Vitro and in Vivo*. Journal of Medicinal Chemistry, 2018. **61**(5): p. 2009-2017.
121. Shukla, R., et al., *Mode of action of teixobactins in cellular membranes*. Nat Commun, 2020. **11**(1): p. 2848.
122. Shukla, R., et al., *Teixobactin kills bacteria by a two-pronged attack on the cell envelope*. Nature, 2022. **608**(7922): p. 390-396.
123. Yang, X., et al., *Isolation and Structural Elucidation of Brevibacillin, an Antimicrobial Lipopeptide from Brevibacillus laterosporus That Combats Drug-Resistant Gram-Positive Bacteria*. Appl Environ Microbiol, 2016. **82**(9): p. 2763-2772.
124. Barsby, T., et al., *Bogorol A produced in culture by a marine Bacillus sp. reveals a novel template for cationic peptide antibiotics*. Org Lett, 2001. **3**(3): p. 437-40.
125. Yang, X. and A.E. Yousef, *Antimicrobial peptides produced by Brevibacillus spp.: structure, classification and bioactivity: a mini review*. World J Microbiol Biotechnol, 2018. **34**(4): p. 57.
126. Yang, X., E. Huang, and A.E. Yousef, *Brevibacillin, a cationic lipopeptide that binds to lipoteichoic acid and subsequently disrupts cytoplasmic membrane of Staphylococcus aureus*. Microbiol Res, 2017. **195**: p. 18-23.
127. Jiang, H., et al., *Antibacterial and antitumor activity of Bogorol B-JX isolated from Brevibacillus laterosporus JX-5*. World J Microbiol Biotechnol, 2017. **33**(10): p. 177.
128. Zhao, X., et al., *Brevibacillin 2V, a Novel Antimicrobial Lipopeptide With an Exceptionally Low Hemolytic Activity*. 2021. **12**(1501).

Chapter 2

Bacterial pH homeostasis, ion homeostasis and ATP synthesis

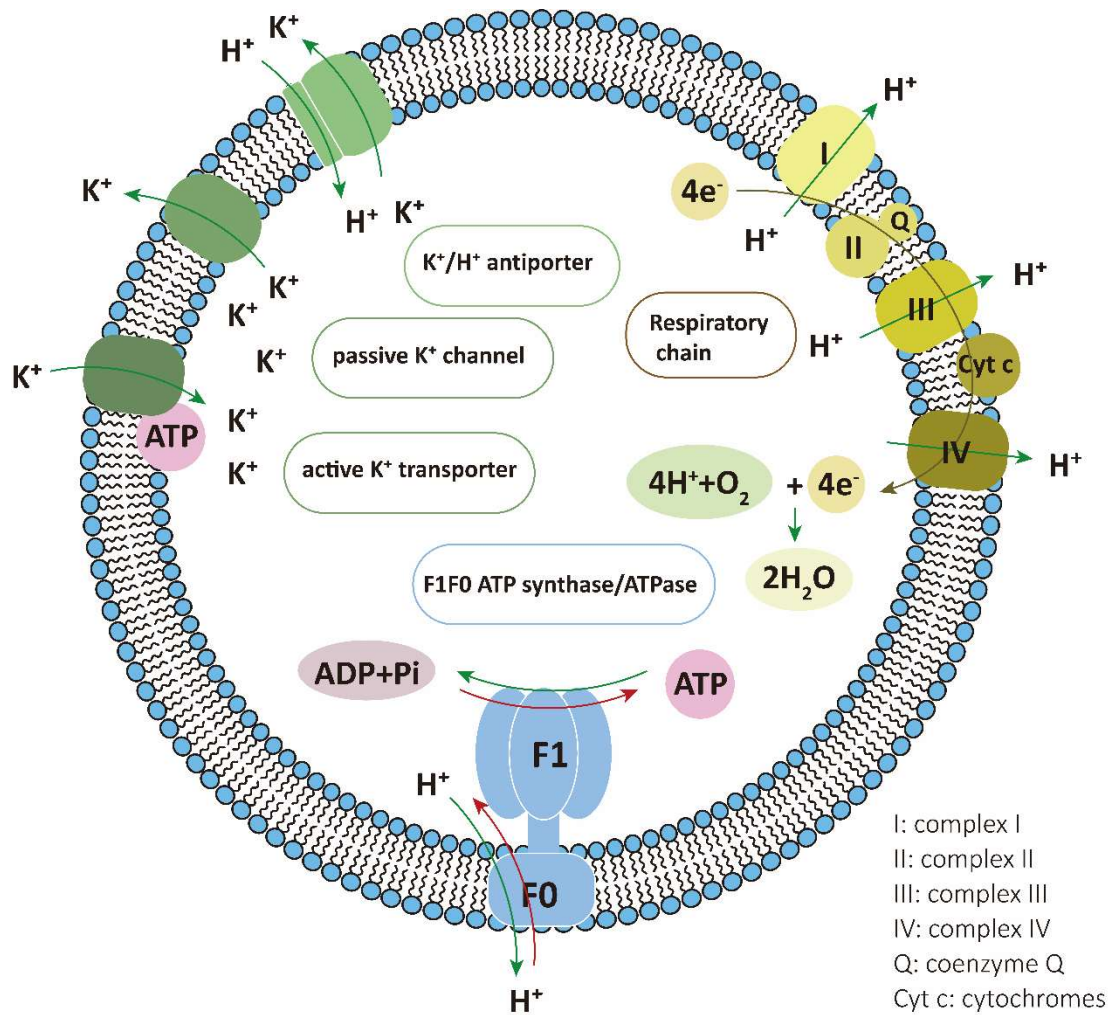


Figure 1. Players that are involved in pH homeostasis, ion homeostasis and ATP synthesis and that will be discussed in this chapter.

2.1 Introduction: The pH homeostasis, ion homeostasis and ATP synthesis in bacteria are tightly linked.

Most of the known AMPs inhibit bacteria by targeting the cytoplasmic membrane resulting in a series of effects such as membrane depolarization, permeabilization, ion leakage. Those effects directly influence the proton motive force (PMF) in the membrane. PMF (Δp) is a respiratory chain (also known as the electron transport chain) generated electrochemical gradient of protons [1]. The respiratory chain complexes continuously pump out protons which establish an transmembrane proton gradient

(ΔpH) [2]. The resulting non-equilibrium distribution of protons establishes an electrical gradient which contributes to the membrane potential ($\Delta\psi$) [3]. This membrane potential drives membrane-permeant cations to the cytoplasm, while membrane-permeant anions are excreted [3]. The whole non-equilibrium distribution of ions contributes to the $\Delta\psi$ [3]. The PMF is thus composed of a ΔpH and $\Delta\psi$ component, that can be formulated as $\Delta p = \Delta\psi - 2.3 \cdot (RT/F) \Delta\text{pH}$ (R, gas constant; T, absolute temperature; F, Faraday constant) [4] and it is the major driving force for ATP synthesis [5]. Additionally, proton homeostasis and ion homeostasis are tightly linked with each other due to the presence of H^+ /ion antiporters and symporters. Understanding the regulation of ΔpH , $\Delta\psi$ and ATP synthesis/hydrolysis is important to elucidate how bacteria react under stresses such as those induced by AMPs treatment, and thereby it also provides insight into the modes of action of these peptides (Fig. 1).

2.2 The regulation of proton homeostasis

Proton homeostasis in bacteria is vital for basal physicochemical reactions such as oxidoreduction and ionization [6]. The first proton pump of the respiratory chain (complex I) which is also known as NADH–quinone oxidoreductase is important for the oxidation of NADH and the reduction of ubiquinone [7, 8]. Most proteins and biomolecules require a stable pH for maintaining an ionization status to keep activities or functions. Proton pumps are membrane enzymes that are responsible for generating the ΔpH and for the regulation of proton homeostasis. They include primary proton pumps such as the respiratory chain pumps, energy-driven pumps and secondary active pumps such as ion/proton antiporters [9].

To adapt to the living environment that may have various pH values, bacteria evolved different proton regulation strategies to maintain intracellular proton homeostasis. The most well-known examples are acidophile and alkaliphile bacteria that live in extreme pH conditions. Here we focus on how the “normal” or neutrophile bacteria deal with environmental pH changes. For instance, under an acid challenge, the aerobically growing *Escherichia coli* upregulated the expression of respiratory chain complexes to increase the flow of protons from the cells. Simultaneously, the expression of ATP synthase was downregulated to decrease proton influx [9]. When *E. coli* faced an alkaline condition challenge, the reverse occurred; it downregulated the expression of respiratory chain complexes and upregulated the ATP synthase expression to maintain the proton concentration inside the cell sufficiently high [9]. For the anaerobically growing *Streptococcus faecalis* only upregulation of the F_1F_0 ATP synthase expression was observed upon an acid challenge [10], while under alkaline conditions, it downregulated the expression of this complex [10].

The secondary ion/proton antiporters (in bacteria mainly Na^+/H^+ and K^+/H^+ antiporters) are important for proton homeostasis as well. The ion/ H^+ antiporters extrude ions and take up H^+ via the force generated by the primary proton pumps [9]. Their activities

depend on the proton electrochemical gradient [9, 11]. The activity of Na^+/H^+ antiporters and K^+/H^+ antiporters could be significantly enhanced to accelerate H^+ uptake and ion efflux when bacteria were faced with an internal alkalized threat [12, 13]. Moreover, the Na^+/H^+ and K^+/H^+ antiporters do not work independently; they cooperate as regulators of cytoplasmic pH [6, 14].

Besides the primary and secondary pumps, lots of metabolic processes are also involved in the regulation of proton homeostasis [9]. For instance, *E. coli* was found to regulate pathways of amino acid consumption and flagellar motility genes to stabilize the internal pH under external acidic or alkaline conditions [15]. For example, at low pH, the expression of acetate-induced proteins and tricarboxylic acid (TCA) enzymes were enhanced to accelerate acid consumption [15]. At high pH, enzymes for arginine and glutamate catabolic pathways are expressed to metabolize carbon to acid [15]. Moreover, pH affects the flagellar synthesis and its motility of *E. coli*. When *E. coli* is brought under alkaline conditions, proton import is enhanced to maintain the PMF and energy consuming processes like flagellar synthesis are suppressed [16]. When placed in acid conditions, the large ΔpH contributes to the PMF which vigorously drives flagellar rotation [17]. As stated above, proton homeostasis is tightly linked with ion homeostasis due to the presence of ion/proton antiporters. The regulation of ion homeostasis will now be discussed.

2.3 The regulation of ion homeostasis

Besides its relation to proton homeostasis, ion homeostasis is also important for the membrane potential, osmoregulation and enzyme activation within cells. Ion transporters regulate ion homeostasis by active and passive transport. Most bacteria have several ion transport systems to deal with various situations [3]. Here, several representative types of potassium transporters are introduced to show how bacteria regulate intracellular ions. There are two types of ion channels: passive ion channels that allow ions to flow down an electrochemical gradient, and active ion transporters that are powered by ATP or the PMF to transport ions against electrochemical gradients.

KcsA is a typical 2-TM potassium channel that is highly selective for potassium [18]. It forms a homotetramer, with each subunit consisting of 2 transmembrane helices and a cytoplasmic domain [19]. The activity of KcsA is pH sensitive as its cytoplasmic domain is involved in pH-dependent gating [3, 20]. In *in vitro* experiments, when the pH was shifted from 7/7.5 to 4, KcsA's helical bundle was shown to open, whereupon potassium ions could flow along the electrochemical gradient [21, 22]. Regulators of K^+ conductance (RCKs) are domains that are responsible for ligand binding in potassium channels [23, 24]. Except KcsA, most potassium channels are regulated by RCK domains of which the conformational changes are triggered by different ligands such as Ca^{2+} , ADP and ATP [3]. For instance, MthK uses Ca^{2+} to open the channel and

GsuK requires Ca^{2+} and ADP/NAD^+ to be activated [25, 26].

When the external potassium concentration is low, bacteria need active potassium uptake to maintain a sufficiently high concentration in the cell. The heterotetrameric K^+ pump KdpFABC is a common K^+ transport system that drives K^+ into the cell when the intracellular K^+ concentration drops to micromolar levels [27]. It is a complex driven by a P-type ATPase domain and has high affinity for K^+ [3]. KdpFABC consists of 4 subunits that each have different functions. KdpF has one transmembrane helix and is assumed to be responsible for stabilization of the whole complex [28]. KdpA belongs to the superfamily of K^+ transporters (SKT) and contains 10 TM helices that function as a selectivity filter [29]. KdpB is the P-type ATPase subunit of the complex that provides the energy necessary for K^+ transport via ATP hydrolysis [30]. KdpC has a soluble periplasmic domain and one TM helix [31]. It increases the ATP-binding affinity of KdpB and is essential for the enzyme complex KdpFABC to assemble together [31-33].

2.4 The regulation of intracellular ATP

Three types of ATP synthases and ATPases are known that are bi-functional as they possess both ATP synthesis and ATPase activity [34]. These are F_1F_0 (in bacteria, mitochondria, chloroplasts), A_1A_0 (in archaea) and V_1V_0 (in vacuolar membranes) [34]. In bacteria, F_1F_0 is responsible for most of the production of ATP in the cell [35]. F-type ATP synthases consist of 8 different types of subunits with different stoichiometries (α , β_2 , c_{9-12} , α_3 , β_3 , γ , δ and ϵ). Depending on where the subunits locate, the structural units of F-type ATP synthase can be divided into the membrane-integral sector F_0 (subunits α , β and c) and the water-soluble peripheral sector F_1 (subunits α , β , γ , δ and ϵ) [36]. The F_0 sector is responsible for the transmembrane translocation of protons (we will only consider the proton pumping ATPases here) and the F_1 sector is responsible for the catalysis of ATP synthesis or hydrolysis [36]. Depending on the movement of subunits during catalyzation, the structural units of F-type ATP synthase can be divided into rotor (c , γ and ϵ) and stator (α , β and δ) [37].

The ATP synthesis is powered by the PMF [38, 39]. A proton translocates from the periplasmic side to the cytoplasmic side through the F_0 sector and thereby drives the rotational torque of the motor [37]. Reversely, the hydrolysis of ATP by F_1 sector drives the rotation of γ subunit [40]. Hereby, the rotation force of γ rotates the ring of c subunits, which results in translocation of a proton out of the cell [41]. The directions of rotation of the motor during ATP synthesis or ATP hydrolysis are opposite of each other [42].

As mentioned above, ATP synthase, catalyzing ATP from ADP and inorganic phosphate (P_i), is driven by the PMF (Δp). Although ΔpH and $\Delta \psi$ are thermodynamically equivalent according to the equation $\Delta p = \Delta \psi - 2.3 \cdot (\text{RT/F}) \cdot \Delta \text{pH}$, they are not kinetically equivalent as $\Delta \psi$ is indispensable for the bacterial ATP synthesis,

while the ΔpH is dispensable [43, 44]. A previous study using *E. coli* ATP synthase reconstituted in proteoliposomes showed that $\Delta\psi$ was mandatory for ATP synthesis while ΔpH is not necessary for ATP synthesis [43]. When ATP synthase works as proton/ion-pumping ATPase, it builds up and maintains the PMF. The catalytic rate of ATP hydrolysis can be limited by PMF backward pressure such that the ATPase activity increases when the PMF is abolished [45, 46].

2.5 ΔpH , $\Delta\psi$ and ATP measurements

The AMP effects towards bacterial membranes usually start with membrane depolarization and permeabilization, likely in this order. These effects cause changes in both components of the PMF, the ΔpH and $\Delta\psi$. Additionally, as mentioned above dissipation of PMF is coupled to the synthesis and hydrolysis of ATP. By monitoring of ΔpH , $\Delta\psi$ and ATP in cells, we can detect subtle effects of antibiotics on bacteria. To detect changes in the components of the PMF, compounds that show fluorescence or absorption changes upon changes in the ΔpH or $\Delta\psi$ are commonly used.

Fluorophores that are pH dependent and easily enter the cells are used for monitoring the internal pH and thus also report on the ΔpH . 5 (and 6-)-carboxyfluorescein diacetate succinimidyl ester (CFDA, SE) is widely used for measuring intracellular pH of bacteria [47]. It enters into cells and following de-esterification it becomes fluorescent [47, 48]. Additionally, the succinimidyl group covalently couples to intracellular amines (mainly originating from proteins) thereby limiting the efflux of the probe, which significantly reduces the error in these measurements [47-49]. FITC-dextran (MW 4000) (incorporated into bacterial vesicles or submitochondrial particles) and bromothymol blue can be used as pH indicators as well [4]. However, FITC-dextran requires a large pH change in order for its fluorescence intensity to change, making this method not useful for measuring minor ΔpH changes [4]. The absorbance of bromothymol blue changes as the pH changes, which can be used to determine pH values. However, the distribution of bromothymol blue on internal or external membrane surfaces is highly dependent on the metabolic state which result in ambiguous absorbance changes [4].

For $\Delta\psi$ monitoring, voltage-sensitive dyes such as safranin and cyanine dyes such as 3,3'-Diethylthiadicarbocyanine iodide (DiSC₂(5)) are mostly used [50]. Changes in the membrane potential induce a spectral change in the absorbance of the positively charged dye safranin, which is linearly responsive to K⁺ or H⁺ diffusion potentials [51, 52]. In the presence of a membrane potential, cyanine dyes absorb into the bilayer and presumably accumulate in the inner leaflet of the plasma membrane resulting in self-quenching [53]. The dyes are released after depolarization of the membrane and as a result the self-quenching is relieved [54-56]. Besides voltage-sensitive dyes, membrane permeable cations such as tetraphenylphosphonium (TPP⁺) can be used in membrane potential measurements [57]. The accumulated TPP⁺ will efflux when the

membrane potential is dissipated [58]. The concentration of TPP⁺ can be determined by a TPP⁺-selective electrode.

The most common way to monitor ATP concentrations is by luciferase-based assays [59-61]. The hydrolysis of ATP catalyzed by luciferase in the presence of O₂ and Mg²⁺ results in light emission with a wavelength of 560 nm, which can be quantified by a luminometer. For detecting the ATP concentration in bacteria, cells are lysed by lysis buffer and then the released ATP is determined by the luminescence intensity after the addition of luciferase [62]. BacTiter-Glo™ assay reagent composed of luciferase and lysis buffer is widely used in ATP determination [63-65].

2.6 Antibiotic lethality and the intracellular pH homeostasis

It has been suggested that the lethality of antibiotics in general may not only be due to their targeting mechanism, but is also caused by a series of disturbances of intracellular homeostasis [1]. Numerous antibiotics inhibit bacteria by targeting ATP consuming processes such as cell wall synthesis, protein synthesis and DNA synthesis [66-69]. The inhibition of various ATP consuming processes inevitably leads to an intracellular ATP increase that in turn limits the rate of ATP synthesis. It leads to reduction of proton flow that enters the cytoplasm via the F₁F₀-ATPase. Together these effects result in intracellular alkalization and membrane hyperpolarization leading to cell death. Based on this, a pH homeostasis hypothesis was proposed claiming that bactericidal antibiotics kill bacteria indirectly by disrupting pH homeostasis of the cell [1, 59]. This was supported by research that showed that a reduction of proton influx increased antibiotic sensitivity and that promoting proton influx increased antibiotic tolerance in *Mycobacterium smegmatis* [59].

Most AMPs depolarize and permeabilize cell membrane as their modes of action [70]. AMPs usually are positively charged and active under acidic conditions [71, 72]. Membrane disruption results in proton influx into the cell causing intracellular acidification. In addition, the PMF is dissipated, reducing the rate of ATP synthesis. Thus, either alkalization or acidification of cells disrupt basal metabolism processes in the cell such as ATP synthesis, protein synthesis, eventually resulting in cell death. Therefore, it is important to measure all these three interdependent parameters: the $\Delta\psi$, ΔpH and ATP levels in bacteria when studying AMP's modes of action.

2.7 Conclusions

The regulation of pH homeostasis, ion homeostasis and ATP synthesis in bacteria is very complicated due to their mutual dependencies and different strains have various ways to do this. This chapter briefly described these phenomena in bacteria and how they affect each other. Previous studies have put effort into how bacteria react when

faced with extreme environments such as high salt or alkaline conditions. On the other hand, relatively little is known how homeostasis of bacteria is affected when facing antibiotics or AMPs. Studying how antibiotics or AMPs influence bacterial pH homeostasis, ion homeostasis and ATP synthesis may give novel insights into improving their efficacy.

2.8 References

1. Voskuil, M.I., C.R. Covey, and N.D. Walter, *Antibiotic Lethality and Membrane Bioenergetics*. Adv Microb Physiol, 2018. **73**: p. 77-122.
2. Stuchebrukhov, A.A., *Redox-Driven Proton Pumps of the Respiratory Chain*. Biophys J, 2018. **115**(5): p. 830-840.
3. Stautz, J., et al., *Molecular Mechanisms for Bacterial Potassium Homeostasis*. J Mol Biol, 2021. **433**(16): p. 166968.
4. Rottenberg, H., *The measurement of membrane potential and ΔpH in cells, organelles, and vesicles*. Methods Enzymol, 1979. **55**: p. 547-69.
5. Maloney, P.C., E.R. Kashket, and T.H. Wilson, *A Protonmotive Force Drives ATP Synthesis in Bacteria*. Proceedings of the National Academy of Sciences, 1974. **71**(10): p. 3896.
6. Padan, E., D. Zilberstein, and S. Schuldiner, *pH homeostasis in bacteria*. Biochim Biophys Acta, 1981. **650**(2-3): p. 151-66.
7. Friedrich, T., *Complex I: a chimaera of a redox and conformation-driven proton pump?* J Bioenerg Biomembr, 2001. **33**(3): p. 169-77.
8. Bonora, M., et al., *ATP synthesis and storage*. Purinergic Signal, 2012. **8**(3): p. 343-57.
9. Krulwich, T.A., G. Sachs, and E. Padan, *Molecular aspects of bacterial pH sensing and homeostasis*. Nature Reviews Microbiology, 2011. **9**(5): p. 330-343.
10. Kobayashi, H., T. Suzuki, and T. Unemoto, *Streptococcal cytoplasmic pH is regulated by changes in amount and activity of a proton-translocating ATPase*. J Biol Chem, 1986. **261**(2): p. 627-30.
11. West, I.C. and P. Mitchell, *Proton/sodium ion antiport in Escherichia coli*. Biochem J, 1974. **144**(1): p. 87-90.
12. Taglicht, D., E. Padan, and S. Schuldiner, *Overproduction and purification of a functional Na^+/H^+ antiporter coded by *nhaA* (*ant*) from Escherichia coli*. J Biol Chem, 1991. **266**(17): p. 11289-94.
13. Nakamura, T., H. Tokuda, and T. Unemoto, *K^+/H^+ antiporter functions as a regulator of cytoplasmic pH in a marine bacterium, Vibrio alginolyticus*. Biochim Biophys Acta, 1984. **776**(2): p. 330-6.
14. Kakinuma, Y. and K. Igarashi, *Isolation and properties of Enterococcus hirae mutants defective in the potassium/proton antiport system*. J Bacteriol, 1999. **181**(13): p. 4103-5.
15. Stancik, L.M., et al., *pH-dependent expression of periplasmic proteins and amino acid catabolism in Escherichia coli*. J Bacteriol, 2002. **184**(15): p. 4246-58.

Chapter 2

16. Maurer, L.M., et al., *pH regulates genes for flagellar motility, catabolism, and oxidative stress in Escherichia coli K-12*. J Bacteriol, 2005. **187**(1): p. 304-19.
17. Khan, S. and R.M. Macnab, *Proton chemical potential, proton electrical potential and bacterial motility*. J Mol Biol, 1980. **138**(3): p. 599-614.
18. Schrempf, H., et al., *A prokaryotic potassium ion channel with two predicted transmembrane segments from Streptomyces lividans*. Embo j, 1995. **14**(21): p. 5170-8.
19. Doyle, D.A., et al., *The structure of the potassium channel: molecular basis of K⁺ conduction and selectivity*. Science, 1998. **280**(5360): p. 69-77.
20. Hirano, M., et al., *Role of the KcsA channel cytoplasmic domain in pH-dependent gating*. Biophysical journal, 2011. **101**(9): p. 2157-2162.
21. Baker, K.A., et al., *Conformational dynamics of the KcsA potassium channel governs gating properties*. Nat Struct Mol Biol, 2007. **14**(11): p. 1089-95.
22. Cordero-Morales, J.F., et al., *Molecular determinants of gating at the potassium-channel selectivity filter*. Nat Struct Mol Biol, 2006. **13**(4): p. 311-8.
23. Pau, V.P., et al., *Structure and function of multiple Ca²⁺-binding sites in a K⁺ channel regulator of K⁺ conductance (RCK) domain*. Proc Natl Acad Sci U S A, 2011. **108**(43): p. 17684-9.
24. Kuang, Q., P. Purhonen, and H. Hebert, *Structure of potassium channels*. Cellular and molecular life sciences : CMLS, 2015. **72**(19): p. 3677-3693.
25. Jiang, Y., et al., *Crystal structure and mechanism of a calcium-gated potassium channel*. Nature, 2002. **417**(6888): p. 515-22.
26. Kong, C., et al., *Distinct gating mechanisms revealed by the structures of a multi-ligand gated K(+) channel*. Elife, 2012. **1**: p. e00184.
27. Epstein, W., V. Whitelaw, and J. Hesse, *A K⁺ transport ATPase in Escherichia coli*. J Biol Chem, 1978. **253**(19): p. 6666-8.
28. Gassel, M., et al., *The KdpF subunit is part of the K(+)-translocating Kdp complex of Escherichia coli and is responsible for stabilization of the complex in vitro*. J Biol Chem, 1999. **274**(53): p. 37901-7.
29. Durell, S.R., E.P. Bakker, and H.R. Guy, *Does the KdpA subunit from the high affinity K(+)-translocating P-type KDP-ATPase have a structure similar to that of K(+) channels?* Biophys J, 2000. **78**(1): p. 188-99.
30. Stock, C., et al., *Cryo-EM structures of KdpFABC suggest a K(+) transport mechanism via two inter-subunit half-channels*. Nat Commun, 2018. **9**(1): p. 4971.
31. Gassel, M. and K. Altendorf, *Analysis of KdpC of the K(+)-transporting KdpFABC complex of Escherichia coli*. Eur J Biochem, 2001. **268**(6): p. 1772-81.

32. Irzik, K., et al., *The KdpC subunit of the Escherichia coli K⁺-transporting KdpB P-type ATPase acts as a catalytic chaperone*. Febs j, 2011. **278**(17): p. 3041-53.
33. Gassel, M., et al., *Assembly of the Kdp complex, the multi-subunit K⁺-transport ATPase of Escherichia coli*. Biochim Biophys Acta, 1998. **1415**(1): p. 77-84.
34. Cross, R.L. and V. Müller, *The evolution of A-, F-, and V-type ATP synthases and ATPases: reversals in function and changes in the H⁺/ATP coupling ratio*. FEBS Lett, 2004. **576**(1-2): p. 1-4.
35. Kühlbrandt, W., *Structure and Mechanisms of F-Type ATP Synthases*. Annu Rev Biochem, 2019. **88**: p. 515-549.
36. Penefsky, H.S. and R.L. Cross, *Structure and mechanism of FoF1-type ATP synthases and ATPases*. Adv Enzymol Relat Areas Mol Biol, 1991. **64**: p. 173-214.
37. Dimroth, P., G. Kaim, and U. Matthey, *Crucial role of the membrane potential for ATP synthesis by F1F0 ATP synthases*. The Journal of experimental biology, 2000. **203**: p. 51-9.
38. von Ballmoos, C., A. Wiedenmann, and P. Dimroth, *Essentials for ATP synthesis by F1F0 ATP synthases*. Annu Rev Biochem, 2009. **78**: p. 649-72.
39. Feniouk, B.A. and M. Yoshida, *Regulatory mechanisms of proton-translocating F(O)F (1)-ATP synthase*. Results Probl Cell Differ, 2008. **45**: p. 279-308.
40. Omote, H., et al., *The gamma-subunit rotation and torque generation in F1-ATPase from wild-type or uncoupled mutant Escherichia coli*. Proc Natl Acad Sci U S A, 1999. **96**(14): p. 7780-4.
41. Nakanishi-Matsui, M., et al., *The mechanism of rotating proton pumping ATPases*. Biochimica et Biophysica Acta (BBA) - Bioenergetics, 2010. **1797**(8): p. 1343-1352.
42. Diez, M., et al., *Proton-powered subunit rotation in single membrane-bound F0F1-ATP synthase*. Nat Struct Mol Biol, 2004. **11**(2): p. 135-41.
43. Kaim, G. and P. Dimroth, *ATP synthesis by the F1Fo ATP synthase of Escherichia coli is obligatorily dependent on the electric potential*. FEBS Lett, 1998. **434**(1-2): p. 57-60.
44. Kaim, G. and P. Dimroth, *ATP synthesis by F-type ATP synthase is obligatorily dependent on the transmembrane voltage*. Embo j, 1999. **18**(15): p. 4118-27.
45. Lapashina, A.S. and B.A. Feniouk, *ADP-Inhibition of H⁺-F(O)F(1)-ATP Synthase*. Biochemistry (Mosc), 2018. **83**(10): p. 1141-1160.
46. Feniouk, B.A., T. Suzuki, and M. Yoshida, *Regulatory interplay between proton motive force, ADP, phosphate, and subunit epsilon in bacterial ATP synthase*. J Biol Chem, 2007. **282**(1): p. 764-72.
47. Breeuwer, P., et al., *A Novel Method for Continuous Determination of the Intracellular pH in Bacteria with the Internally Conjugated Fluorescent Probe 5 (and 6)-Carboxyfluorescein Succinimidyl Ester*. Appl Environ Microbiol, 1996. **62**(1): p. 178-83.

48. Quah, B.J.C., H.S. Warren, and C.R. Parish, *Monitoring lymphocyte proliferation in vitro and in vivo with the intracellular fluorescent dye carboxyfluorescein diacetate succinimidyl ester*. Nature Protocols, 2007. **2**(9): p. 2049-2056.
49. Wang, X.Q., et al., *Carboxyfluorescein diacetate succinimidyl ester fluorescent dye for cell labeling*. Acta Biochim Biophys Sin (Shanghai), 2005. **37**(6): p. 379-85.
50. Singh, A.P. and P. Nicholls, *Cyanine and safranin dyes as membrane potential probes in cytochrome c oxidase reconstituted proteoliposomes*. J Biochem Biophys Methods, 1985. **11**(2-3): p. 95-108.
51. Huttunen, M.T. and K.E. Akerman, *Measurements of membrane potentials in Escherichia coli K-12 inner membrane vesicles with the safranin method*. Biochim Biophys Acta, 1980. **597**(2): p. 274-84.
52. Moore, A. and W. Bonner, *Measurements of Membrane Potentials in Plant Mitochondria with the Safranin Method*. Plant physiology, 1982. **70**: p. 1271-6.
53. Cabrini, G. and A.S. Verkman, *Localization of cyanine dye binding to brush-border membranes by quenching of n-(9-anthroyloxy) fatty acid probes*. Biochim Biophys Acta, 1986. **862**(2): p. 285-93.
54. Sims, P.J., et al., *Mechanism by which cyanine dyes measure membrane potential in red blood cells and phosphatidylcholine vesicles*. Biochemistry, 1974. **13**(16): p. 3315-3330.
55. Krasne, S.J.B.j., *Interactions of voltage-sensing dyes with membranes. I. Steady-state permeability behaviors induced by cyanine dyes*. 1980. **30**(3): p. 415-439.
56. Krasne, S., *Interactions of voltage-sensing dyes with membranes. II. Spectrophotometric and electrical correlates of cyanine-dye adsorption to membranes*. Biophysical journal, 1980. **30**(3): p. 441-462.
57. Serviddio, G. and J. Sastre, *Measurement of mitochondrial membrane potential and proton leak*. Methods Mol Biol, 2010. **594**: p. 107-21.
58. Prasad, R. and M. Höfer, *Tetraphenylphosphonium is an indicator of negative membrane potential in Candida albicans*. Biochim Biophys Acta, 1986. **861**(2): p. 377-80.
59. Bartek, I.L., et al., *Antibiotic Bactericidal Activity Is Countered by Maintaining pH Homeostasis in Mycobacterium smegmatis*. mSphere, 2016. **1**(4).
60. Ruokonen, A., et al., *Screening of bacteria in urine using luciferin-luciferase assay of microbial ATP: a comparative study*. Ann Clin Biochem, 1982. **19**(6): p. 416-20.
61. DeLuca, M. and W.D. McElroy, *Kinetics of the firefly luciferase catalyzed reactions*. Biochemistry, 1974. **13**(5): p. 921-5.
62. de Rautlin de la Roy, Y., et al., *Kinetics of bactericidal activity of antibiotics measured by luciferin-luciferase assay*. J Biolumin Chemilumin, 1991. **6**(3): p. 193-201.

63. Farhat, N., et al., *A uniform bacterial growth potential assay for different water types*. Water Research, 2018. **142**: p. 227-235.
64. Roshan, N., et al., *Natural products show diverse mechanisms of action against Clostridium difficile*. J Appl Microbiol, 2019. **126**(2): p. 468-479.
65. Jarrad, A.M., et al., *Detection and Investigation of Eagle Effect Resistance to Vancomycin in Clostridium difficile With an ATP-Bioluminescence Assay*. Front Microbiol, 2018. **9**: p. 1420.
66. Brötz, H., et al., *Mode of action of the lantibiotic mersacidin: inhibition of peptidoglycan biosynthesis via a novel mechanism?* Antimicrobial agents and chemotherapy, 1995. **39**(3): p. 714-719.
67. Sheldrick, G.M., et al., *Structure of vancomycin and its complex with acetyl-D-alanyl-D-alanine*. Nature, 1978. **271**(5642): p. 223.
68. Apirion, D. and D. Schlessinger, *Coresistance to neomycin and kanamycin by mutations in an Escherichia coli locus that affects ribosomes*. J Bacteriol, 1968. **96**(3): p. 768-76.
69. Blondeau, J.M., *Fluoroquinolones: mechanism of action, classification, and development of resistance*. Surv Ophthalmol, 2004. **49 Suppl 2**: p. S73-8.
70. Feng, X., et al., *Antiinfectives targeting enzymes and the proton motive force*. Proc Natl Acad Sci U S A, 2015. **112**(51): p. E7073-82.
71. Mortvedt-Abildgaa, C., et al., *Production and pH-Dependent Bactericidal Activity of Lactocin S, a Lantibiotic from Lactobacillus sake L45*. Applied and Environmental Microbiology, 1995. **61**(1): p. 175-179.
72. Lombardi, L., et al., *Insights into the antimicrobial properties of hepcidins: advantages and drawbacks as potential therapeutic agents*. Molecules, 2015. **20**(4): p. 6319-41.

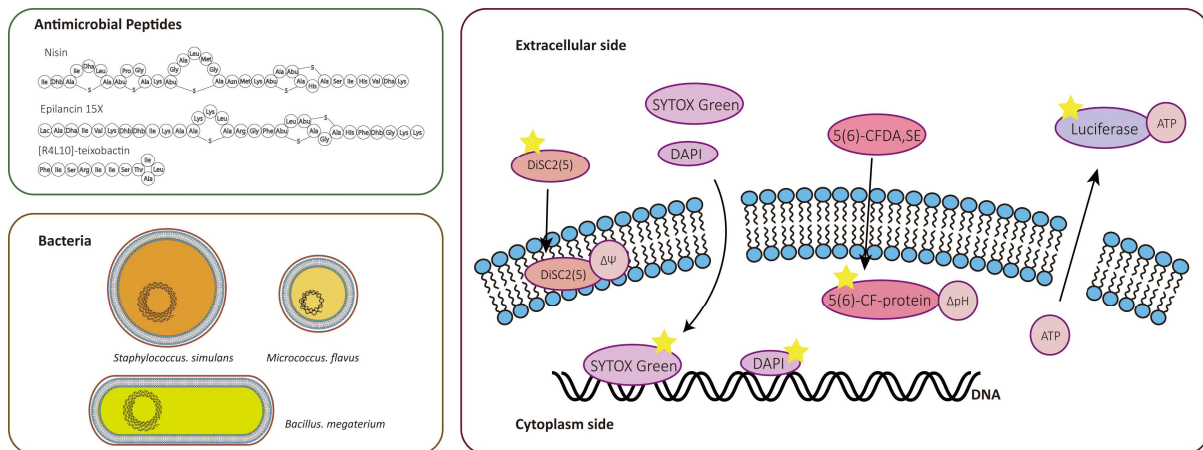
Chapter 3

Analyzing mechanisms of action of antimicrobial peptides on bacterial membranes requires multiple complimentary assays and different bacterial strains

This chapter is based on:

Xiaoqi Wang, Roy A. M. van Beekveld, Yang Xu, Anish Parmar, Sanjit Das, Ishwar Singh, and Eefjan Breukink. "Analyzing Mechanisms of Action of Antimicrobial Peptides on Bacterial Membranes Requires Multiple Complimentary Assays and Different Bacterial Strains." *Biochimica et Biophysica Acta (BBA) - Biomembranes* (2023/04/24/2023):184160.

<https://dx.doi.org/https://doi.org/10.1016/j.bbamem.2023.184160>.



Abstract

Antimicrobial peptides (AMPs) commonly target bacterial membranes and show broad-spectrum activity against microorganisms. In this research we used three AMPs (nisin, epilancin 15X, [R4L10]-teixobactin) and tested their membrane effects toward three strains (*Staphylococcus simulans*, *Micrococcus flavus*, *Bacillus megaterium*) in relation with their antibacterial activity. We describe fluorescence and luminescence-based assays to measure effects on membrane potential, intracellular pH, membrane permeabilization and intracellular ATP levels. The results show that our control peptide, nisin, performed mostly as expected in view of its targeted pore-forming activity, with fast killing kinetics that coincided with severe membrane permeabilization in all three strains. However, the mechanisms of action of both Epilancin 15X as well as [R4L10]-teixobactin appeared to depend strongly on the bacterium tested. In certain specific combinations of assay, peptide and bacterium, deviations from the general picture were observed. This was even the case for nisin, indicating the importance of using multiple assays and bacteria for mode of action studies to be able to draw proper conclusions on the mode of action of AMPs.

3.1 Introduction

Antimicrobial resistance is becoming a global threat to human health as more and more antibiotics are losing their efficacy. Antimicrobial peptides (AMPs) showing broad-spectrum activity against microorganisms have been considered already for a long time as promising substitutions for these antibiotics [1-3]. AMPs are mostly positively charged and amphiphilic, properties that are essential for their (initial) interaction with the negatively charged membranes of target bacteria [4]. Currently, there are three main models that are describing the possible mechanisms of action of AMPs, i.e., the barrel-stave model, carpet model and toroidal-pore model [4-6]. However, these three classic models cannot account for the modes of action of many AMPs. In addition, mechanisms of actions are often ascribed to peptides while using improper model systems (e.g. composed of only one lipid) [6, 7]. Increasingly more models have been proposed by which AMPs destabilize the target membrane. Examples of these are thinning of the membrane, clustering of anionic lipids or non-lytic membrane depolarization [8-11]. Alternatively, the AMPs induce phase separations that lead to destabilization of the bacterial membranes via blebbing, budding, or vascularization [12-15]. Recently, it was shown that many AMPs lacked a correlation between membrane permeabilization and antibiotic activity. This led to the suggestion that these AMPs inhibit bacteria by perturbing the membrane and causing intracellular biomass aggregation [16]. What all AMPs have in common is their affinity for the bacterial membrane, and even those that have internal targets but do not cause permeabilization have mechanisms to pass this membrane that are similar to certain pore-forming mechanisms [16]. Importantly, what mechanism a peptide is proposed to follow largely depends on the method and bacterium used for determining the peptide's effects [17, 18]. Thus, the way in which membrane permeabilization by an AMP is determined has major implications for the conclusions that can (and will) be drawn on the proposed mechanism.

AMPs' effects on bacterial membranes can be subtle, such as membrane depolarization or more severe, like pore-formation or disruption via the carpet model and several methods exist that can measure these effects on membranes. Dissipation of the membrane potential ($\Delta\Psi$) and/or ΔpH , are the subtlest indications of membrane perturbation that can be measured. Both constitute the so-called proton-motive force (PMF, Δp) where $\Delta p = \Delta\psi - 2.3RT/F \cdot \Delta\text{pH}$ [19]. The dissipation of the PMF is triggered by proton leakage or membrane potential depolarization (ion leakage, in case of bacteria mostly K^+). The depolarization of the membrane can be measured by voltage-sensitive cyanine dyes such as 3,3'-Diethylthiadicarbocyanine ($\text{DiSC}_2(5)$) [20-23]. In the presence of a membrane potential, these dyes are absorbed into the bilayer and accumulate presumably in the inner leaflet of the plasma membrane resulting in self-quenching [24]. The dyes are released after depolarization of the membrane and as a result the self-quenching is relieved [25-27]. Changes in the pH gradient are mostly

measured by determining the pH of the cytosol via internalized pH-sensitive fluorophores. Carboxyfluorescein diacetate succinimidyl ester can be used for this, where its esterized form can enter the cell and following de-esterification it becomes fluorescent [28]. The succinimidyl ester ensures stable intracellular localization. Besides dissipation of the PMF due to loss of ions or proton influx, more severe membrane damage, such as pore-formation, can be measured by determining the efflux of (much) larger intracellular components. The earliest method used for this was detecting the release of UV-absorbing components of the cell [29]. In addition, the loss of ATP by the cells can be determined by a luciferase based assay [30]. An alternative way to determine the membrane damage is using probes that can enter the cells when their membrane is damaged. DNA-binding probes such as SYTOX green or 4',6-diamidino-2-phenylindole (DAPI) are membrane impermeable and they stain the DNA only when the membrane barrier is compromised [31-38].

Members of the family of lantibiotics, which belongs to AMPs, usually have specific mechanisms and large amount of them harbors the Lipid II targeting family members [39, 40]. Nisin (Fig. S1A) is one of the most well studied member of the lantibiotics family that targets Lipid II and forms stable pores together with Lipid II in the bacterial membrane [17, 41-43]. The A and B ring-system of nisin is responsible for binding to Lipid II and the C-terminal part of nisin including rings D/E has been suggested to be important for pore-formation [44]. A recent high-resolution NMR study revealed more details on the nisin-Lipid II binding in membrane bilayers, where the N20-K22 (the hinge) of nisin was shown to be flexible and lines the pore lumen. This was suggested to be important for the adaption of the pores to the thickness of the membrane [45]. The C-terminal (S29-K34) part of nisin was shown to still be dynamic in the pore structure and it is proposed to pierce through the membrane [45]. Pores formed by nisin are very stable and black lipid bilayer studies have shown that nisin pores have a pore-size of about 2 to 2.5 nm, thus allowing molecules the size of ATP (Stokes radius of ~0.7) through the pore [43, 46]. The mode of action of epilancin 15X (Fig. S1B), another member of the lantibiotics family, is still unknown. Therefore we aimed to study the antibacterial activity of this peptide in comparison to nisin. Epilancin 15X, which has one of the lowest MICs against pathogenic bacteria and has potent activity especially against *Staphylococci* [47]. It is produced by *Staphylococcus epidermidis* 15X154 and was isolated and structurally characterized in 2005 [48]. The C-terminus of epilancin 15X, especially rings B and C, is very similar to nisin, which may point to pore-formation as its mechanism [47]. However, epilancin 15X lacks nisin's N-terminal lipid II signature binding A/B rings system, which makes it uncertain if it interacts with Lipid II. As mentioned, how epilancin 15X acts is still unclear, but given the similarity of the C-terminal lanthionine rings it may, like nisin, attack bacteria via membrane permeabilization. Teixobactin, which is produced by *Eleftheria terrae*, kills pathogens via targeting Lipid II and the wall teichoic acid precursor Lipid III, thus its mode of action includes inhibition of the bacterial cell wall synthesis machinery [49]. Recently it was shown that teixobactin has a dual mode of action that besides cell wall synthesis

inhibition also includes membrane disruption via fibril formation together with Lipid II on the membrane surface [50]. This aggregational behavior with Lipid II had been shown before for an improved teixobactin analogue, D-Arg4-Leu10-teixobactin ([R4L10]-teixobactin, Fig. S1C) [51, 52]. Hence, we also explored the permeabilization activity of this teixobactin analogue compared to that of nisin and epilancin 15X.

During our efforts in studying the membrane effects of these AMPs we noticed that even a well-known pore-former, the lantibiotic nisin, sometimes behaved differently from what can be expected from a pore-forming peptide in different methods and bacteria. Our results indicate that it is important to use multiple assays and bacteria for mode of action studies to be able to draw proper conclusions on the mode of action of AMPs.

3.2 Method and materials

3.2.1 Materials and strains

Nisin A, epilancin 15X were prepared as previously described [48, 53]. [R4L10]-teixobactin was obtained from Ishwar Singh (University of Liverpool). 3,3'-Diethylthiadicarbocyanine iodide (DiSC₂(5)), 4',6-diamidino-2-phenylindole (DAPI) and Triton X-100 were purchased from Sigma-Aldrich. SYTOX™ Green Nucleic Acid Stain (SYTOX green) and 5(6)-CFDA, SE, Luria Broth (LB) and Tryptone Soya Broth (TSB) were purchased from ThermoFisher. M9 medium supplemented with vitamins and salts was prepared as described [54]. BacTiter-Glo™ Microbial Cell Viability Assay Kit was purchased from Promega. All other chemicals or reagents used were of analytical grade. Strains used in this study: *Staphylococcus simulans* 22 [55]; *Micrococcus flavus* DSM 1790; *Bacillus megaterium* ATCC 14581.

3.2.2 Methods

3.2.2.1 General procedures

Precultures of the indicator strains were grown at 37 °C in TSB for *S. simulans* and *M. flavus* or LB for *B. megaterium* while shaking at 200 rpm overnight and then diluted to an OD₆₀₀ of 0.05 with fresh medium. The cultures were further grown for 4 hours and spun down at 3000 × g for 10 min at 4 °C. The cells were washed twice with buffer A (250 mM glucose, 5 mM MgSO₄, 100 mM KCl, 10 mM potassium-phosphate buffer at pH 7) for *S. simulans* and *M. flavus* or M9 medium for *B. megaterium*. They were then resuspended to an OD₆₀₀ of 5 and kept on ice until use on the same day. The bacteria remained viable under these conditions for at least 2 hours.

The concentration of peptides was determined using the Pierce™ BCA Protein Assay

Kit (Thermo Fisher) using BSA as a standard. Fluorescence and luminescence related experiments (membrane potential depolarization assay, membrane permeability assay, ATP leakage assay, proton permeability assay) were performed using a Cary Eclipse fluorescence spectrophotometer (FL0904M005) in a 10 x 4-mm quartz cuvette at 25 °C.

To determine the number of surviving cells in the fluorescence cuvette at a given time, 5 µL of the suspension was plated onto TSB agar plates and incubated at 37 °C overnight.

Per species of bacteria all the experiments were done on the same day and due to time restraints, per experiment, one set of data could only be obtained. For each bacterium this was repeated at least twice, thus generating fully independent measurements.

3.2.2.2 MIC determination

The lowest concentrations of AMPs (nisin, epilancin 15X and teixobactin) that did not allow growth of the indicator strains after 18 hours were defined as the MICs. This was determined using 1 mL cultures of indicator strains at a start OD₆₀₀ of 0.05 in fresh medium (TSB for *S. simulans* and *M. flavus* or LB for *B. megaterium*) containing a serial dilution of antibiotics in sterilized glass tubes. The tubes were shaken at 37 °C, 200 rpm and the OD₆₀₀ was determined after incubation for 18 hours on a Novaspec II. MIC determinations were repeated three times.

3.2.2.3 Membrane potential depolarization assay

The fluorescent dye DiSC₂(5) (excitation at 650 nm and emission at 670 nm) was used to test the effect of the antibiotics on the membrane potential of the bacteria. From the concentrated cell suspension, cells were diluted to OD₆₀₀=0.05 in a cuvette containing 1 ml of buffer A, followed by the addition of 2 µL of a stock solution of 0.1 mM DiSC₂(5) dissolved in DMSO. Antibiotics were added after 1 minute, or left out for the blank. At the end of the experiment 10 µL of 20% Triton X-100 was added to fully dissipate the membrane potential.

3.2.2.4 Membrane permeability assay (DNA binding stain)

The fluorescent dyes SYTOX green (excitation at 504 nm and emission at 523 nm) and DAPI (excitation at 364 nm and emission at 454 nm) were used to inspect the abilities of the antibiotics to disrupt the bacterial membrane. From the concentrated cell suspension 10 µL was added into a cuvette containing 1 mL buffer A to reach an OD₆₀₀ of 0.05, followed by the addition of 1 µL of a stock solution of 0.25 µM SYTOX green dissolved in DMSO or 1 µL of a stock solution of 1 mg/mL DAPI dissolved in 10 mM PBS at pH 7. Antibiotics were added after 1 minute, or left out for the blank. At the end

Analyzing mechanisms of action of antimicrobial peptides on bacterial membranes requires multiple complimentary assays and different bacterial strains

of the experiment 10 μ L of 20% Triton X-100 for SYTOX green or BacTiter-Glo™ disruption buffer for DAPI was added to fully disrupt the cells.

3.2.2.5 ATP leakage assay

The BacTiter-Glo™ Microbial Cell Viability Assay Kit was used to inspect the abilities of the antibiotics to cause ATP leakage from the bacteria. Luciferase signal was recorded using the Bio/Chemi-luminescence mode with the emission set at 556 nm. The BacTiter-Glo™ substrate stock solution containing the luciferase enzyme and substrate was made by dissolving the lyophilized substrate/enzyme mixture provided in the kit in 1 mL of buffer A, which was then divided into 50 μ L aliquots and stored at -80 °C until use. From the concentrated cell suspension 10 μ L was added into a cuvette containing 1 mL buffer A, followed by the addition of 5 μ L of BacTiter-Glo™ substrate solution. Antibiotics were added after 1 minute, or left out for the blank. At the end of the experiment 10 μ L of BacTiter-Glo™ disruption buffer was added to measure the amount of residual ATP that was left inside the cells. Experiments using *B. megaterium* were performed in M9 medium to maintain viability of the cells. Unfortunately, ATP measurements were incompatible with M9 medium.

3.2.2.6 Proton permeability assay

The 5(6)-CFDA, SE (excitation at 490 nm and emission at 525 nm) was used to inspect the proton permeabilities of the antibiotics against the bacteria. Precultures of indicator strains were grown at 37 °C, 200 rpm overnight, and then diluted to an OD₆₀₀ of 0.05 with fresh medium. The culture was further grown for 4 hours and spun down at 3000 \times g for 10 min at 4 °C. Then cells were resuspended in buffer B containing 50 mM HEPES, 20 mM glucose, 1 mM MgSO₄ at pH 7 to an OD₆₀₀ of 0.5 and incubated with 3 μ M 5(6)-CFDA, SE for 30 min at 30 °C, 200 rpm. The cells were washed twice with the same buffer and were resuspended to an OD₆₀₀ of 5. From this cell suspension 10 μ L was added into a cuvette containing 1 mL buffer B set at pH 5. Antibiotics were added after 30 seconds, or left out for the blank. At the end of the experiment 20 μ L of a 1 mg/mL carbonyl cyanide m-chlorophenyl hydrazone (CCCP) solution in DMSO was added to fully dissipate the Δ pH of the bacteria.

3.2.2.7 Analysis of lipid compositions of bacteria

Bacteria were grown overnight at 37°C while shaking @200 rpm in TSB in the case of *S. simulans*, or at 30°C while shaking at 200 RPM for *B. megaterium* (in LB) and *M. flavus* (in TSB). The overnight culture was diluted to an OD₆₀₀ of 0.05 in 10 mL and grown to mid-log phase (OD₆₀₀ = 0.3 - 0.4) at the same conditions as for the overnight growth. Bacteria were harvested, resuspended in 0.8 mL H₂O, after which 2 mL MeOH and 1 mL CHCl₃ were added and the samples were vortexed extensively. Subsequently,

1 mL of CHCl_3 and H_2O were added, the sample vortexed and then centrifuged at $1,000\times g$ for 2 min. The organic layer (bottom) was dried under a N_2 stream at 40°C . The dried lipids were weighed and redissolved in $250\ \mu\text{L}$ 2:1 CHCl_3 :MeOH. Lipids were then spotted onto a NP-TLC (HPTLC-Fertigplatten Nano-ADAMANT®) at $20\ \mu\text{g}$ total lipids per lane using a Camag Linomat 5. The TLC was developed in 48:48:3:1, CHCl_3 :EtOH: NH_3 : H_2O with 0.2 g/L NH_4Ac , dried under vacuum and then stained with iodine prior to imaging. Phospholipid species were assigned based on pure references and the bacterial lipid extracts were analyzed as three independent cultures per species.

For analysis of the acyl chain compositions, approximately 1 mg of the bacterial extracts were redissolved in 1 mL n-hexane. Subsequently, $200\ \mu\text{L}$ MeOH containing 100 g/L KOH was added and the samples were extensively vortexed for 1 min to obtain fatty acid methyl esters (FAMES). The n-hexane layer was taken, dried under a N_2 -stream and redissolved in $50\ \mu\text{L}$ n-hexane. The FAMES were then analyzed using gas chromatography with flame-ionization detection on a Trace GC Ultra (Thermo Fisher Scientific) equipped with a biscyanopropyl polysiloxane column (Restek) and N_2 as a carrier gas. A temperature gradient was used that started at 40°C and held for one minute, followed by a linear gradient to 160°C in 4 min and a subsequent linear gradient to 220°C in 15 min. Peak identification was performed using FAME standards Mixture BR2 (Larodan; 90-1052) for branched species and certain straight chain fatty acids or 63-B (Nu-Chek-Prep) for various unsaturated and straight chain fatty acid species.

3.3 Results

The peptides under study here are targeted. Hence, to ensure that unspecific (non-targeted) mechanisms do not play a role we deliberately selected strains with low MICs to avoid clouding the results with a-specific effects.

3.3.1 Nisin causes severe membrane disruption in *S. simulans* and *B. megaterium* typical for pore-formation.

Nisin displayed MIC values equal to 80 nM, 50 nM and 75 nM toward *S. simulans*, *M. flavus* and *B. megaterium* respectively. In general, severe membrane disruption, e.g. pore-formation, of a bacterium leads to rapid death. This fast-killing rate should also correspond to the effects observed in the assays that are employed to determine membrane effects of AMPs if their mode of action involves membrane disruption. Therefore, we also determined the number of cells killed by nisin by determining the amount of colony forming units (CFU) after 5 minutes incubation, the average time needed for the assays employed here, at the different concentrations mentioned above. To exclude any environmental influence on the results we determined the CFUs that

are present in the same cuvette and under the identical conditions used for the fluorescence experiments. From these plate assays it becomes clear that nisin is able to kill rapidly, as can be expected from its targeted pore-forming mechanism. At 5X and 10X MIC there is about a 3 and 4 log reduction respectively in viable cells after 5 minutes and after 1 minute already more than 99% of the bacteria have been killed (Fig. P1). At lower nisin concentrations (1X and 2X MIC) only a 1 or 2 log reduction was achieved in 5 minutes and killing clearly takes longer.

The activity of AMPs, expressed in their MIC-values, towards different strains and in comparison to others can vary quite extensively from nanomolar to micromolar values depending on the killing mechanism they use. Therefore, in order to allow easy comparison, we used AMP-concentrations equal to 1X, 2X, 5X and 10X the respective MICs of the different strains in all the assays that report on membrane effects by the AMPs.

When testing the effects of nisin on the membrane potential with the dye DiSC₂(5) or the effect on membrane permeability to a DNA probe with the dye Sytox green/DAPI, in all cases, a picture emerges where the membrane effects parallel the killing rates (Fig. 1A, B and S2A). At low MICs relative minor effects can be seen, while at the highest concentrations (5X and 10X MIC) the effects are maximal of what can be achieved in the assay. The Δ pH measurements deviate from this picture where already a maximum effect was achieved with a concentration of only 1X MIC in about 1 minute (Fig. 1C). An interesting case is presented when we tested for ATP leakage in an on-line assay using luciferase to determine both intra cellular ATP levels as well as ATP-leakage from the cells. As luciferase is unable to enter the cell spontaneously and is too large to leak through the pores formed by nisin, this assay allowed us to determine i) the extent of ATP leakage from the bacteria in time and ii) the total amount of ATP remaining in the bacteria after 5 minutes of incubation with nisin. The low MIC traces (1X and 2X MIC) are especially interesting as it shows that two simultaneously occurring processes have to be considered (Fig. 1D). The addition on nisin at this concentration clearly induced some leakage of ATP in 5 minutes, amounting to a little over 10 % of the original amount of ATP in the cells (as deduced from the maximal signal obtained from the blank after lysis of the cells). However, simultaneously the total amount of ATP present in the cells had dropped considerable. Only about 50% of the ATP was left with respect to the control, meaning that an additional 40% of ATP was lost somehow. This drop in cellular ATP can be explained by taking into account that, within 1 minute, nisin induced a complete dissipation of the Δ pH, the main driving force for the generation of ATP in the bacteria [56]. As all ATP-consuming processes (e.g. protein synthesis, a major ATP-consumer) within the cell are still active, this results in a dramatic drop of the ATP-levels. At the highest concentration of nisin a little over 20% of the original amount of ATP has leaked out of the cells in five minutes, while nothing remains as there is no extra increase of signal upon complete lysis of the cells. Thus the remaining cells are completely devoid of ATP and have lost their ATP due to

the combined losses due to leakage and consumption in the absence of ATP regeneration. So far, studies on luciferase-based ATP determination for cells have been off-line-and only determined the amount of ATP that leaked out after separating the cells from the medium. Our method is able to determine both the amount of ATP leakage in time and the total amount of ATP that is left in the cells at a given timepoint, a valuable improvement of the assay.

We next tested nisin's activity towards *B. megaterium*, a bacterium with a similar sensitivity towards nisin as *S. simulans* (both 75 nM). Surprisingly, *B. megaterium* seemed to be much more sensitive in the membrane disruption assays (even in M9 medium) as its MIC would suggest. Membrane effects could be observed in all assays at concentrations starting 100-fold lower than the MIC, which also correlated with a rapid drop in CFUs at similar concentrations (Fig. P2). Apparently, this bacterium is much more sensitive towards nisin under the conditions of the membrane permeability tests (M9 medium) opposed to MIC tests in growth medium (LB-broth). Yet, at these lower concentrations, a fairly similar behavior of nisin was seen towards *B. megaterium* as compared to *S. simulans* with all membrane disruption assays (Fig. S2E-H). Here, the disruption of the ΔpH was very fast as well and already complete within a minute, but also the membrane-potential measurements showed fast dissipation kinetics. Thus, both the two components of the PMF, $\Delta\Psi$ and ΔpH , were affected early as compared to the more severe membrane effects measured by the DNA probes. Taken together, the results with these two bacteria show that there is a good correlation between the killing rates observed and the membrane disruption measured by the different assays¹.

3.3.2 Deviations from ideal behavior as a pore-former with *M. flavus*

M. flavus is a bit more sensitive to nisin (MIC of 50 nM) as compared to *S. simulans* (75 nM). The killing rate of nisin towards this bacterium is similarly fast as compared to *S. simulans* as at a 10-fold MIC concentration of nisin 3-4 log killing was achieved in 5 minutes (Fig. P3).

The effects of nisin in the membrane potential assay, Sytox green assay and ATP-leakage assay on *M. flavus*, were all comparable to the effects observed for the other bacteria (Fig. S2B-C and Fig. 1F). Surprisingly, the effects of nisin on the ΔpH of *M. flavus* was much less pronounced. Instead of a rapid decrease of the signal in the first minutes as seen for the other bacteria, a gradual decrease over time was observed (Fig. 1E). This coincided with a low drop of ATP levels within the cells at the lower concentrations, again showing that the ΔpH and the ATP content of the cells are correlated. Importantly, the leakage assay using DAPI was completely non-responsive to the effects of nisin on *M. flavus* (Fig. S2D). Since DAPI is a factor of ~ 2 times smaller than Sytox green the size of the probe cannot explain this difference in responsiveness.

Analyzing mechanisms of action of antimicrobial peptides on bacterial membranes requires multiple complimentary assays and different bacterial strains

This deviation from the ideal behavior signifies that relying on only one bacterium and one assay for determining membrane effects can be very limiting and can lead to complete misinterpretation of the mode of action. The non-responsiveness of DAPI stands out (also for the other peptides, see below) and makes this probe unsuitable for this kind of membrane permeability assays, at least in combination with *M. flavus*.

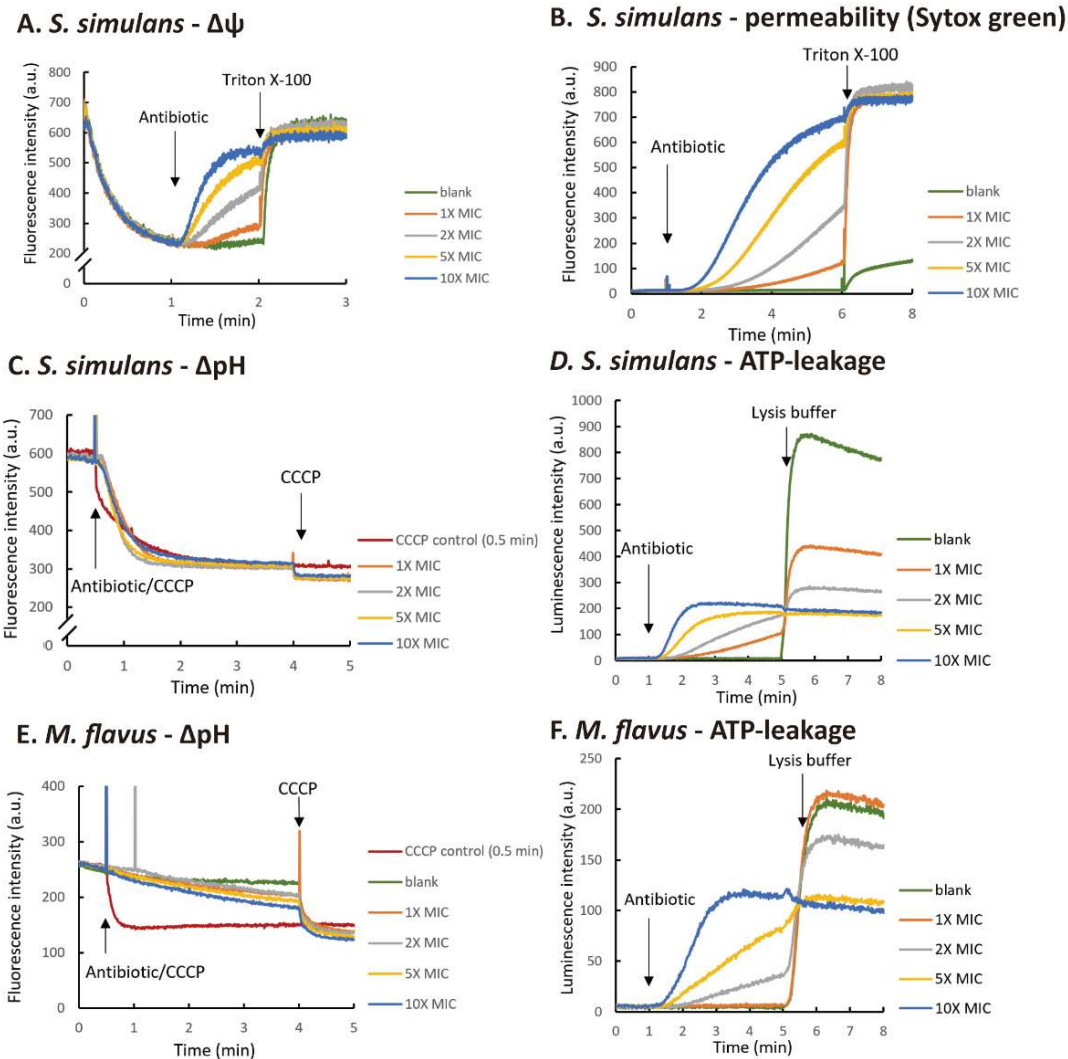


Figure 1. Effects of nisin on the membranes of *S. simulans* and *M. flavus* determined using different fluorescent probes on (A) the membrane potential of *S. simulans*; (B) the membrane permeability of *S. simulans* determined using Sytox green; (C) the intracellular pH of *S. simulans*; (D) the intracellular ATP levels and leakage of ATP from *S. simulans*; (E) the intracellular pH of *M. flavus*; (F) the intracellular ATP levels and leakage of ATP from *M. flavus*. The addition of samples (antibiotics, TritonX-100, CCCP, Lysis buffer) is indicated by arrows. Different amounts of nisin which were equal to 1X MIC (orange), 2X MIC (grey), 5X MIC (yellow) and 10X MIC (blue) are indicated by different color. Blank and CCCP control trace are indicated by green and red. For each bacterium this was repeated twice, thus generating fully independent measurements. Experiment 1E was repeated three times.

3.3.3 Epilancin 15X does not cause major membrane disruptions in *M. flavus* and *S. simulans*.

Epilancin 15X (abbreviated to epilancin) displayed MIC values equal to 100 nM, 75 nM and 100 nM toward *S. simulans*, *M. flavus*, *B. megaterium* respectively. Epilancin behaved quite differently from nisin towards *S. simulans* and *M. flavus*. In contrast to nisin, epilancin was shown to be bacteriostatic towards both *S. simulans* and *M. flavus*; only 1-2 log of cells were killed at the highest concentration (10X MIC) in 5 min (Fig. P4 and P5). The bacteriostatic effect of epilancin towards these strains would suggest that it has less severe membrane perturbing activity. This, we tested using the assays we have validated with nisin as a reference compound above.

First, we used DiSC₂(5) and 5(6)-CFDA, SE to test the membrane depolarization activity and proton permeabilization activity of epilancin toward the two strains. Epilancin causes clear effects in both assays with *S. simulans* that increase with increasing concentration (Fig. 2A and C) albeit that the effects on the Δ pH were not as strong as those of nisin (compare Figures 1C and 2C). Interestingly, concentrations of epilancin of 0.5X MIC and 1X MIC do not appear to cause proton permeability in *M. flavus* (Fig. 2E). On the contrary, the signal has a clear increase, pointing to increased outflow protons from the cells.

In line with epilancin's bacteriostatic activity, it barely shows effects on membrane permeability in experiments using Sytox green, DAPI and luciferase (Fig. 2B and D, Fig. S3A, C and E). Only at high concentrations (5x & 10X MICs) some minor effects can be seen. Furthermore, although epilancin barely causes any ATP leakage from *S. simulans* or *M. flavus*, it did cause the internal ATP concentration to drop in both cells at the higher concentrations (Fig. 2D and S3E) albeit not to a large extent.

Previously, epilancin was predicted to kill bacteria via pore-formation in view of similarities between the structures of epilancin and nisin [47]. Our results show that this cannot be the case, at least not with respect to its activity towards *S. simulans* and *M. flavus*.

3.3.4 Epilancin 15X activity towards *B. megaterium*

Similar to what we observed for nisin, *B. megaterium* was also very sensitive to epilancin. It was clearly bactericidal as at 5X MIC it caused a 4-log reduction in cells after 5 minutes (Fig. P6). This high sensitivity was also reflected in the membrane depolarization assay, where epilancin, like nisin, showed membrane depolarization activity below its MIC value. At 0.1X MIC, epilancin exhibited already more than 50% membrane depolarization in two minutes and effects were maximal at concentrations of 1X MIC or higher (Fig. S3F). The proton permeability assay showed similar results

Analyzing mechanisms of action of antimicrobial peptides on bacterial membranes requires multiple complimentary assays and different bacterial strains

(Fig. S3H). Moreover, the Sytox green and DAPI assays indicated severe membrane damage at these higher concentrations (Fig. 2F and S3G) and these effects parallel the killing rates. Thus, these results suggest that the bactericidal activity of epilancin towards *B. megaterium* is mainly due to its membrane damaging effect.

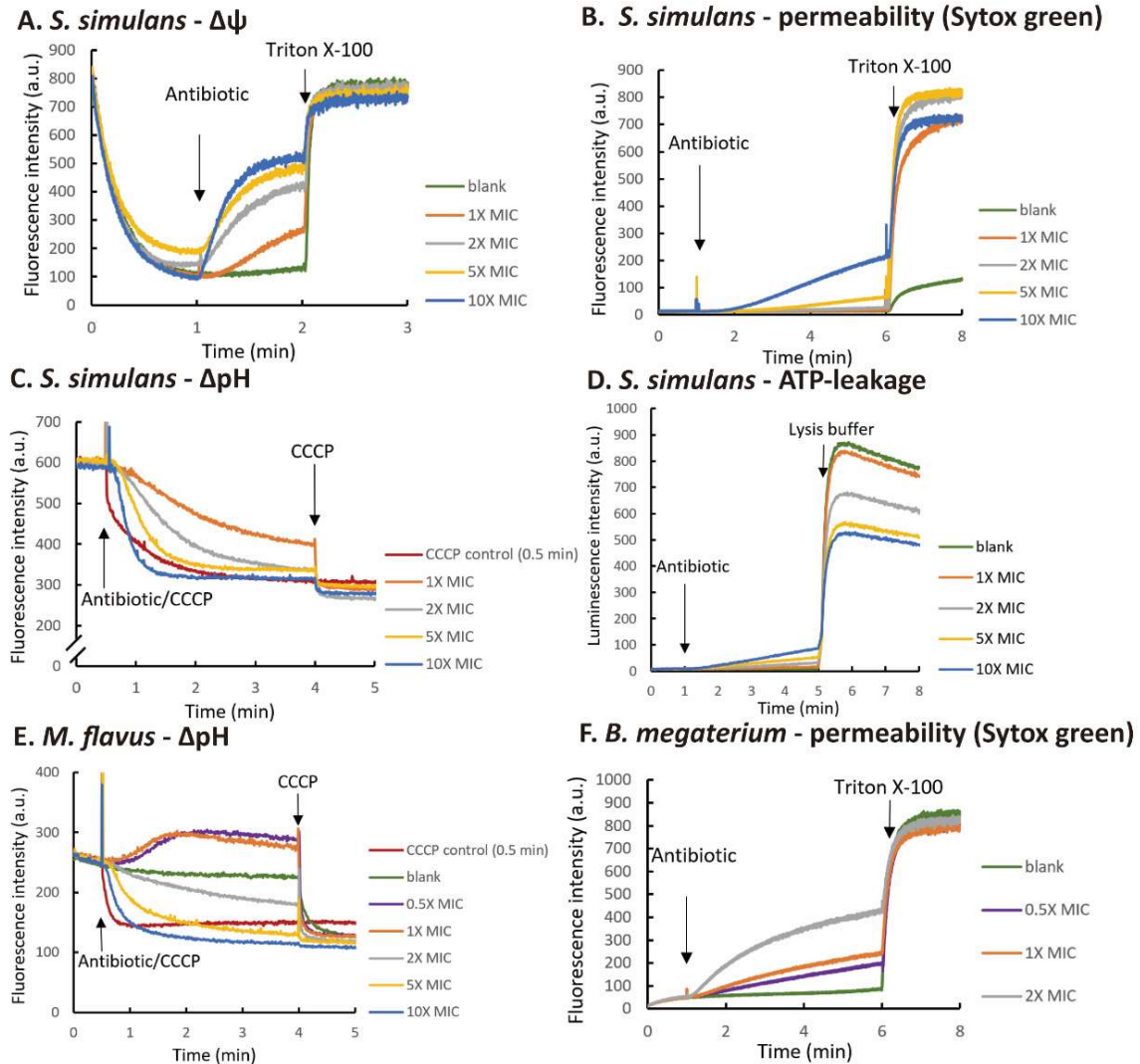


Figure 2. Effects of epilancin 15X on the membrane of *S. simulans*, *M. flavus* and *B. megaterium* determined using different fluorescent probes on (A) the membrane potential of *S. simulans*; (B) the membrane permeability of *S. simulans* determined using Sytox green; (C) the intracellular pH of *S. simulans*; (D) the intracellular ATP levels and leakage of ATP from *S. simulans*; (E) the intracellular pH of *M. flavus*; (F) the membrane permeability of *B. megaterium* determined using Sytox green. The addition of samples (antibiotics, TritonX-100, CCCP, Lysis buffer) is indicated by arrows. Different amounts of epilancin 15X which were equal to 0.5X MIC (purple), 1X MIC (orange), 2X MIC (grey), 5XMIC (yellow) and 10X MIC (blue) are indicated by different color. Blank and CCCP control trace are indicated by green and red. For each bacterium this was repeated twice, thus generating fully independent measurements. Experiment 2E was repeated three times.

3.3.5 [R4L10]-teixobactin induced membrane permeabilization.

[R4L10]-teixobactin displayed a MIC value of 0.125 $\mu\text{g/ml}$ (100 nM) which is 2-fold lower MIC than that of the natural version against MRSAATCC 33591 [52]. Besides, it displays MICs in the range of 0.25-1 $\mu\text{g/ml}$ (200-800 nM) against VRE, 0.03-0.5 $\mu\text{g/ml}$ (24-400 nM) against MRSA, and 0.125-0.5 $\mu\text{g/ml}$ (100-400 nM) against *Bacillus* spp. [52]. In this research, [R4L10]-teixobactin displayed MIC values equal to 1000 nM, 750 nM and 500 nM toward *S. simulans*, *M. flavus*, *B. megaterium* respectively. Thus, our MIC values were close to the range of MIC-values found in the literature even though we used a different method to determine them. The MIC values of [R4L10]-teixobactin toward our three test strains are 6-10 folds higher than that of nisin and epilancin 15X, therefore, to prevent possible a-specific effects due to high peptide concentrations, we only used concentrations equal to 1X, 2X and 5X the MICs of [R4L10]-teixobactin in our membrane disruption assays.

At lower [R4L10]-teixobactin concentrations (1X and 2X MIC), it barely killed *S. simulans* until at 5X MIC, the number of viable cells dropped with 90% in 5 min (Fig. P7). Similar to the case of epilancin, [R4L10]-teixobactin only showed killing activity toward *S. simulans* at the highest concentrations. The time killing assay indicated that [R4L10]-teixobactin should have a relatively low membrane perturbing activity compared to nisin, at least within the short time frame used here.

The membrane depolarization activity of [R4L10]-teixobactin toward *S. simulans* was in line with its low membrane-perturbing activity. Only at the highest concentration (5X MIC) a clear membrane depolarization effect could be observed and the maximal amount of dissipation that was reached in the experiment stayed below the 50% (Fig. 3A). Similarly, the ΔpH was dissipated at concentrations higher than 1x MIC, with maximal effects only at a 5X MIC concentration (Fig. S4B). While similar results were observed in the DAPI assay (Fig. S4A), the Sytox green assay showed a different picture. A clear membrane permeability effect was observed already at 1X MIC and the maximal effect that was obtained at 5X MIC was above 70% (Fig. 3B). In line with these results, [R4L10]-teixobactin induced ATP leakage, and a low but significant amount of ATP was released from the cells at 1X MIC (Fig. 3C). Like nisin, a dual effect could be seen here as the cytosolic ATP concentration dropped significantly at concentrations equal to 2X and 5X MIC (Fig. 3C).

Similar to its activity towards *S. simulans*, [R4L10]-teixobactin killed 90% of *M. flavus* cells in 5 minutes at a concentration equal to 5X MIC (Fig. P8). Likewise, its effects on the membrane potential (Fig. 3D) and ΔpH were also comparable (Fig. 3E) including the rise of the cellular pH at low concentrations of the peptide. No severe permeabilization could be observed at all concentrations in the Sytox assay and ATP only leaked out of the cells at the highest 5X MIC concentration (Fig. S4D and 3F). The DAPI results were (again) hardly showing any response with *M. flavus*, only some

Analyzing mechanisms of action of antimicrobial peptides on bacterial membranes requires multiple complimentary assays and different bacterial strains

effect at 5X MIC could be observed (Fig. S4C). A very interesting effect could be observed for low concentrations (1 and 2X MIC) of [R4L10]-teixobactin on the internal ATP levels. A clear increase in total ATP levels of this bacterium could be observed, which we have never seen before in this test and seems unique for this combination of antibiotic and bacterial strain (Fig. 3F).

As observed for the other peptides, *B. megaterium* was more sensitive towards [R4L10]-teixobactin as well. More severe effects in the time-killing assay was paralleled by severe effects in the assays reporting on membrane permeabilization. [R4L10]-teixobactin at 2X MIC killed 3-log of cells in 5 min while at lower concentrations the effect was substantially lower in this time period (Fig. P9). In all membrane perturbation assays with *B. megaterium*, [R4L10]-teixobactin exhibited clear effects at 0.5X MIC and reached nearly 100% at the concentration of 2X MIC (Fig. S4E-H).

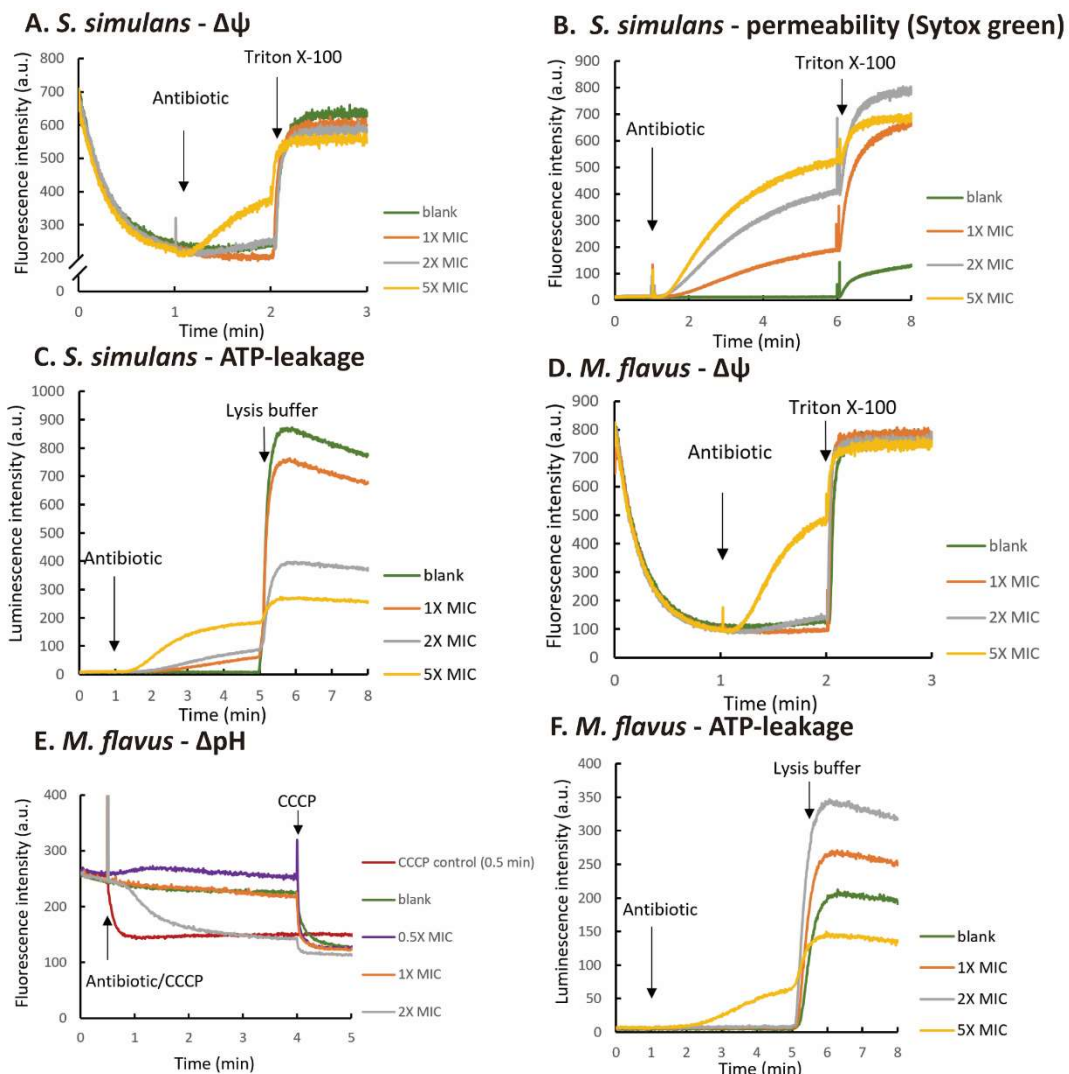


Figure 3. Effects of [R4L10]-teixobactin on the membrane of *S. simulans* and *M. flavus* determined using different fluorescent probes on (A) the membrane potential of *S. simulans* determined using DiSC₂(5); (B) the membrane permeability of *S. simulans* determined using Sytox green; (C) the

ATP levels and leakage of ATP from *S. simulans*; (D) the membrane potential of *M. flavus*; (E) the intracellular pH of *M. flavus* determined, SE; (F) the ATP levels and leakage of ATP from *M. flavus*. The addition of samples (antibiotics, TritonX-100, Lysis buffer) is indicated by arrows. Different amounts of [R4L10]-teixobactin which were equal to 0.5X MIC (purple), 1X MIC (orange), 2X MIC (grey) and 5X MIC (yellow) are indicated by different color. Blank and CCCP control trace are indicated by green and red. For each bacterium this was repeated twice, thus generating fully independent measurements. Experiments 3E and 3F were repeated three times.

3.3.6 The ultra-sensitivity of *B. megaterium* may be related to membrane lipid composition.

What stood out in the experiments above was that the *B. megaterium* cells were very sensitive and rapidly killed by all three antibiotic peptides. This was always paralleled by severe membrane perturbation. To test if this may be caused by the membrane lipid composition of this strain compared to the other strains we determined their composition with respect to the acyl chain and headgroup. There were some differences observed in acyl chain composition between the three strains (Fig. S5). However, these small differences do likely not explain the high sensitivity of *B. megaterium* vs the other strains. This changed when the headgroup composition was determined (Fig. S6). Phosphatidylglycerol (PG) and cardiolipin (CL) were predominantly found in *S. simulans* and *M. flavus*, while phosphatidylethanolamine (PE) could only be observed for *B. megaterium*. Most conspicuous was the absence of Lysyl-PG, a version of PG with a lysine attached making it the only known naturally occurring cationic lipid [57], in the *B. megaterium* extract. Lysyl-PG is synthesized from PG and flopped to the outer monolayer of the plasma membrane by MprF, and is involved in resistance against positively charged AMPs [58]. *B. megaterium* lacks the gene encoding for MprF, which explains the absence of this lipid in the extracts. Therefore, it is tempting to speculate that this absence of Lysyl-PG causes *B. megaterium* to be highly sensitive to the membrane-disruptive effects of the AMPs from in this study.

3.4 Discussion

Fluorescent probes that can measure, somehow, the extent of membrane damage are often used for determining the mode of action of antimicrobial peptides or other antibiotic compounds. Depending on the probe used, moderate or more severe effects on the permeability barrier of the bacterial plasma membrane are measured. Here we used five different assays and three different bacterial strains and compared how they report on the mode of action of three different antimicrobial peptides. First we tested how the different assays report on the well-established mode of action of nisin, that together with Lipid II efficiently forms pores in target membranes. Then, we tested

these systems on two other peptide antibiotics. One peptide with a so far unknown mode of action was the lantibiotic epilancin 15X. The mode of action of the other, the [R4L10] analog of teixobactin, also involves targeting Lipid II and, similar to nisin, it clusters into higher order oligomers in a Lipid II dependent way. Recently, natural teixobactin was shown to induce membrane disruption in conjunction to its assembly into higher order oligomers. Whether this is also the case for the [R4L10] analog was not known [50].

3.4.1 General considerations

Changes in the internal pH of the cell that we measured using 5(6)-CFDA, SE or in the trans-membrane potential measured by DiSC₂(5) were considered as moderate membrane permeabilization effects as they report on leakage of protons into and of (mainly) potassium ions out of the cells respectively. More severe membrane effects we determined by measuring the leakage of DNA probes into, or ATP from the cells. For the latter we devised an on-line luciferase-based assay that is able to determine both the leakage of ATP from the cells as well as the remaining ATP pool left in the cytosol. The membrane potential and Δ pH are directly linked to the cell's ability to generate ATP [56]. Thus, these three assays are, in principle, connected. The two DNA-dye based assays differ in terms of the size of the dye where SYTOX-green (MW 600 g/mol) is more than twice the size of DAPI (MW 277 g/mol) and thus may report differently based on the severity of the membrane perturbation. We have no evidence of these probe interference by the peptides.

Data from the previous century on polymeric exclusion thresholds of gram-positive cell walls indicated that this threshold is rather high (e.g. number average molecular weight, $M_n=30,000$ to $57,000$ for *B. megaterium* and $M_n=25,000$ for *Micrococcus lysodeikticus*) [59]. Likely the *staphylococci* have similar thresholds. This fits nicely with more recent data on the architecture of gram-positive cell walls of *B. subtilis* and *S. aureus* of which the smallest determined pore-size present at the inner side of the peptidoglycan layer was ~ 6 nm [60]. Thus, the different dyes are not expected to be affected by different cell wall architectures. Indeed, we haven't detected any evidence for different behavior of the dyes with the different bacterial strains.

We consider severe membrane perturbation as the fastest way to kill bacteria and we could clearly find a good correlation between the killing kinetics of nisin and the assays that report on severe membrane disruption. An existing correlation between killing kinetics and membrane permeabilization is important to draw proper conclusions on whether the mechanism of action involves membrane perturbation. However, it should be noted that it is impossible to immediately stop the killing of bacteria by nisin (or any other AMP) while determining the number of CFUs after treatment. The amount of viable cells will likely continue to drop to some extent after plating out and incubation overnight, leading to a possible over estimation of the killing rate, especially if the AMPs

have fast killing kinetics. Additionally, it should be realized that the membrane permeability experiments are only “sensitive” for up to two log reductions in cell numbers, as they cannot discriminate between 99% killing (2-log reduction) or 99.9% killing (3-log reduction). Nevertheless, whenever we noticed a higher than 2-log reduction of cell numbers after 5 minutes, this always correlated with the occurrence of severe membrane disruption in the assays. We noticed that, in general, there seemed to be a specific order in which these membrane perturbation effects are occurring. The ion and proton gradients are the first to be dissipated. Often, within the first minute after addition on the AMPs maximal effects were seen in the assays that measured the ΔpH and $\Delta\Psi$, while ATP-leakage and the Sytox green signal only appeared after a lag time (usually 30 seconds to 1 minute). Yet, only the Sytox, DAPI and ATP assays correlated with bacterial killing, which implies that the effect on the ΔpH and $\Delta\Psi$ alone, although stress related, are not sufficient to conclude that AMP's (or other compound's) killing mode involves membrane perturbation.

3.4.2 Specific observations.

3.4.2.1 Nisin

From a targeted pore-former such as nisin it is to be expected that, provided it is able to reach Lipid II in the target membrane, it will cause severe membrane disruption. The pore-size of the nisin-lipid II pore-complex, estimated to be of about 2 nm in diameter, would easily allow passage of ATP and the DNA probes used in this study [46]. This was indeed what we observed, as virtually all assays indicated fast and severe membrane effects. There were however two exceptions; the DAPI assay with *M. flavus* and the proton permeability assay with the same bacteria. In combination with *M. flavus*, the DAPI probe displayed strange behavior compared to Sytox green with all the peptides tested here. This suggests that this combination of probe and bacterium is for some reason not compatible, emphasizing the need for multiple probes and bacteria when testing membrane effects of AMPs and proper positive controls. Our observation that nisin didn't cause a rapid and full dissipation of the proton gradient in *M. flavus* even at very high (10 X MIC) concentrations was especially surprising in relation to the results obtained with the other probes that all show (at least some) membrane perturbation at 1-2 X MIC. The other two peptides did show dissipation of the ΔpH , which, together with the behavior of the control (CCCP), rule out that 5(6)-CFDA is, similar to DAPI, not compatible with *M. flavus*. We currently do not have a good explanation for this aberrant effect of nisin on the pH gradient in *M. flavus*.

3.4.2.2 Epilancin 15X

The mechanism of action of epilancin 15X appeared to be different for all the three test strains we used. It acted bactericidal towards *B. megaterium* and, in line with this, it

clearly induced membrane permeabilization in all our experiments even at concentrations lower than the MIC. The clear effects in the Sytox green and DAPI assays indicate a severe membrane damaging effect in this bacterium, possibly involving pore-formation. In contrast, epilancin 15X acted bacteriostatic towards *S. simulans* and *M. flavus* and displayed severe membrane effects (Sytox green influx and ATP-leakage) at relative high concentrations only with *S. simulans*. While with most assays a similar activity could be observed with the two bacteria, *M. flavus* showed a surprising increase of the internal pH in the presence of low (0.5 and 1 X MIC) peptide concentrations. At these concentrations no drop in cellular ATP levels and only a small dissipation of the membrane potential could be detected. This picture suggests that epilancin 15X targets an ATP-consuming process, while also the ATP-synthesis is inhibited, which in turn decreases the influx of protons [61]. In the meantime, protons are still pumped out of the cells by the respiratory chain. These effects together led to the increase of the cellular pH [62].

The inhibition of ATP-synthesis is most likely the result of the epilancin-induced dissipation of the membrane potential, the main determinant of the activity of the ATP-synthase [63-65]. Because bacteria maintained a ΔpH (which even increased at low concentrations) this suggests that the membrane is still intact. Therefore, the dissipation of the membrane potential is unlikely caused by a direct effect on the bilayer lipids of *M. flavus*, but may rather involve perturbation of the ion homeostasis in another way. A direct effect on ion transporters cannot be ruled out.

3.4.2.3 [R4L10]-teixobactin

The binding mode of [R4L10]-teixobactin to Lipid II in bacterial membranes was elucidated recently. The C-terminal depsi-cycle of teixobactin binds the pyrophosphate and MurNAc parts of Lipid II whereupon it assembles into antiparallel β -sheets in the membrane [51]. This is followed by a slower formation of a supramolecular fibrillar structure. For natural teixobactin, this was recently also shown [50]. The multimeric structure of the natural form contains, like the [R4L10] variant a concentrated hydrophobic patch and displays curvature that results in local thinning of the membrane upon fibril formation, which was considered as the reason for teixobactin's ability to cause membrane permeabilization. The polyprenyl tails of Lipid II that are concentrated within the hydrophobic patch are proposed to also play an active role in the membrane perturbation [50]. Although the 10th amino acid *allo*-enduracididine of teixobactin is replaced by leucine in [R4L10]-teixobactin which reduces Lipid II binding affinity, the interaction of R4L10 teixobactin with Lipid II resembles that of natural teixobactin in these aspects [50, 51]. Indeed, we could show with our assays that also [R4L10]-teixobactin was able to permeabilize bacterial membranes, albeit that the severity of this permeabilization depended on the strain tested.

Similar as was observed for epilancin 15X, [R4L10]-teixobactin displayed different

behavior towards the three different indicator strains. Towards *B. megaterium*, killing was paralleled by membrane perturbations in all assays, suggesting that membrane perturbation is a major aspect of [R4L10]-teixobactin's mechanism of action towards this bacterium. While [R4L10]-teixobactin induced somewhat less severe membrane effects towards *S. simulans*, which were in line with previous results, *M. flavus* was not that sensitive to [R4L10]-teixobactin [50]. What again stood out with this bacterium was an increased intracellular pH at 0.5 X MIC, that was also observed for epilancin, albeit that the effect was less severe with the [R4L10]-teixobactin variant. Interestingly and contrasting the effects of epilancin on this bacterium, [R4L10]-teixobactin caused an increase in intracellular ATP at the lower concentrations. This suggests that at least one major ATP-consuming biosynthesis pathway has been stopped and that the ATP-synthase remained active. Inhibition of ATP-consumption in the cells is most likely caused by blocking peptidoglycan and wall teichoic acid biosynthesis pathways via binding of the teixobactin analog to the isoprenoid-based precursors [50, 51]. The lack of effect on the membrane potential in these bacteria would explain that the ATP-synthase activity remains intact. Active ATP-synthase would then explain the lesser effects on the internal pH at low concentrations (0.5 and 1.0 x MIC), as protons would be flowing back to the cytosol via the ATP-synthase.

3.5 Conclusions

In this research, we have developed an on-line ATP measurement which determines the extent of ATP leakage from the bacteria in time and the total amount of ATP remaining in the bacteria. The on-line ATP measurements combined with membrane potential depolarization assays and proton permeability assays reflect how antibiotics interfere with the intracellular homeostasis of the pH, ions and ATP, which are highly interconnected and regulated. These three assays combined form a very powerful tool to reveal antimicrobial mechanisms. In view of their connectedness, we recommend to always combine these three assays if membrane effects of AMPs or other compounds are studied.

Almost all assays were consistent with the mode of action of nisin as the typical example of a targeted pore-former. Yet, even for such a clear MOA, deviations were observed in certain assay-bacterium combinations. This points to the importance of using multiple assays and bacteria for (general) mode of action studies.

The different behavior of epilancin 15X to the three strains makes it difficult to propose one general mode of action for this peptide. This, together with the recently found antagonization of the activity of epilancin 15X by Lipid II and, to a lesser extent, DOPG [40], indicates the need for further investigation of epilancin's mechanism of action in relation to its possible target.

For [R4L10]-teixobactin it is clear that its primary target, like natural teixobactin, is Lipid

II and other prenyl-pyrophosphate-linked precursors [49]. The interaction with Lipid II leads to the formation of supramolecular fibrillar structures on the target membrane [50]. Whether the formation of these fibrillar structures leads to membrane damaging effects seems to depend on the membrane lipid composition of the target strain that is tested.

Footnotes:

1. Triton X-100 only induced a 100% effect in the control situation of our Sytox-green with *B. megaterium*. For the other two bacteria, a 100% effect was only obtained upon Triton X-100 addition to the cells in the presence of the peptides. Triton X-100 addition did cause a 100% effect with all bacteria in the membrane depolarization assay. Another example of the higher sensitivity of this assay to relative minor membrane perturbations.

The lysis buffer supplied with the BacTiter-Glo kit seemed to be an efficient way for bacterial cell lysis and was compatible with the membrane depolarization, where it gave the same results, and DAPI assays. However, it was not compatible with the Sytox-green assay as this led to significant quenching of the fluorescence.

3.6 References

1. Wimley, W.C. and K. Hristova, *Antimicrobial peptides: successes, challenges and unanswered questions*. The Journal of membrane biology, 2011. **239**(1-2): p. 27-34.
2. Reddy, K., R. Yedery, and C. Aranha, *Antimicrobial peptides: premises and promises*. International journal of antimicrobial agents, 2004. **24**(6): p. 536-547.
3. Koczulla, A.R. and R. Bals, *Antimicrobial peptides*. Drugs, 2003. **63**(4): p. 389-406.
4. Brogden, K.A., *Antimicrobial peptides: pore formers or metabolic inhibitors in bacteria?* Nature Reviews Microbiology, 2005. **3**(3): p. 238-250.
5. Oren, Z. and Y. Shai, *Mode of action of linear amphipathic α - helical antimicrobial peptides*. Peptide Science, 1998. **47**(6): p. 451-463.
6. Huang, H.W., F.-Y. Chen, and M.-T. Lee, *Molecular mechanism of peptide-induced pores in membranes*. Physical review letters, 2004. **92**(19): p. 198304.
7. Matsuzaki, K., *Membrane Permeabilization Mechanisms*. Adv Exp Med Biol, 2019. **1117**: p. 9-16.
8. Lohner, K., *New strategies for novel antibiotics: peptides targeting bacterial cell membranes*. Gen Physiol Biophys, 2009. **28**(2): p. 105-16.
9. Epand, R.M. and R.F. Epand, *Bacterial membrane lipids in the action of antimicrobial agents*. J Pept Sci, 2011. **17**(5): p. 298-305.
10. Haukland, H.H., et al., *The antimicrobial peptides lactoferricin B and magainin 2 cross over the bacterial cytoplasmic membrane and reside in the cytoplasm*. FEBS Letters, 2001. **508**(3): p. 389-393.
11. Nguyen, L.T., E.F. Haney, and H.J. Vogel, *The expanding scope of antimicrobial peptide structures and their modes of action*. Trends Biotechnol, 2011. **29**(9): p. 464-72.
12. Gidalevitz, D., et al., *Interaction of antimicrobial peptide protegrin with biomembranes*. Proc Natl Acad Sci U S A, 2003. **100**(11): p. 6302-7.
13. Kalfa, V.C., et al., *Congeners of SMAP29 kill ovine pathogens and induce ultrastructural damage in bacterial cells*. Antimicrob Agents Chemother, 2001. **45**(11): p. 3256-61.
14. Falagas, M.E. and S.K. Kasiakou, *Colistin: the revival of polymyxins for the management of multidrug-resistant gram-negative bacterial infections*. Clin Infect Dis, 2005. **40**(9): p. 1333-41.
15. Schmidt, N.W. and G.C.L. Wong, *Antimicrobial peptides and induced membrane curvature: Geometry, coordination chemistry, and molecular engineering*. Current Opinion in Solid State and Materials Science, 2013. **17**(4): p. 151-163.
16. Chongsiriwatana, N.P., et al., *Intracellular biomass flocculation as a key mechanism of rapid*

Analyzing mechanisms of action of antimicrobial peptides on bacterial membranes requires multiple complimentary assays and different bacterial strains

- bacterial killing by cationic, amphipathic antimicrobial peptides and peptoids*. Scientific Reports, 2017. **7**(1): p. 16718.
17. Breukink, E., et al., *Use of the cell wall precursor lipid II by a pore-forming peptide antibiotic*. Science, 1999. **286**(5448): p. 2361-2364.
 18. Galván Márquez, I.J., et al., *Mode of action of nisin on Escherichia coli*. Can J Microbiol, 2020. **66**(2): p. 161-168.
 19. Rottenberg, H., *The measurement of membrane potential and ΔpH in cells, organelles, and vesicles*. Methods Enzymol, 1979. **55**: p. 547-69.
 20. Peña, A., et al., *The use of a cyanine dye in measuring membrane potential in yeast*. Archives of Biochemistry and Biophysics, 1984. **231**(1): p. 217-225.
 21. Singh, A.P. and P. Nicholls, *Cyanine and safranin dyes as membrane potential probes in cytochrome c oxidase reconstituted proteoliposomes*. Journal of Biochemical and Biophysical Methods, 1985. **11**(2): p. 95-108.
 22. Milligan, G. and P.G. Strange, *Reduction in accumulation of [^3H]triphenylmethylphosphonium cation in neuroblastoma cells caused by optical probes of membrane potential: Evidence for interactions between carbocyanine dyes and lipophilic anions*. Biochimica et Biophysica Acta (BBA) - Molecular Cell Research, 1983. **762**(4): p. 585-592.
 23. Waggoner, A.S., *Dye Indicators of Membrane Potential*. Annual Review of Biophysics and Bioengineering, 1979. **8**(1): p. 47-68.
 24. Cabrini, G. and A.S. Verkman, *Localization of cyanine dye binding to brush-border membranes by quenching of n-(9-anthroyloxy) fatty acid probes*. Biochim Biophys Acta, 1986. **862**(2): p. 285-93.
 25. Sims, P.J., et al., *Mechanism by which cyanine dyes measure membrane potential in red blood cells and phosphatidylcholine vesicles*. Biochemistry, 1974. **13**(16): p. 3315-3330.
 26. Krasne, S.J.B.j., *Interactions of voltage-sensing dyes with membranes. I. Steady-state permeability behaviors induced by cyanine dyes*. 1980. **30**(3): p. 415-439.
 27. Krasne, S., *Interactions of voltage-sensing dyes with membranes. II. Spectrophotometric and electrical correlates of cyanine-dye adsorption to membranes*. Biophysical journal, 1980. **30**(3): p. 441-462.
 28. Breeuwer, P., et al., *A Novel Method for Continuous Determination of the Intracellular pH in Bacteria with the Internally Conjugated Fluorescent Probe 5 (and 6-)Carboxyfluorescein Succinimidyl Ester*. Applied and environmental microbiology, 1996. **62**(1): p. 178-183.
 29. Kuo, S.C. and J.O. Lampen, *Osmotic Regulation of Invertase Formation and Secretion by Protoplasts of *Saccharomyces**. Journal of Bacteriology, 1971. **106**(1): p. 183.

30. Lomakina, G.Y., Y.A. Modestova, and N.N. Ugarova, *Bioluminescence assay for cell viability*. Biochemistry (Mosc), 2015. **80**(6): p. 701-13.
31. Roth, B.L., et al., *Bacterial viability and antibiotic susceptibility testing with SYTOX green nucleic acid stain*. Applied and Environmental Microbiology, 1997. **63**(6): p. 2421.
32. Yasir, M., D. Dutta, and M.D.P. Willcox, *Comparative mode of action of the antimicrobial peptide melimine and its derivative Mel4 against Pseudomonas aeruginosa*. Scientific reports, 2019. **9**(1): p. 7063-7063.
33. Rathinakumar, R., W.F. Walkenhorst, and W.C. Wimley, *Broad-spectrum antimicrobial peptides by rational combinatorial design and high-throughput screening: the importance of interfacial activity*. Journal of the American Chemical Society, 2009. **131**(22): p. 7609-7617.
34. Pérez-Peinado, C., et al., *Mechanisms of bacterial membrane permeabilization by crotalidicin (Ctn) and its fragment Ctn(15-34), antimicrobial peptides from rattlesnake venom*. The Journal of biological chemistry, 2018. **293**(5): p. 1536-1549.
35. Coleman, A.W., M.J. Maguire, and J.R. Coleman, *Mithramycin- and 4'-6-diamidino-2-phenylindole (DAPI)-DNA staining for fluorescence microspectrophotometric measurement of DNA in nuclei, plastids, and virus particles*. Journal of Histochemistry & Cytochemistry, 1981. **29**(8): p. 959-968.
36. Mangoni, M.L., et al., *Effects of the antimicrobial peptide temporin L on cell morphology, membrane permeability and viability of Escherichia coli*. 2004. **380**(3): p. 859-865.
37. Urfer, M., et al., *A peptidomimetic antibiotic targets outer membrane proteins and disrupts selectively the outer membrane in Escherichia coli*. 2016. **291**(4): p. 1921-1932.
38. Chudzik, B., et al., *A new look at the antibiotic amphotericin B effect on Candida albicans plasma membrane permeability and cell viability functions*. European Biophysics Journal, 2015. **44**(1): p. 77-90.
39. Chatterjee, C., et al., *Biosynthesis and Mode of Action of Lantibiotics*. Chemical Reviews, 2005. **105**(2): p. 633-684.
40. Wang, X., Q. Gu, and E. Breukink, *Non-lipid II targeting lantibiotics*. Biochimica et Biophysica Acta (BBA) - Biomembranes, 2020. **1862**(8): p. 183244.
41. Breukink, E., et al., *Lipid II is an intrinsic component of the pore induced by nisin in bacterial membranes*. J Biol Chem, 2003. **278**(22): p. 19898-903.
42. Hasper, H.E., B. de Kruijff, and E. Breukink, *Assembly and Stability of Nisin-Lipid II Pores*. Biochemistry, 2004. **43**(36): p. 11567-11575.
43. van Heusden, H.E., B. de Kruijff, and E. Breukink, *Lipid II induces a transmembrane orientation of the pore-forming peptide lantibiotic nisin*. Biochemistry, 2002. **41**(40): p. 12171-8.
44. Wiedemann, I., et al., *Specific binding of nisin to the peptidoglycan precursor lipid II combines*

Analyzing mechanisms of action of antimicrobial peptides on bacterial membranes requires multiple complimentary assays and different bacterial strains

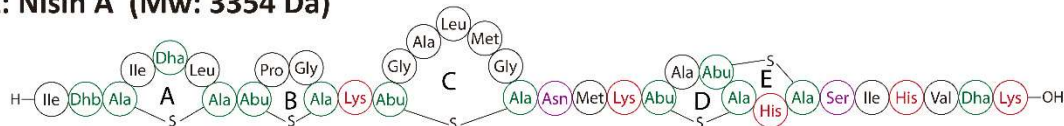
- pore formation and inhibition of cell wall biosynthesis for potent antibiotic activity.* Journal of Biological Chemistry, 2001. **276**(3): p. 1772-1779.
45. Medeiros-Silva, J., et al., *High-resolution NMR studies of antibiotics in cellular membranes.* Nature Communications, 2018. **9**(1): p. 3963.
 46. Wiedemann, I., R. Benz, and H.-G. Sahl, *Lipid II-Mediated Pore Formation by the Peptide Antibiotic Nisin: a Black Lipid Membrane Study.* Journal of Bacteriology, 2004. **186**(10): p. 3259.
 47. Velásquez, J.E., X. Zhang, and W.A. Van Der Donk, *Biosynthesis of the antimicrobial peptide epilancin 15X and its N-terminal lactate.* Chemistry & biology, 2011. **18**(7): p. 857-867.
 48. Ekkelenkamp, M.B., et al., *Isolation and structural characterization of epilancin 15X, a novel lantibiotic from a clinical strain of Staphylococcus epidermidis.* FEBS Letters, 2005. **579**(9): p. 1917-1922.
 49. Ling, L.L., et al., *A new antibiotic kills pathogens without detectable resistance.* Nature, 2015. **517**(7535): p. 455-9.
 50. Shukla, R., et al., *Teixobactin kills bacteria by a two-pronged attack on the cell envelope.* Nature, 2022. **608**(7922): p. 390-396.
 51. Shukla, R., et al., *Mode of action of teixobactins in cellular membranes.* Nat Commun, 2020. **11**(1): p. 2848.
 52. Parmar, A., et al., *Design and Syntheses of Highly Potent Teixobactin Analogues against Staphylococcus aureus, Methicillin-Resistant Staphylococcus aureus (MRSA), and Vancomycin-Resistant Enterococci (VRE) in Vitro and in Vivo.* Journal of Medicinal Chemistry, 2018. **61**(5): p. 2009-2017.
 53. Paiva, A.D., E. Breukink, and H.C. Mantovani, *Role of lipid II and membrane thickness in the mechanism of action of the lantibiotic bovicin HC5.* Antimicrobial agents and chemotherapy, 2011. **55**(11): p. 5284-5293.
 54. Egan, A.J.F., et al., *Induced conformational changes activate the peptidoglycan synthase PBP1B.* Molecular Microbiology, 2018. **110**(3): p. 335-356.
 55. Sahl, H.-G. and H. Brandis, *Production, purification and chemical properties of an antistaphylococcal agent produced by Staphylococcus epidermidis.* Microbiology, 1981. **127**(2): p. 377-384.
 56. Maloney, P.C., E.R. Kashket, and T.H. Wilson, *A Protonmotive Force Drives ATP Synthesis in Bacteria.* Proceedings of the National Academy of Sciences, 1974. **71**(10): p. 3896.
 57. Rashid, R., M. Veleba, and K.A. Kline, *Focal Targeting of the Bacterial Envelope by Antimicrobial Peptides.* Front Cell Dev Biol, 2016. **4**: p. 55.
 58. Friedman, L., J.D. Alder, and J.A. Silverman, *Genetic changes that correlate with reduced susceptibility to daptomycin in Staphylococcus aureus.* Antimicrob Agents Chemother, 2006.

- 50(6):** p. 2137-45.
59. Scherrer, R. and P. Gerhardt, *Molecular sieving by the Bacillus megaterium cell wall and protoplast*. J Bacteriol, 1971. **107(3)**: p. 718-35.
 60. Pasquina-Lemonche, L., et al., *The architecture of the gram-positive bacterial cell wall*. Nature, 2020. **582(7811)**: p. 294-297.
 61. Bartek, I.L., et al., *Antibiotic Bactericidal Activity Is Countered by Maintaining pH Homeostasis in Mycobacterium smegmatis*. mSphere, 2016. **1(4)**.
 62. Kaila, V.R.I. and M. Wikström, *Architecture of bacterial respiratory chains*. Nat Rev Microbiol, 2021. **19(5)**: p. 319-330.
 63. Kaim, G. and P. Dimroth, *ATP synthesis by the F1Fo ATP synthase of Escherichia coli is obligatorily dependent on the electric potential*. FEBS Lett, 1998. **434(1-2)**: p. 57-60.
 64. Kaim, G. and P. Dimroth, *Voltage-generated torque drives the motor of the ATP synthase*. Embo j, 1998. **17(20)**: p. 5887-95.
 65. Kaim, G. and P. Dimroth, *ATP synthesis by F-type ATP synthase is obligatorily dependent on the transmembrane voltage*. Embo j, 1999. **18(15)**: p. 4118-27.

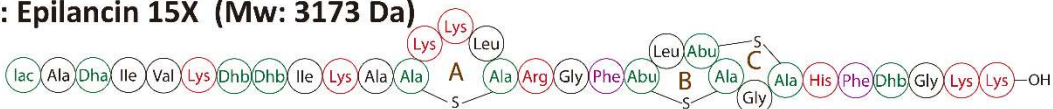
3.7 Supplement information

Antimicrobial Peptides

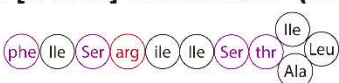
A: Nisin A (Mw: 3354 Da)



B: Epilancin 15X (Mw: 3173 Da)



C: [R4L10]-teixobactin (Mw: 1230 Da)



- Non-Polar amino acid
- Polar amino acid
- Negative charged amino acid
- Positive charged amino acid
- Modified amino acid

Figure S1. Structures of nisin A, Epilancin 15X and [R4L10]-teixobactin. D-amino acids were indicated in non-capital letters. Nisin contains 5 positive charged amino acids, and its charge is +3 to +5 depending on the pH. Epilancin 15X contains 8 positive charged amino acids, and its charge is +6 to +7 depending on the pH. [R4L10]-teixobactin contains 1 positive charged amino acid, and its charge is +2. Modified amino acids abbreviations: Dha (2,3-dehydroalanine), Dhb ((Z)-2,3-dehydrobutyrine), Abu (2-aminobutyric acid), Lac (Lactate).

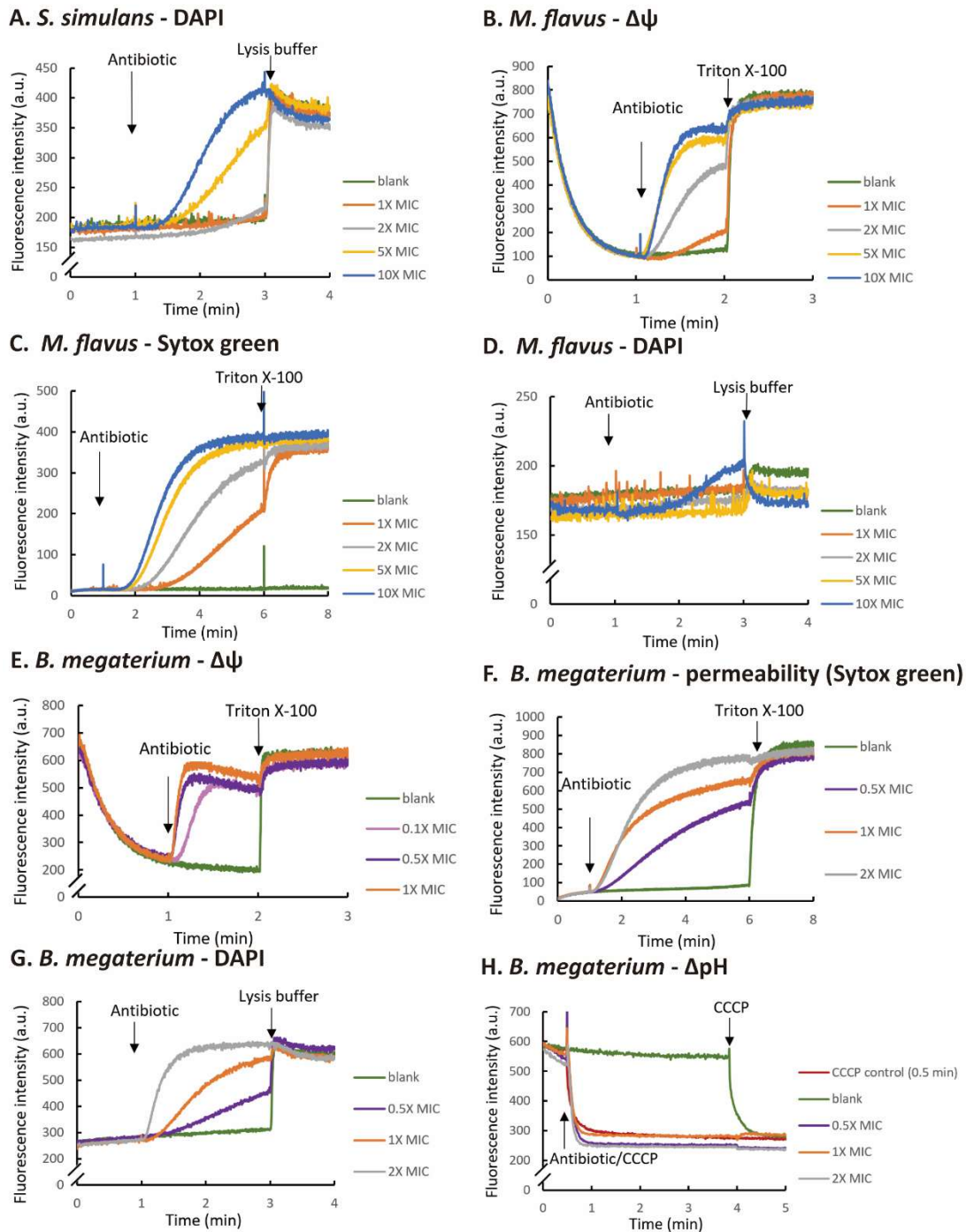


Figure S2. Effects of nisin on the membranes of *S. simulans*, *M. flavus* and *B. megaterium* determined using different fluorescent probes on (A) the membrane permeability of *S. simulans* determined using DAPI (B) the membrane potential of *M. flavus* (C) the membrane permeability of *M. flavus* determined using Sytox green (D) the membrane permeability of *M. flavus* determined using DAPI (E) on the membrane potential of *B. megaterium* (F) the membrane permeability of *B. megaterium* determined using Sytox green (G) the membrane permeability of *B. megaterium* determined using DAPI (H) the intracellular pH of *B. megaterium*. The addition of samples (antibiotics, Triton-100X, CCCP, Lysis buffer) is indicated by arrows. Different amounts of nisin

Analyzing mechanisms of action of antimicrobial peptides on bacterial membranes requires multiple complimentary assays and different bacterial strains

which were equal to 0.1X MIC (pink), 0.5X MIC (purple), 1X MIC (orange), 2X MIC (grey), 5X MIC (yellow) and 10X MIC (blue) are indicated by different color. Blank and CCCP control trace are indicated by green and red. For each bacterium this was repeated at least twice, thus generating fully independent measurements.

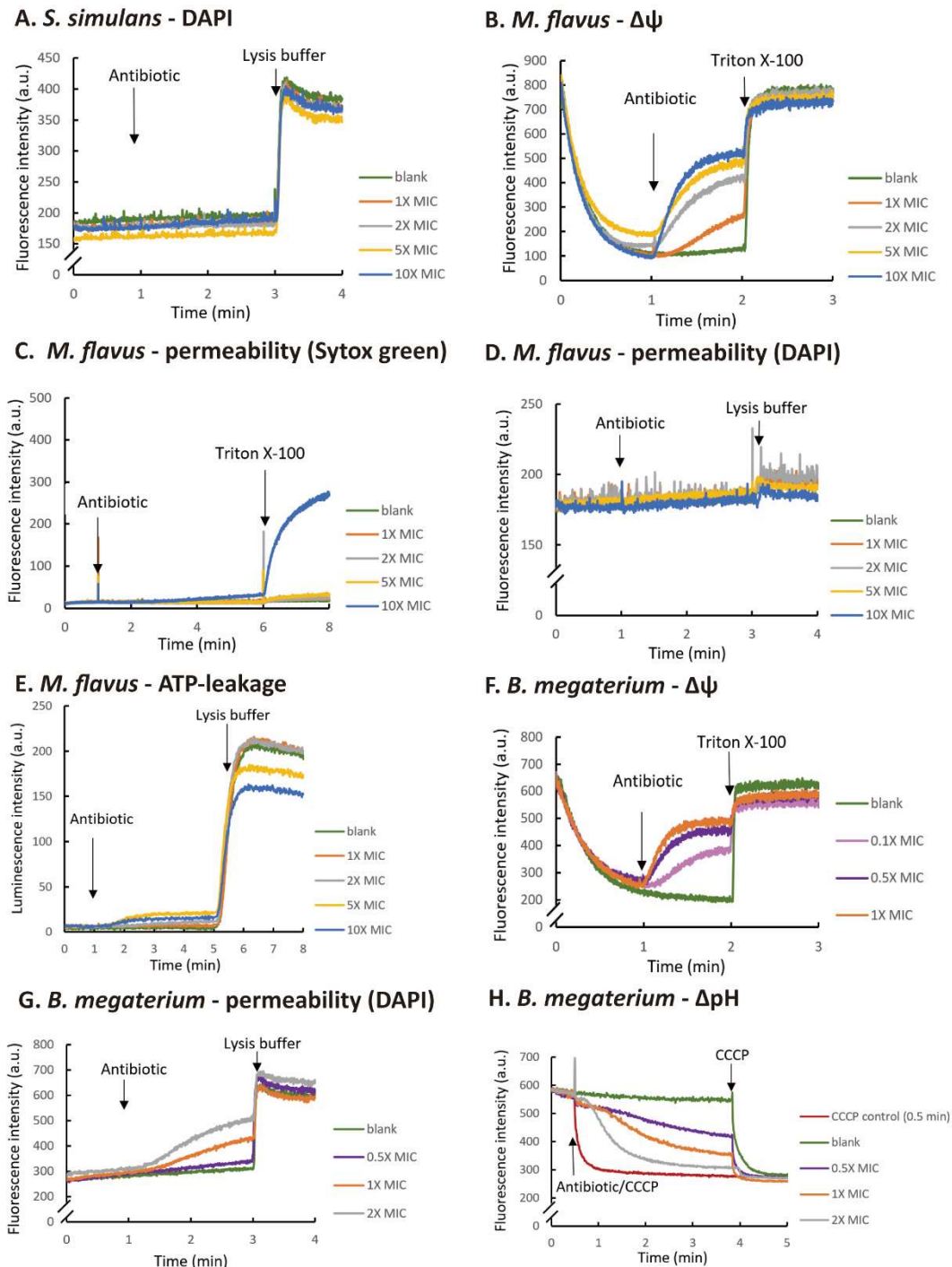


Figure S3. Effects of epilancin 15X on the membrane of *S. simulans*, *M. flavus* and *B. megaterium* determined using different fluorescent probes on (A) the membrane permeability of *S. simulans*

determined using DAPI (B) the membrane potential of *M. flavus* (C) the membrane permeability of *M. flavus* determined using Sytox green (D) the membrane permeability of *M. flavus* determined using DAPI (E) the intracellular ATP levels and leakage of ATP from *M. flavus* (F) the membrane potential of *B. megaterium* (G) the membrane permeability of *B. megaterium* determined using DAPI (H) the intracellular pH of *B. megaterium*. The addition of samples (antibiotics, Triton-100X, CCCP, Lysis buffer) were indicated by arrows. Different amounts of epilancin 15X which were equal to 0.1X MIC (pink), 0.5X MIC (purple), 1X MIC (orange), 2X MIC (grey), 5X MIC (yellow) and 10X MIC (blue) are indicated by different color. Blank and CCCP control trace are indicated by green and red. For each bacterium this was repeated at least twice, thus generating fully independent measurements.

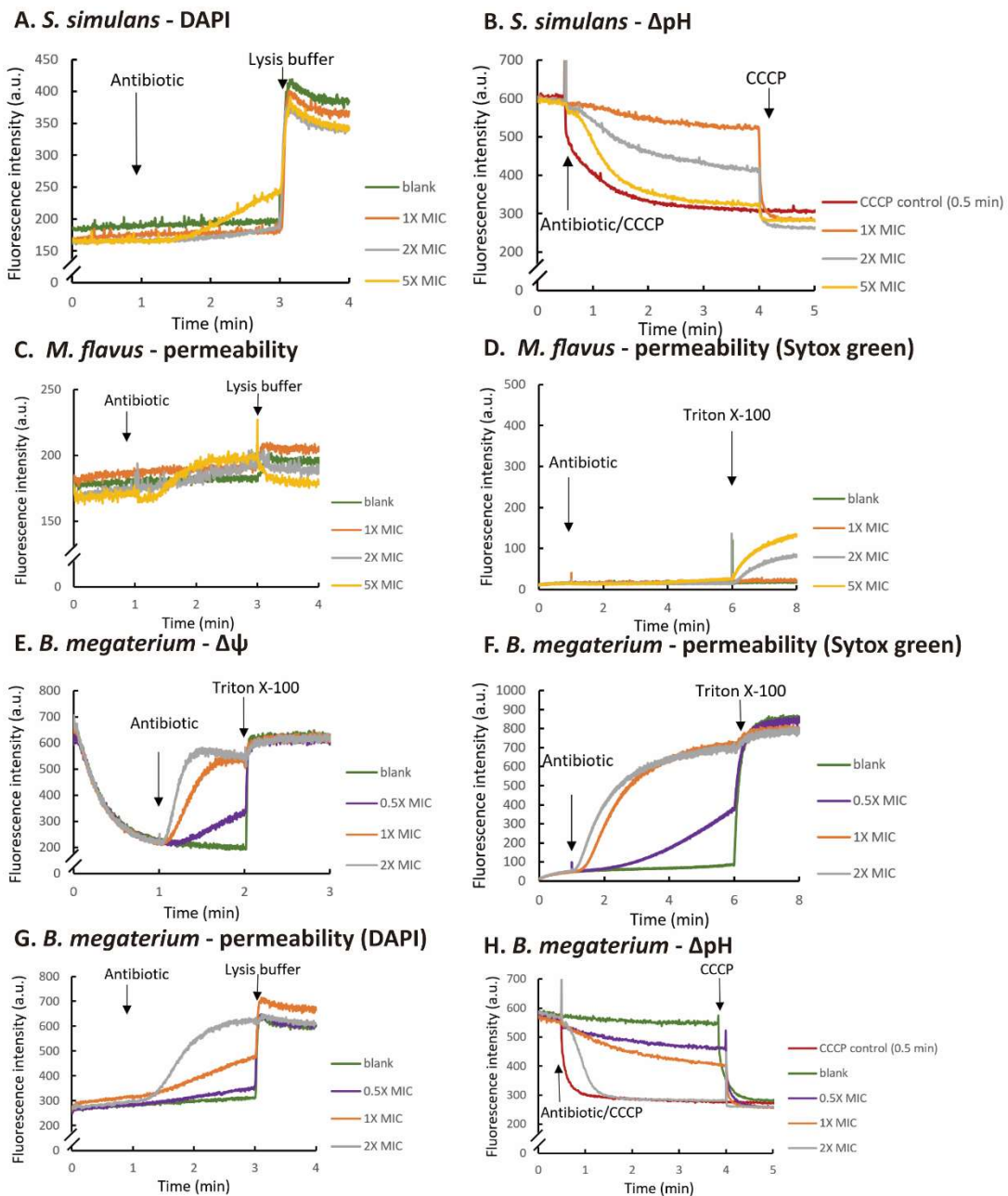


Figure S4. Effects of [R4L10]-teixobactin on the membrane of *S. simulans*, *M. flavus* and *B. megaterium* determined using different fluorescent probes on (A) the membrane permeability of *S. simulans* determined using DAPI (B) the intracellular pH of *S. simulans* (C) the membrane of *M. flavus* determined permeability using DAPI (D) the membrane permeability of *M. flavus* determined using Sytox green (E) the membrane potential of *B. megaterium* (F) the membrane permeability of *B. megaterium* determined using Sytox green (G) the membrane permeability of *B. megaterium* determined using DAPI (H) the intracellular pH of *B. megaterium*. The addition of samples (antibiotics, Triton-100X, CCCP, Lysis buffer) is indicated by arrows. Different amounts of [R4L10]-teixobactin which were equal to 0.5X MIC (purple), 1X MIC (orange), 2X MIC (grey) and 5X MIC (yellow) are indicated by different color. Blank and CCCP control trace are indicated by green and red. For each bacterium this was repeated at least twice, thus generating fully independent measurements.

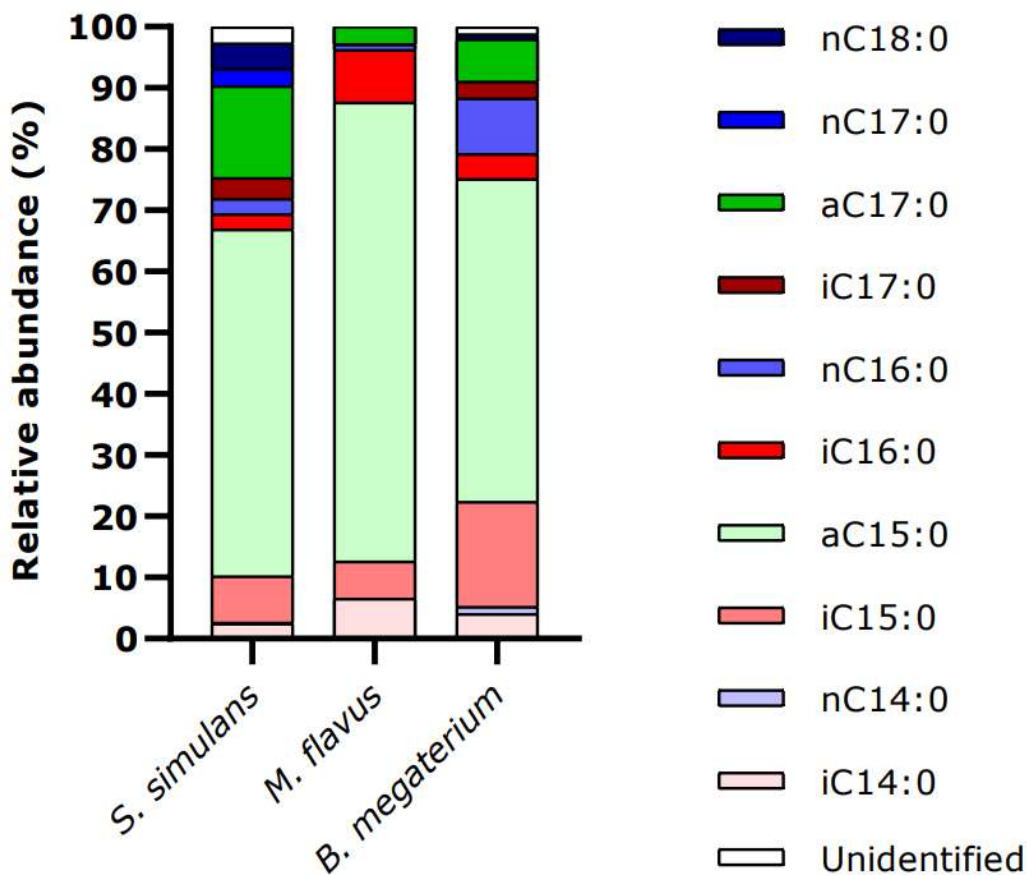


Figure S5. Analysis of the acyl chain compositions of *S. simulans*, *M. flavus*, *B. megaterium*

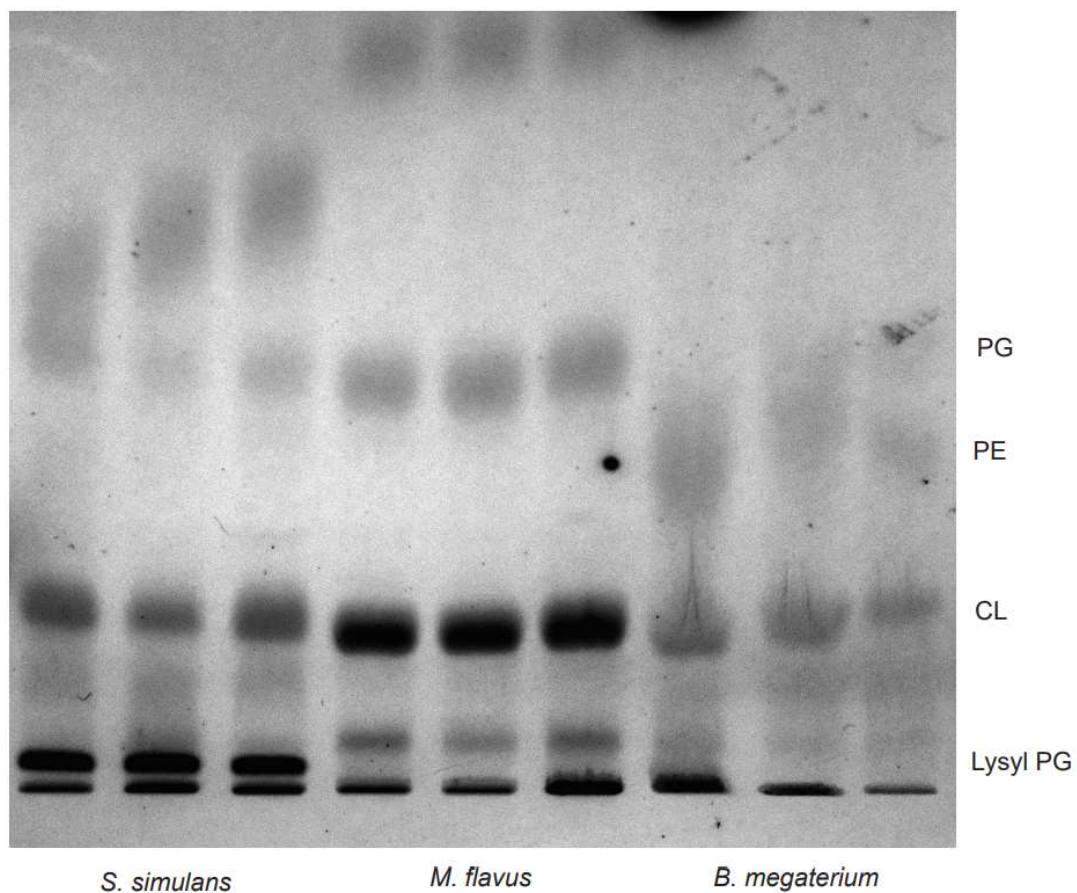


Figure S6. TLC analysis of lipid compositions of *S. simulans*, *M. flavus* and *B. megaterium*. Positions of phospholipid references are indicated at the right of the TLC. The TLC was scanned, the blue channel of the RGB picture was used for the grey-scale image and the levels were adapted such to provide maximal contrast of the different lipid bands using Adobe Photoshop. A cut out from just below the front of the TLC is shown. Three samples from independently grown cells are spotted per strain.

Plates section

This section mainly focused on the killing activity of nisin, epilancin 15X, [R4L10]-teixobactin towards *S. simulans*, *M. flavus*, *B. megaterium*. For each figure, the first line of plates was the count of 5 μ L of bacteria at OD_{600nm}=0.05 by 10-folds series dilution. Nisin, epilancin 15X, [R4L10]-teixobactin which were equal to different times of MICs treated with bacteria in 0-5 min. 5 μ L of bacteria at each minute was taken and spread on plates. The number of bacteria after 5min treatment of antibiotics were counted by 10-folds series dilution.

Chapter 3

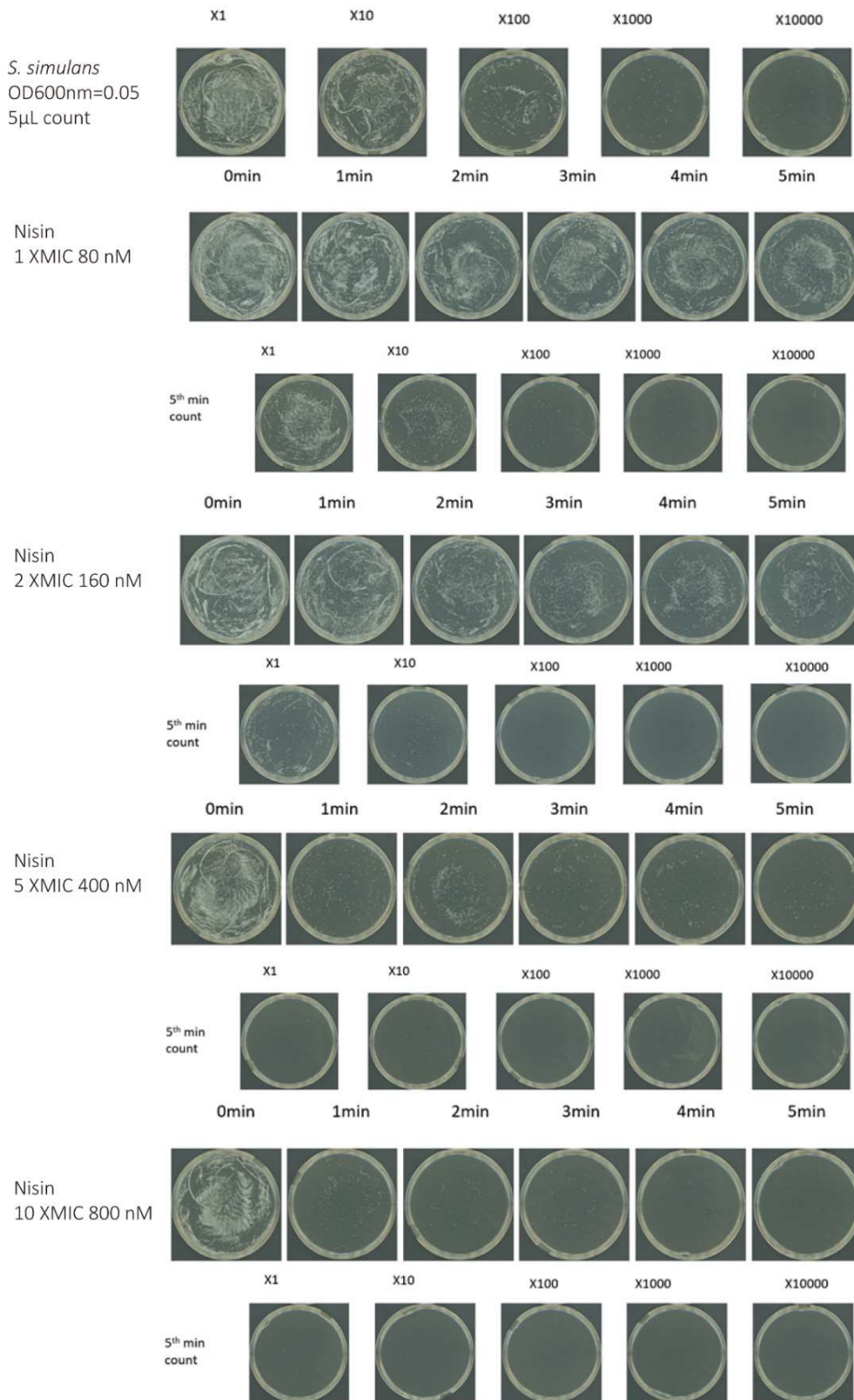


Figure P1. Time killing assay of nisin towards *S. simulans*.

Analyzing mechanisms of action of antimicrobial peptides on bacterial membranes requires multiple complimentary assays and different bacterial strains

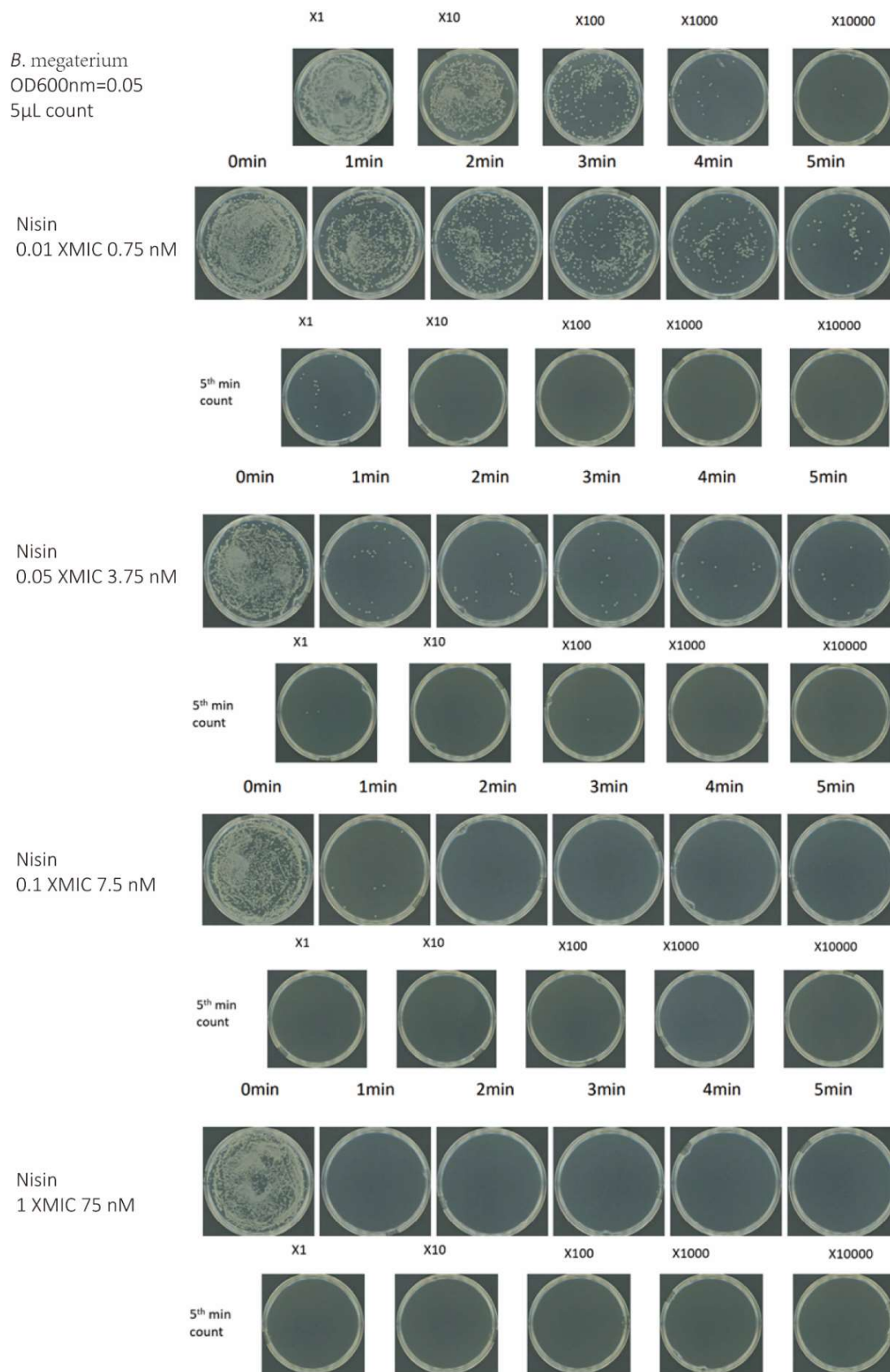


Figure P2. Time killing assay of nisin towards *B. megaterium*.

Chapter 3

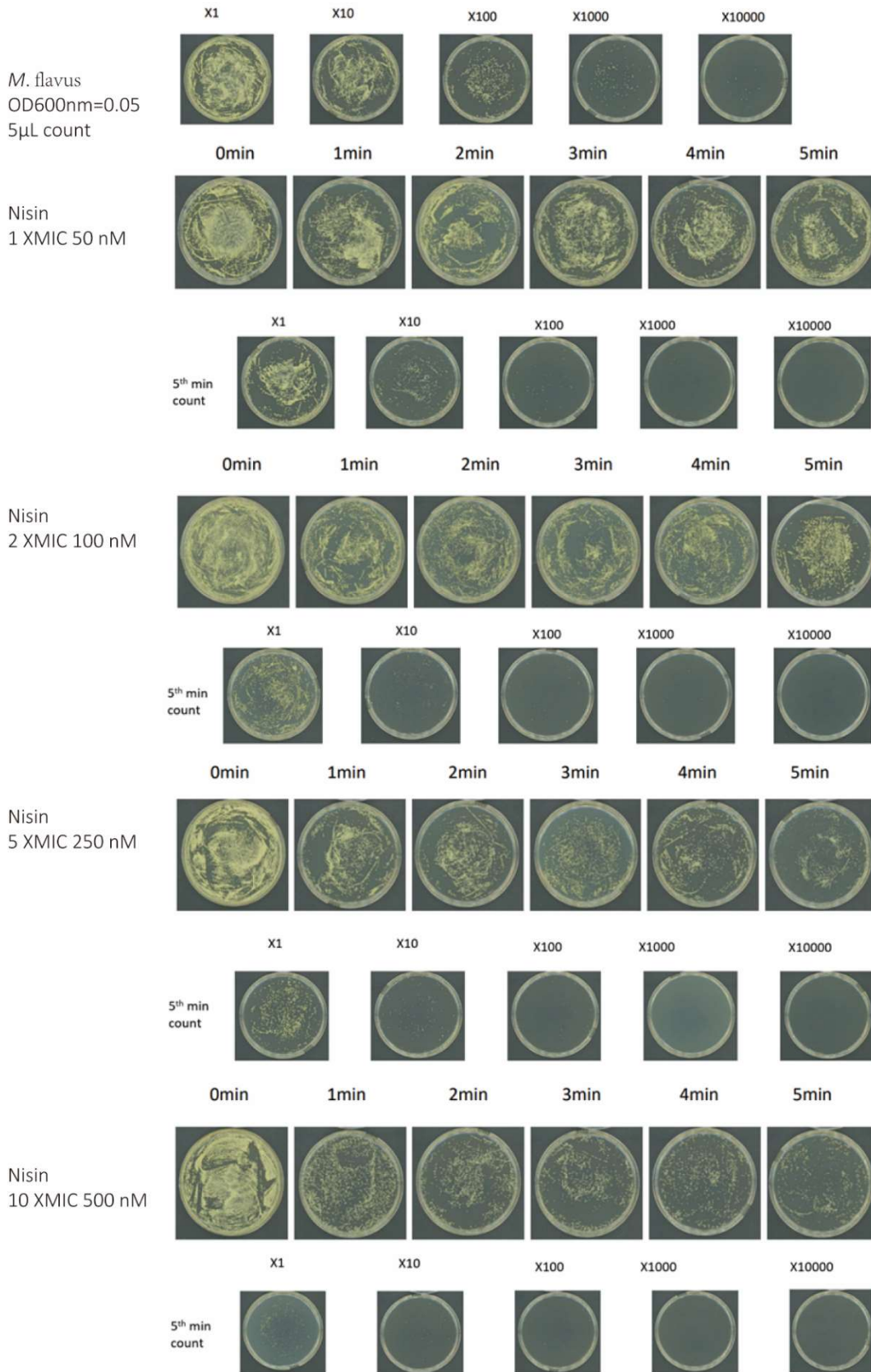


Figure P3. Time killing assay of nisin towards *M. flavus*.

Analyzing mechanisms of action of antimicrobial peptides on bacterial membranes requires multiple complimentary assays and different bacterial strains

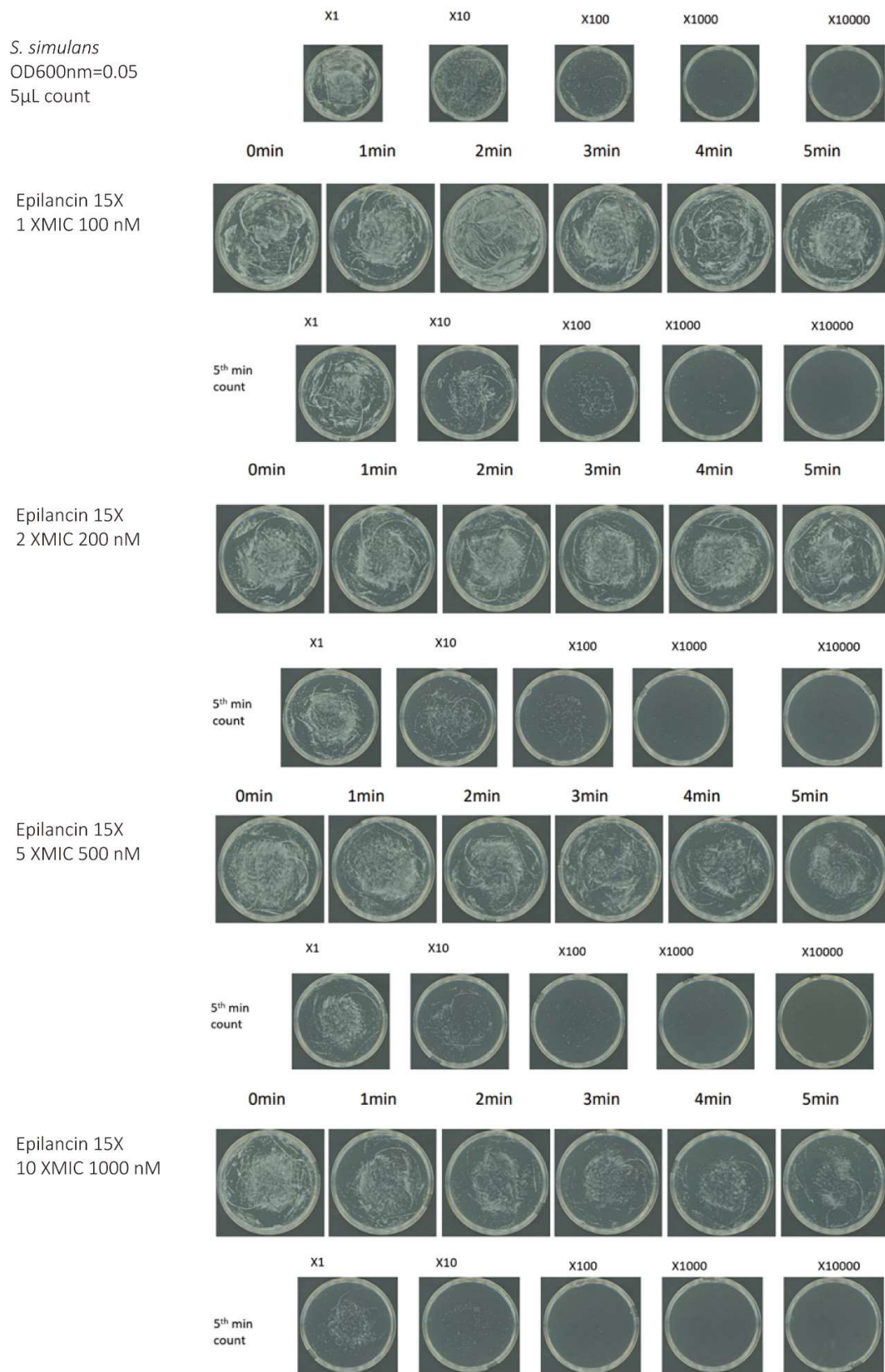


Figure P4. Time killing assay of epilancin 15X towards *S. simulans*.

Chapter 3

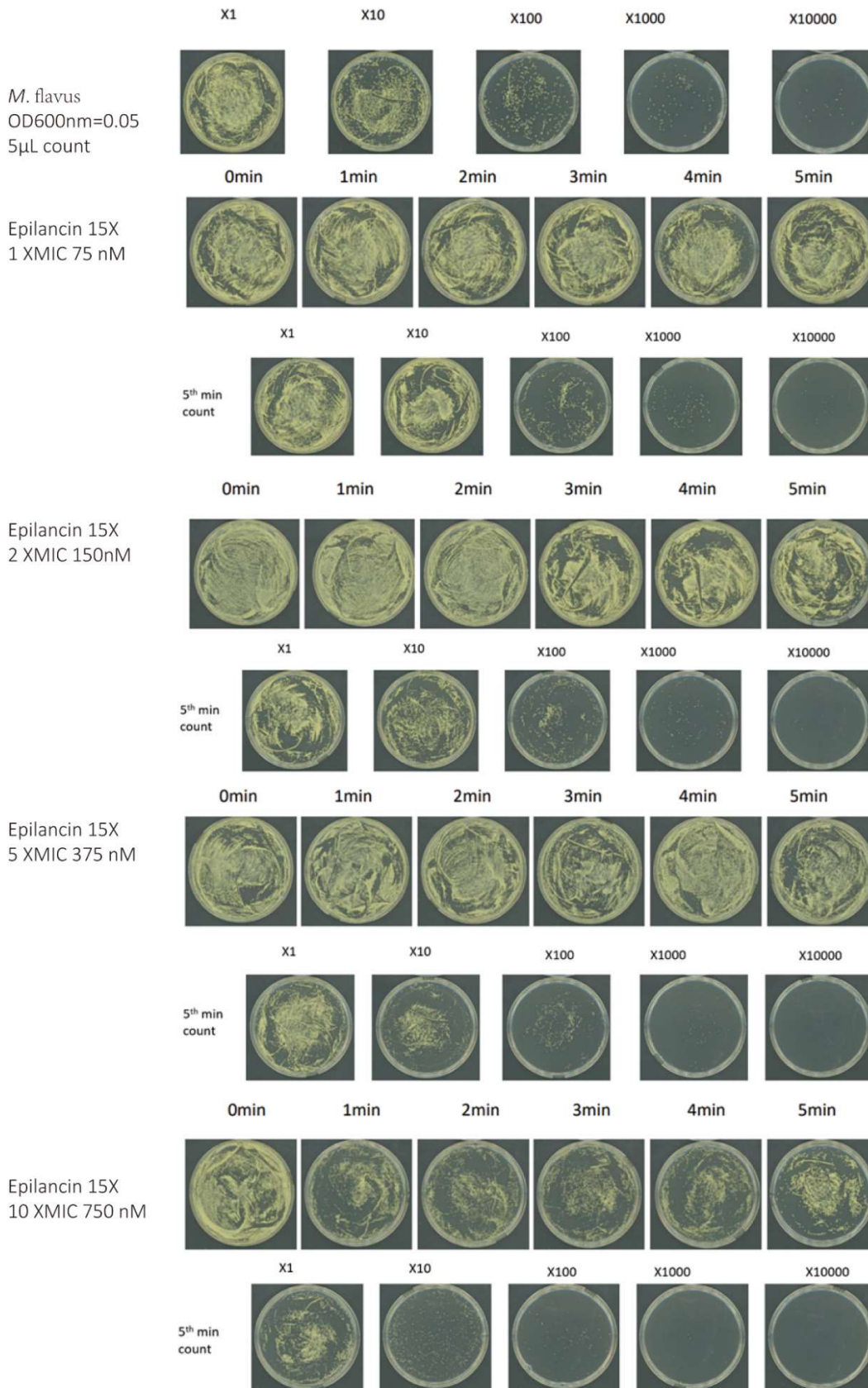


Figure P5. Time killing assay of epilancin 15X towards *M. flavus*.

Analyzing mechanisms of action of antimicrobial peptides on bacterial membranes requires multiple complimentary assays and different bacterial strains

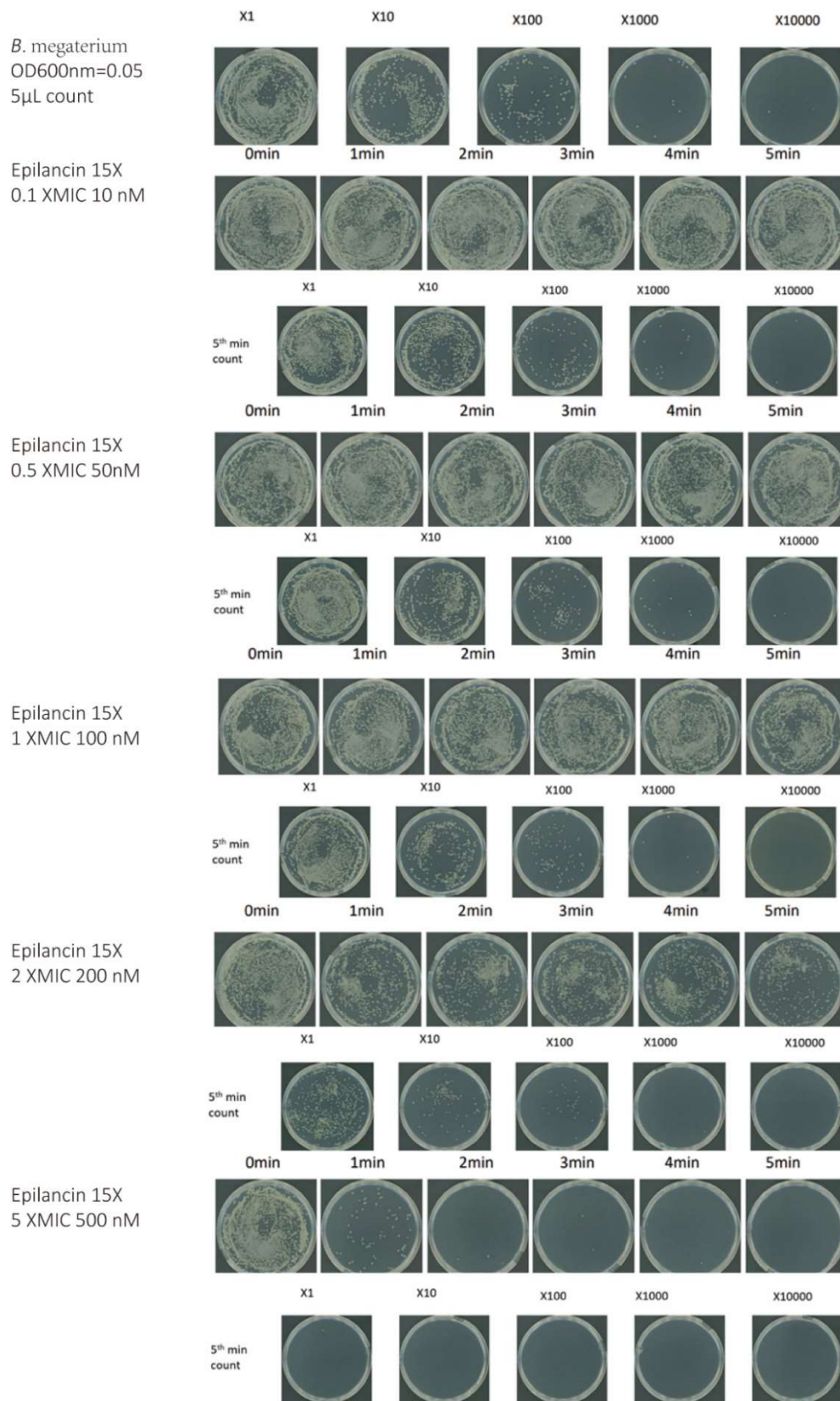


Figure P6. Time killing assay of epilancin 15X towards *B. megaterium*.

Chapter 3

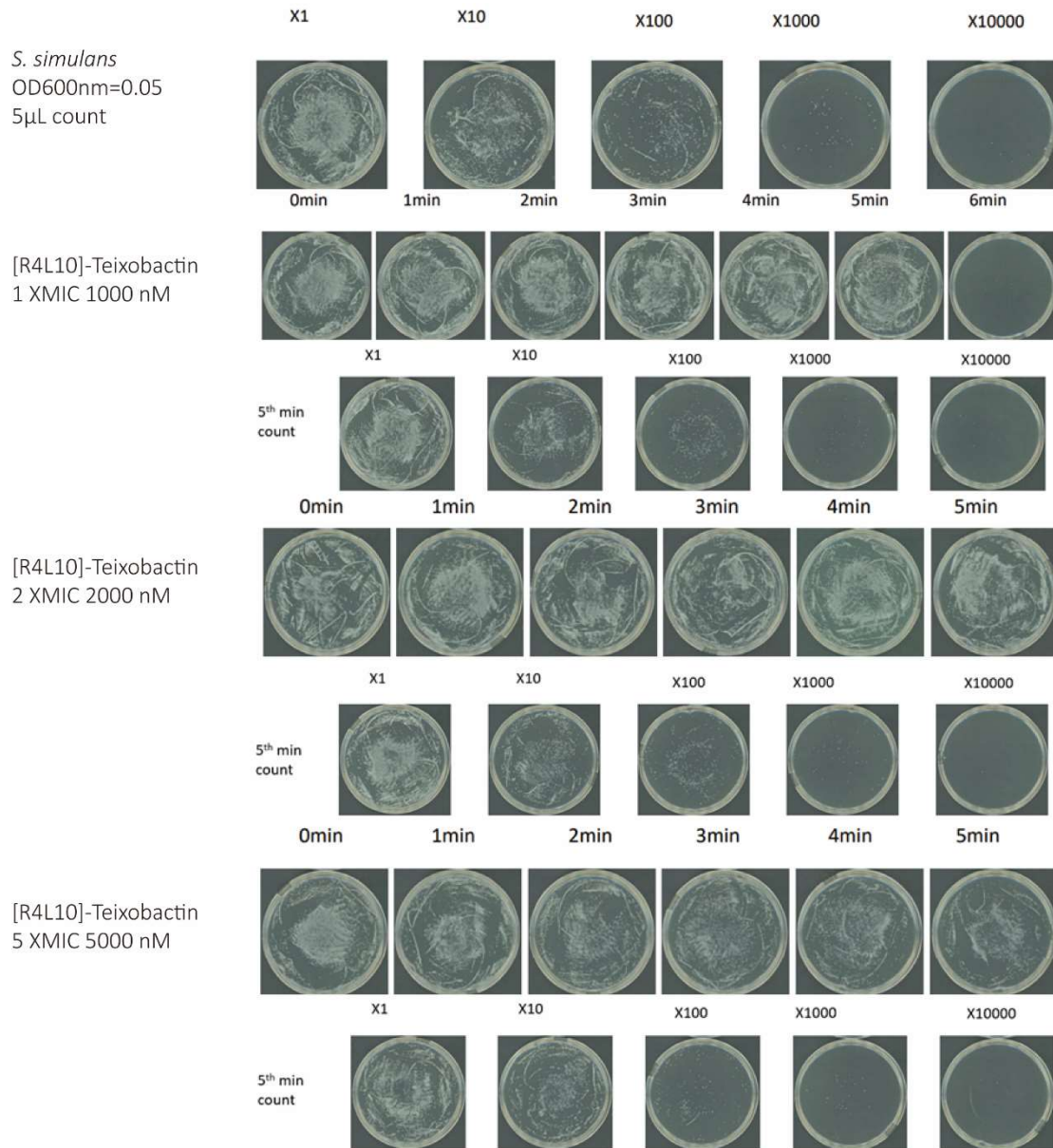


Figure P7. Time killing assay of [R4L10]-teixobactin towards *S. simulans*.

Analyzing mechanisms of action of antimicrobial peptides on bacterial membranes requires multiple complimentary assays and different bacterial strains

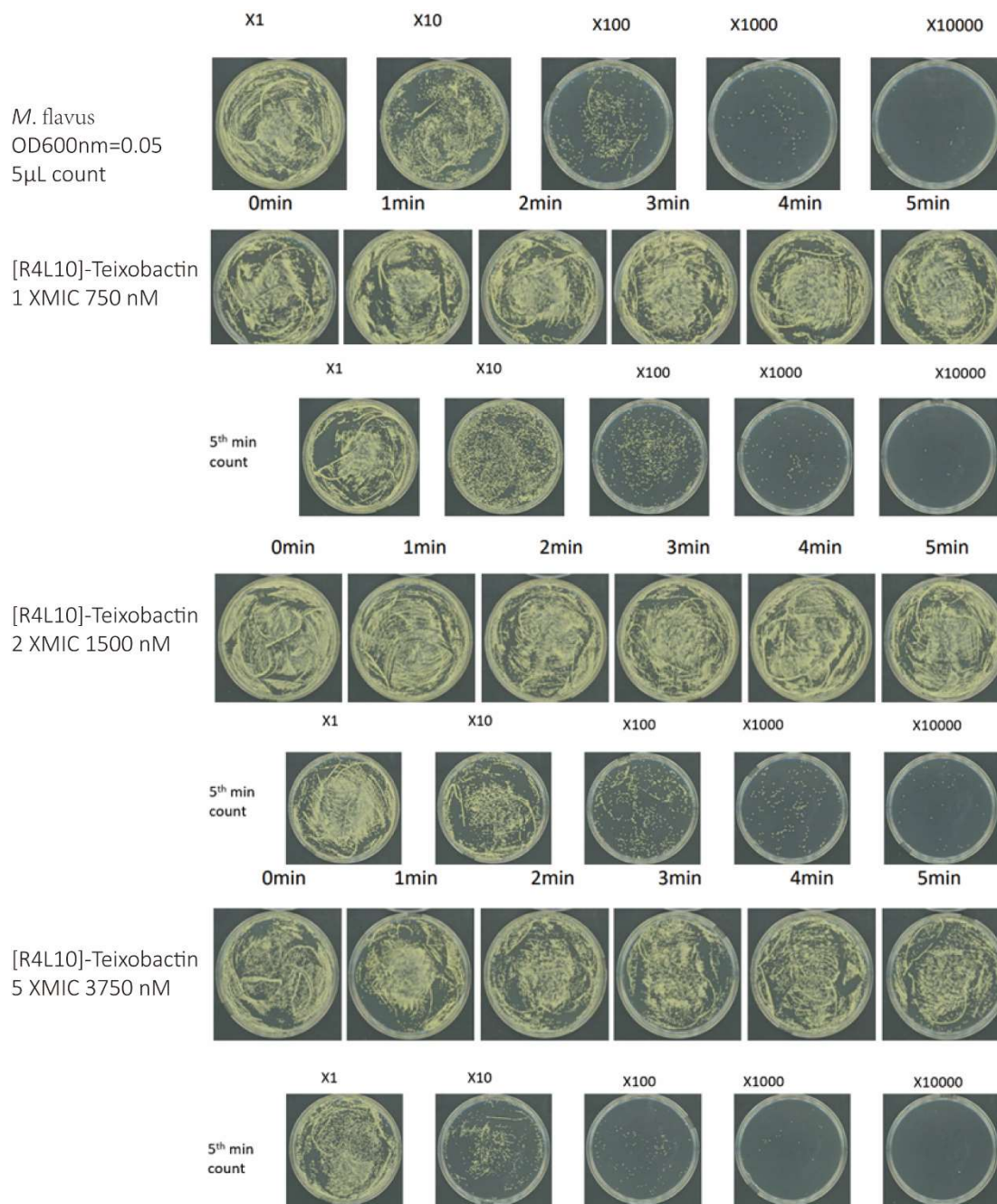


Figure P8. Time killing assay of [R4L10]-teixobactin towards *M. flavus*.

Chapter 3

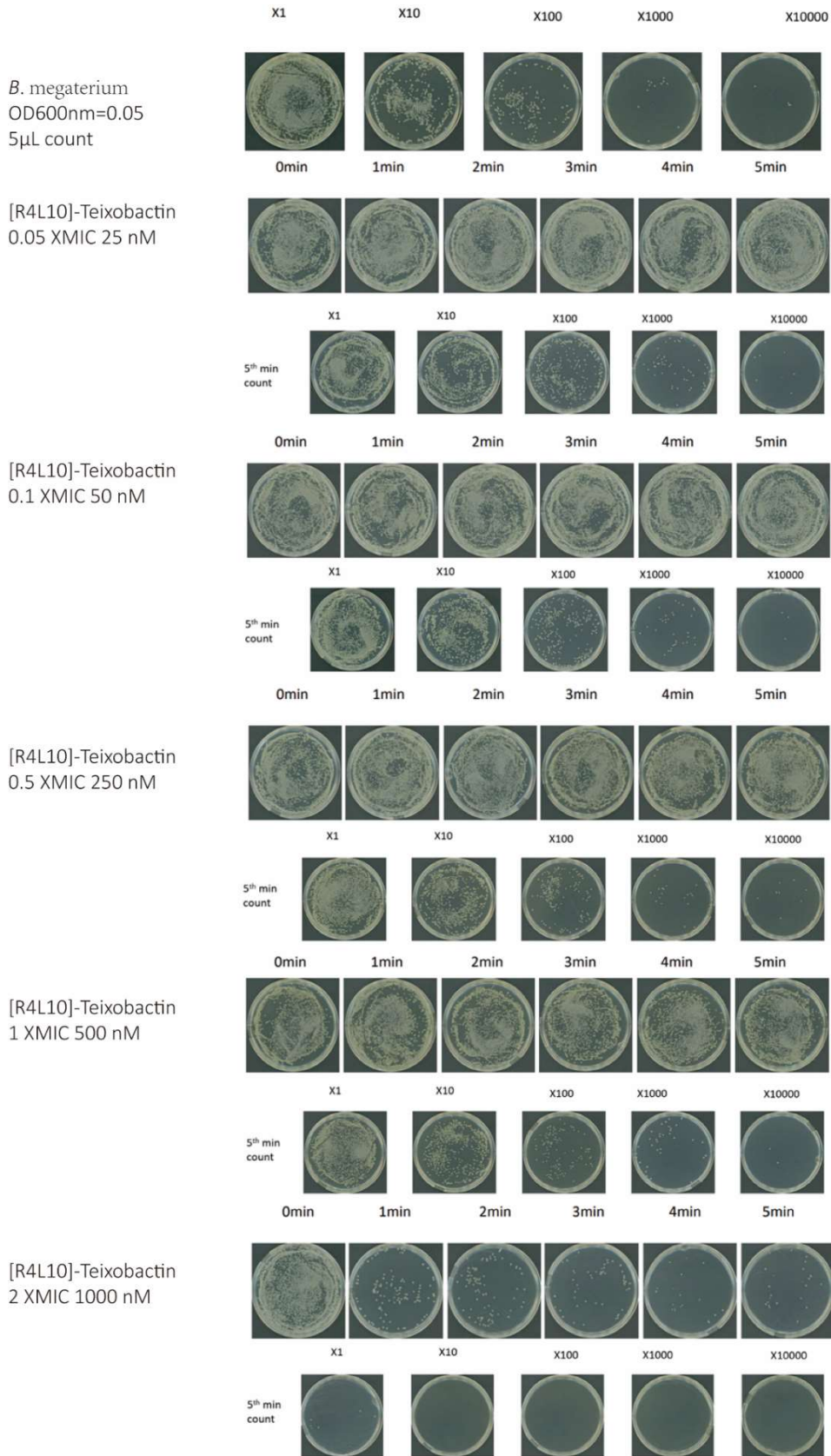


Figure P9. Time killing assay of [R4L10]-teixobactin towards *B. megaterium*.

Chapter 4

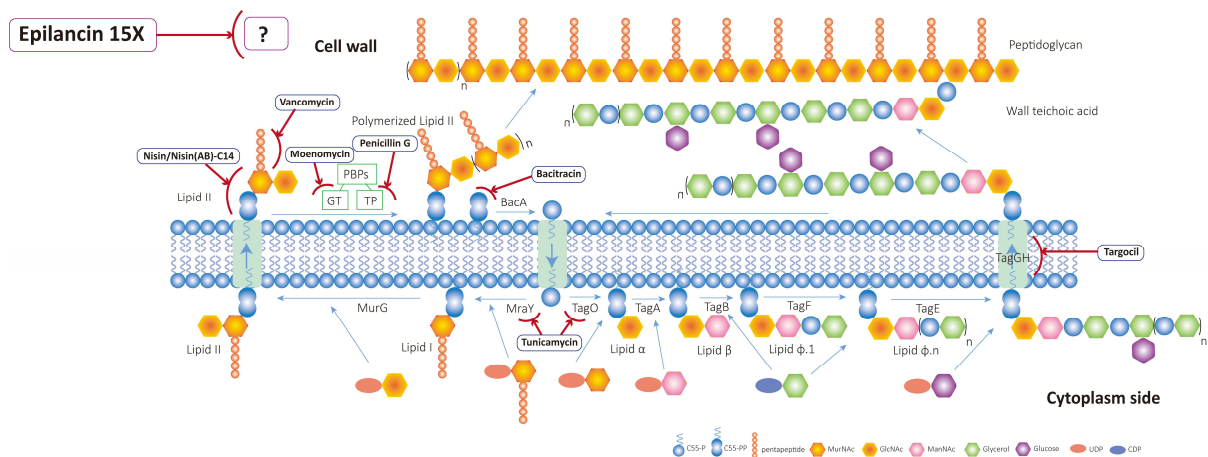
Exploring potential targets of the lantibiotic epilancin 15X on bacterial membranes

Xiaoqi Wang¹, Yang Xu¹, Nathaniel I. Martin³, Eefjan Breukink^{1,2},

1 Membrane Biochemistry and Biophysics, Department of Chemistry, Faculty of Science, Utrecht University, Utrecht, The Netherlands.

2 Zhejiang Provincial Key Laboratory of Food Microbiotechnology Research of China, the Zhejiang Gongshang University of China, Hangzhou, China

3 Biological Chemistry Group, Institute of Biology, Leiden University, Leiden, The Netherlands.



Abstract

Epilancin 15X is a lantibiotic that has an antimicrobial activity in the nanomolar concentration range toward *Staphylococcus simulans*. This implies the involvement of a specific target in its mode of action (MoA). In our previous study, epilancin 15X's ability to dissipate the membrane potential of intact *S. simulans* cells was observed. Here we studied its MoA by using this effect. The membrane depolarization assays showed that treatment of the bacteria by antibiotics which were known to affect the bacterial cell wall synthesis pathway decreased the membrane depolarization effects of epilancin 15X. Disruption of the Lipid II cycle in intact bacteria using several methods led to a decrease in the activity of epilancin 15X. Antagonism-based experiments on 96-well plate and agar diffusion plate pointed towards a possible interaction between epilancin 15X and Lipid II and this was confirmed by Circular Dichroism (CD) based experiments. However, this interaction did not lead to a detectable effect on either carboxyfluorescein (CF) leakage or proton permeability. All experiments point to the involvement of a target within a polyisoprene-based biosynthesis pathway, yet the exact target remains obscure so far.

4.1 Introduction

Bacterial resistance to traditional antibiotics is a growing concern. Therefore, there is an urgent demand for substitutes. Peptides from the family of lantibiotics exhibit high antibacterial activity against a broad spectrum of gram-positive bacteria including several antibiotic-resistant pathogens [1]. Lantibiotics are a type of peptide antibiotics with an extremely low minimal inhibitory concentration (MIC). They belong to bacteriocin Class I and are ribosomally synthesized peptides produced by gram-positive bacteria [2, 3]. These peptides contain the dehydrated amino acids 2,3-didehydroalanine (Dha) and 2,3-didehydrobutyrine (Dhb) as well as lanthionine (Lan) and/or methyllanthionine (MeLan) residues that form the typical thio-ether linked rings (Fig. 1). These rings and unnatural amino acids are formed by post-translational modification [1]. The low MIC of the lantibiotics implies that there are specific targets on the bacterial cells accounting for their efficient killing. The most well-known lantibiotic nisin, uses the essential bacterial cell wall precursor, Lipid II, to efficiently kill bacteria by forming pores in the cytoplasmic membrane [4, 5]. There are several lantibiotics with unknown MoAs [6]. One example of such a lantibiotic is epilancin 15X, which has an antibacterial activity in the nanomolar concentration range toward *Staphylococcus simulans*. Elucidating the mechanism of action of epilancin 15X may provide novel insight in tackling the problematic multi-resistant staphylococci.

Epilancin 15X is produced by *Staphylococcus epidermidis* 15X154 and was isolated and structurally characterized in 2005 (Fig. 1A) [7]. It contains 31 amino acid residues including 10 modified residues and 3 lanthionine rings with a molecular weight of 3172.75 Da [7]. Epilancin 15X is a highly positive charged lantibiotic. It has 8 positively charged amino acids that probably play an important role in supporting electrostatic interactions between the cationic peptides and components of the bacterial envelope, such as the negatively charged membrane lipids. Moreover, epilancin 15X acts against several antibiotic-resistant pathogens including vancomycin-resistant *Enterococci* (VRE) and methicillin-resistant *Staphylococcus aureus* (MRSA) displaying low MICs in the range of 0.125-0.5 µg/ml [8, 9]. It implies that epilancin 15X targets a special binding site different from vancomycin and methicillin.

Epilancin K7 highly resembles epilancin 15X. It has 31 amino acid residues, including 10 modified residues and 3 lanthionine rings similar to epilancin 15X, and a molecular weight of 3033 Da (Fig. 1B) [10]. Interestingly, the C-terminal half of the structures of epilancin 15X and K7 starting from residue 17 are very similar to the C-terminal half of nisin (starting from residue 20) (Fig. 1C). This C terminal part of nisin including the hinge region and rings D/E has been suggested to be important for pore-formation [11]. Additionally, the rings D and E of nisin have been implicated in recognition by NisFEG, proteins that are important for the self-protection of nisin-producing strains [12]. Hence, the B/C rings of the epilancins might have a similar function. Notably, the epilancins do

not have the A/B-ring system of nisin that is responsible for binding to Lipid II. Indeed, for epilancin K7, earlier results showed that it could not induce leakage from model membranes containing Lipid II, which led the authors to conclude that it does not target Lipid II [13].

Lipid II is an important precursor within the bacterial peptidoglycan biosynthesis pathway, which harbors many potential targets of antibiotics especially in gram-positive bacteria. The peptidoglycan (PG) layer is a main constituent of the gram-positive cell wall together with the wall teichoic acids (wTA) that are embedded within this PG-layer [14, 15]. The PG synthesis steps start with the synthesis of Lipid I on the cytosolic side of the plasma membrane from UDP-N-acetylmuramyl-pentapeptide (UDP-MurNAc-pentapeptide) and undecaprenyl phosphate (C55-P). This step is catalyzed by the integral membrane protein MraY [16]. Then, an N-acetyl-D-glucosamine (GlcNAc) moiety of UDP-GlcNAc is transferred to Lipid I by MurG to produce Lipid II [5]. Lipid II is flipped to the external leaflet of the plasma membrane and polymerized and linked to the existing PG-layer by penicillin binding proteins (PBPs) [17-20]. The C55-PP that is resulting from the Lipid II polymerization step is dephosphorylated to C55-P by BacA and the C55-P is recycled to the cytosolic side of the plasma membrane to complete the cycle [21]. The wTA synthesis pathway is connected with PG synthesis via the shared use of the precursor C55-P. There are two main types of wTA known, the poly(glycerol-phosphate) based wTA and the poly(ribitol-phosphate) based that have very similar biosynthesis pathways. What follows is a description of the poly(glycerol-phosphate) based wTA synthesis pathway of *Bacillus subtilis*. The first teichoic acid synthesis step that takes place on the cytosolic side of the membrane starts with the synthesis of lipid α from UDP-GlcNAc and C55-P, a step catalyzed by the integral membrane enzyme TagO, a paralogue of MraY [22]. Then a N-acetylmannosamine (ManNAc) moiety from UDP-ManNAc is transferred to lipid α to produce a lipid β by TagA [23]. TagB adds an sn-glycerol-3-phosphate unit from CDP-glycerol to lipid β to form lipid $\phi.1$ and more glycerol-phosphate units (n) are polymerized onto lipid $\phi.1$ by TagF to form lipid $\phi.n$ [24, 25]. Lipid $\phi.n$ is modified with glucose units by TagE before it is transferred to the external leaflet of the plasma membrane, presumably by TagGH [26, 27]. Finally, the wTA polymer is D-alanylated and transferred from its polyisoprenoid anchor to the PG layer [28]. The remaining, C55-PP is dephosphorylated and recycled as described above. In this research, we used both *S. simulans* and *B. subtilis* to study effects of antibiotics towards the PG and wTA biosynthesis pathways.

Precursors, enzymes, and products of the above-described biosynthesis pathways are popular targets for many antibiotics. For instance, nisin bind to peptidoglycan precursor Lipid II; Bacitracin binds to C55-PP; penicillin binds to the transpeptidation domain and moenomycin binds to the transglycosylation domain of PBPs. Targocil targets wTA translocase TarGH and tunicamycin inhibits both MraY and TagO of both pathways, albeit with different efficacies [29-37].

This research mainly explores potential targets of epilancin 15X by tackling precursors and enzymes that are involved in the pathways involved in the bacterial cell wall synthesis. This may also provide insights on how to study the MoA of other membrane targeting antibiotics.

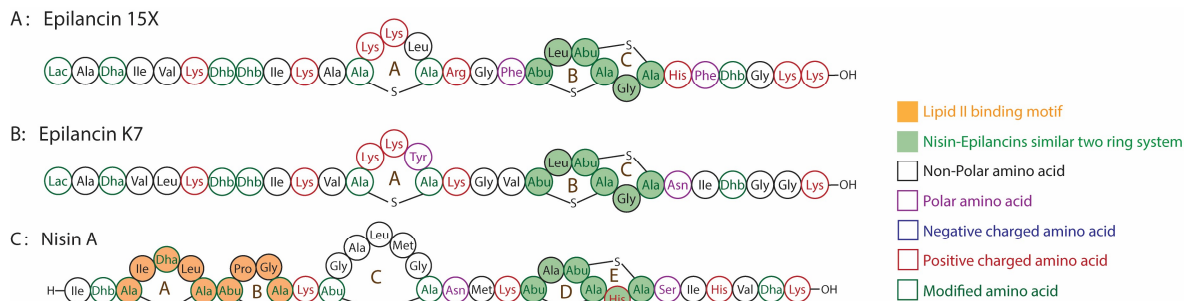


Figure 1. Structures of the lantibiotics epilancin 15X, epilancin K7, nisin A. The lipid II binding motif is highlighted in orange. The similar two C-terminal ring systems are highlighted in green.

4.2 Materials and Methods

4.2.1 Materials

Nisin A and Lipid II (DAP/Lys) was prepared as previously described [11, 38]. Nisin(AB)-C14 was obtained from Nathaniel I. Martin (Leiden University). Plasmid pDML924 encoding His6-PBP1b- γ was obtained from Mohammed Terrak (Liège University), and the plasmid pQ318A encoding PBP1b Q318A was obtained from Waldemar Vollmer (Newcastle University). The TagO mutant of *B. subtilis* was obtained from Richard Daniel (The Centre for Bacterial Cell Biology, Newcastle University).

All other chemicals used were of analytical or reagent grade. 1,2-Dioleoyl-*sn*-glycero-3-phosphocholine (DOPC), 1,2-dioleoyl-*sn*-glycero-3-phosphoglycerol (DOPG), 1,2-dioleoyl-*sn*-glycero-3-(cytidine diphosphate) (CDP-DAG) were purchased from Avanti Polar Lipids. Carboxyfluorescein (CF) was obtained from Molecular Probes. DiSC₂(5), HPTS were purchased from Sigma-Aldrich. G-25 Sephadex and G-50 Sephadex were from Amersham Pharmacia Biotech AB. Tween-20 was purchased from Merck. Triton X-100 was purchased from Sigma-Aldrich. All other chemicals used were of analytical or reagent grade.

4.2.2 Methods

4.2.2.1 General procedures

The concentration of peptides was determined using the Pierce™ BCA Protein Assay

Kit (Thermo Fisher). The tubes used were siliconized by SurfaSil Siliconizing Fluid (Thermo Scientific™) using Siliconizing Fluids. All fluorescence related experiments were measured by a Cary Eclipse fluorescence spectrophotometer.

4.2.2.2 Bacterial strains and culture conditions

Epilancin 15X producer strain *Staphylococcus epidermidis* 15X154 [39] was grown on Muller-Hinton broth at 37°C. Indicator strain *S. simulans* 22 was grown on Tryptic Soy Broth (TSB) at 37°C [11].

4.2.2.3 Epilancin 15X purification

The strain *S. epidermidis* 15X154 was inoculated in 60 mL Muller-Hinton broth at 37°C and 200 rpm overnight. The pre-culture was transferred into sterile 6 × 1 L TSB in 2 L Erlenmeyer flasks and grown for 18 hours at 37°C aerobically (1% inoculum). The cells were removed by centrifugation at 8000×g for 20 min at 4°C, and the supernatant was sterilized using a 200 nm filter. The supernatant was applied to a cation exchange column (SP Sepharose Fast Flow) which was equilibrated with 20 mM sodium acetate, pH5. Epilancin 15X was eluted using a linear gradient from 100 mM to 1 M NaCl in 20 mM sodium acetate pH5. Fractions containing antibacterial activity were collected and applied to a RP-18 column (LiChrosprep, 40-63 µm of 23.5 mm x 50 mm, d x h) and epilancin 15X was eluted by a step gradient of 10% methanol, 50% methanol, 90% methanol, and 95% acetonitrile in water. Finally, epilancin was purified from the fractions containing antimicrobial activity using a C18 RP-HPLC column (LiChrospher, 250 mm × 4.6 mm, 5 µm) equilibrated in eluent A (5% acetonitrile, 95% water, 0.05% TFA) and using a linear gradient from 0% to 100% eluent B (95% acetonitrile, 5% water, 0.05% TFA) in 30 min (flow rate at 0.8 mL/min, UV detection at 214 nm). Epilancin 15X appeared as a broad peak at ~90% B (Fig. S1).

To reach maximal activity of epilancin 15X it was necessary to remove the peptide-bound TFA. For this, 13.5µL of 1 M HCl was added for every 100 ml epilancin 15X solution containing 0.01% TFA. Hereafter, the sample was evaporated at 40 °C to dryness and the peptide was re-dissolved in 20 ml of methanol/water (1:1, v/v). Then, the sample was evaporated again. This last step was done a total of three times. Finally, epilancin 15X was dissolved in water and freeze-dried for 24h. The molecular weight was determined by Mass spectrometry, and epilancin appeared in 4 main peaks of 636.2 (5 H⁺), 794.8 (4 H⁺), 1059.5 (3 H⁺) and 1588.4 (2 H⁺) (Thermo Finnigan) (Fig. S2).

4.2.2.4 Minimal inhibitory concentration (MIC) determination

The minimal concentration of epilancin 15X that did not allow *S. simulans* growth after 24 hours was defined as the MIC. This was determined using 1 mL cultures of *S.*

simulans at a start OD₆₀₀ of 0.05 in TSB broth containing a serial dilution of epilancin 15X in sterilized and siliconized glass tubes. The tubes were shaken at 37°C, 200 rpm and the OD₆₀₀ was read after incubation for 24 hours.

4.2.2.5 Membrane potential depolarization assay

The fluorescent dye 3,3'-Diethylthiadicarbocyanine iodide DiSC₂(5) (excitation at 650 nm and emission at 670 nm) was used to inspect the ability of epilancin 15X to dissipate the membrane potential of *S. simulans* [40]. Precultures of *S. simulans* were grown at 37 °C, 200 rpm overnight, and then diluted to an OD₆₀₀ of 0.05 with fresh TSB medium. The culture was further grown for 4 hours and spun down at 4000 × g for 20 min at 4°C. The cells were washed twice with 250 mM glucose, 5 mM MgSO₄, 100 mM KCl, 10 mM PBS at pH 7 (buffer A). The cells were then resuspended to an OD₆₀₀ of 5. From this cell suspension 10 µL was added into a cuvette containing 1 mL buffer A, followed by the addition of 2 µL of a stock solution of 0.1 mM DiSC₂(5) dissolved in DMSO. Antibiotics were added after a stable curve was obtained and at the end of the experiment 10 µL of 20% Triton X-100 was added to fully dissipate the membrane potential.

4.2.2.6 Preincubation of *S. simulans* with vancomycin

Precultures of *S. simulans* were grown at 37°C, 200 rpm overnight, and then diluted to an OD₆₀₀ of 0.05 with fresh TSB medium. The culture was further grown for 4 hours and diluted to OD₆₀₀ of 0.05 again with fresh TSB medium. The diluted *S. simulans* culture was divided into 3 tubes containing 30 ml of bacteria. Then 10 µM (final concentration) of vancomycin was added to each tube. Cells in the first tube were immediately centrifuged and washed twice with buffer A. The pellet was put on ice. The second and the third tubes were incubated at 37°C, 200 rpm for 5 and 10 min respectively, and were then centrifuged and washed as for the first sample and stored on ice. Cells from the three tubes were then resuspended to an OD₆₀₀ of 5. From this cell suspension 10 µL was added into a cuvette containing 1 mL buffer A for the membrane potential assay.

4.2.2.7 Agar diffusion assay

Preculture of *S. simulans* was grown at 37°C, 200 rpm overnight. 100 µL of pre-cultured *S. simulans* was added into 10 mL 0.6% agar TSB medium at around 50°C. After the agar TSB medium in the plates solidified, 10 µL of samples were spotted on the agar. The plate was incubated at 37°C overnight.

The ability of Lipid II to antagonize antibiotic activity was also tested using an agar diffusion assay, normally used to determine antibiotic activity. 20 µL of epilancin 15X and nisin stock solution (20 µM) were added on 1% pre-cultured *S. simulans* containing

agar plate, and it was incubated at 30°C overnight. Then the diameters of inhibition haloes were measured. Subsequently, Lipid II-Lys, lipid II-DAP (0.02 nmol, 0.1 nmol and 0.2 nmol dissolved in 0.1% Tween-20) and DOPG (0.04 nmol, 0.2 nmol, 0.4 nmol dissolved in 0.1% Tween-20) were spotted on a new 1% pre-cultured *S. simulans* containing agar plate at a distance from the planned antibiotic spot that corresponds to the previously measured radius of the inhibition halo. The lipid spots were allowed to dry, which was then followed by spotting 20 µL of an epilancin 15X and nisin stock solution (20 µM). The plate was incubated at 30°C overnight.

4.2.2.8 Assay for antagonism by Lipid II in liquid medium

Overnight pre-cultured *S. simulans* was diluted by TSB medium containing 0.01% Tween-20 to an OD₆₀₀ of 0.05. The molecular ratios of lantibiotics (epilancin 15X and nisin) to Lipid II-Lys, Lipid II-DAP were varied from 1:0 to 1:10. DOPG was used as a control for electrostatic effect of concentration two times that of Lipid II. Lipids, lantibiotics and *S. simulans* were added into 96 well plate (Ultra-Low Attachment Surface, 3474 Corning) with the final volume of 200 µL each well. The 96 well plates were incubated at 37°C and 200 rpm overnight.

4.2.2.9 Model membrane vesicle preparation

Large unilamellar vesicles (LUVs) containing phospholipids (DOPC, DOPG) with/without Lipid II were prepared for the CF leakage assay, the proton permeability assay and the direct binding assay. Lipids were dried by N₂ and were hydrated by adding 25 mM Tris-HCl, 150 mM NaCl, pH 7.5 (buffer B) containing 50 mM CF for the CF leakage assay, or by adding buffer 0.2 M pH 7 PBS (buffer C) containing 2 mM HPTS for the proton permeability assay, or by adding 25 mM Tris-HCl, 150 mM NaCl, pH 7.5 (Buffer D) for the direct binding assay.

The LUVs were prepared in 10 freeze-thaw cycles in liquid nitrogen and extruded over a 200 nm filter for 10 times. The vesicles for the CF leakage assay were passed through a 2.5 mL spin column filled with sephadex G50 which was equilibrated with buffer B. The vesicles for the proton permeability assay were passed through a 2.5 mL spin column filled with sephadex G25 column which was equilibrated with buffer C.

Small unilamellar vesicles (SUVs) containing phospholipids (DOPC, DOPG) with/without Lipid II were prepared for Circular Dichroism (CD) measurements. Lipids were dried by N₂ and were hydrated by adding 20 mM HEPES, 40 mM Na₂SO₄, pH 7.4 (buffer E). The SUVs were prepared by sonication using a Branson 250 tip sonicator for about 5 min with 10-s time intervals and an input power of 40 W until the dispersions were clear. Residual particles of vesicles for direct binding assay were removed by centrifugation at 14000 rpm for 20 min at 4°C.

The concentrations of phospholipids and vesicle preparations were determined as

described [41]. The phospholipids dispersed in phosphate buffer were extracted using the method described by Bligh and Dyer [42].

4.2.2.10 CF leakage assay using model membrane vesicles

LUVs with the fluorescent dye CF (excitation at 492 nm and emission at 515 nm) enclosed were used to measure the pore-forming ability of epilancin 15X [43]. LUVs were diluted with buffer B to a concentration of 5 μM in a 1 mL cuvette, followed by the addition of the lantibiotics after 30s. Maximum fluorescence was reached by adding 10 μL of 20% Triton X-100 to destroy all LUVs.

4.2.2.11 Proton permeability assay using model membrane vesicles.

Proton permeability assay was performed using LUVs, using the fluorescent signal of 8-hydroxypyrene-1,3,6-trisulfonic acid trisodium salt (HPTS) (excitation at 450 nm and emission at 508 nm) which is a type of pH-dependent fluorescent probe [44]. The LUVs were diluted in buffer C to a final concentration of 35 μM in 1 mL cuvette, and antibiotics were added after 1 min. Maximum fluorescence was reached by adding 10 μL of 20% Triton X-100.

4.2.2.12 CD Measurements

CD spectra were measured with a Jasco-810 spectropolarimeter in a quartz cuvette with a 2 mm path length. The temperature was kept at 20°C by a Jasco Peltier CDF 426S. The ellipticity was recorded between 190 nm and 260 nm at a 0.2-nm step size with 1-s response time. The spectra were averaged over 5 recordings with a scanning speed of 50 nm/min. Samples contained 50 μM epilancin 15X and buffer E was used for preparation and dilution. The lipid II containing SUVs were added to a final lipid II concentration of 50 μM . The DOPG containing SUVs were added to a final DOPG concentration of 100 μM .

4.3 Results and Discussion

4.3.1 Epilancin 15X has a low MIC which indicates that it uses a specific target.

In the course of our studies on the MoA of epilancin 15X, there were two major aspects that negatively affected the determination of the MIC value: glass adhesion and an inhibitory effect of TFA. Of note is the property of epilancin 15X to adhere to glass surfaces, hence it was essential that the glass tubes used during MIC determination

were siliconized beforehand. Siliconization resulted in a reduction of the measured MIC towards *S. simulans* from 750 nM to 500 nM. The second, more severe effect was caused by the presence of TFA (as it is used in the HPLC-purification step) in the epilancin 15X solution, which significantly decreased the peptide's activity. Removal of the TFA from the peptide resulted in a 5-fold reduction of the measured MIC towards *S. simulans* from 500 nM to 100 nM. This large effect of TFA on the activity of epilancin 15X maybe a general problem with HPLC-purified antimicrobial peptides (AMPs) that are highly positively charged.

These low MICs are indicative for a specific target of epilancin 15X. Previous studies showed that epilancin 15X clearly dissipated membrane potential of *S. simulans* at concentrations equal to its MIC, while it did not cause severe membrane disruption [45]. In view of this correlation, the effect on the membrane potential is likely to be related to its MoA and we therefore used this assay in our attempts to identify the target of epilancin 15X.

4.3.2 Epilancin 15X likely interacts with the cell wall synthesis precursor Lipid II.

We used the membrane depolarization assay for exploring the MoA of epilancin 15X with respect to possible targets of this lantibiotic. First, we performed the membrane depolarization assay with nisin and epilancin 15X at 200 nM and 500 nM, respectively and a rapid dissipation of the membrane potential was observed, similar as found in our previous study [45] (Fig. 2A). Nisin uses the essential cell wall precursor, Lipid II, as a target with which it efficiently forms pores [4]. We have shown before that vancomycin, an antibiotic that targets the D-Ala-D-Ala terminus of the pentapeptide of Lipid II, can inhibit the pore-forming activity of nisin [46]. Indeed, addition of vancomycin to the *S. simulans* cells before the addition of nisin caused a significant inhibition of the ability of nisin to dissipate the membrane potential of these cells (Fig. 2B). As epilancin 15X does not have the archetypical A/B ring system of Lipid II targeting lantibiotics, we did not expect an effect of vancomycin on epilancin 15X. Indeed, addition of vancomycin could not inhibit the membrane permeability of epilancin 15X, even at two-fold higher concentration (Fig. 2C). The membrane depolarization effect of epilancin 15X was even slightly enhanced.

This picture completely changed when we used a truncated form of nisin which is composed of rings A and B fused to a lipid chain containing 14 carbon atoms (nisin(AB)-C14) that, like nisin, binds to the pyrophosphate part of Lipid II but cannot form pores [47]. It was shown before that this truncated and acylated form of nisin can inhibit the Lipid II-dependent pore-formation of wild-type nisin in model membranes [47]. Fig. 2D shows that this truncated form of nisin could also inhibit the pore-formation of wild-type nisin in intact bacterial cells as a clear effect on the dissipation of the

membrane potential by nisin could be observed (blue and green traces). Much to our surprise, we also observed an effect of nisin(AB)-C14 on the ability of epilancin 15X to dissipate the membrane potential of intact cells (Fig. 2D, orange and yellow traces). nisin(AB)-C14 caused a clear inhibition of the activity of epilancin 15X, albeit that nisin was more sensitive to the acylated fragment as a higher inhibition could be observed at a two-fold lower concentration of the fragment. These results suggest that Lipid II may also be targeted by epilancin 15X despite that it lacks the archetypical A/B-ring system of Lipid II-targeting lantibiotics.

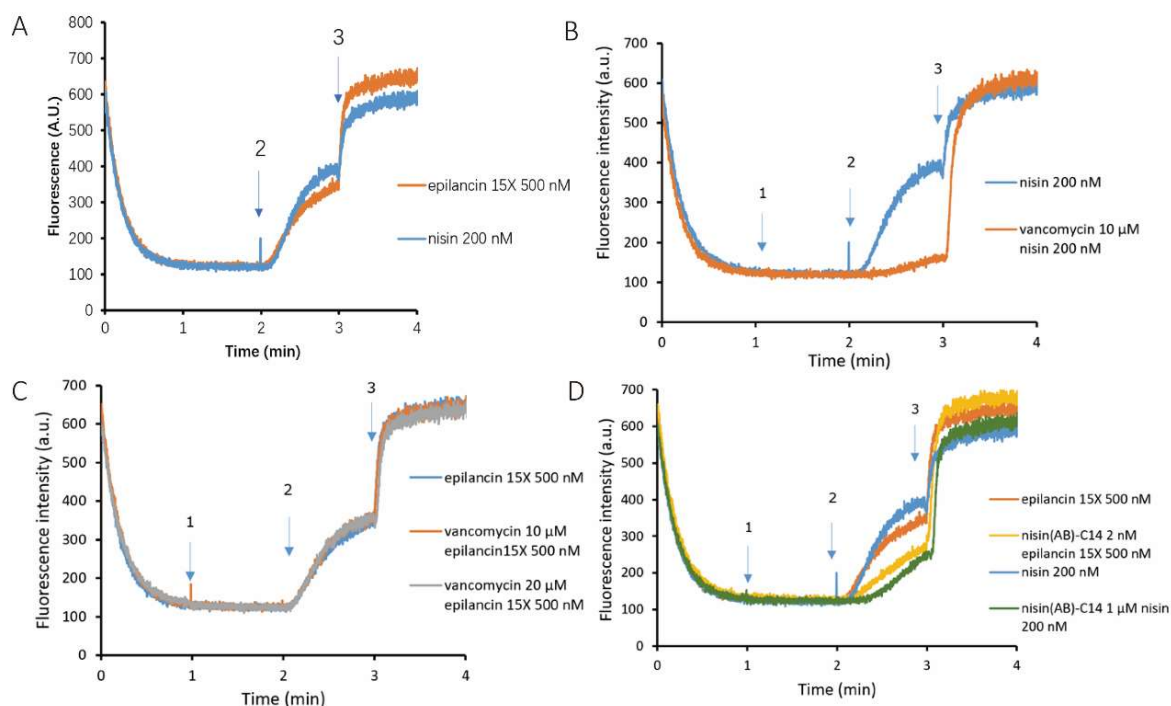


Figure 2. Effect of addition of vancomycin and nisin(AB)-C14 on the ability of epilancin 15X and nisin to disrupt the membrane potential of *S. simulans* cells. (A) 200 nM nisin (blue) and 500 nM epilancin 15X (orange) were added at 2 min. (B) 200 nM nisin was added at 2 min (blue); 10 μ M vancomycin was added at 1 min and 200 nM nisin added at 2 min (orange). (C) 500 nM epilancin 15X was added at 2 min (blue); 10 μ M (orange) and 20 μ M (gray) vancomycin was added at 1 min and 500 nM epilancin 15X added at 2 min. (D) 500 nM epilancin 15X was added at 2 min (orange), 2 μ M nisin(AB)-C14 was added at 1 min and 500 nM epilancin 15X was added at 2 min (yellow); 200 nM nisin 15X added at 2 min (blue), 1 μ M nisin(AB)-C14 was added at 1 min and 200 nM nisin was added at 2 min (green). Arrows mark the addition of antagonists (1), lantibiotics (2), and 20 μ L 20% Triton X-100 (3), which was added to fully dissipate the membrane potential.

4.3.3 Lipid II binds to epilancin 15X and induces conformational change.

To check whether epilancin 15X and Lipid II indeed interact, we first tested if Lipid II is able to antagonize the antibacterial action of epilancin 15X towards *S. simulans* in two different ways. In one of the approaches, we grew *S. simulans* cells in 96 wells plates in the presence of 5 times the MIC of nisin or epilancin 15X and increasing concentrations of Lipid II. In the case of nisin, bacterial growth could be observed at Lipid II concentrations above 225 nM. Hardly any difference could be observed between the lysine form of Lipid II or the diaminopimelic acid (DAP) form (Fig. 3A). Lipid II could also antagonize the antibacterial activity of epilancin 15X, albeit that the concentration of Lipid II needed for this antagonization effect was about 10-fold higher irrespective of the Lipid II variant used. This suggests that epilancin 15X and Lipid II do interact. DOPG, a control to test for electrostatic effects, also displayed antagonistic effects towards epilancin 15X at concentrations above 5 μ M while DOPG did not affect the antibiotic activity of nisin.

As an alternative and independent approach, we tested the antagonization effect of Lipid II on epilancin 15X in an agar diffusion assay. For this we spotted different amounts of Lipid II at positions around the spot where the lantibiotic was applied. These positions were located at the predicted rim of the halo formed by the antibacterial action of the lantibiotic in the absence of any antagonist, which was determined using identical circumstances (e.g., amount of lantibiotic spotted, thickness of agar plate) (Fig. 3B)[6]. In case of nisin, clear deformations of the halo could be observed for amounts of Lipid II as low as 20 pmol. There did not appear to be a difference between the variants of Lipid II tested and DOPG had no effect on the nisin activity. The halos of epilancin 15X also showed deformation when Lipid II was added and like above, higher concentrations of Lipid II were needed to observe an effect on the halo. Again, DOPG had an effect on the activity of epilancin 15X as well.

These results clearly show that epilancin 15X interacts with Lipid II. However, the apparent affinity of epilancin 15X toward Lipid II seems to be lower as compared to that of nisin, as significantly higher concentrations of Lipid II were needed to observe an antagonistic effect. This difference in affinity may point to a difference in binding mode between the two lantibiotics, as can be expected from the large differences in primary structure. Alternatively, this may point to a different target for epilancin 15X. We could detect no significant difference between Lipid II-Lys and Lipid II-DAP, suggesting that the penta-peptide part of Lipid II is not an important part of the interaction interface. In both test systems, DOPG had an effect on the activity of epilancin 15X. This may suggest that the interaction of epilancin with Lipid II is mainly caused by (unspecific) electrostatic interactions, which may be stronger in the case of Lipid II as it contains more negative charges. Yet, since DAP-Lipid II has one negative

charge more than the lysine form and we could not detect any difference between the two, this suggests that electrostatics aren't the main driving force for this interaction.

Next, we checked if the lantibiotic changes its conformation upon binding to Lipid II by CD. We observed a clear change in the CD-spectrum of epilancin 15X in the presence of SUVs containing Lipid II (Fig. 4A). This points to a Lipid II induced change in the secondary structure of epilancin 15X. It remains unclear what kind of secondary structure is induced upon binding to Lipid II. SUVs containing double the amount of DOPG as compared to Lipid II, to correct for the charge, did not induce any structural change in the peptide (Fig. 4B). Thus, the binding of epilancin to Lipid II is likely to be specific, and not only governed by electrostatics.

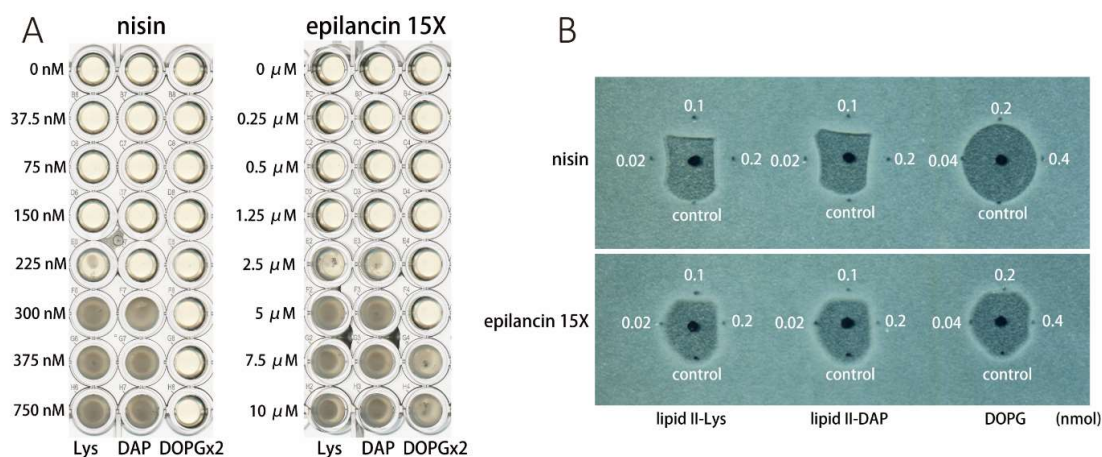


Figure 3. Antagonistic effect of externally added Lipid II on the antimicrobial activities of epilancin 15X and nisin. (A) The concentration of nisin and epilancin 15X used were 375 nM and 250 nM respectively. The numbers display to the left of the wells are the concentration of externally added Lipid II. Lys and DAP refer to the lysine or DAP variant of Lipid II, the concentration of externally added DOPG was twice that of Lipid II. (B) Different amount of Lipid II-Lys and Lipid II-DAP equal to 0.02 nmol, 0.1 nmol, 0.2 nmol were added at the edge of the inhibition halo where the lowest concentration of lantibiotic that still inhibits *S. simulans* growth is present. Twice the amount of DOPG was added as compared to Lipid II (Fig. 3B was published in [6], figure 10).

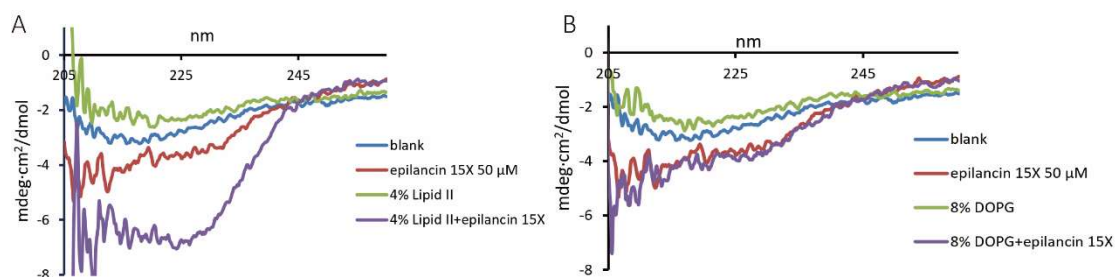


Figure 4. Lipid II-induced secondary structure of epilancin 15X. CD spectra recorded for 50 μM epilancin 15X in buffer E (tracing Red) and the buffer E control (tracing blue). (A) tracing purple

was recorded for 50 μM epilancin 15X in the presence of 50 μM Lipid II in DOPC SUVs (4 mol %) and green was recorded for 50 μM Lipid II in DOPC SUVs (4 mol %) only. (B) tracing purple and green were recorded for 50 μM epilancin 15X in the presence of 100 μM DOPG in DOPC SUVs (8 mol %) and 100 μM DOPG in DOPC SUVs (8 mol %) control.

4.3.4 Epilancin 15X -Lipid II binding does not lead to pore-formation.

Next, we checked whether the interaction between epilancin 15 X and Lipid II leads to membrane permeabilization of model membrane vesicles loaded with either carboxy fluorescein (CF) or 8-Hydroxypyrene-1,3,6-trisulfonic acid (HPTS). CF is loaded in self quenching concentrations into the vesicles thus monitoring the release of the probe (molar mass 376 Da). Nisin could efficiently induce CF leakage as expected from a pore-former where about 50% leakage could be observed from Lipid II containing LUVs at a nisin concentration of only 5 nM (Fig. S3A, red trace). No leakage could be observed from vesicles devoid of Lipid II (blue trace). Epilancin 15X did not cause leakage either in the absence or presence of Lipid II at ten times higher concentrations of 50 nM (Fig. S3B). Similar results were obtained when vesicles were used that also contained negatively charged phospholipids with the composition DOPC/DOPG (1:1) with/without 0.1% Lipid II (Fig. S4).

In our previous study, proton permeability activity of epilancin 15X toward *S. simulans*, *M. flavus* and *B. megaterium* were observed [45]. Furthermore, we even observed that epilancin 15X caused an increase in the pH_{in} of *M. flavus* at low concentrations. Thus, it may be possible that epilancin 15X and Lipid II together might form small pores that allow only protons instead of bigger molecular such as CF (1 nm of molecular radius) to pass through. To check whether epilancin 15X causes proton permeabilization in the presence of Lipid II in model vesicles, we tested for proton leakage using HPTS containing LUVs [44, 48]. HPTS is a pH sensitive fluorescent probe, and its fluorescent signal will decrease when protons from the more acidic exterior can enter the vesicles and lower the pH. As expected, nisin caused a rapid decrease in fluorescence when Lipid II was present (Fig. S3C). However, epilancin 15X failed to have any effect on the pH gradient even in the presence of Lipid II (Fig. S3D). Thus, even though epilancin 15X showed specific binding to Lipid II in vitro, this interaction did not lead to a detectable effect on the permeability of model membranes.

4.3.5 Interfering with the cell wall biosynthesis pathways affects epilancin 15X.

The observation that nisin(AB)-C14 could inhibit epilancin while vancomycin could not can be explained by the differences in substrate specificity of the two compounds.

Vancomycin targets the D-Ala-D-Ala terminus of the pentapeptide of Lipid II and nascent peptidoglycan and thus prevents both further transglycosylation and transpeptidation. Nisin(AB)-C14 targets not only Lipid II, but also other undecaprenyl-pyrophosphoryl-linked precursors including C55-PP, lipid α , lipid β and lipid ϕ .1 (and n). Thus, epilancin may target another undecaprenyl-pyrophosphoryl-linked precursor rather than Lipid II. This would explain the failure of epilancin 15X to cause permeabilization in model membranes containing Lipid II.

In order to check whether C55-PP is the target of epilancin 15X, we made use of bacitracin in the membrane depolarization assays. Bacitracin binds to C55-PP and thus blocks the lipid II cycle at that position resulting in PG synthesis inhibition. This assay showed that the presence of bacitracin inhibited the activity of both epilancin 15X and nisin (Fig. 5A). A two-fold higher concentration of bacitracin was needed to inhibit epilancin 15X to the same extent as that of nisin. These results suggest that C55-PP may play a role in the MoA of epilancin, so we tested it for possible antagonization activity in an agar diffusion assay. For this, we used farnesyl-pyrophosphate (C15-PP) that is water soluble and more stable as compared to C55-PP. The only difference between C55-PP and C15-PP is the length of lipid chain which is embedded in the cell membrane. No effect of 7.5 μ mol of C15-PP could be observed on the shape of the halo formed by epilancin 15X's antibacterial activity (Fig. S5B). We also checked the effect of C15-PP on the secondary structure of epilancin 15X in the presence of 0.1% Tween. In line with the agar diffusion assay, C15-PP did not induce any structural change in the peptide (Fig. S5A). Both these results suggest that it is unlikely that C55-PP is the direct target of epilancin 15X. However, the effect of bacitracin on the epilancin activity can be explained by an indirect effect of bacitracin on the pool of other undecaprenyl-pyrophosphoryl-linked precursors. Bacitracin addition to the cells will lead to an accumulation of C55-PP in the external leaflet of the plasma membrane, which in turn will cause a depletion of undecaprenyl-phosphate and other members of the Lipid II cycle. This will also affect other biosynthesis pathways that rely on this compound, such as the wTA pathway.

Considering this indirect effect of bacitracin, it is hard to explain why vancomycin did not inhibit the membrane depolarization activity of epilancin 15X, while bacitracin did. A possible explanation for this is that vancomycin needs more time to completely block the lipid II cycle before it can have an effect on epilancin's activity. To test this, we prolonged the preincubation time of *S. simulans* with vancomycin to 5 and 10 minutes. Indeed, the depolarization activity of epilancin 15X was greatly suppressed already after 5 min preincubation with vancomycin and a complete inhibition could be observed after 10 min (Fig. 5B). Notably, at time point 0 minutes, the activity of epilancin was already affected a bit (compare epilancin traces in figures 5A and 5B), which can be explained by an increased dead-time of the experiment due to a washing step. Thus, vancomycin induced accumulation of Lipid II and concomitant disruption of the Lipid II cycle also leads to inhibition of epilancin's effect on the membrane potential. Moreover,

also these results indicate that Lipid II is probably not the target of epilancin 15X, as addition of vancomycin inhibited nisin but not epilancin 15X.

Our previous study showed that when studying MoAs of AMPs, one should not rely on only one bacterium [45]. We therefore tested whether the above effects could also be observed for *M. flavus*. Indeed, similar inhibitory effects of bacitracin, nisin(AB)-C14 and vancomycin to nisin and epilancin 15X were observed using *M. flavus* (Fig. S6). With these bacteria, a prolonged incubation time with vancomycin was not needed to inhibit the membrane depolarization activity of epilancin 15X. From the results above a picture emerges in which the inhibitory activity of epilancin 15X is dependent on the correct functioning of the Lipid II cycle. Possibly, inhibition of this cycle has an effect on the availability of epilancin's target. While Lipid II itself and C55-PP are ruled out as possible targets within the PG biosynthesis pathway, another (biosynthesis) pathway that is affected by a blockage of the Lipid II cycle likely harbors the target of epilancin 15X.

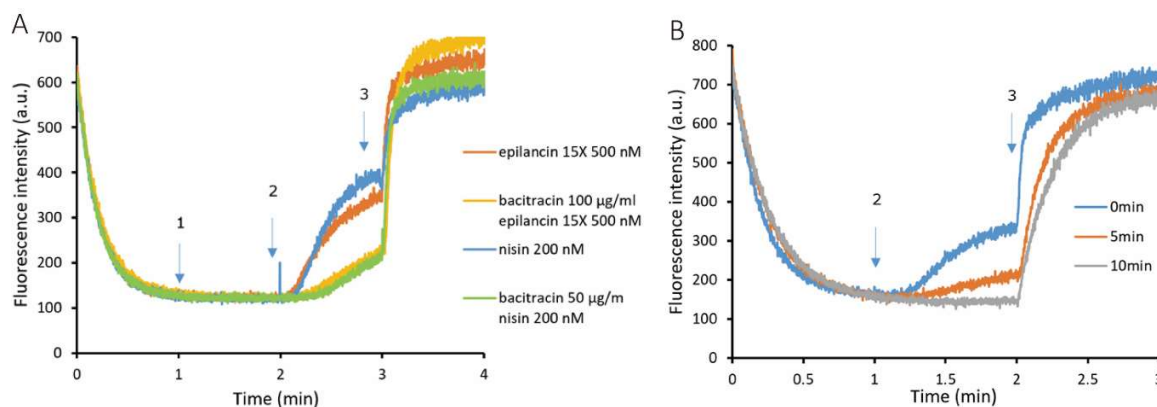


Figure 5. Effects of bacitracin and prolonged incubation with vancomycin on epilancin 15X's ability to disrupt the membrane potential of *S. simulans* cells. (A) 500 nM epilancin 15X was added at 2 min (orange), 100 µg/ml bacitracin was added at 1 min and 500 nM epilancin 15X was added at 2 min (yellow); 200 nM nisin 15X added at 2 min (blue), 50 µg/ml bacitracin was added at 1 min and 200 nM nisin was added at 2 min (green). (B) Intact cells were treated with 10 µM vancomycin for 0 min (blue), 5 min (orange), 10 min (grey). 200 nM epilancin 15X was added at 1 min. Arrows match the addition of antagonists (1), lantibiotics (2), and 20 µL 20% Triton X-100 (3), which was added to dissipate 100% membrane potential.

4.3.6 PG-synthesis inhibition at the level of PBPs and their effects on the activity of epilancin 15X.

All the antibiotics that we used to test for possible targets of epilancin, i.e. vancomycin, bacitracin and nisin(AB)-C14 act at the level of the Lipid II cycle of the PG-biosynthesis pathway. Next, we disrupted the PG pathway at the level of the PBPs to test effects of epilancin 15X. For this we used two PBP-targeting antibiotics penicillin G and

moenomycin. Penicillin targets the transpeptidation activity of both monofunctional and bifunctional PBPs, which inhibits the crosslinking of polymerized peptidoglycan strains [31]. Moenomycin targets the transglycosylase domain of PBP which blocks the Lipid II polymerization step [32]. The addition of penicillin did not affect the membrane depolarization activity of nisin and epilancin 15X as can be expected since blocking transpeptidation/crosslinking does not have an effect on the Lipid II cycle (Fig. 6). Addition of moenomycin completely blocked the depolarization activity of nisin and also inhibits that of epilancin 15X, albeit to a lesser extent. The complete block of nisin (and also the partly block of epilancin) activity came as a surprise as it's known that moenomycin accumulates Lipid II in the bacterial membrane, which is also true for the *S. simulans* cells (unpublished observations). These observations can only be explained if the accumulated Lipid II is located at the cytosolic side of the plasma membrane, which would point to a (strict) coupling of transport of Lipid II to its use in the polymerization step of the PG synthesis pathway. Hence, moenomycin causes an (indirect) block of the transport of Lipid II. Eventually, this accumulation will lead to a depletion of the undecaprenyl-phosphate pool available to the other biosynthesis pathways that rely on this pool. Thus, only the antibiotics that block the Lipid II cycle of the PG biosynthesis pathway inhibit the activity of nisin and epilancin 15X. Again, similar results were obtained with *M. flavus* as the test bacterium (Fig. S7), albeit that the effect of moenomycin on epilancin was less severe.

Interestingly, the addition of moenomycin caused a small decrease of the fluorescence, which points to a possible moenomycin induced increase in the membrane potential of the bacteria. In this, the effect resembles the effect of adding nigericin, a H^+/K^+ antiporter that increases the membrane potential at the expense of the ΔpH [49]. The origin of this effect of moenomycin remains unclear, but may be related to the block in Lipid II transport.

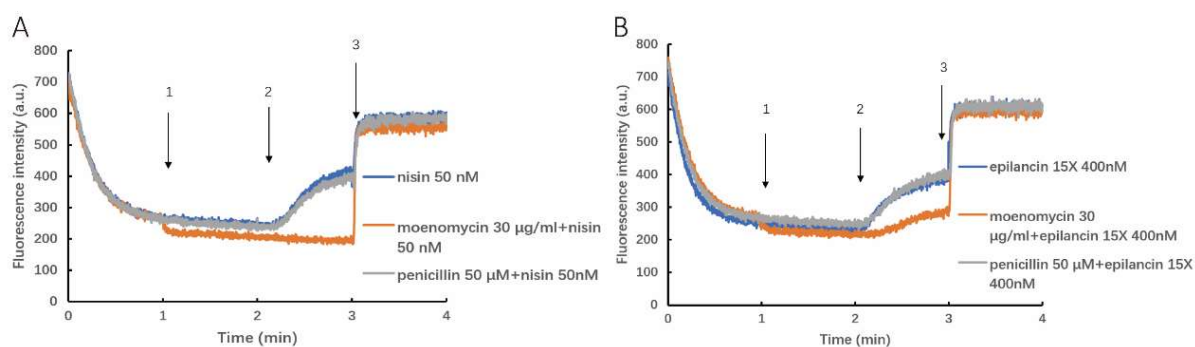


Figure 6. Effects of penicillin and moenomycin on the membrane depolarization activity of nisin and epilancin 15X in *S. simulans* cells. (A) 50 nM nisin was added at 2 min (blue); 30 µg/ml moenomycin was added at 1 min and 50 nM nisin added at 2 min (orange), 50 µM penicillin was added at 1 min and 50 nM nisin was added at 2 min (gray). (B) 400 nM epilancin 15X was added at 2 min (blue); 30 µg/ml moenomycin was added at 1 min and 400 nM epilancin 15X was added at 2 min (orange), 50 µM penicillin was added at 1 min and 400 nM epilancin 15X was added at 2

min (gray) Arrows mark the addition of antagonists (1), lantibiotics (2), and 20 μ L 20% Triton X-100 (3), which was added to fully dissipate the membrane potential.

4.3.7 wTA precursor is not the target of epilancin 15X.

Direct inhibition of the Lipid II cycle by means of the compounds used so far all affected the activity of epilancin 15X, but this can also be attributed to their indirect effect on other pathways that make use of undecaprenyl-phosphate as a carrier. The other main pathway in gram-positive bacteria that uses this precursor is the wTA pathway. To check whether epilancin 15X targets the wTA synthesis pathway, we first tried to use tunicamycin and targocil (a wTA flippase inhibitor) as antagonists in the membrane depolarization activity of nisin or epilancin 15X towards *S. simulans*. Unfortunately, both compounds had an effect on the membrane potential on their own account, where tunicamycin decreased the membrane potential of cells at 10 μ g/ml and the addition of targocil somehow causes an increased membrane potential (Fig. S8), making it impossible to use these compounds in our assay. Thus, we took an alternative way that used a *B. Subtilis* TagO deletion mutant to check whether wTA precursors are involved in the mode of action of epilancin 15X. TagO is a phosphosugar transferase that forms GlcNAc-pp-undecaprenyl, which is a reversible step [50]. After deleting the *tagO* gene, cells will not be able to form wTA. We performed an agar diffusion assay with a 2-fold serial dilution of epilancin 15X on the *B. Subtilis* Δ TagO strain (Fig. S9A) and the corresponding wildtype (Fig. S9B). The halo sizes indicate that the Δ TagO strain was much more sensitive to epilancin 15X than the wild-type strain. The concentration of epilancin 15X in NO.8 (0.16 μ M) clearly caused a halo on the plates with the *B. Subtilis* Δ TagO strain and for wild type, epilancin 15X showed its inhibition at the concentration in No.4 (2.5 μ M) which is 16 time higher than that of TagO mutant. So, a wTA precursor is not the target of epilancin 15X. Instead, the negative charged wTA may even play a protective role in bacteria by trapping the positive charged epilancin 15X, thereby preventing the peptide to reach the membrane.

4.3.8 Recognition of lipid-linked pyrophosphates by epilancin 15X.

The effects of the inhibition of the Lipid II cycle on the activity of epilancin 15X and the interaction of epilancin 15X with Lipid II as shown by CD points to a target that resides in a polyprenol-based biosynthesis pathway. Yet, Lipid II is not likely to be that target in view of epilancin 15X's low affinity for Lipid II as well as the lack of any effect on the membrane permeability in model systems containing Lipid II. Similarly, wTA precursors are also not likely to be the target in view of the results with the TagO deletion mutant. This makes it difficult to draw conclusions on what constitutes the target of epilancin 15X. In all likelihood this target concerns a pyrophosphate containing molecule, which made us wonder if epilancin 15X would be able to recognize CDG-DAG. This lipid, an important precursor in the phospholipid biosynthesis routes, contains a diacylglycerol-

linked pyrophosphate to which a cytidyl group is attached (Fig. S10A). So, some resemblance to the polyprenyl-pyrophosphate-linked sugars is apparent. We tested the possible interaction of epilancin 15X by CD, and could observe a significant change in the secondary structure of the peptide in the presence of CDP-DAG (Fig. S10B). This shows that epilancin 15X can recognize pyrophosphoryl groups that are not polyisoprenoid-linked and a hexose sugar following the pyrophosphoryl group isn't necessary either. As epilancin 15X did not interact with farnesyl-pyrophosphate, this indicates that epilancin 15X recognizes pyrophosphate groups that are derivatized on both sides, i.e. containing phosphodiester.

4.4 Conclusions

This study focused on exploring potential targets of epilancin 15X within the bacterial membrane and involved in the PG and wTA biosynthesis cycles. Several results suggested that the target of epilancin 15X is located in polyprenol-based biosynthesis pathways. Although a clear interaction between epilancin 15X and Lipid II was observed and Lipid II induced conformation change of epilancin 15X, this interaction failed to result in permeabilization of model membrane, which indicated that Lipid II is likely not the actual target. Similarly, C55-PP and wTA precursors are also unlikely to be the target of epilancin 15X. Interestingly, we could show an interaction between epilancin 15X and CDP-DAG, which implied that epilancin 15X does target phosphodiester containing molecules. However, the actual target of epilancin 15X was not identified yet, but it cannot be ruled out that epilancin 15X uses multiple targets within a bacterium.

Footnote:

1. In Fig. 4, buffer 20 mM HEPES, 40 mM Na₂SO₄, pH 7.4 was used and the concentration of epilancin 15X was 50 μM. In Fig. S5A, buffer 0.1% Tween-20, 50 mM phosphate, pH 5 was used and the concentration of epilancin 15X was 80 μM. The CD spectrums of epilancin 15X were changed likely due to Tween-20.

4.5 References

1. van Kraaij, C., et al., *Lantibiotics: biosynthesis, mode of action and applications*. Natural product reports, 1999. **16**(5): p. 575-587.
2. Heng, N.C. and J.R. Tagg, *What's in a name? Class distinction for bacteriocins*. Nature Reviews Microbiology, 2006. **4**(2).
3. McAuliffe, O., R.P. Ross, and C. Hill, *Lantibiotics: structure, biosynthesis and mode of action*. FEMS microbiology reviews, 2001. **25**(3): p. 285-308.
4. Breukink, E. and B. de Kruijff, *The lantibiotic nisin, a special case or not?* Biochimica et Biophysica Acta (BBA) - Biomembranes, 1999. **1462**(1–2): p. 223-234.
5. de Kruijff, B., V. van Dam, and E. Breukink, *Lipid II: a central component in bacterial cell wall synthesis and a target for antibiotics*. Prostaglandins, leukotrienes and essential fatty acids, 2008. **79**(3): p. 117-121.
6. Wang, X., Q. Gu, and E. Breukink, *Non-lipid II targeting lantibiotics*. Biochimica et Biophysica Acta (BBA) - Biomembranes, 2020. **1862**(8): p. 183244.
7. Ekkelenkamp, M.B., et al., *Isolation and structural characterization of epilancin 15X, a novel lantibiotic from a clinical strain of Staphylococcus epidermidis*. FEBS Letters, 2005. **579**(9): p. 1917-1922.
8. Velásquez, J.E., X. Zhang, and W.A. Van Der Donk, *Biosynthesis of the antimicrobial peptide epilancin 15X and its N-terminal lactate*. Chemistry & biology, 2011. **18**(7): p. 857-867.
9. Verhoef, J., Milatovic, D., and Ekkelenkamp, M.B., *Antimicrobial compounds*. 2005.
10. Van De Kamp, M., et al., *Sequence Analysis by NMR Spectroscopy of the Peptide Lantibiotic Epilancin K7 from Staphylococcus epidermidis K7*. European Journal of Biochemistry, 1995. **227**(3): p. 757-771.
11. Wiedemann, I., et al., *Specific binding of nisin to the peptidoglycan precursor lipid II combines pore formation and inhibition of cell wall biosynthesis for potent antibiotic activity*. Journal of Biological Chemistry, 2001. **276**(3): p. 1772-1779.
12. Immonen, T. and P.E.J. Saris, *Characterization of the nisFEG Operon of the Nisin Z Producing Lactococcus Lactis Subsp. Lactis N8 Strain*. DNA Sequence, 1998. **9**(5-6): p. 263-274.
13. Brötz, H., et al., *Role of lipid-bound peptidoglycan precursors in the formation of pores by nisin, epidermin and other lantibiotics*. Molecular Microbiology, 1998. **30**(2): p. 317-327.
14. D'Elia, M.A., et al., *Probing teichoic acid genetics with bioactive molecules reveals new interactions among diverse processes in bacterial cell wall biogenesis*. Chem Biol, 2009. **16**(5): p. 548-56.

15. Sewell, E.W. and E.D. Brown, *Taking aim at wall teichoic acid synthesis: new biology and new leads for antibiotics*. J Antibiot (Tokyo), 2014. **67**(1): p. 43-51.
16. Chung, B.C., et al., *Crystal structure of MraY, an essential membrane enzyme for bacterial cell wall synthesis*. Science, 2013. **341**(6149): p. 1012-1016.
17. Sham, L.T., et al., *Bacterial cell wall. MurJ is the flippase of lipid-linked precursors for peptidoglycan biogenesis*. Science, 2014. **345**(6193): p. 220-2.
18. Mohammadi, T., et al., *Specificity of the transport of lipid II by FtsW in Escherichia coli*. J Biol Chem, 2014. **289**(21): p. 14707-18.
19. Jeong, J.H., et al., *Crystal structures of bifunctional penicillin-binding protein 4 from Listeria monocytogenes*. Antimicrob Agents Chemother, 2013. **57**(8): p. 3507-12.
20. Egan, A.J., et al., *Activities and regulation of peptidoglycan synthases*. Philos Trans R Soc Lond B Biol Sci, 2015. **370**(1679).
21. Manat, G., et al., *Membrane Topology and Biochemical Characterization of the Escherichia coli BacA Undecaprenyl-Pyrophosphate Phosphatase*. PLoS One, 2015. **10**(11): p. e0142870.
22. Soldo, B., V. Lazarevic, and D. Karamata, *tagO is involved in the synthesis of all anionic cell-wall polymers in Bacillus subtilis 168*. Microbiology (Reading), 2002. **148**(Pt 7): p. 2079-2087.
23. Zhang, Y.H., et al., *Acceptor substrate selectivity and kinetic mechanism of Bacillus subtilis TagA*. Biochemistry, 2006. **45**(36): p. 10895-904.
24. Bhavsar, A.P., R. Truant, and E.D. Brown, *The TagB protein in Bacillus subtilis 168 is an intracellular peripheral membrane protein that can incorporate glycerol phosphate onto a membrane-bound acceptor in vitro*. J Biol Chem, 2005. **280**(44): p. 36691-700.
25. Schertzer, J.W. and E.D. Brown, *Purified, recombinant TagF protein from Bacillus subtilis 168 catalyzes the polymerization of glycerol phosphate onto a membrane acceptor in vitro*. J Biol Chem, 2003. **278**(20): p. 18002-7.
26. Allison, S.E., et al., *Studies of the genetics, function, and kinetic mechanism of TagE, the wall teichoic acid glycosyltransferase in Bacillus subtilis 168*. J Biol Chem, 2011. **286**(27): p. 23708-16.
27. Lazarevic, V. and D. Karamata, *The tagGH operon of Bacillus subtilis 168 encodes a two-component ABC transporter involved in the metabolism of two wall teichoic acids*. Mol Microbiol, 1995. **16**(2): p. 345-55.
28. Neuhaus, F.C. and J. Baddiley, *A continuum of anionic charge: structures and functions of D-alanyl-teichoic acids in gram-positive bacteria*. Microbiol Mol Biol Rev, 2003. **67**(4): p. 686-723.
29. Breukink, E. and B. de Kruijff, *Lipid II as a target for antibiotics*. Nature Reviews Drug Discovery, 2006. **5**: p. 321.
30. Stone, K.J. and J.L. Strominger, *Mechanism of action of bacitracin: complexation with metal ion*

- and C55-isoprenyl pyrophosphate. Proceedings of the National Academy of Sciences, 1971. **68**(12): p. 3223-3227.
31. Yocum, R.R., J.R. Rasmussen, and J.L. Strominger, *The mechanism of action of penicillin. Penicillin acylates the active site of Bacillus stearothermophilus D-alanine carboxypeptidase.* J Biol Chem, 1980. **255**(9): p. 3977-86.
 32. Ostash, B. and S. Walker, *Moenomycin family antibiotics: chemical synthesis, biosynthesis, and biological activity.* Nat Prod Rep, 2010. **27**(11): p. 1594-617.
 33. Lee, K., et al., *Development of improved inhibitors of wall teichoic acid biosynthesis with potent activity against Staphylococcus aureus.* Bioorg Med Chem Lett, 2010. **20**(5): p. 1767-70.
 34. Brandish, P.E., et al., *Modes of action of tunicamycin, liposidomycin B, and mureidomycin A: inhibition of phospho-N-acetylmuramyl-pentapeptide translocase from Escherichia coli.* Antimicrob Agents Chemother, 1996. **40**(7): p. 1640-4.
 35. Hancock, I.C., G. Wiseman, and J. Baddiley, *Biosynthesis of the unit that links teichoic acid to the bacterial wall: inhibition by tunicamycin.* FEBS Lett, 1976. **69**(1): p. 75-80.
 36. Dengler, V., et al., *Deletion of hypothetical wall teichoic acid ligases in Staphylococcus aureus activates the cell wall stress response.* FEMS Microbiol Lett, 2012. **333**(2): p. 109-20.
 37. Chen, W., et al., *Characterization of the tunicamycin gene cluster unveiling unique steps involved in its biosynthesis.* Protein Cell, 2010. **1**(12): p. 1093-105.
 38. Kuipers, O.P., et al., *Engineering dehydrated amino acid residues in the antimicrobial peptide nisin.* Journal of Biological Chemistry, 1992. **267**(34): p. 24340-24346.
 39. Sahl, H.-G. and H. Brandis, *Production, purification and chemical properties of an antistaphylococcal agent produced by Staphylococcus epidermidis.* Microbiology, 1981. **127**(2): p. 377-384.
 40. van Kan, E.J., et al., *Membrane activity of the peptide antibiotic clavamin and the importance of its glycine residues.* Biochemistry, 2001. **40**(21): p. 6398-6405.
 41. Rouser, G., S. Fleischer, and A. Yamamoto, *Two dimensional thin layer chromatographic separation of polar lipids and determination of phospholipids by phosphorus analysis of spots.* Lipids, 1970. **5**(5): p. 494-496.
 42. Bligh, E. and W. Dyer, *Canadian Journal of Biochemistry and Physiology.* A rapid method of lipid extraction and purification, 1959. **37**: p. 911-917.
 43. van Kan, E.J., et al., *The role of the abundant phenylalanines in the mode of action of the antimicrobial peptide clavamin.* Biochimica et Biophysica Acta (BBA)-Biomembranes, 2003. **1615**(1): p. 84-92.
 44. Te Welscher, Y.M., et al., *Natamycin blocks fungal growth by binding specifically to ergosterol without permeabilizing the membrane.* Journal of Biological Chemistry, 2008. **283**(10): p. 6393-

6401.

45. Wang, X., et al., *Analyzing mechanisms of action of antimicrobial peptides on bacterial membranes requires multiple complimentary assays and different bacterial strains*. *Biochim Biophys Acta Biomembr*, 2023. **1865**(6): p. 184160.
46. Knox, J.R. and R.F. Pratt, *Different modes of vancomycin and D-alanyl-D-alanine peptidase binding to cell wall peptide and a possible role for the vancomycin resistance protein*. *Antimicrobial Agents and Chemotherapy*, 1990. **34**(7): p. 1342-1347.
47. Koopmans, T., et al., *Semisynthetic lipopeptides derived from nisin display antibacterial activity and lipid II binding on par with that of the parent compound*. *Journal of the American Chemical Society*, 2015. **137**(29): p. 9382-9389.
48. van Kan, E.J., et al., *Clavanin permeabilizes target membranes via two distinctly different pH-dependent mechanisms*. *Biochemistry*, 2002. **41**(24): p. 7529-39.
49. Prabhananda, B.S. and M.M. Ugrankar, *Nigericin-mediated H⁺, K⁺ and Na⁺ transports across vesicular membrane: T-jump studies*. *Biochim Biophys Acta*, 1991. **1070**(2): p. 481-91.
50. Swoboda, J.G., et al., *Wall Teichoic Acid Function, Biosynthesis, and Inhibition*. *Chembiochem : a European journal of chemical biology*, 2010. **11**(1): p. 35-45.

4.6 Supplement information

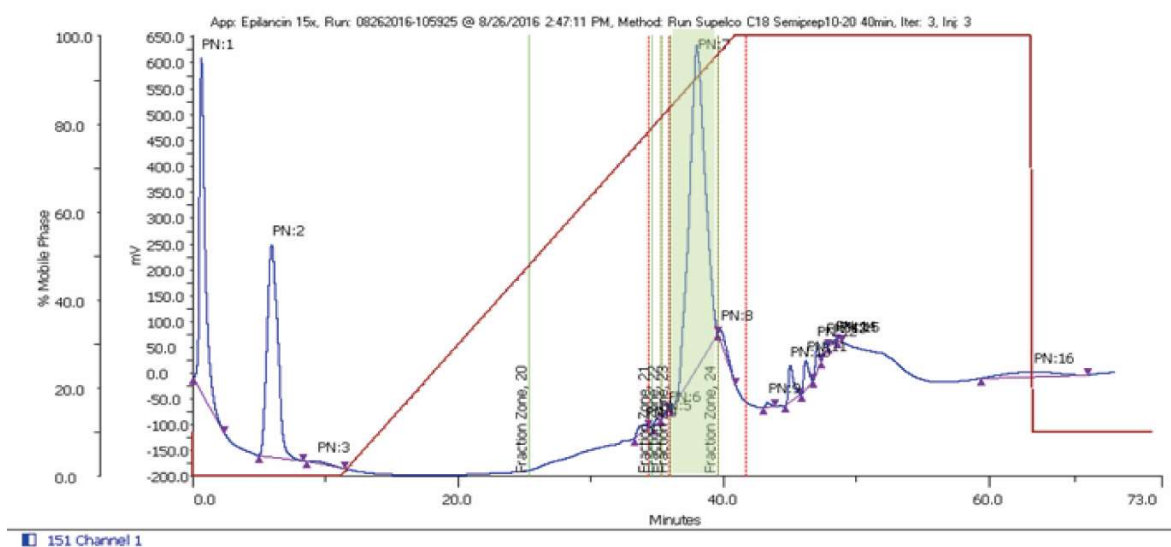


Figure S1. A typical HPLC spectrum of Epilancin 15X. Epilancin 15X was purified from the fractions containing antimicrobial activity using a C18 RP-HPLC column (LiChrospher, 250 mm × 4.6 mm, 5 μm) equilibrated in eluent B (95% acetonitrile, 5% water, 0.05% TFA) and using a linear gradient from 0% to 100% eluent B in 30 min (flow rate at 0.8 mL/min, UV detection at 214 nm). Epilancin 15X appeared as a broad peak at 98% B, marked with green highlight.

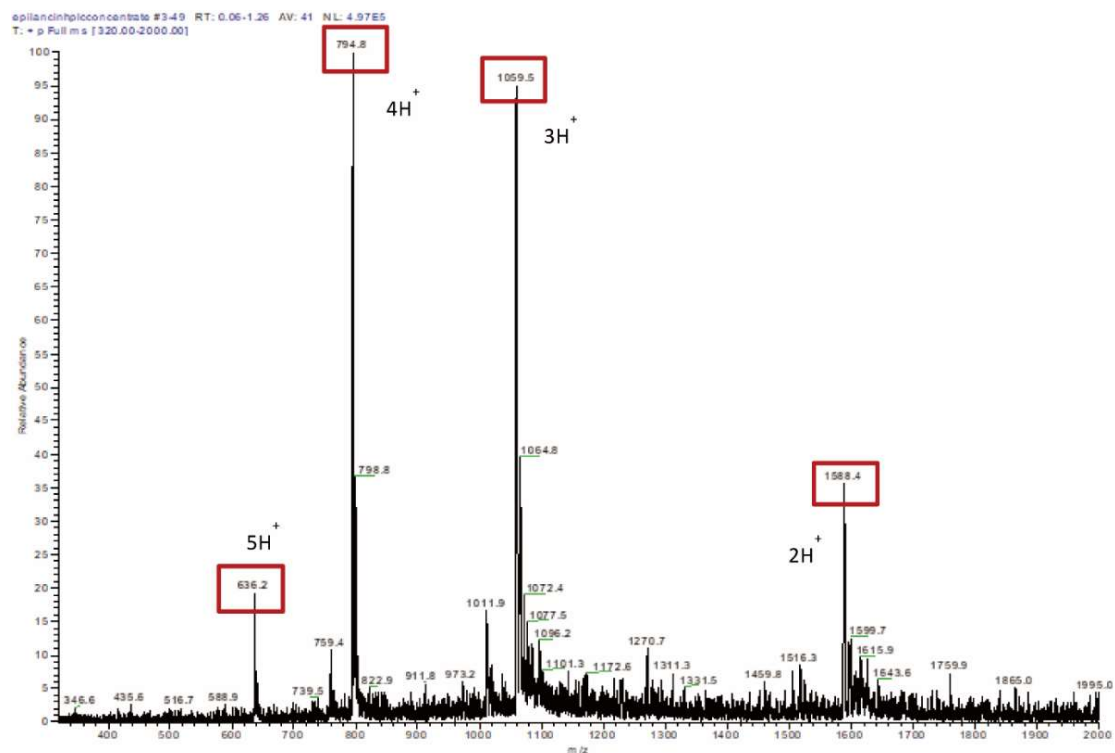


Figure S2. Mass Spectrum of epilancin 15X. The spectrum contains 4 main peaks at m/z of 636.2

(5 H⁺), 794.8 (4 H⁺), 1059.5 (3 H⁺) and 1588.4 (2 H⁺) pointing to a molecular weight 3176 Da (Thermo Finnigan).

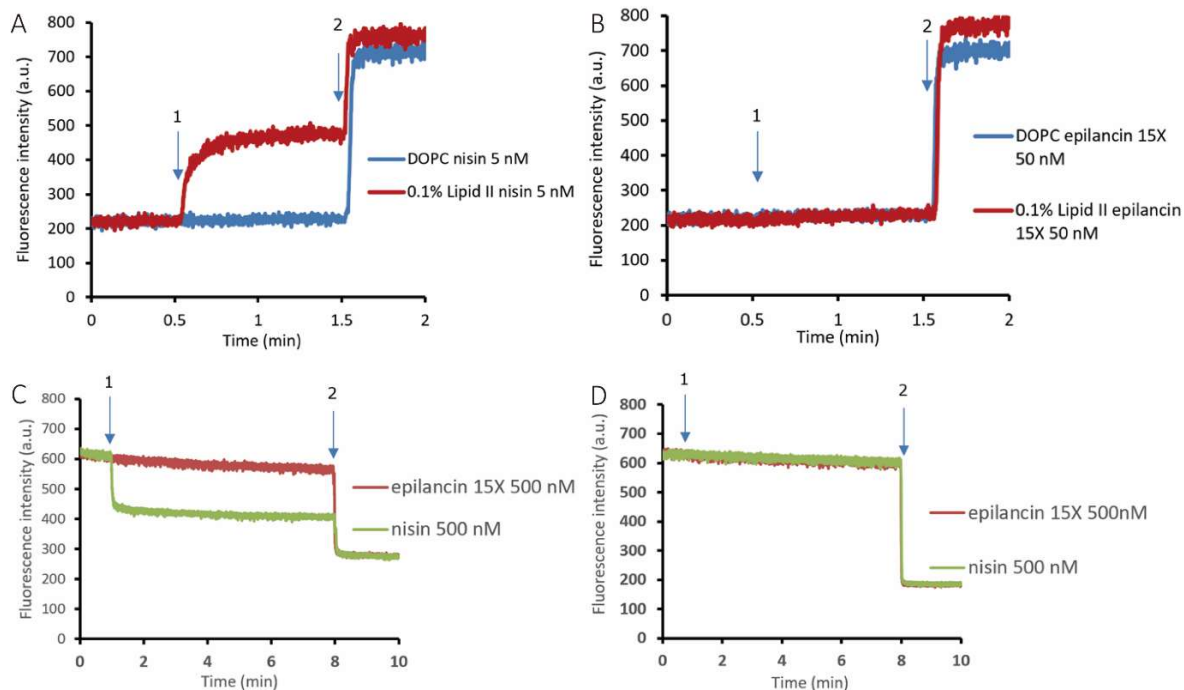


Figure S3. Effect of epilancin 15X and nisin on the CF leakage and proton permeability of LUVs with or without Lipid II. (A) 5 nM nisin was added to DOPC LUVs (blue) and 0.1% Lipid II containing DOPC LUVs (red). (B) 50 nM epilancin 15X was added to DOPC LUVs (blue) and 0.1% Lipid II containing DOPC LUVs (red). (C) 500 nM epilancin 15X (red) and 500 nM nisin (green) were added to LUVs containing 4% Lipid II and 96% DOPC. (D) 500 nM epilancin 15X (red) and 500 nM nisin (green) were added to LUVs containing 8% DOPG and 92% DOPC. Arrows match the addition of lantibiotics (1) and 20 μ L 20% Triton X-100 (2), which was added to obtain the maximum leakage or permeability.

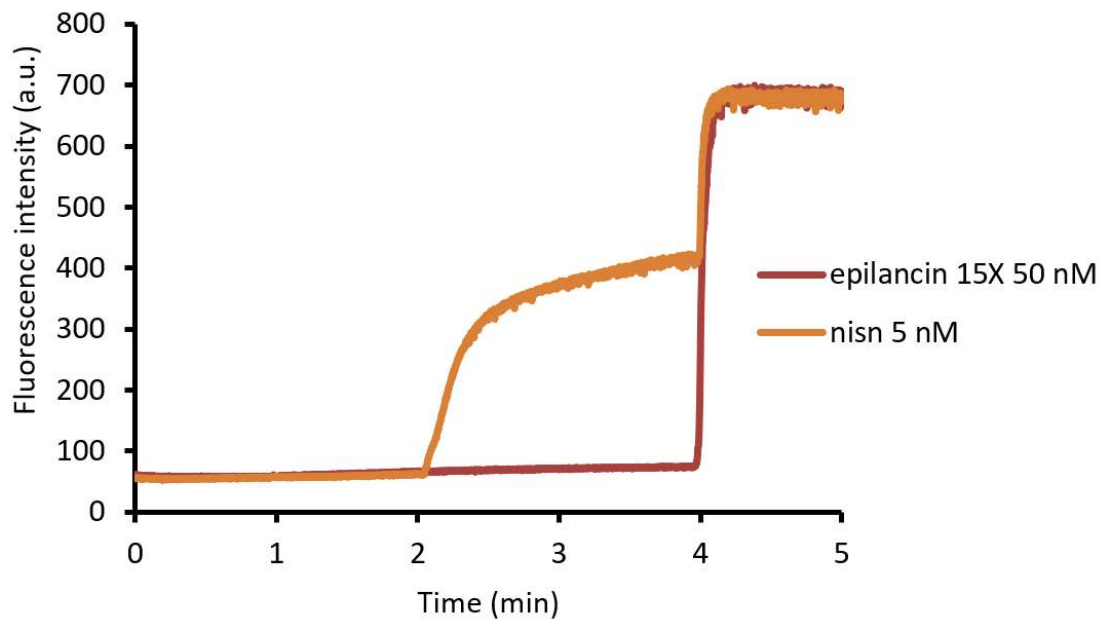


Figure S4. Model membrane permeabilization assay using CF leakage. Vesicles were composed of 50% DOPC and 50% DOPG LUVs containing 0.1% Lipid II. 50 nM epilancin 15X was added at 1 min (Red), 5 nM nisin was added at 2 min (orange). Although epilancin 15X and nisin were added at different time, 5 nM nisin causes 50% CF leakage, while epilancin 15X does not.

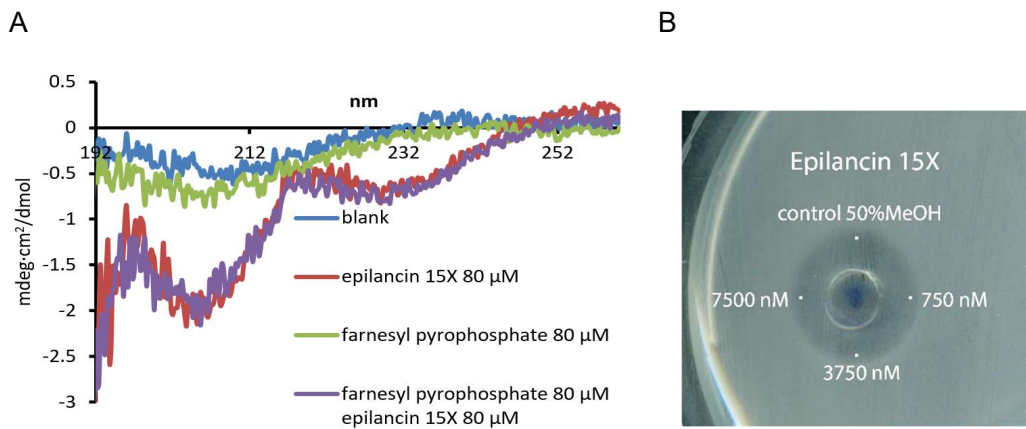


Figure S5. (A) CD spectrum of epilancin 15X and farnesyl pyrophosphate. CD spectra recorded in 50 mM phosphate buffer pH5 containing 0.1% tween-20. Tracing purple was recorded for 80 μ M epilancin 15X in the presence of 80 μ M farnesyl pyrophosphate which shows no different compared to tracing red. Tracing red and green were recorded for 80 μ M epilancin 15X and 80 μ M farnesyl pyrophosphate. Tracing blue is buffer control. (B) Antagonist action between epilancin 15X and farnesyl pyrophosphate. We add 2 μ L farnesyl pyrophosphate at the concentration of 750 nM, 3750 nM, 7500 nM. No antagonist reaction between epilancin 15X and farnesyl pyrophosphate was detected.

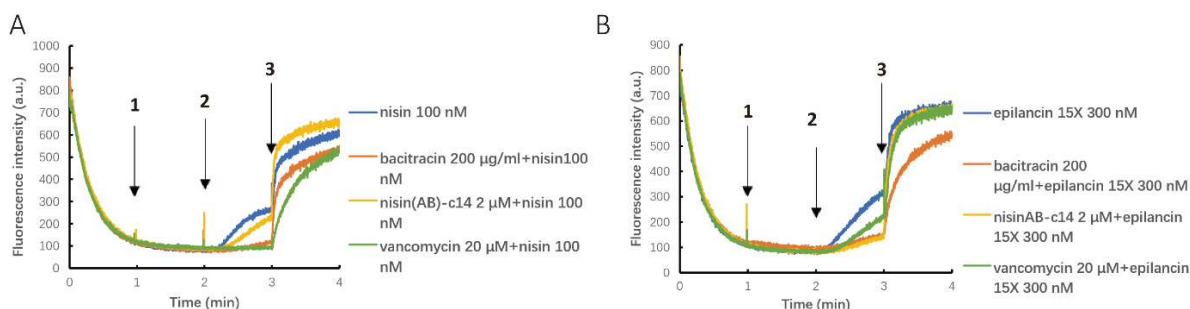


Figure S6. Test for antagonization activity of bacitracin, nisin(AB)-C14 and vancomycin towards the membrane depolarization activity of nisin or epilancin 15X in *M. flavus*. (A) 100 nM nisin was added at 2 min (blue); 200 µg/ml bacitracin was added at 1 min and 100 nM nisin added at 2 min (orange), 2 µM nisin(AB)-c14 was added at 1 min and 100 nM nisin was added at 2 min (yellow), 20 µM vancomycin was added at 1 min and 100 nM nisin was added at 2 min (green). (B) 300 nM epilancin 15X was added at 2 min (blue); 200 µg/ml bacitracin was added at 1 min and 300 nM epilancin 15X was added at 2 min (orange), 2 µM nisin(AB)-c14 was added at 1 min and 300 nM epilancin 15X was added at 2 min (green), 20 µM vancomycin was added at 1 min and 300 nM epilancin 15X was added at 2 min (green). Arrows mark the addition of antagonists (1), lantibiotics (2), and 20 µL 20% Triton X-100 (3), which was added to fully dissipate the membrane potential.

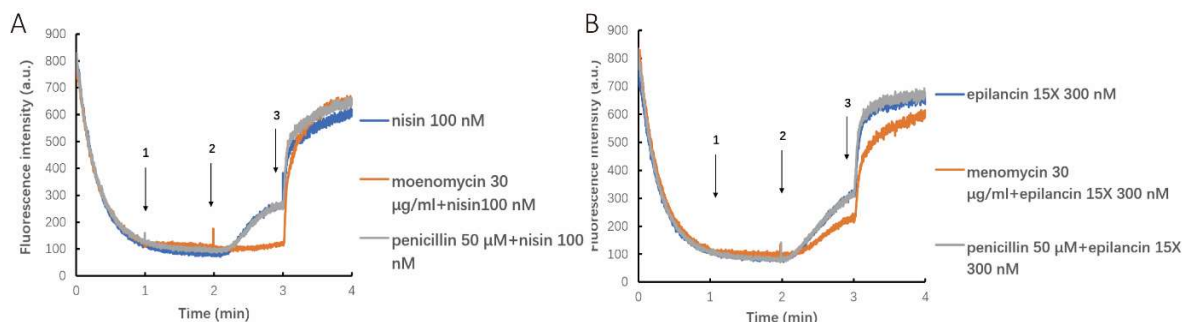


Figure S7. Test for antagonization activity of penicillin and moenomycin towards the membrane depolarization activity of nisin or epilancin 15X in *M. flavus*. (A) 100 nM nisin was added at 2 min (blue); 30 µg/ml moenomycin was added at 1 min and 100 nM nisin added at 2 min (orange), 50 µM penicillin was added at 1 min and 100 nM nisin was added at 2 min (gray). (B) 300 nM epilancin 15X was added at 2 min (blue); 30 µg/ml moenomycin was added at 1 min and 300 nM epilancin 15X was added at 2 min (orange), 50 µM penicillin was added at 1 min and 300 nM epilancin 15X was added at 2 min (gray) Arrows mark the addition of antagonists (1), lantibiotics (2), and 20 µL 20% Triton X-100 (3), which was added to fully dissipate the membrane potential.

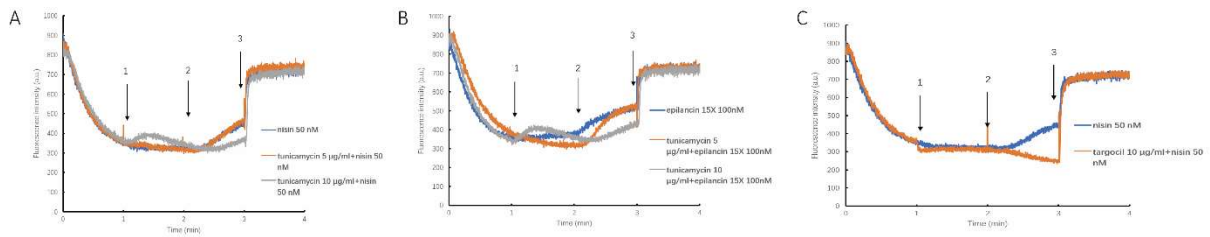


Figure S8. Test for antagonization activity of tunicamycin and targocil towards the membrane depolarization activity of nisin or epilancin 15X in *S. simulans*. (A) 50 nM nisin was added at 2 min (blue); 5 µg/ml tunicamycin was added at 1 min and 50 nM nisin added at 2 min (orange), 10 µg/ml tunicamycin was added at 1 min and 50 nM nisin was added at 2 min (gray). (B) 100 nM epilancin 15X was added at 2 min (blue); 5 µg/ml tunicamycin was added at 1 min and 100 nM epilancin 15X was added at 2 min (orange), 10 µg/ml tunicamycin was added at 1 min and 100 nM epilancin 15X was added at 2 min (gray). (C) 50 nM nisin was added at 2 min (blue); 10 µg/ml targocil was added at 1 min and 50 nM nisin added at 2 min (orange). Arrows mark the addition of antagonists (1), lantibiotics (2), and 20 µL 20% Triton X-100 (3), which was added to fully dissipate the membrane potential.

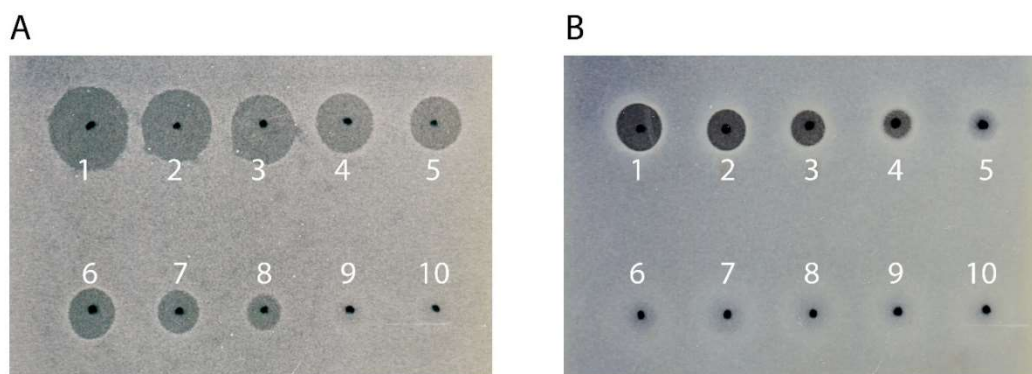


Figure S9. Agar diffusion assay of epilancin 15X with *B. subtilis* TagO Mutant and *B. subtilis* wild type. (A) The indicator strain was *B. subtilis* TagO Mutant. (B) The indicator strain was *B. subtilis* wild type. 10 µL 2-fold serial dilutions of epilancin 15X (from 1 to 10) were spotted on an agar plate, the initial concentration of epilancin 15X was 50 µM.

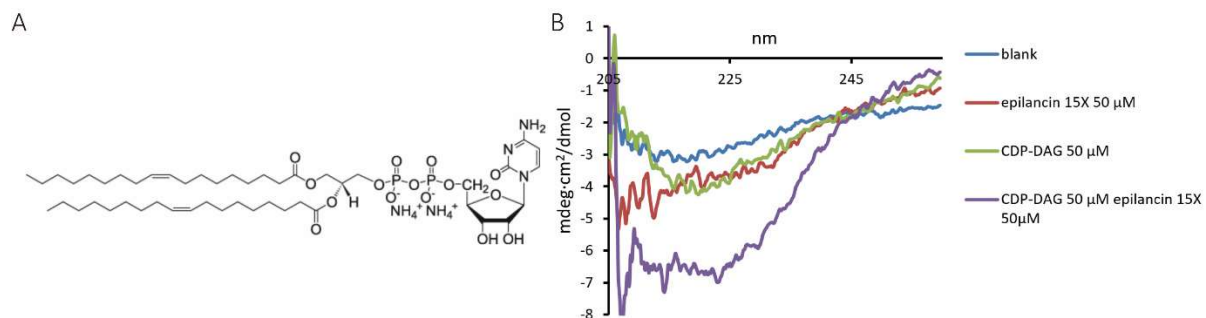


Figure S10. Interaction of epilancin 15X with CDP-DAG. (A) Chemical structure of CDP-DAG (B) CD spectrum of epilancin 15X and CDP-DAG. CD spectra recorded in 50 mM phosphate buffer pH5 containing 0.1% tween-20. Tracing purple was recorded for 50 μ M epilancin 15X in the presence of 50 μ M CDP-DG which shows dramatic change compared to tracing red. Tracing red and green were recorded for 50 μ M epilancin 15X and 50 μ M CDP-DG. Tracing blue is buffer control.

Chapter5

The interactions of brevibacillin and brevibacillin 2V with Lipid II

This chapter is based on:

Xinghong Zhao, Xiaoqi Wang, Rhythm Shukla, Raj Kumar, Markus Weingarth, Eefjan Breukink, and Oscar P. Kuipers. "Brevibacillin 2v Exerts Its Bactericidal Activity Via Binding to Lipid II and Permeabilizing Cellular Membranes." *Front Microbiol* 12 (2021): 694847. <https://dx.doi.org/10.3389/fmicb.2021.694847>.

Xinghong Zhao, Xiaoqi Wang, Rhythm Shukla, Raj Kumar, Markus Weingarth, Eefjan Breukink, and Oscar P. Kuipers. "Brevibacillin 2v, a Novel Antimicrobial Lipopeptide with an Exceptionally Low Hemolytic Activity." *Original Research*, 12, no. 1501 (2021-June-17 2021). <https://dx.doi.org/10.3389/fmicb.2021.693725>.

Abstract

Brevibacillins are non-ribosomally lipo-tridecapeptides which show potential against antimicrobial resistance bacteria. Here two of these peptides, brevibacillin and brevibacillin 2V, that have similar antimicrobial activity but differ greatly in hemolytic activity are studied. We found an antagonist effects of Lipid II on the activity of both brevibacillins in an agar diffusion assay, which led us to perform a series of experiments to study the interaction between brevibacillin/brevibacillin 2V and Lipid II. CD spectra using 3-Lipid II and 7-Lipid II suggested that brevibacillins bind to the head group of Lipid II instead of the undecaprenyl tail. Experiments using pyrene-labeled Lipid II indicated that brevibacillin/brevibacillin 2V did not cluster together with Lipid II into an organized structure such as a pore. Results from ITC experiments suggested brevibacillin had a higher affinity to Lipid II than brevibacillin 2V. A carboxyfluorescein (CF) leakage assay showed that brevibacillin and brevibacillin 2V cause membrane permeabilization without the help of Lipid II, which suggest that the brevibacillins have two independent antimicrobial mechanisms: (1) binding to Lipid II to interfere with cell wall synthesis and (2) membrane permeabilization. The permeabilization activity of brevibacillin 2V was 2 times lower than that of brevibacillin, possibly explaining its lower hemolytic activity.

5.1 Introduction

In recent years, antimicrobial resistance has become a growing concern which severely threatens the medical system and human health [1]. Discovering new antibiotics and studying their antimicrobial mechanisms is considered as a promising way to deal with this problem. Antimicrobial non-ribosomally produced peptides (NRPs) include many clinical use antibiotics such as penicillin, vancomycin, chloramphenicol and colistin [2]. NRPs are highly chemically modified and contain lots of non-canonical amino acids which makes them stable towards proteolytic degradation. Lipopeptides such as brevivacillins, bogorols and brevicidine, are NRPs which were found to inhibit bacterial strains that harbor antibiotic resistance [3-6]. From these antibiotics, bogorols were found to form pores in the membrane while the modes of action of the others are still not clear yet [7]. Due to the high structural similarity of bogorols and brevivacillins, we here assume that brevivacillins also target bacterial membranes [3].

Lipid II is a peptidoglycan precursor that is essential for cell wall synthesis. It comprises a hydrophilic head group composed of the basic building block of the peptidoglycan layer that contains two amino sugars (GlcNAc-MurNAc-) and a pentapeptide chain. This building block is attached to a hydrophobic lipid tail composed of 11 isoprene units via a pyrophosphate moiety [8]. The essentiality of Lipid II makes it a desirable target for an extensive list of antibiotics that includes vancomycin, nisin, teixobactin, ramoplanin to name but a few [8, 9]. Although, they all bind to Lipid II, their binding modes are quite different. For instance, vancomycin targets the D-Ala-D-Ala terminus of the pentapeptide of Lipid II and thereby inhibits cell wall synthesis [10]. Nisin binds to the pyrophosphate part of Lipid II and forms stable pores in the membrane leading to leakage of cellular content [11].

Here we study a novel class of NRPs, brevivacillins, which belongs to the linear lipotridecapeptide family and has potential use towards antibiotic resistant gram-positive pathogens including methicillin-resistant *Staphylococcus aureus* (MRSA) and vancomycin-resistant *Enterococcus faecalis* (VRE) [3]. Brevivacillins were isolated from *Brevibacillus laterosporus* and share high degree of structural similarity [12]. The primary structures of brevivacillin, brevivacillin I, brevivacillin V, brevivacillin 2V are represented by the following formula: FA-Dhb-Leu-Orn-Ile/Val-Ile/Val-Val-Lys-Ile/Val-Val-Lys-Tyr-Leu-valinol (Fig. 1). The 4th, 5th, 8th amino acids are either Ile or Val, and their conserved cationic amino acids at 3(Orn), 7(Lys), and 10(Lys) positions provide them with positive charges which help brevivacillins in membrane permeabilization [13, 14].

In this research, we study the modes of action of brevivacillin and brevivacillin 2V, which were isolated from *Brevibacillus laterosporus* DSM 25. They exhibit bactericidal activities toward *Staphylococcus aureus* (MRSA) at concentrations equal to 10 X MICs. Being highly positively charged, brevivacillins are likely to accumulate at the highly

negatively charged bacterial membranes and cause membrane disruption. Indeed, it was shown that the two peptides cause membrane depolarization and membrane permeabilization using different assays. In addition, agar-diffusion and circular dichroism (CD) assays indicated that the antibiotics target Lipid II. Yet, model membrane leakage assays showed that this interaction with Lipid II is not required for the membrane permeabilization activities of brevicacillin and brevicacillin 2V. We suggest that the Lipid II binding and membrane permeabilization are two independent antimicrobial mechanisms of the brevicacillins, which combined, make them efficient in killing bacteria.

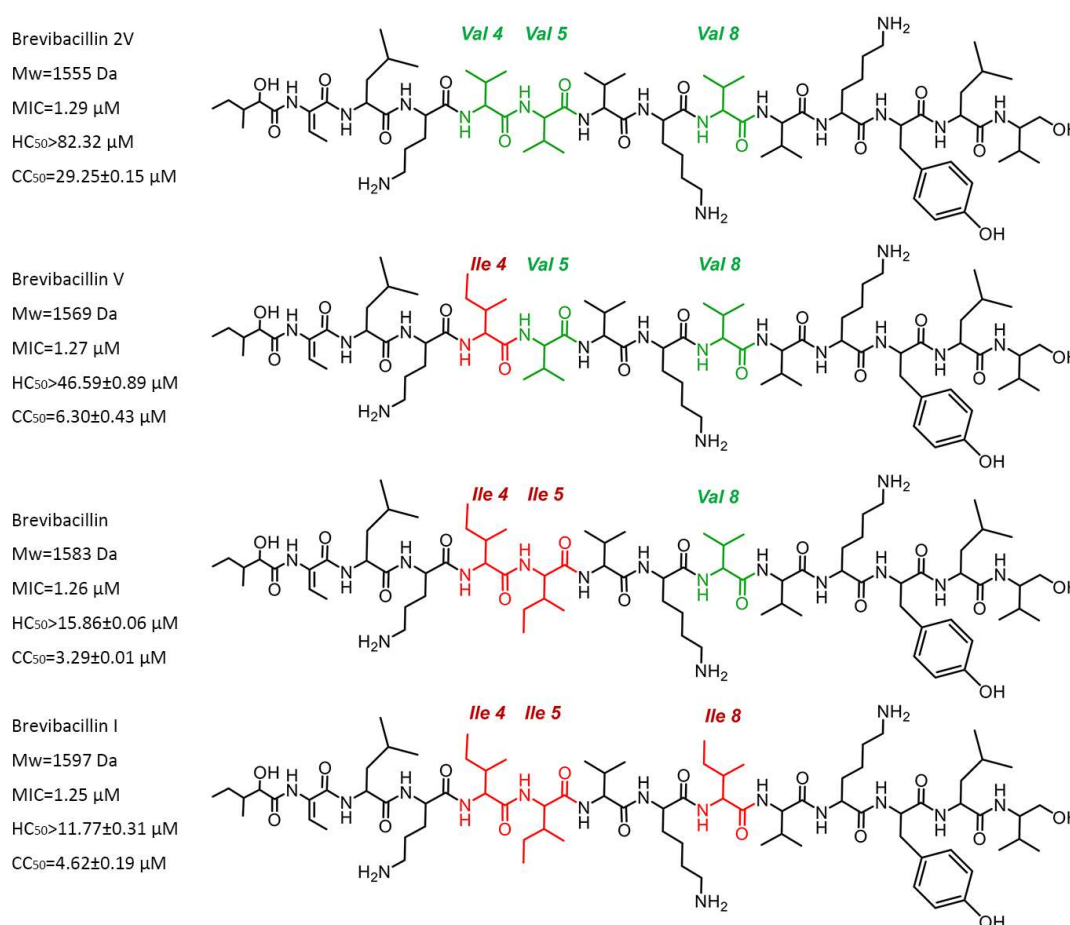


Figure 1. Structures of brevicacillins (brevicacillin 2V, brevicacillin, brevicacillin I, brevicacillin V). MIC represents the minimum inhibitory concentration against *Staphylococcus aureus* (MRSA). HC₅₀ is the concentration that causes 50% Human blood cell hemolysis. CC₅₀ is the 50% cell (HepG2) toxicity concentration.

5.2 Materials and Methods

5.2.1 Materials

Brevivacillin and brevivacillin 2V were provided by Xinghong Zhao and Oscar P. Kuipers (Department of Molecular Genetics, University of Groningen). Nisin A, Lipid II, pyrene-labeled Lipid II was prepared as previously described [15-17]. 1,2-Dioleoyl-*sn*-glycero-3-phosphocholine (DOPC) was purchased from Avanti Polar Lipids. Carboxyfluorescein (CF) was obtained from Molecular Probes. G-50 Sephadex was purchased from Amersham Pharmacia Biotech AB. Triton X-100 was purchased from Sigma-Aldrich. All other chemicals used were of analytical or reagent grade. The 200 nm membrane for Lipids extrusion was purchased from Whatman Nuclepore, Track-Etch Membranes.

5.2.2 Methods

5.2.2.1 Lipids preparation

(1) Lipids for CD measurements: 3-Lipid II was dissolved in 10 mM Boric-NaOH pH 7.5. 7-Lipid II and DOPC were resuspended as mixed micelles in 10 mM Boric-NaOH pH 7.5 containing 0.1% CHAPS. The peptide concentration was 50 μ M. 3-Lipid II and 7-Lipid II were added to a final concentration of 50 μ M, while the DOPC containing micelles were added to a final concentration of 100 μ M. **(2) Lipids for Fluorescence quenching assay:** 5 mM 0.5% pyrene-Lipid II/DOPC (mol/mol) lipids solutions were dried by a nitrogen stream and hydrated with 10 mM Tris and 100 mM NaCl, pH 8.0. LUVs (Large unilamellar vesicles) were obtained after 10 freeze-thaw cycles followed by 10 rounds of extrusion through 200 nm membrane filters. **(3) Lipids for Isothermal Titration Calorimetry (ITC) assay:** LUVs containing Lipid II (2%, mol/mol) were prepared by mixing the appropriate volumes of Lipid II and DOPC stock solutions in $\text{CHCl}_3/\text{MeOH}$ (2:1, v/v). The lipid solutions were dried by a nitrogen stream and hydrated with 10 mM Tris-HCl, 100 mM NaCl, pH 8 buffer to a lipid-phosphate concentration of \sim 20 mM. LUVs were obtained after 10 freeze-thaw cycles followed by 10 rounds of extrusion through 200 nm membrane filters. **(4) Lipids for CF leakage assay:** LUVs that contain DOPC or DOPC+0.1% Lipid II were prepared for CF leakage assay. Lipids were dried by N_2 and put under vacuum for 2 hours. Then, they were hydrated by adding 25 mM Tris-HCl, 150 mM NaCl, pH 7.5 containing 50 mM carboxyfluorescein. The suspensions were frozen and thawed for 10 times, followed by extrusion over 200 nm filter for 10 times. The excess dye was removed by loading vesicles on a spin column (Sephadex G50) for 2 min at 500 \times g. The concentration of lipid-phosphate was determined as described [18].

5.2.2.2 CD measurements

CD spectra were measured with a Jasco-810 spectropolarimeter in a quartz cuvette with a 1 mm path length. The temperature was kept at 20°C by a Jasco Peltier CDF 426S. The ellipticity was recorded between 185 nm and 260 nm at a 0.2-nm step size with 1-s response time. The spectra were averaged over 5 recordings with a scanning speed of 50 nm/min.

5.2.2.3 Fluorescence quenching using pyrene-labeled lipid II

The fluorescence spectrum was recorded between 360 and 600 nm with an excitation wavelength at 350 nm. Samples were stirred in a quartz cuvette at 20°C. LUVs were diluted to a concentration of 50 µM in a 1 mL cuvette and then were titrated with brevivacillin or brevivacillin 2V.

5.2.2.4 ITC assay

ITC was performed with the Low Volume NanoITC (Waters LLC, New Castle, DE, USA) to determine the interaction between LUVs and brevivacillins. Brevivacillins were diluted in a buffer (10 mM Tris-HCl, 100 mM NaCl, pH 8) to a final concentration of 50 µM. Samples were degassed before use. The chamber was filled with 177 µL of the brevivacillins solutions, and the LUVs were titrated into the chamber at a rate of 2 µL/300 s with a stirring rate of 300 rpm. Experiments were performed at 25°C. Control experiments were performed with Lipid II-free LUVs. The K_d values of brevivacillins to Lipid II were calculated using the Nano Analyse Software (Waters LLC).

5.2.2.5 CF leakage assay

The excitation wavelength and emission wavelength were set to 492 nm and 515 nm. The vesicles were diluted to a concentration of 5 µM in a 1 mL cuvette. The brevivacillins-induced release of CF from the vesicles was monitored by measuring the increase in fluorescence intensity. The maximum fluorescence was reached by adding 10 µL of 20% Triton X-100.

5.3 Results

5.3.1 Brevivacillin and brevivacillin 2V act bactericidal and cause membrane depolarization and permeabilization.

Brevivacillin and brevivacillin 2V exhibited similar MICs against antimicrobial resistant

bacteria such as MRSAATCC15975 (2 µg/mL ≈1.3 µM), VRE LMG16216 (2 µg/mL≈1.3 µM) and VRE LMG16003 (2 µg/mL ≈1.3 µM) (Table S1). Both peptides displayed bactericidal activity in a time killing assay. Compared to nisin, brevivacillin showed better activity at concentrations equal to 10 X MIC, while the activity of brevivacillin 2V was close to that of nisin (Fig. S1). Similar to our observations in Chapter 3, these bactericidal activities were paralleled by membrane depolarization activities of both brevivacillins, where brevivacillin caused more severe membrane depolarization than brevivacillin 2V. Moreover, brevivacillin and brevivacillin 2V acted faster than nisin in the first 10 min (Fig. S2A). These membrane permeabilization activities were confirmed using a live-death staining approach with the probes SYTO® 9 and propidium iodide (Fig. S2B). Here, the brevivacillins showed lower membrane permeabilization activities than nisin at relatively low concentrations (100 nM) while at higher concentrations (1600 nM) their permeabilization activities were >90% (Fig. S2C). The permeabilization activity of brevivacillin 2V was lower than that of brevivacillin at all concentrations tested, consistent with the membrane depolarization assay.

5.3.2 Lipid II changes the conformation of brevivacillin and brevivacillin 2V.

Testing for a possible lipid II interaction of an antibiotic can be done in a sensitive way via an agar diffusion assay [19]. This assay clearly showed that the halos of antibiotic activity were distorted for the brevivacillins at the sites where Lipid II was spotted, thus this indicated that both the brevivacillins interact with Lipid II (Fig. S3). Next, we checked if this interaction leads to a conformational change in the peptides. For this we determined their secondary structure by CD in absence and presence of the water-soluble Lipid II variant 3-Lipid II (farnesyl version of Lipid II [17]) in 10 mM Boric acid-NaOH pH7.5, a buffer that had minimal absorption at the low wavelength range used for CD. Conformational changes were observed for brevivacillin and brevivacillin 2V in the presence of 3-lipid II (Fig. S4), indicative for an interaction with 3-Lipid II.

Next, we used a membrane-mimicking environment to test the interaction of the brevivacillins with heptaprenyl-Lipid II containing CHAPS micelles. While DOPC in CHAPS did not induce any conformational change, more extensive conformational changes could be observed for brevivacillin and brevivacillin 2V in the presence of 7-lipid II as compared to the water-soluble 3-Lipid II. Especially for brevivacillin 2V the presence of Lipid II seemed to induce more of a helical conformation as judged from the presence of minima at 208 and 222 nm. Thus, a more membrane-mimicking environment seemed to enhance the interaction of the brevivacillins with Lipid II.

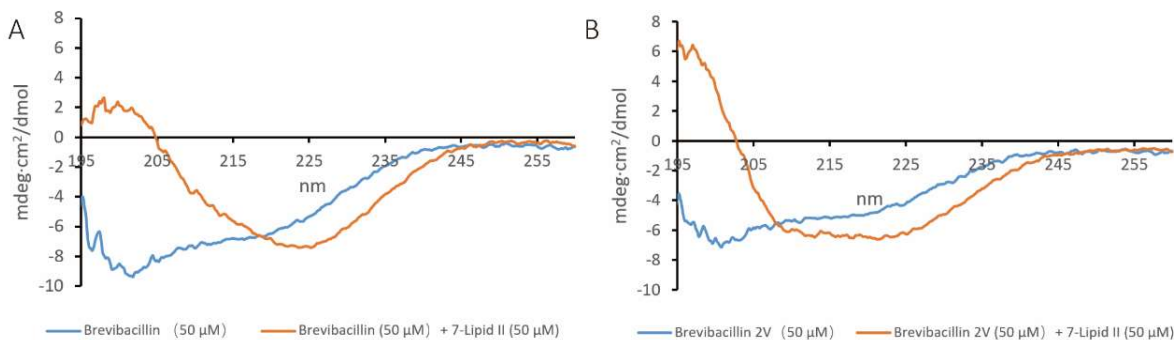


Figure 2. 7-Lipid II induced conformational change of brevivacillin and brevivacillin 2V. (A) CD spectrum of brevivacillin with the present of 7-Lipid II or DOPC. (B) CD spectrum of brevivacillin 2V with the present of 7-Lipid II or DOPC. (Brevivacillin and brevivacillin 2V curves were corrected for the buffer signal. Brevivacillin + 7-Lipid II and brevivacillin 2V + 7-Lipid II were corrected for the signal of 7-Lipid II in buffer.)

5.3.3 Binding constants of brevivacillin and brevivacillin 2V with Lipid II determined by ITC.

To determine the binding constants of the interaction of the brevivacillins with Lipid II we used ITC. Brevivacillin and brevivacillin 2V were titrated with LUVs containing 2 mol % Lipid II. Brevivacillin-Lipid II exhibited a binding curve with a binding constant of 0.869 μM which was calculated by the independent mode of interaction (Fig. 3A). The Brevivacillin 2V-Lipid II curve indicated a lower binding affinity, as clearly a less steep curve was obtained resulting in an almost ten-fold higher binding constant of 7.9 μM (Fig. 3B).

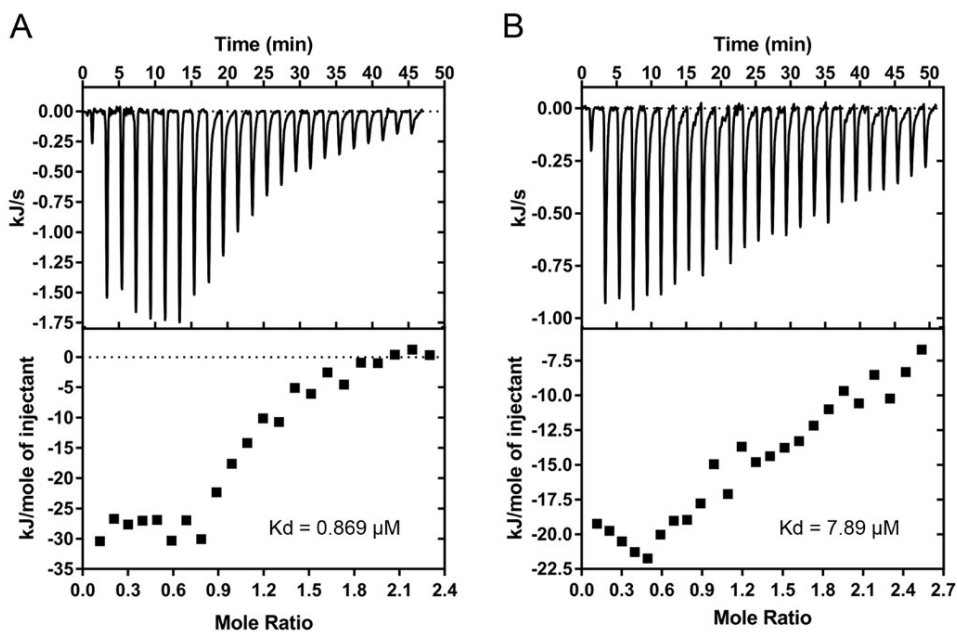


Figure 3. ITC analysis of the binding of brevivacillin and brevivacillin 2V to Lipid II. (A) ITC binding experiments of brevivacillin and Lipid II (2 mol % in DOPC LUVs). (B) ITC binding experiments of brevivacillin 2V and Lipid II (2 mol % in DOPC LUVs). The K_d values of brevivacillins to Lipid II were calculated using the Nano Analyse Software (Waters LLC).

5.3.4 Brevivacillin and brevivacillin 2V quenched the fluorescence of pyrene-labeled Lipid II

For certain antibiotics that interact with Lipid II it has been shown that they are able to cluster Lipid II molecules together in specific higher order oligomers. To test this for brevivacillins we made use of pyrene-labeled Lipid II that could show the assembly of Lipid II together with nisin as well as R4L10-teixobactin into higher order oligomers [17, 20]. In monomeric form pyrene shows emission wavelength maxima at about 378 nm, 398 nm and 417 nm. When two pyrenes are in close proximity, within ~ 10 Å, they can form an excimer which results in the appearance of a broad fluorescence around 490 nm and a concomitant decrease of the triplet of peaks of the monomeric form [17]. This is illustrated for the nisin-Lipid II system where in the presence of increasing amounts of nisin the monomeric signals (at about 378 nm, 398 nm and 417 nm) were significantly quenched and a peak at around 490 nm arose (Fig 4C). Thus nisin clusters together with Lipid II into a pore-complex [11]. In the case of brevivacillin and brevivacillin 2V only quenching of the pyrene monomer fluorescence could be observed, while no excimer fluorescence at 490 nm appeared (Fig. 4A and 4B). These results suggest that brevivacillin and brevivacillin 2V bound to Lipid II, which results in quenching of the fluorescence, but this interaction did not lead to the formation of higher order oligomers. Moreover, brevivacillin at concentration of 1500 nM quenched the 378 nm peak of pyrene-labeled Lipid II from about ~ 800 A.U. to ~ 550 A.U. and brevivacillin 2V at the same concentration quenched the 378 nm peak from ~ 800 A.U. to ~ 630 A.U. These results are consistent with the ITC experiments, which showed that brevivacillin had a higher affinity for Lipid II than brevivacillin 2V.

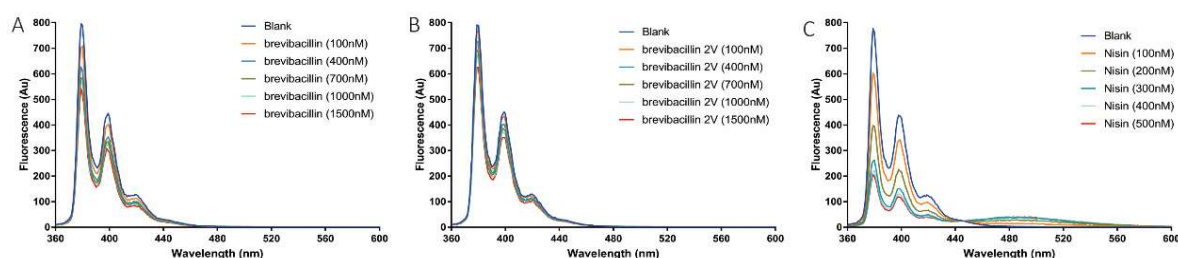


Figure 4. Brevivacillin and brevivacillin 2V quenched the fluorescence signal of pyrene-labeled Lipid II. (A) Fluorescence spectrum of pyrene-labeled Lipid II (0.5 mol % in DOPC LUVs) which was titrated with increasing concentration of brevivacillin. (B) Fluorescence spectrum of pyrene-

labeled Lipid II (0.5 mol % in DOPC LUVs) which was titrated with increasing concentration of brevivacillin 2V. (C) Fluorescence spectrum of pyrene-labeled Lipid II (0.5 mol % in DOPC LUVs) which was titrated with increasing concentration of nisin.

5.3.5 Brevivacillin and brevivacillin 2V caused CF leakage without the help of Lipid II

Time killing assay and fluorescence microscopy assay showed brevivacillins were bactericidal via permeabilizing cell membrane. Model membranes with or without Lipid II were used to check whether brevivacillins-Lipid II binding leads to membrane permeabilization. Brevivacillin and brevivacillin 2V at 100 nM both caused CF leakage in LUVs with (Fig. 5A) or without (Fig. 5B) Lipid II. Moreover, the percentage of CF leakage caused by brevivacillin was about 2 times higher than brevivacillin 2V. This explains why brevivacillin 2V showed an exceptional low hemolytic activity [12]. Interestingly, the presence of Lipid II did not enhance the permeabilization activity of brevivacillins. On the contrary, brevivacillin caused a higher percentage of CF leakage from the vesicles in the absence of Lipid II. Apparently, binding of the brevivacillins to Lipid II reduced their permeabilization activities. These CF leakage assays suggested that the Lipid II binding and membrane permeabilization are two independent antimicrobial mechanisms of brevivacillins.

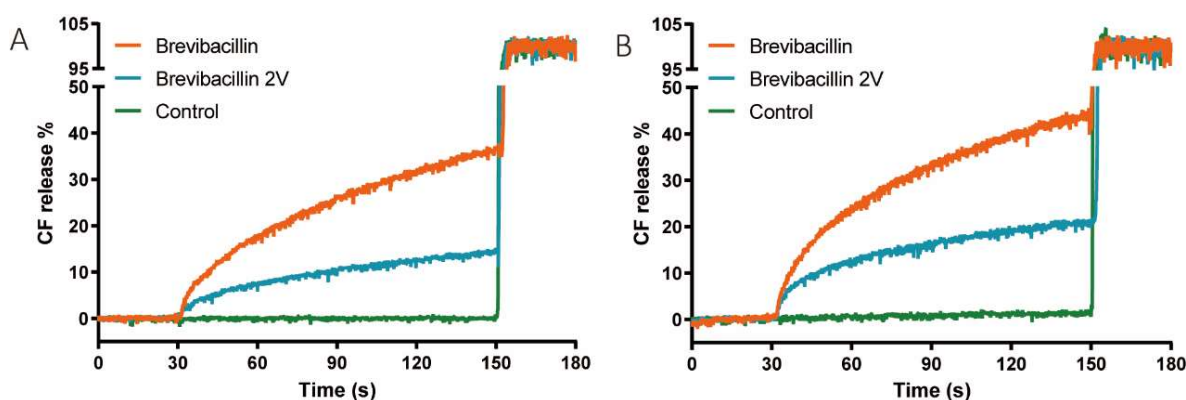


Figure 5. Brevivacillin and brevivacillin 2V permeabilized model membranes without the help of Lipid II. (A) Fluorescence spectrum of CF leakage (%) at the present of 100 nM brevivacillin or brevivacillin 2V using DOPC+ 0.1% Lipid II LUVs. (B) Fluorescence spectrum of CF leakage (%) at the present of 100 nM brevivacillin or brevivacillin 2V using DOPC LUVs. Brevivacillin or brevivacillin 2V was added at 30 s, and 10 μ L of 20% Triton X-100 was added at 150 s.

5.4 Discussion

The brevivacillins and bogorols can, in view of their high similarity, be considered as a family of linear lipo-tridecapeptides summarized with the following formula: FA-Dhb-

Leu/Val/Met-Orn-Ile/Val-Ile/Val-Val-Lys-Ile/Val-Val/Leu-Lys-Tyr-Leu-valinol [14, 21]. The variable 2nd, 4th, 5th, 8th, 9th positions of these antibiotics are all hydrophobic nonpolar amino acids. In this research, we have investigated the mechanism of action of brevivacillin and the closely related brevivacillin 2V. We could show that both brevivacillins display membrane permeabilization activity. In addition, both peptides also interact with Lipid II. However, the two properties seemed to be independent of each other.

Despite brevivacillins' three positive charges, our ³¹P solid-state NMR (ssNMR) data did not suggest an interaction between brevivacillins and the pyrophosphate of Lipid II (Fig. S5). Brevivacillins more likely bind to the hydrophilic head group of Lipid II (GlcNAc-MurNAc moiety and/or the pentapeptide), where, in general, the pentapeptide also carries two negative charges at the C-terminal D-Ala and the C-terminus of the Glu at position 2.

Interestingly, while the structural difference between brevivacillin and brevivacillin 2V is a mere 2 methyl-groups, the K_d of brevivacillin for Lipid II is 0.869 μ M, almost a factor of 10 lower than the K_d of brevivacillin 2V for Lipid II (7.9 μ M). This higher affinity for Lipid II was paralleled by a higher ability of brevivacillin over brevivacillin 2V to permeabilize bacterial and model membranes. This suggests that a higher intrinsic membrane affinity of the peptide increases its affinity for Lipid II. This can be explained by the positive influence of two-dimensional diffusion on the plane of the membrane on the affinity for a membrane embedded target, similar to the vancomycin variants that have been outfitted with a lipophilic anchor [22]. The downside of this increased membrane affinity seems to be a higher hemolytic activity. In this respect it would be interesting to test what effects further increases in hydrophobicity at the variable three positions (in bold above) have on the affinity for Lipid II, membrane permeabilization activity and hemolytic activity.

5.5 References

1. McEwen, S.A. and P.J. Collignon, *Antimicrobial Resistance: a One Health Perspective*. Microbiol Spectr, 2018. **6**(2).
2. Süssmuth, R.D. and A. Mainz, *Nonribosomal Peptide Synthesis-Principles and Prospects*. Angew Chem Int Ed Engl, 2017. **56**(14): p. 3770-3821.
3. Yang, X., et al., *Isolation and Structural Elucidation of Brevibacillin, an Antimicrobial Lipopeptide from Brevibacillus laterosporus That Combats Drug-Resistant Gram-Positive Bacteria*. Appl Environ Microbiol, 2016. **82**(9): p. 2763-2772.
4. Barsby, T., et al., *Bogorol A produced in culture by a marine Bacillus sp. reveals a novel template for cationic peptide antibiotics*. Org Lett, 2001. **3**(3): p. 437-40.
5. Jiang, H., et al., *Antibacterial and antitumor activity of Bogorol B-JX isolated from Brevibacillus laterosporus JX-5*. World J Microbiol Biotechnol, 2017. **33**(10): p. 177.
6. Li, Y.X., et al., *Discovery of cationic nonribosomal peptides as gram-negative antibiotics through global genome mining*. Nat Commun, 2018. **9**(1): p. 3273.
7. Li, Z., et al., *Novel Modifications of Nonribosomal Peptides from Brevibacillus laterosporus MG64 and Investigation of Their Mode of Action*. Appl Environ Microbiol, 2020. **86**(24).
8. Breukink, E. and B. de Kruijff, *Lipid II as a target for antibiotics*. Nature Reviews Drug Discovery, 2006. **5**: p. 321.
9. Ling, L.L., et al., *A new antibiotic kills pathogens without detectable resistance*. Nature, 2015. **517**(7535): p. 455-9.
10. Knox, J.R. and R.F. Pratt, *Different modes of vancomycin and D-alanyl-D-alanine peptidase binding to cell wall peptide and a possible role for the vancomycin resistance protein*. Antimicrobial Agents and Chemotherapy, 1990. **34**(7): p. 1342-1347.
11. Medeiros-Silva, J., et al., *High-resolution NMR studies of antibiotics in cellular membranes*. Nature Communications, 2018. **9**(1): p. 3963.
12. Zhao, X., et al., *Brevibacillin 2V, a Novel Antimicrobial Lipopeptide With an Exceptionally Low Hemolytic Activity*. 2021. **12**(1501).
13. Yang, X., E. Huang, and A.E. Yousef, *Brevibacillin, a cationic lipopeptide that binds to lipoteichoic acid and subsequently disrupts cytoplasmic membrane of Staphylococcus aureus*. Microbiol Res, 2017. **195**: p. 18-23.
14. Yang, X. and A.E. Yousef, *Antimicrobial peptides produced by Brevibacillus spp.: structure, classification and bioactivity: a mini review*. World J Microbiol Biotechnol, 2018. **34**(4): p. 57.
15. Kuipers, O.P., et al., *Engineering dehydrated amino acid residues in the antimicrobial peptide*

- nisin*. Journal of Biological Chemistry, 1992. **267**(34): p. 24340-24346.
16. Wiedemann, I., et al., *Specific binding of nisin to the peptidoglycan precursor lipid II combines pore formation and inhibition of cell wall biosynthesis for potent antibiotic activity*. Journal of Biological Chemistry, 2001. **276**(3): p. 1772-1779.
 17. Breukink, E., et al., *Lipid II is an intrinsic component of the pore induced by nisin in bacterial membranes*. J Biol Chem, 2003. **278**(22): p. 19898-903.
 18. Rouser, G., S. Fleischer, and A. Yamamoto, *Two dimensional thin layer chromatographic separation of polar lipids and determination of phospholipids by phosphorus analysis of spots*. Lipids, 1970. **5**(5): p. 494-496.
 19. Wang, X., Q. Gu, and E. Breukink, *Non-lipid II targeting lantibiotics*. Biochimica et Biophysica Acta (BBA) - Biomembranes, 2020. **1862**(8): p. 183244.
 20. Shukla, R., et al., *Mode of action of teixobactins in cellular membranes*. Nat Commun, 2020. **11**(1): p. 2848.
 21. Barsby, T., et al., *The Bogorol family of antibiotics: template-based structure elucidation and a new approach to positioning enantiomeric pairs of amino acids*. J Org Chem, 2006. **71**(16): p. 6031-7.
 22. Benton, B.M., et al., *O258 Telavancin inhibits peptidoglycan biosynthesis through preferential targeting of transglycosylation: evidence for a multivalent interaction between telavancin and lipid II*. 2007. **29**.

5.6 Supplement information

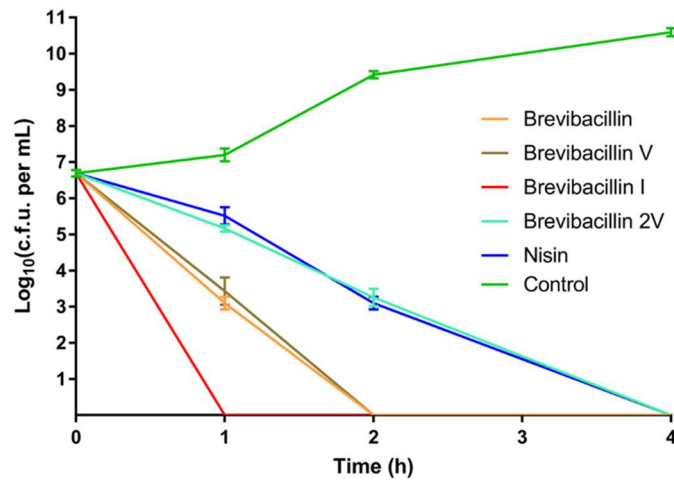


Figure S1. Time killing curves of brevivacillins and nisin at the concentrations equal to 10 X MICs against *Staphylococcus aureus* (MRSA).

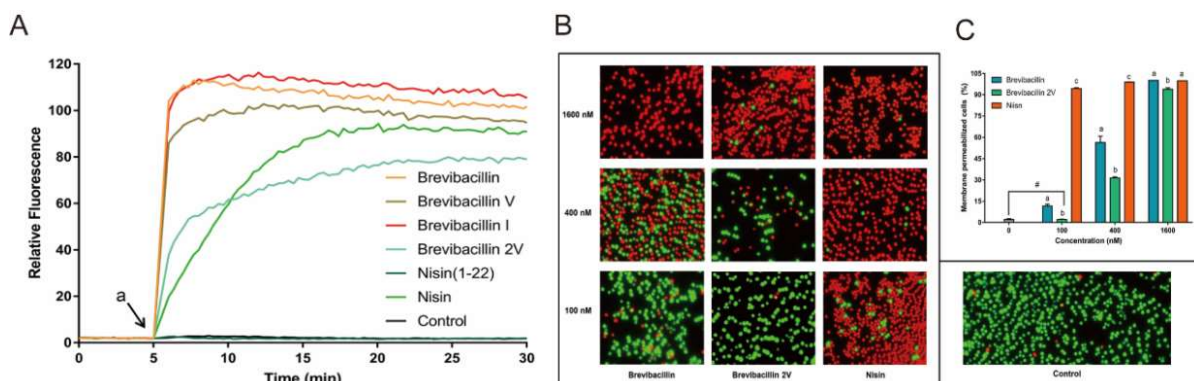


Figure S2. (A) DiSC₃(5) fluorescence in *S. aureus* (MRSA) upon exposure (at 2 × MIC) to brevivacillins, nisin, nisin (1-22), and MQ (Control); a, when peptides were added. (B) fluorescence microscopic images of *S. aureus* (MRSA) after having been treated by a series concentrations of brevivacillins and nisin for 15 min. (C) The ratio of membrane permeabilized cells that was quantified by Adobe Photoshop 2021; the data are representative of three independent experiments. Significant differences were considered at $p < 0.05$; a, b, c bars at the same concentration without the same superscripts differ significantly ($p < 0.05$); and #brevivacillin 2V did not induce membrane permeabilization at a concentration of 100 nm, which showed no significant difference on the ratio of membrane permeabilized cells with untreated group.

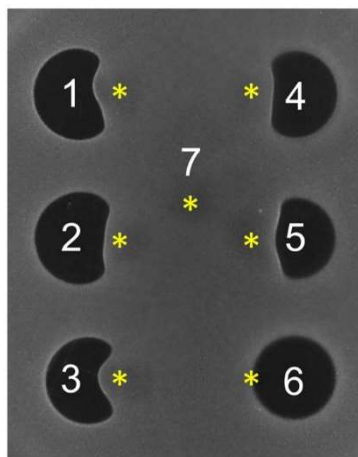


Figure S3. Agar diffusion assay using *S. aureus* (MRSA). 1, brevivacillin; 2, brevivacillin V; 3, brevivacillin I; 4, brevivacillin 2V; 5, nisin; 6, daptomycin; 7, MQ. 6.8 μ L of brevivacillins were spotted at a concentration of 100 μ g/mL; 6.8 μ L of nisin and daptomycin were spotted at a concentration of 200 μ g/mL, * marks the position of 4 μ L of Lipid II that was spotted at a concentration of 300 μ M.

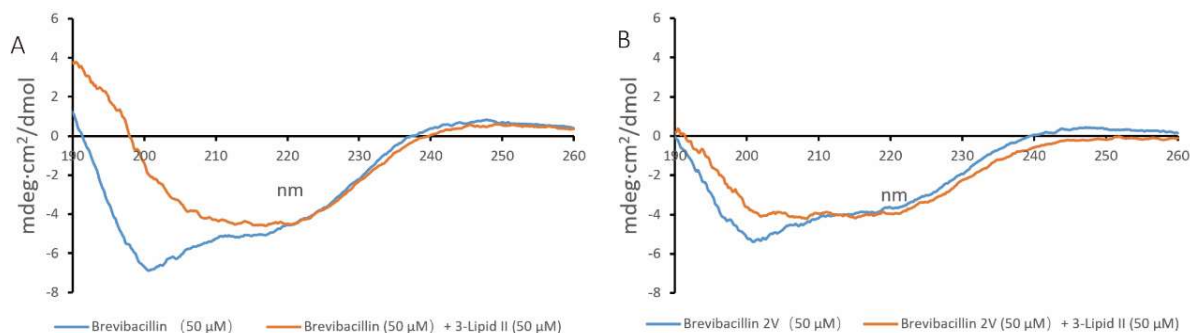


Figure S4. 3-Lipid II induced conformational change of brevivacillin and brevivacillin 2V. (A) CD spectrum of brevivacillin in the presence or absence of 3-Lipid II. (B) CD spectrum of brevivacillin 2V in the presence or absence of 3-Lipid II. (Brevivacillin and brevivacillin 2V curves were corrected for the buffer signal. Brevivacillin + 3-Lipid II and brevivacillin 2V + 3-Lipid II were corrected for the signal of 3-Lipid II in buffer.)

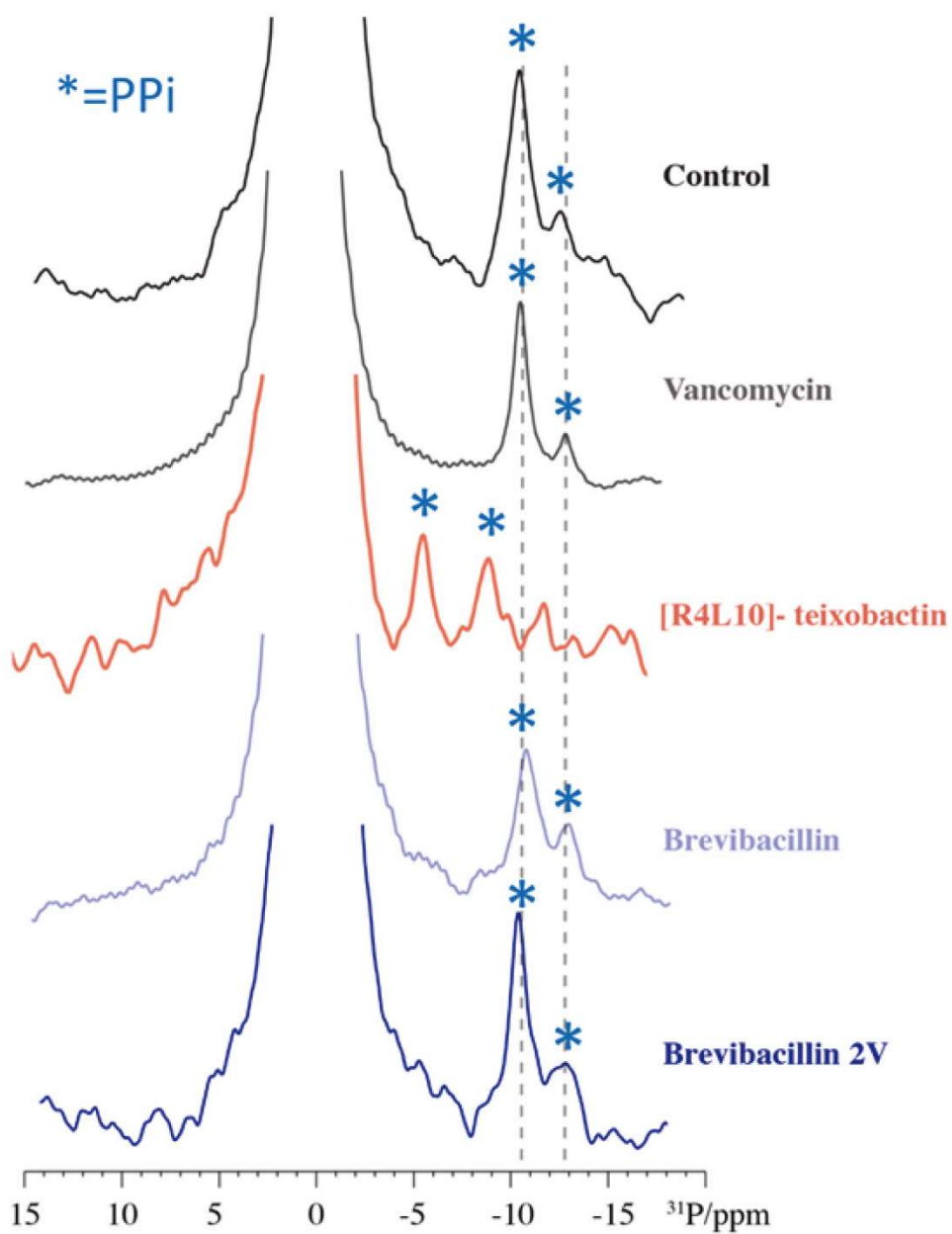


Figure S5. ^{31}P solid-state NMR spectra of Lipid II in liposomes in the presence of vancomycin, [R4L10]-teixobactin, brevibacillin, and brevibacillin 2V. Blue * mark PPI signals; bulk lipids come around 0 ppm.

Table S1. MIC values of brevivacillins against pathogenic bacteria.

Microorganism	MIC ($\mu\text{g/mL}$)					
	Bre	Bre V	Bre I	Bre 2V	Poly B	Nisin
Gram-positive pathogenic bacteria						
<i>Staphylococcus aureus</i> ATCC15975 (MRSA)	2	1-2	2	2	32	4-8
<i>Enterococcus faecium</i> LMG16003 (VRE)	2	2	2	2	16	4
<i>Enterococcus faecium</i> LMG16003 (VRE) plus 10% Human blood plasma	2	2	2	2	16	4-8
<i>Enterococcus faecalis</i> LMG16216 (VRE)	2	2	2	2	16	4
<i>Bacillus cereus</i> ATCC14579	1	1	2	2	8	4
Gram-negative pathogenic bacteria						
<i>Acinetobacter baumannii</i> ATCC17978	32	64	64	32	4	32
<i>Escherichia coli</i> ATCC25922	32	32	32	16	2	64
<i>Pseudomonas aeruginosa</i> LMG6395	64	64	64	64	1	128
<i>Klebsiella pneumoniae</i> LMG20218	32	64	64	32	2	128

VRE, vancomycin resistant *Enterococcus*; MRSA, methicillin resistant *S. aureus*; Poly B, polymyxin B.

Chapter 6

Summary and discussion

Antimicrobial resistance is becoming an increasing challenge that threatens the human health system. The overuse of antibiotics has led to an acceleration in the emergence of antibiotic-resistant bacteria, the result of bacterial adaptation to evolutionary pressure when they encounter antibiotics. Thus, bacteria constantly evolve resistance genes in order to survive, which makes it hard if not impossible to find an effective antibiotic that does not induce any antibiotic resistance at all. Chemical modification has helped to extend the useful lifetime of clinically used antibiotics that encountered resistance. Yet, this likely only postpones the inevitable clinical failure of a whole class of antibiotics in the future. Hence, it is important to discover new antibiotics and study their modes of action. This thesis is centered on studying the mode of action (MoA) of antimicrobial peptides (AMPs). These AMPs form a large family of peptides that have broad spectrum antibiotic activity against bacteria including antibiotic-resistant bacteria. They are regarded as potential candidates to tackle the rising antimicrobial resistant problem.

Chapter 1 introduces the bacterial cell wall synthesis pathway and its central precursor Lipid II as well as the family of lantibiotics, a large family of post-translationally modified AMPs. The cell wall is the first barrier of gram-positive bacteria that faces outside threats. Many AMPs inhibit the growth of bacteria by interfering with the cell wall synthesis. This includes the lantibiotic family that harbors quite some peptides that interfere with the cell wall biosynthesis by targeting Lipid II. For instance, nisin, the first example of a targeted pore-former uses Lipid II to efficiently form pores. The lantibiotics family also harbors members that do not target Lipid II but are still very efficient in killing bacteria, making it worthwhile to study their MoA and uncover their target. One of these is epilancin 15X, one of the key players in the next chapters. Besides lantibiotics, teixobactins and brevibacillins are also introduced in this chapter. Both target Lipid II, have been discovered recently and have the potential to tackle the antibiotic-resistant bacteria problem.

In **Chapter 2**, we briefly describe the regulation of intracellular pH homeostasis, ion homeostasis and ATP synthesis, three interrelated phenomena, in bacteria. The intracellular proton gradient (ΔpH), electrical potential ($\Delta\psi$) and ATP synthesis/hydrolysis are actively or passively regulated by bacteria when under outside stresses such as antibiotic treatment. This is especially relevant for AMPs that target the bacterial membrane as the membrane plays a central role in all these processes. Monitoring the changes of ΔpH , $\Delta\psi$ and ATP level thus provides important insight into the MoAs of these AMPs.

Chapter 3 introduces epilancin 15X and the first steps to unravel its mode of action. Here, 5 probes are used to study the membrane effects of epilancin 15X and to compare these to those caused by nisin and the chemical variant of teixobactin, [R4L10]-teixobactin, in the gram-positive bacteria *Staphylococcus simulans*, *Micrococcus flavus* and *Bacillus megaterium*. We introduced here a novel luciferase based ATP assay that will be of great value to the field as it can measure on-line ATP leakage from the cells as well as determine the remaining cellular ATP content. We

measured the effects of AMPs on membrane permeability, ΔpH , $\Delta\psi$, ATP leakage and intracellular levels of ATP. Among the three strains tested, the results with *M. flavus* were most puzzling but also insightful. This strain seemed incompatible with DAPI, a DNA binding probe often used in cell death assays. The most insightful hint of the MoA of epilancin 15X and [R4L10]-teixobactin given by *M. flavus* involved the intracellular pH and luciferase assay. Both peptides induced an increase in intracellular pH and [R4L10]-teixobactin also caused intracellular ATP-levels to increase at low concentrations. Interestingly, these effects mimic those that were observed upon treatment of *Mycobacterium bovis* BCG with inhibitors of cell wall synthesis [1]. Here a burst of intracellular ATP was caused by an increase in oxidative phosphorylation, which contributes to drug induced cell death. The increase in pH in *M. flavus* can be caused by a burst in oxidative phosphorylation, hence *M. flavus* appears to react similar to inhibitors of the cell wall as compared to *Mycobacterium bovis* BCG. This also suggests that epilancin 15X does interfere with the cell wall synthesis of *M. flavus*. Possibly, in view of the increased oxidative phosphorylation, both epilancin and teixobactin may potentiate *M. flavus* (and maybe also other bacteria) to killing by other bactericidal antibiotics [2]. This increase in respiration coupled to increased ATP levels appears to be different from the rise in ATP levels in *Staphylococcus aureus* upon treatment with antibiotics that inhibit protein synthesis such as chloramphenicol, where no increased respiration was observed [2]. This rise in ATP was more likely caused by a surplus of ATP buildup due to the shutdown of the most ATP-consuming process in cells, protein synthesis. Why *M. flavus* behaves different compared to the other strains remains a mystery and may be related to specific properties of its membrane. Yet, this phenomenon emphasizes the importance of using multiple assays and strains in order to be able to draw proper conclusions on the MoA of AMPs. Moreover, it cannot be ruled out that the mechanism of action of a particular peptide differs to some extent for different target strains.

Chapter 4 is zooming in on the mode of action of epilancin 15X and the possible involvement of Lipid II. Clear interaction between epilancin 15X and Lipid II was observed by antagonism-based experiments. This was confirmed by Circular Dichroism (CD) experiments which showed that the interaction is specific rather than merely caused by electrostatic effects. However, epilancin's interaction with Lipid II did not lead to membrane effects. While it remained uncertain if Lipid II is the target of epilancin 15X, depolarization assays did point to the involvement of a target within a polyisoprene-based biosynthesis pathway, as clear effects could be observed on the activity of epilancin 15X by compounds that acted specifically on these pathways. Interestingly, we did observe an interaction with CDP-DAG, which points to the involvement of a lipid-linked pyrophosphate. Yet, unfortunately, the exact target of epilancin 15X remains obscure so far.

Chapter 5 studies the mode of action of brevivacillins. They belong to a novel class of non-ribosomally produced lipo-tridecapeptides and exhibit activity towards

antimicrobial resistant pathogens. As brevivacillins show a similar membrane permeability capacity as nisin, we tested the interaction between brevivacillins and Lipid II. Indeed, clear antagonistic effects were observed of Lipid II on the activity of both brevivacillin and brevivacillin 2V in an agar diffusion assay. Furthermore, interactions of the peptides with Lipid II were confirmed by circular dichroism experiments that showed clear structural changes only in the presence of Lipid II. Quenching of the fluorescence of pyrene-labeled Lipid II in the presence of brevivacillins also supported an interaction. But different from the nisin-Lipid II system that together form a pore-complex which always leads to the appearance of pyrene excimer fluorescence, the brevivacillins showed no such effects, indicating that their binding did not lead to the formation of higher order oligomers that include Lipid II. Brevivacillin and brevivacillin 2V were both found to cause permeabilization of model membranes, but Lipid II did not play a role in their permeability activity. On the contrary, the presence of Lipid II actually decreased the membrane permeability activity of brevivacillins. Binding to Lipid II and membrane permeabilization were thus considered as 2 independent modes of action of brevivacillins.

The role of metabolic state in bacterial susceptibility towards antibiotics

The metabolic state of bacteria is tightly related to their susceptibility towards antibiotics. Studies have indicated that the metabolic state of bacteria, especially the ATP-levels, play an important role in antibiotic lethality when growth rate is related to nutrient availability while the metabolic state is not [3]. In addition, the number of rRNA operons in bacteria is related to antibiotic susceptibility as well. The number of ribosomes is correlated with the number of rRNA operons, and when bacteria with relatively low numbers of ribosomes are treated with ribosome-targeting antibiotics, the protein synthesis and growth by bacteria will be severely hindered [4]. Moreover, antibiotics bind to chain-elongating ribosomes resulting in the production of misread proteins. These misread proteins may incorporate into cell membrane and cause membrane disruption [5]. Thus, by keeping the number of rRNA operons at a high level, the bacteria are more tolerant to antibiotics [4]. On the other hand, bacteria can also manipulate their metabolic status to achieve drug resistance or tolerance as is observed for persisters. These bacterial persisters are a subpopulation of antibiotic tolerant bacteria which are a growing medical concern as they cause a recalcitrance of chronic infections despite antibiotic treatment [6]. Persister formation is coupled to a decrease in intracellular level of ATP, which has been shown to generate antibiotic tolerance [7, 8]. Since ATP synthesis is directly coupled to respiration (CH₂), it doesn't come as a surprise that compromised respiratory complex I generates persistence towards antibiotics [9]. Such a proton translocation compromised respiratory complex I or other perturbations of metabolic homeostasis such as continued ATP consumption without ATP regeneration will lead to the decrease of intracellular pH or in other words: cytoplasmic acidification [9]. Mild cytoplasmic acidification increases RpoS response, a conserved adaptive regulator of which its expression leads to general stress

resistance of the cells with a relation to persister formation [10, 11]. Severe cytoplasmic acidification stops protein synthesis thus making the cells more tolerant to antibiotics that target this pathway [9]. Either mild or severe acidification leads to increased persistence [9]. The above effects demonstrate the importance of determining effect of an antibiotic on the ATP-levels, the ΔpH as well as the $\Delta\psi$ of bacteria, which would allow a prediction of possible persister induction. For instance, the effect of [R4L10]-teixobactin on *M. flavus* that showed an increased ATP levels and intracellular pH, indicates no risk of persister formation, which can be part of the reasons behind the lack of resistance buildup that was seen with teixobactin treated bacteria.

The potential of antibiotics with dual modes of action (MoA) that include membrane targeting.

Nisin, teixobactin and the brevibacillins all have dual MoAs, that include cell wall synthesis targeting (via Lipid II binding) and membrane permeabilization. Similarly, AMPs such as telavancin and daptomycin have dual MoAs where they combine inhibition of peptidoglycan synthesis with membrane effects [12, 13]. Although membrane active properties bring more risks in the form of possible hemolysis issues that may hinder further clinical use, they indeed enhanced their antimicrobial abilities [14, 15].

Another interesting example of combined MoAs of which one targets bacterial membranes was given recently. Compounds SCH-79797 and the derived Irresistin-16 target folate metabolism but were also shown to target the bacterial membrane rendering them both active toward gram-positive and gram-negative bacteria. In addition, these antibiotics were found to hardly induce resistance, probably due to their dual MoAs [16]. Hence, including membrane targeting into the MoA of an antibiotic increases antibacterial efficiency and decreases the emergence of resistance. This is a promising direction of antibiotic development for dealing with antibiotic resistance.

References

1. Shetty, A. and T. Dick, *Mycobacterial Cell Wall Synthesis Inhibitors Cause Lethal ATP Burst*. Front Microbiol, 2018. **9**: p. 1898.
2. Lobritz, M.A., et al., *Antibiotic efficacy is linked to bacterial cellular respiration*. Proc Natl Acad Sci U S A, 2015. **112**(27): p. 8173-80.
3. Lopatkin, A.J., et al., *Bacterial metabolic state more accurately predicts antibiotic lethality than growth rate*. Nature Microbiology, 2019. **4**(12): p. 2109-2117.
4. Levin, B.R., et al., *A Numbers Game: Ribosome Densities, Bacterial Growth, and Antibiotic-Mediated Stasis and Death*. mBio, 2017. **8**(1).
5. Davis, B.D., L.L. Chen, and P.C. Tai, *Misread protein creates membrane channels: an essential step in the bactericidal action of aminoglycosides*. Proc Natl Acad Sci U S A, 1986. **83**(16): p. 6164-8.
6. Fisher, R.A., B. Gollan, and S. Helaine, *Persistent bacterial infections and persister cells*. Nature Reviews Microbiology, 2017. **15**(8): p. 453-464.
7. Shan, Y., et al. *ATP-Dependent Persister Formation in Escherichia coli*. mBio, 2017. **8**, e02267-16 DOI: 10.1128/mbio.02267-16.
8. Conlon, B.P., et al., *Persister formation in Staphylococcus aureus is associated with ATP depletion*. Nature Microbiology, 2016. **1**(5): p. 16051.
9. Van den Bergh, B., et al., *Mutations in respiratory complex I promote antibiotic persistence through alterations in intracellular acidity and protein synthesis*. Nature Communications, 2022. **13**(1): p. 546.
10. Schellhorn, H.E., *Function, Evolution, and Composition of the RpoS Regulon in Escherichia coli*. 2020. **11**.
11. Liu, S., et al., *Variable Persister Gene Interactions with (p)ppGpp for Persister Formation in Escherichia coli*. Front Microbiol, 2017. **8**: p. 1795.
12. Taylor, S.D. and M. Palmer, *The action mechanism of daptomycin*. Bioorg Med Chem, 2016. **24**(24): p. 6253-6268.
13. Saravolatz, L.D., G.E. Stein, and L.B. Johnson, *Telavancin: a novel lipoglycopeptide*. Clin Infect Dis, 2009. **49**(12): p. 1908-14.
14. Belokoneva, O.S., et al., *The hemolytic activity of six arachnid cationic peptides is affected by the phosphatidylcholine-to-sphingomyelin ratio in lipid bilayers*. Biochimica et Biophysica Acta (BBA) - Biomembranes, 2003. **1617**(1): p. 22-30.
15. Dennison, S. and D. Phoenix, *Susceptibility of sheep, human, and pig erythrocytes to haemolysis by the antimicrobial peptide Modelin 5*. European biophysics journal : EBJ, 2014.

43.

16. Martin, J.K., 2nd, et al., *A Dual-Mechanism Antibiotic Kills Gram-Negative Bacteria and Avoids Drug Resistance*. Cell, 2020. **181**(7): p. 1518-1532.e14.

Nederlandse samenvatting en discussie

Antimicrobiële resistentie wordt een steeds grotere uitdaging die de volksgezondheid bedreigt. Het overmatig gebruik van antibiotica heeft geleid tot een versnelde opkomst van antibioticaresistente bacteriën, door aanpassing van bacteriën aan de evolutionaire druk wanneer zij met antibiotica in aanraking komen. Zo evolueren bacteriën voortdurend resistentiegenen om te overleven, wat het moeilijk, zo niet onmogelijk maakt om een effectief antibioticum te vinden dat helemaal geen resistentie opwekt. Chemische modificatie heeft geholpen om de nuttige levensduur van klinisch gebruikte antibiotica die op resistentie stuiten te verlengen. Maar dit stelt het onvermijdelijke klinische falen van een hele klasse antibiotica in de toekomst waarschijnlijk enkel uit. Daarom is het belangrijk nieuwe antibiotica te ontdekken en hun werkingsmechanismen te bestuderen. In dit proefschrift staat de studie van het werkingsmechanisme van antimicrobiële peptiden (AMP's) centraal. Deze AMP's vormen een grote familie van peptiden die een breed spectrum aan antibiotische activiteit hebben tegen bacteriën, waaronder antibioticaresistente bacteriën. Ze worden hierdoor beschouwd als potentiële kandidaten om het toenemende probleem van antimicrobiële resistentie aan te pakken.

Hoofdstuk 1 introduceert de bacteriële celwandsynthese en de centrale precursor hiervan, Lipide II, alsook de familie van lantibiotica, een grote familie van post-translationeel gemodificeerde AMP's. De celwand is de eerste barrière van gram-positieve bacteriën die bedreigingen van buitenaf tegenkomen. Veel AMP's remmen de groei van bacteriën door de celwandsynthese te verstoren. Zo ook de familie van de lantibiotica, die een groot aantal peptiden bevat die de biosynthese van de celwand verstoren door zich te richten op Lipide II. Zo gebruikt nisine, het eerste voorbeeld van een porievormende AMP, Lipide II om efficiënt poriën te vormen. De lantibiotica-familie omvat ook leden die niet gericht zijn op Lipide II, maar toch zeer efficiënt zijn in het doden van bacteriën, waardoor zowel het bestuderen van hun mechanismen als hun doelwit ontdekken belangrijk is. Een daarvan is epilancine 15X, een hoofdrolspeler in de volgende hoofdstukken. Naast lantibiotica worden in dit hoofdstuk ook teixobactines en brevibacillines geïntroduceerd. Beide zijn gericht tegen Lipide II, zijn onlangs ontdekt, en hebben het potentieel om het probleem van antibioticaresistente bacteriën aan te pakken.

In hoofdstuk 2 beschrijven we kort de regulatie van de intracellulaire pH-homeostase, ionenhomeostase, en ATP-synthese, drie onderling samenhangende verschijnselen, in bacteriën. De intracellulaire protonengradiënt (ΔpH), elektrisch potentiaal ($\Delta\psi$) en de ATP-synthese/hydrolyse worden actief of passief gereguleerd door bacteriën wanneer zij worden blootgesteld aan stress van buitenaf, zoals behandeling met antibiotica. Dit is vooral relevant voor AMP's die gericht zijn op het bacteriële membraan, aangezien het membraan een centrale rol speelt in al deze processen. Het monitoren van de veranderingen van ΔpH , $\Delta\psi$ en ATP-niveau geeft dus een belangrijk

inzicht in de mechanismen van deze AMP's.

Hoofdstuk 3 introduceert epilancine 15X en de eerste stappen om het werkingsmechanisme ervan te ontrafelen. Hier worden 5 probes gebruikt om de effecten van epilancine 15X op het membraan te bestuderen en deze te vergelijken met die van nisine en de chemische variant van teixobactine, [R4L10]-teixobactine, in de grampositieve bacteriën *Staphylococcus simulans*, *Micrococcus flavus* en *Bacillus megaterium*. Wij introduceerde hier een nieuwe op luciferase gebaseerde ATP-test, die van grote waarde is voor dit onderzoek, omdat hiermee zowel on-line ATP-lekkage uit de cellen, alsook de resterende cellulaire ATP-inhoud kan worden gemeten. We maten het effect van AMP's op membraanpermeabiliteit, ΔpH , $\Delta\psi$, ATP-lekkage en intracellulaire ATP-niveaus. Van de drie geteste stammen waren de resultaten met *M. flavus* het meest raadselachtig, maar ook inzichtelijk. Deze stam leek niet compatibel met DAPI, een DNA-bindende probe die vaak wordt gebruikt in celdoodtests. De meest inzichtelijke aanwijzing voor het mechanisme van epilancine 15X en [R4L10]-teixobactine bij *M. flavus* betrof de intracellulaire pH en de luciferase-test. Beide peptiden induceerden een verhoging van de intracellulaire pH en [R4L10]-teixobactine veroorzaakte ook een verhoging van het intracellulaire ATP-gehalte bij lage concentraties. Interessant genoeg lijken deze effecten op de effecten die werden waargenomen bij behandeling van *Mycobacterium bovis* BCG met remmers van de celwandsynthese [1]. Daar werd een sterke verhoging van intracellulair ATP veroorzaakt door een toename van de oxidatieve fosforylering, wat bijdraagt tot de door het geneesmiddel veroorzaakte celdood. De verhoging van de pH in *M. flavus* kan worden veroorzaakt door een excessieve activatie van oxidatieve fosforylering, waardoor *M. flavus* vergelijkbaar lijkt te reageren op remmers van de celwand als *Mycobacterium bovis* BCG. Dit suggereert ook dat epilancine 15X de celwandsynthese van *M. flavus* verstoort. Gezien de verhoogde oxidatieve fosforylering, potentiëren zowel epilancine als teixobactine mogelijk andere antibiotica om *M. flavus* (en misschien ook andere bacteriën) te doden [2]. Deze toename van de respiratie gekoppeld aan verhoogde ATP-niveaus lijkt te verschillen van de stijging van de ATP-niveaus bij *Staphylococcus aureus* na behandeling met antibiotica die de eiwitsynthese remmen, zoals chlooramfenicol, waar geen verhoogde respiratie werd waargenomen [2]. Deze stijging in ATP werd waarschijnlijker veroorzaakt door een overschot aan ATP opbouw als gevolg van de uitschakeling van het meest ATP-verbruikende proces in de cel: de eiwitsynthese. Waarom *M. flavus* zich anders gedraagt dan de andere stammen blijft een raadsel en kan verbonden zijn met specifieke eigenschappen van zijn membraan. Toch benadrukt dit verschijnsel het belang van meerdere tests en stammen te gebruiken om goede conclusies te kunnen trekken over de werkingsmechanismen van AMP's. Bovendien kan niet worden uitgesloten dat het werkingsmechanisme van een bepaald peptide tot op zekere hoogte verschilt voor verschillende bacteriestammen.

In hoofdstuk 4 wordt ingezoomd op het werkingsmechanisme van epilancine 15X en

de mogelijke betrokkenheid van Lipide II daarbij. Een duidelijke interactie tussen epilancine 15X en Lipide II werd waargenomen met op antagonisme gebaseerde experimenten. Dit werd bevestigd met behulp van circulair dichroïsme (CD), waaruit bleek dat de interactie specifiek is en niet alleen door elektrostatische effecten wordt veroorzaakt. De interactie van epilancine met Lipide II leidde echter niet tot membraaneffecten. Hoewel het onzeker bleef of Lipide II het doelwit is van epilancine 15X, wezen depolarisatietests op de betrokkenheid van een doelwit binnen een op polyisopreen-gebaseerde biosyntheseroute, aangezien duidelijke effecten op de activiteit van epilancine 15X konden worden waargenomen door verbindingen die specifiek op deze routes werkten. Interessant is dat wij een interactie van epilancine 15X met CDP-DAG waarnamen, wat wijst op de betrokkenheid van een lipidegebonden pyrofosfaat. Helaas blijft het precieze doelwit van epilancine 15X tot dusver onbekend.

In hoofdstuk 5 wordt het werkingsmechanisme van brevibacillinen bestudeerd. Deze behoren tot een nieuwe klasse van niet-ribosomaal geproduceerde lipotridecapeptiden en vertonen activiteit tegen antimicrobieel resistente pathogenen. Aangezien brevibacillinen een soortgelijke membraanpermeabiliteit vertonen als nisine, hebben wij de interactie tussen brevibacillines en Lipide II getest. Er werden inderdaad duidelijke antagonistische effecten waargenomen van Lipide II op de activiteit van zowel brevibacilline als brevibacilline 2V in een agar diffusietest. Bovendien werden interacties van de peptiden met Lipide II bevestigd door circulair dichroïsme experimenten die alleen in aanwezigheid van Lipide II duidelijke structurele veranderingen lieten zien, bevestigde ook een interactie. Uitdoving van de fluorescentie van pyreen-gelabelde Lipide II in de aanwezigheid van brevibacillines ondersteunde ook het bestaan van een interactie. Maar anders dan het nisine-Lipide II-systeem dat samen een porie-complex vormt en altijd leidt tot het verschijnen van pyreen excimer fluorescentie, vertoonden de brevibacillines geen dergelijke effecten, wat erop wijst dat hun binding niet leidde tot de vorming van oligomeren van hogere orde die Lipide II omvatten. Brevibacilline en brevibacilline 2V bleken beide permeabilisatie van modelmembranen te veroorzaken, maar Lipide II speelde geen rol in hun permeabilisatie-activiteit. Integendeel, de aanwezigheid van Lipide II verminderde juist de membraanpermeabilisatie-activiteit van brevibacillines. Binding aan Lipide II en membraanpermeabilisatie werden dus beschouwd als twee onafhankelijke werkingswijzen van brevibacillines.

De rol van metabolische toestand bij de gevoeligheid van bacteriën voor antibiotica

De metabolische toestand van bacteriën is nauw verbonden met hun gevoeligheid voor antibiotica. Studies hebben aangetoond dat de metabolische toestand van bacteriën, vooral de ATP-niveaus, een belangrijke rol spelen bij de dodelijkheid van antibiotica wanneer de groeisnelheid gerelateerd is aan de beschikbaarheid van voedingsstoffen, terwijl de metabole toestand dat niet is [3]. Bovendien is ook het aantal rRNA-operons

in bacteriën gerelateerd aan antibioticagevoeligheid. Het aantal ribosomen is gecorreleerd met het aantal rRNA-operons, en wanneer bacteriën met een relatief laag aantal ribosomen worden behandeld met ribosoom-gerichte antibiotica, worden de eiwitsynthese en de groei van bacteriën ernstig belemmerd [4]. Bovendien binden antibiotica zich aan actief translaterende ribosomen, wat leidt tot de productie van verkeerd gelezen eiwitten. Deze verkeerd gelezen eiwitten kunnen in het celmembraan terechtkomen en membraanverstoring veroorzaken [5]. Door het aantal rRNA-operons op een hoog niveau te houden, zijn bacteriën dus toleranter tegen antibiotica [4]. Anderzijds kunnen bacteriën ook hun metabolische toestand manipuleren om resistentie of tolerantie te bereiken, zoals bij persisters wordt waargenomen. Deze bacteriële persisters zijn een subpopulatie van antibioticatolerante bacteriën die een groeiend medisch probleem vormen, omdat zij een recalcitrantie van chronische infecties veroorzaken ondanks antibacteriële behandeling [6]. Persister-vorming is gekoppeld aan een afname van het intracellulaire ATP-niveau, waarvan is aangetoond dat het antibioticatolerantie genereert [7, 8]. Aangezien ATP-synthese rechtstreeks gekoppeld is aan respiratie (CH₂), is het geen verrassing dat defecten in respiratoir complex I persistentie tegen antibiotica genereert [9]. Problemen met proton translocatie door zo'n gecompromitteerd respiratoir complex I of andere verstoringen van de metabole homeostase, zoals aanhoudend ATP verbruik zonder ATP-regeneratie, zal leiden tot een daling van de intracellulaire pH of met andere woorden: cytoplasmatische verzuring [9]. Milde verzuring van het cytoplasma verhoogt de RpoS-respons, een geconserveerde adaptieve regulator waarvan de expressie leidt tot algemene stressbestendigheid van cellen, wat gerelateerd is aan persister-vorming [10, 11]. Ernstige cytoplasmatische verzuring stopt de eiwitsynthese, waardoor de cellen toleranter worden voor antibiotica die gericht zijn op translatie [9]. Zowel milde als ernstige verzuring leidt tot verhoogde persistentie [9]. De bovenstaande effecten tonen het belang aan van het bepalen van het effect van een antibioticum op de ATP-niveaus, de Δ pH en de Δ ψ van bacteriën, wat een voorspelling van mogelijke persister-vorming mogelijk maakt. Zo wijst het effect van [R4L10]-teixobactine op *M. flavus*, dat een verhoogd ATP-gehalte en een verhoogde intracellulaire pH liet zien, erop dat er geen risico van persister-vorming bestaat, wat een van de redenen kan zijn voor het uitblijven van resistentieopbouw bij met teixobactine behandelde bacteriën.

Het potentieel van antibiotica met een dubbel mechanisme, waaronder membraaneffecten

Nisine, teixobactine en de brevibacillines hebben een dubbel werkingsmechanisme, die zowel gericht is op celwandsynthese (via binding aan lipide II) als op membraanpermeabilisatie. Evenzo hebben AMP's zoals telavancine en daptomycine dubbele mechanismen waarbij zij remming van peptidoglycan-synthese combineren met membraaneffecten [12, 13]. Hoewel membraanactieve eigenschappen meer risico's inhouden in de vorm van mogelijke hemolyseproblemen die toekomstig klinisch gebruik kunnen belemmeren, verbeteren ze wel de antimicrobiële capaciteiten [14, 15].

Een ander interessant voorbeeld van een gecombineerd mechanisme waarvan er één deel zich richt op bacteriële membranen werd onlangs gegeven. De verbindingen SCH-79797 en het daarvan afgeleide Irresistin-16 richten zich op het folaatmetabolisme, maar bleken zich ook te richten tegen het bacteriële membraan, waardoor zij beide actief zijn tegen zowel gram-positieve en Gram-negatieve bacteriën. Bovendien bleken deze antibiotica nauwelijks resistentie op te wekken, waarschijnlijk vanwege hun dubbele mechanisme [16]. Het opnemen van membraaneffecten in het mechanisme van een antibioticum verhoogt dus de antibacteriële efficiëntie en vermindert het ontstaan van resistentie. Dit is een veelbelovende richting voor de ontwikkeling van antibiotica om antibioticaresistentie aan te pakken.

Referenties

1. Shetty, A. and T. Dick, *Mycobacterial Cell Wall Synthesis Inhibitors Cause Lethal ATP Burst*. Front Microbiol, 2018. **9**: p. 1898.
2. Lobritz, M.A., et al., *Antibiotic efficacy is linked to bacterial cellular respiration*. Proc Natl Acad Sci U S A, 2015. **112**(27): p. 8173-80.
3. Lopatkin, A.J., et al., *Bacterial metabolic state more accurately predicts antibiotic lethality than growth rate*. Nature Microbiology, 2019. **4**(12): p. 2109-2117.
4. Levin, B.R., et al., *A Numbers Game: Ribosome Densities, Bacterial Growth, and Antibiotic-Mediated Stasis and Death*. mBio, 2017. **8**(1).
5. Davis, B.D., L.L. Chen, and P.C. Tai, *Misread protein creates membrane channels: an essential step in the bactericidal action of aminoglycosides*. Proc Natl Acad Sci U S A, 1986. **83**(16): p. 6164-8.
6. Fisher, R.A., B. Gollan, and S. Helaine, *Persistent bacterial infections and persister cells*. Nature Reviews Microbiology, 2017. **15**(8): p. 453-464.
7. Shan, Y., et al. *ATP-Dependent Persister Formation in Escherichia coli*. mBio, 2017. **8**, e02267-16 DOI: 10.1128/mbio.02267-16.
8. Conlon, B.P., et al., *Persister formation in Staphylococcus aureus is associated with ATP depletion*. Nature Microbiology, 2016. **1**(5): p. 16051.
9. Van den Bergh, B., et al., *Mutations in respiratory complex I promote antibiotic persistence through alterations in intracellular acidity and protein synthesis*. Nature Communications, 2022. **13**(1): p. 546.
10. Schellhorn, H.E., *Function, Evolution, and Composition of the RpoS Regulon in Escherichia coli*. 2020. **11**.
11. Liu, S., et al., *Variable Persister Gene Interactions with (p)ppGpp for Persister Formation in Escherichia coli*. Front Microbiol, 2017. **8**: p. 1795.
12. Taylor, S.D. and M. Palmer, *The action mechanism of daptomycin*. Bioorg Med Chem, 2016. **24**(24): p. 6253-6268.
13. Saravolatz, L.D., G.E. Stein, and L.B. Johnson, *Telavancin: a novel lipoglycopeptide*. Clin Infect Dis, 2009. **49**(12): p. 1908-14.
14. Belokoneva, O.S., et al., *The hemolytic activity of six arachnid cationic peptides is affected by the phosphatidylcholine-to-sphingomyelin ratio in lipid bilayers*. Biochimica et Biophysica Acta (BBA) - Biomembranes, 2003. **1617**(1): p. 22-30.
15. Dennison, S. and D. Phoenix, *Susceptibility of sheep, human, and pig erythrocytes to haemolysis by the antimicrobial peptide Modelin 5*. European biophysics journal : EBJ, 2014.

43.

16. Martin, J.K., 2nd, et al., *A Dual-Mechanism Antibiotic Kills Gram-Negative Bacteria and Avoids Drug Resistance*. Cell, 2020. **181**(7): p. 1518-1532.e14.

Acknowledgments

In **2010**, just before I went to university to have my college life, I bought a T-shirt. In **2014**, I wore it and took my bachelor's degree photo (right side). In **2016**, I came to Netherlands and had the best 4.5 years of my life. In **2023**, I finally will get my PhD degree. I'm a very rational person who deeply believes in science. But I would like to say it here in a romantic way: **I came to Utrecht and have my PhD is meant to be.**



Thank you, **Eefjan**. I am lucky to have you as my supervisor. Thank you for always being patient with me and understanding my thoughts (Sometimes, I do not even understand what I am talking about #^_#.). You support my ideas, give me quite insightful suggestions, and teach me how to think critically. When experiments went not well, you always shrugged your shoulders and said: Shit happens. Your words, "Shit happens", comfort me a lot.

Thank you, **Antoinette**, for being my promotor. You set a role model for me as a respectable female scientist. Professor **Qing Gu**, thanks for giving me this opportunity to study in the Netherlands. **Maarten**, you are critical to my research and give me good advice. **Linda**, you are such a warm-hearted girl who always gives me your hand with your smile. **Martijn, Ruud and Eveline**, thanks for making our lab run smoothly and helping me whenever I needed help. **Toon**, you are always being so gentle. **Joseph**, thanks for your endless jokes.

Xue Bao, my roommate, my friend, my colleague, my sister. I cannot even imagine the live without you in Utrecht, thanks for helping me so so much. Hope you have a dream-like life with **Wouter**, an excellent man. **Sabine** and **Lisette**, I am grateful to have you to as my office roommates, helping me settle down in Utrecht, give me the strength to start with my lab work. **Yao Liu, Yang Xu, Min Xie, Hannah Jiang, Heqin Ma, Huifang Cai, Zhihong Lv, Beili Wang, Luwen Zhuang, Ying Liu**, it is nice to have you people in the Netherlands that makes me feel at home. **Juan, Mike, Jonas, Adrian, Maik, Amrah, Joao, Rhythm, Max, Renée, Noortje, Monica, Saran, Kees** and **Michal**, you are really good colleagues that have diverse interesting personalities.

Thanks to my family members. **My parents**, who always protect me, supply me with the best they have and support my dream. You are the best parents in the whole world. My husband, **Dong Xu**, who stayed late every night to talk to me, listened my complaints, flew to Netherlands because I said I missed him. My baby girl **Lai Xu**, thank you for being so healthy and happy. I am lucky to be your mother.

Acknowledgments

谢谢我的家庭成员们。我的父母，谢谢你们永远这样保护我，给我你们能提供的最好的条件，无条件支持我的梦想。你们是世界上最好的爸爸妈妈。谢谢我的先生徐栋，谢谢你每天熬夜陪我聊天，倾听我的各种抱怨，当我说想你的时候毫不犹豫地飞来荷兰。谢谢我的宝贝女儿徐莱，感谢你生的这样的健康和快乐，我很荣幸成为你的妈妈。

Curriculum vitae

Xiaoqi Wang was born on 24th November 1991 in Hangzhou Zhejiang province in China. She majored in “Food quality and safety” and obtained her bachelor’s degree in China Jiliang University in 2014. Afterwards, she pursued her master’s degree with the major “Food engineering” and graduated from Zhejiang Gongshang University in 2017. She got a China Scholarship Council (CSC) scholarship in 2015 and started her PhD project under the supervision of Prof. dr. Eefjan Breukink in Membrane Biochemistry & Biophysics group (MBB), Department of Chemistry, Utrecht University, Utrecht, the Netherlands in 2016. Her PhD research is centered on membrane effects of antimicrobial peptides which are described in this thesis.

List of publications

1. **X. Wang**, Q. Gu, E. Breukink, Non-lipid II targeting lantibiotics, *Biochimica et Biophysica Acta (BBA) - Biomembranes*, 1862 (2020) 183244.
2. X. Zhao, **X. Wang**, R. Shukla, R. Kumar, M. Weingarh, E. Breukink, O.P. Kuipers, Brevibacillin 2V, a Novel Antimicrobial Lipopeptide With an Exceptionally Low Hemolytic Activity, *12* (2021).
3. X. Zhao, **X. Wang**, R. Shukla, R. Kumar, M. Weingarh, E. Breukink, O.P. Kuipers, Brevibacillin 2V Exerts Its Bactericidal Activity via Binding to Lipid II and Permeabilizing Cellular Membranes, *Front Microbiol*, 12 (2021) 694847.
4. Y. Xu, V.M. Hernández-Rocamora, J.H. Lorent, R. Cox, **X. Wang**, X. Bao, M. Stel, G. Vos, R.M. van den Bos, R.J. Pieters, J. Gray, W. Vollmer, E. Breukink, Metabolic labeling of the bacterial peptidoglycan by functionalized glucosamine, *iScience*, 25 (2022) 104753.
5. R. Shukla, F. Lavore, S. Maity, M.G.N. Derks, C.R. Jones, B.J.A. Vermeulen, A. Melcrová, M.A. Morris, L.M. Becker, **X. Wang**, R. Kumar, J. Medeiros-Silva, R.A.M. van Beekveld, A. Bonvin, J.H. Lorent, M. Lelli, J.S. Nowick, H.D. MacGillavry, A.J. Peoples, A.L. Spoering, L.L. Ling, D.E. Hughes, W.H. Roos, E. Breukink, K. Lewis, M. Weingarh, Teixobactin kills bacteria by a two-pronged attack on the cell envelope, *Nature*, 608 (2022) 390-396.
6. **X. Wang**, R.A.M. van Beekveld, Y. Xu, A. Parmar, S. Das, I. Singh, E. Breukink, Analyzing mechanisms of action of antimicrobial peptides on bacterial membranes requires multiple complimentary assays and different bacterial strains, *Biochimica et Biophysica Acta (BBA) - Biomembranes*, (2023) 184160.
7. **Xiaoqi Wang**, Yang Xu, Nathaniel I. Martin, Eefjan Breukink, The enigmatic mode of action of the lantibiotic epilancin 15X, (*BBA*) – *Biomembranes*, (2023). Submitted.